UNIVERSIDADE FEDERAL DE MINAS GERAIS

Instituto de Ciências Biológicas

Programa de Pós-Graduação em Biologia Celular

JORDANE CLARISSE PIMENTA

ALTERAÇÕES NEUROQUÍMICAS E COMPORTAMENTAIS INDUZIDAS PELA INFECÇÃO POR CORONAVÍRUS, TANTO NO CONTEXTO AGUDO COMO NAS SEQUELAS

Belo Horizonte

2025

JORDANE CLARISSE PIMENTA

ALTERAÇÕES NEUROQUÍMICAS E COMPORTAMENTAIS INDUZIDAS PELA INFECÇÃO POR CORONAVÍRUS, TANTO NO CONTEXTO AGUDO COMO NAS SEQUELAS

Tese apresentada ao Programa de Pós-Graduação em Biologia Celular do Departamento de Morfologia, do Instituto de Ciências Biológicas, da Universidade Federal de Minas Gerais, como requisito parcial para obtenção do título de Doutora em Ciências.
Área de concentração: Biologia Celular

Orientador (a): Profa. Dra. Vivian Vasconcelos Costa
Coorientador (a): Profa. Dra. Aline Silva de Miranda

Belo Horizonte
2025

043 Pimenta, Jordane Clarisse.
Alterações neuroquímicas e comportamentais induzidas pela infecção por Coronavírus, tanto no contexto agudo como nas sequelas [manuscrito] / Jordane Clarisse Pimenta. – 2025.
199 f. : il. ; 29,5 cm.

Orientador (a): Profa. Dra. Vivian Vasconcelos Costa. Coorientador (a): Profa. Dra. Aline Silva de Miranda.
Tese (doutorado) – Universidade Federal de Minas Gerais, Instituto de Ciências Biológicas. Programa de Pós-Graduação em Biologia Celular.

1. Biologia Celular. 2. Infecções por Coronavirus. 3. Betacoronavirus. 4. Comportamento Animal. 5. Sistema Nervoso Central. I. Litwinski, Vivian Vasconcelos Costa. II. Miranda, Aline Silva de. III. Universidade Federal de Minas Gerais. Instituto de Ciências Biológicas. IV. Título.

CDU: 576

Ficha catalográfica elaborada pela bibliotecária Fabiane C M Reis – CRB 6 – 2680

UNIVERSIDADE FEDERAL DE MINAS GERAIS
ICB - COLEGIADO DE PÓS-GRADUAÇÃO EM BIOLOGIA CELULAR - SECRETARIA

ATA DE DEFESA DE DISSERTAÇÃO/TESE

JORDANE CLARISSE PIMENTA

Às **treze horas** do dia **05 de fevereiro de 2025**, reuniu-se, no Instituto de Ciências Biológicas da UFMG, a Comissão Examinadora da Tese, indicada pelo Colegiado do Programa, para julgar, em exame final, o trabalho final intitulado: **"ALTERAÇÕES NEUROQUÍMICAS E COMPORTAMENTAIS INDUZIDAS PELA INFECÇÃO POR CORONAVÍRUS, TANTO NO CONTEXTO AGUDO COMO NAS SEQUELAS"**, requisito final para obtenção do grau de Doutora em Biologia Celular. Abrindo a sessão, a Presidente da Comissão, **Dra. Vivian Vasconcelos Costa Litwinski**, após dar a conhecer aos presentes o teor das Normas Regulamentares do Trabalho Final, passou a palavra à candidata, para apresentação de seu trabalho. Seguiu-se a arguição pelos examinadores, com a respectiva defesa da candidata. Logo após, a Comissão se reuniu, sem a presença da candidata e do público, para julgamento e expedição de resultado final. Foram atribuídas as seguintes indicações:

Prof./Pesq.	Instituição	Indicação
Dra. Vivian Vasconcelos Costa Litwinski	UFMG	Aprovada
Dra. Aline Silva de Miranda	UFMG	Aprovada
Dra. Karina Ramalho Bortoluci	UNIFESP	Aprovada
Dr. Antônio Carlos Pinheiro de Oliveira	UFMG	Aprovada
Dr. André Ricardo Massensini	UFMG	Aprovada
Dr. Antônio Lúcio Teixeira Júnior	UNIVERSITY OF TEXAS HEALTH SCIENCE CENTER AT HOUSTON	Aprovada

Pelas indicações, a candidata foi considerada: APROVADA
O resultado final foi comunicado publicamente à candidata pela Presidente da Comissão. Nada mais havendo a tratar, a Presidente encerrou a reunião e lavrou a presente ATA, que será assinada por todos os membros participantes da Comissão Examinadora. **Belo Horizonte, 05 de fevereiro de 2025.**

Dra. Vivian Vasconcelos Costa Litwinski_____

Dra. Aline Silva de Miranda_____

Dra. Karina Ramalho Bortoluci_____

Dr. Antônio Carlos Pinheiro de Oliveira_____

Dr. André Ricardo Massensini_____

Dr. Antônio Lúcio Teixeira Júnior_____

.

Belo Horizonte, 14 de fevereiro de 2025.

Assinatura dos membros da banca examinadora:

Documento assinado eletronicamente por **Antonio Carlos Pinheiro de Oliveira**, **Professor do Magistério Superior**, em 14/02/2025, às 10:54, conforme horário oficial de Brasília, com fundamento no art. 5º do Decreto nº 10.543, de 13 de novembro de 2020.

Documento assinado eletronicamente por **Karina Ramalho Bortoluci**, **Usuária Externa**, em 14/02/2025, às 13:09, conforme horário oficial de Brasília, com fundamento no art. 5º do Decreto nº 10.543, de 13 de novembro de 2020.

Documento assinado eletronicamente por **Antonio Lucio Teixeira Junior**, **Usuário Externo**, em 14/02/2025, às 13:35, conforme horário oficial de Brasília, com fundamento no art. 5º do Decreto nº 10.543, de 13 de novembro de 2020.

Documento assinado eletronicamente por **Aline Silva de Miranda**, **Servidor(a)**, em 14/02/2025, às 17:39, conforme horário oficial de Brasília, com fundamento no art. 5º do Decreto nº 10.543, de 13 de novembro de 2020.

Documento assinado eletronicamente por **Vivian Vasconcelos Costa Litwinski**, **Professora do Magistério Superior**, em 18/02/2025, às 11:10, conforme horário oficial de Brasília, com fundamento no art. 5º do Decreto nº 10.543, de 13 de novembro de 2020.

A autenticidade deste documento pode ser conferida no site https://sei.ufmg.br/sei/controlador_externo.php?acao=documento_conferir&id_orgao_acesso_externo=0, informando o código verificador **3972114** e o código CRC **6D6D0F4A**.

Dedico este trabalho a Deus,
aos meus queridos pais, amigos e professores.

AGRADECIMENTOS

Chegar ao final desta jornada foi um processo intenso, marcado por desafios, aprendizados e muitas conquistas. Este trabalho é fruto de esforços conjuntos, e é com imensa gratidão que registro aqui meus sinceros agradecimentos a todas as pessoas e instituições que contribuíram direta ou indiretamente para a realização deste sonho.

Primeiramente, agradeço a Deus pela força, saúde, resiliência que me sustentaram em cada etapa do percurso e por ter honrado todo meu esforço ao final do processo. À minha família, minha base sólida e meu maior incentivo. Agradeço especialmente aos meus pais, Gesofeta e David, por todo amor, dedicação e pelos valores que me ensinaram, os quais estiveram presente em cada passo desta caminhada. Ao meu companheiro Leonardo pelo apoio incondicional, paciência e compreensão ao longo de tantas noites mal dormidas e dias exaustivos.

À minha orientadora Vivian, expresso minha mais profunda gratidão. Sua sabedoria, comprometimento e generosidade intelectual foram fundamentais para o desenvolvimento deste trabalho. Obrigada por acreditar em mim, mesmo nos momentos mais difíceis, e por sempre me guiar com palavras de encorajamento. Agradeço também à minha coorientadora Aline, por todos os ensinamentos de neuro e pelos treinamentos didáticos em que me descobri professora.

À minha psicóloga, Valkíria, por ter me feito enxergar que a vida vai muito além do que pensamos. Muito obrigada, eu jamais teria conseguido prosseguir sem você.

Aos membros da banca examinadora, por suas valiosas contribuições, sugestões e questionamentos, que enriquecem e proporcionam novas perspectivas acadêmicas.

Aos professores, técnicos e colegas de laboratório do G3, especialmente o Winy (Vinícius Beltrami), meu companheiro do *"Long COVID*", minha eterna gratidão pelo compartilhamento de conhecimentos, pelas colaborações que contribuíram para meu crescimento acadêmico e pessoal, sem você jamais teríamos feito um trabalho tão lindo. Agradeço à Let (Letícia Soldati), a técnica que virou minha amiga confidente, obrigada por tanto.

As instituição de fomento, CAPES, CNPq, FAPEMIG, INCT em Dengue, agradeço o suporte financeiro, sem o qual esta pesquisa não teria sido possível.

Ao meu querido GPA/V, agradeço pela parceria, pela troca de ideias, pelo apoio mútuo e pelos momentos de descontração que tornaram esta caminhada mais leve.

À minha “panelinha”, “quinteto fantástico” que eu tanto amo e vou sentir saudades, Luíz, Felipe Rocha, Dani e Tana. Obrigada por toda colaboração, ensinamentos e risadas. Aos meus amigos, especialmente Jéssica e Brenda, que jamais desistiram de mim.

Por fim, dedico este trabalho a todas as pessoas que, de alguma forma, contribuíram para a realização deste sonho. Agradeço por acreditarem em mim, por suas palavras de incentivo e por seus gestos de generosidade ao longo desta jornada.

A todos, meu mais sincero obrigada.

“Porque dele, e por ele, e para ele, são todas as coisas; glória, pois, a ele eternamente.” Amém.

Romanos 11:36

RESUMO

A COVID-19 (*Coronavirus Disease-2019*), inicialmente descrita como uma doença predominantemente respiratória, revelou-se uma condição multissistêmica. A progressão para formas graves da doença tem sido atribuída tanto à resposta imune exacerbada do hospedeiro, resultando na chamada "tempestade de citocinas", quanto à ampla replicação viral em diversos tecidos devido à expressão ubíqua da enzima conversora de angiotensina 2 (ECA-2), utilizada como receptor viral. No sistema nervoso central (SNC), a neuroinflamação destaca-se pela relevância na etiopatogenia de distúrbios neuropsiquiátricos. Neste estudo, utilizamos modelos de infecção intranasal por betacoronavírus murinos (MHV-3 e MHV-A59) para investigar alterações associadas à infecção aguda e subaguda/crônica, respectivamente. O MHV-3 foi capaz de infectar e se replicar no SNC, induzindo alterações agudas graves como desequilíbrio na produção de mediadores inflamatórios, aumento na liberação de glutamato e no influxo de cálcio, alterações histopatológicas leves e déficits comportamentais, como anedonia, comportamento do tipo ansioso e comprometimento motor. Já o MHV-A59, um vírus de tropismo pulmonar que causa doença de caráter auto resolutivo, foi utilizado como ferramenta para estudar sequelas neuropsiquiátricas da COVID longa. Os resultados indicaram que apenas fêmeas infectadas com MHV-A59 apresentaram alterações neuropsiquiátricas. Esses achados sugerem que as alterações pós-infecção estão diretamente relacionadas ao sexo biológico e à influência de hormônios sexuais. Nesse sentido, foram avaliados estradiol, hormônio folículo estimulante (FSH) e testosterona. Esses hormônios se apresentaram alterados durante a cinética de infecção, mas destacamos os níveis de testosterona que permaneceram reduzidos durante todo período estudado. Assim como demonstrado na literatura, essa redução está diretamente associada aos sintomas da COVID longa, em ambos os sexos. A ovariectomia em fêmeas infectadas resultou em melhora significativa nas sequelas comportamentais e no escore histopatológico cerebral. Nesse contexto, a prova de conceito consistiu no tratamento com o peptídeo anti-inflamatório e pró-resolutivo angiotensina (1-7), administrado na fase aguda da infecção, demonstrando ser eficaz na prevenção das sequelas neuropsiquiátricas observadas previamente. Portanto, os modelos murinos de MHV-3 e MHV-A59 mimetizam aspectos fundamentais da COVID-19 aguda grave e da COVID longa, respectivamente, fornecendo plataformas pré-clínicas robustas para estudos de patogênese e desenvolvimento de intervenções terapêuticas.

Palavras-chave: MHV-3; infecção SNC; COVID-19; comportamento animal; COVID longa; MHV-A59.

ABSTRACT

COVID-19 (Coronavirus Disease-2019), initially described as a predominantly respiratory disease, has proven to be a multisystemic condition. The progression to severe forms of the disease has been attributed both to the exacerbated host immune response, resulting in the so-called "cytokine storm", and to widespread viral replication in several tissues due to the ubiquitous expression of angiotensin-converting enzyme 2 (ACE-2), used as a viral receptor. In the central nervous system (CNS), neuroinflammation stands out for its relevance in the etiopathogenesis of neuropsychiatric disorders. In this study, we used models of intranasal infection by murine betacoronaviruses (MHV-3 and MHV-A59) to investigate changes associated with acute and subacute/chronic infection, respectively. MHV-3 was able to infect and replicate in the CNS, inducing severe acute changes such as imbalance in the production of inflammatory mediators, increased glutamate release and calcium influx, mild histopathological changes, and behavioral deficits such as anhedonia, anxiety-like behavior, and motor impairment. MHV-A59, a pulmonary tropism virus that causes self-resolving disease, was used as a tool to study neuropsychiatric sequelae of long COVID. The results indicated that only females infected with MHV-A59 presented neuropsychiatric changes. These findings suggest that post-infection changes are directly related to biological sex and the influence of sex hormones. In this sense, estradiol, follicle-stimulating hormone (FSH), and testosterone were evaluated. These hormones were altered during the kinetics of infection, but we highlight that testosterone levels remained reduced throughout the study period. As demonstrated in the literature, this reduction is directly associated with the symptoms of long COVID in both sexes. Ovariectomy in infected females resulted in significant improvement in behavioral sequelae and brain histopathological score. In this context, the proof of concept consisted of treatment with the anti-inflammatory and pro-resolution peptide angiotensin (1-7), administered in the acute phase of infection, proving to be effective in preventing the neuropsychiatric sequelae previously observed. Therefore, the murine models of MHV-3 and MHV-A59 mimic fundamental aspects of severe acute COVID-19 and long COVID, respectively, providing robust preclinical platforms for pathogenesis studies and development of therapeutic interventions.

Keywords: MHV-3; CNS infection; COVID-19; animal behavior; long COVID; MHV-A59.

LISTA DE ABREVIATURAS E SIGLAS

AABs	Autoanticorpos
ANAs	Anticorpos antinucleares
Angio (1-7)	Angiotensina (1-7)
Aβ	Proteína β-Amilóide
BDNF	Fator neurotrófico derivado do cérebro
BHE	Barreira hematoencefálica
CCL ()	Quimiocina da família CC
CD14	*Cluster of differentiation 14*- Proteína componente do sistema inato
CDC	Centro de controle e prevenção de doenças
CEACAM	*Carcinoembryonic Antigen-Related Cell Adhesion Molecules* (Molécula de adesão celular relacionada ao antígeno carcinoembrionário)
CMV	Citomegalovírus
COVID-19	*Corona Virus Disease-2019* (Doença do coronavírus-2019)
CoVs	Coronavírus
CXC	Grupo de quimiocina com domínio cisteína-x-cisteína, onde x representa qualquer aminoácido
CXCL ()	Quimiocina da família CXC ()
DENV-3	Vírus do Dengue-3
DM1	Diabetes mellitus 1
DN	*Dark neurons* (Neurônios escurecidos)
E2	Estradiol
EBV	Vírus Epstein-Barr
ECA-2	Enzima conversora de angiotensina 2

ELA	Esclerose lateral amiotrófica
ELISA	*Enzyme-linked immunosorbant assay* (Ensaio imunoenzimático)
EM	Esclerose múltipla
FQN	Fractalquina
FSH	Hormônio folículo estimulante
GFAP	Proteína fibrilar glial ácida
GPCRs	Receptores acoplados à proteína G
H_2O_2	Peróxido de hidrogênio
H_2SO_4	Ácido sulfúrico
HCoVs	Coronavírus que acometem humanos
hECA-2	ECA-2 humana
I	Um
I.p	Intraperitoneal
IBA-1	*Ionized calcium-binding adaptor molecule 1* (Molécula adaptadora de ligação ao cálcio ionizado 1)
IFN-γ	Interferon gama
IgG	Imunoglobulina G
IgM	Imunoglobulina M
II	Dois
III	Três
IL	Interleucina
iNOS	Óxido nítrico sintase induzível
IV	Quatro
LCR	Líquido cefalorraquidiano

LES	Lúpus eritematoso sistêmico
LPS	Lipopolissacarídeo
ME/CFS	Encefalomielite miálgica/síndrome da fadiga crônica
MERS-CoV	Coronavírus da Síndrome Respiratória do Oriente Médio
MHV	Coronavírus da hepatite murina
NB-2	Nível de Biossegurança 2
NB-3	Nível de Biossegurança 3
NMDA	N-metil-D-aspartato
NO	Óxido nítrico
NSCs	Células-tronco neurais
OMS	Organização Mundial da Saúde
OVX	Ovariectomia
PAISs	Síndromes de infecção pós-aguda
PASC	Sequelas pós-agudas da COVID-19
PFC	Córtex pré-frontal
qRT-PCR	*Quantitative Reverse Transcription Polymerase Chain Reaction* (Reação em cadeia da polimerase com transcrição reversa quantitativa)
RdRp	RNA polimerase RNA-dependente
RDV	Remdesivir
RRPs	Receptores reconhecedores de padrão
S100B	*Calcium binding protein B* (Proteína B de ligação ao cálcio)
SARS	Síndrome Respiratória Aguda Grave
SARS-CoV	Coronavírus da Síndrome Respiratória Aguda Grave
SARS-CoV-2	Coronavírus da Síndrome Respiratória Aguda Grave 2
SNC	Sistema nervoso central

SNE	Sistema nervoso entérico
ssRNA	RNA fita simples
TGI	Trato gastrointestinal
TLR	*Toll-like receptor* (Receptores tipo-Toll)
V	Cinco
WHO	*World health organization* (Organização Mundial da Saúde)
ZIKV	Vírus Zika

LISTA DE FIGURAS

‘

SUMÁRIO

APRESENTAÇÃO

Esse trabalho foi estruturado em:

1. Introdução
2. Objetivos
3. Artigos relacionados à tese e resultados não publicados
4. Discussão
5. Conclusão
6. Produção científica
7. Anexos

Referências

Os resultados deste trabalho foram organizados em dois artigos científicos e complementados com dados inéditos ainda não publicados: o primeiro artigo, já publicado, apresenta uma plataforma experimental para o estudo da fase aguda da COVID-19 grave. Essa plataforma foi desenvolvida a partir de um modelo murino de infecção pelo betacoronavírus MHV-3, permitindo a investigação de aspectos neuroquímicos, comportamentais e inflamatórios associados à doença. O segundo artigo, atualmente em revisão e em pré-print (https://www.biorxiv.org/content/10.1101/2024.01.10.575003v1), introduz uma nova plataforma baseada em um modelo murino de infecção pelo betacoronavírus MHV-A59. Essa abordagem ampliou a análise para incluir não apenas a fase aguda da infecção, mas também as sequelas prolongadas induzidas pelo vírus, comumente chamadas de COVID longa ou síndrome pós-COVID. Além desses artigos, os resultados não publicados reforçam o valor do modelo de COVID longa como uma ferramenta importante para o estudo de intervenções terapêuticas. Esses dados sugerem que o modelo pode ser crucial para identificar estratégias que previnam ou atenuem os efeitos debilitantes dessa condição crônica.

1. INTRODUÇÃO

1.1 Os Coronavírus

Em dezembro de 2019, um surto de uma nova Síndrome Respiratória Aguda Grave (SARS) foi identificado em Wuhan, província de Hubei, na China. No início de 2020, foi confirmado que essas infecções eram causadas por um novo coronavírus (CoVs), posteriormente, denominado SARS-CoV-2, agente etiológico da doença COVID-19 (do inglês, *Corona virus disease* 2019) (Uddin et al., 2020). Esse vírus possui alto potencial de disseminação, e em janeiro de 2020, a Organização Mundial de Saúde (OMS) declarou a COVID-19 como uma emergência de saúde pública global e, em março de 2020, foi anunciada como uma pandemia (OMS, 2020).

Os CoVs foram descobertos na década de 1960 e organizados taxonomicamente na família *Coronaviridae*, a maior família da ordem *Nidovirales* (Woo et al., 2010; Ashour et al., 2020). A família *Coronaviridae* abrange duas subfamílias: a *Orthocoronavirinae* e a *Torovirinae*. A subfamília *Orthocoronavirinae* é dividida em quatro gêneros: alfacoronavírus, betacoronavírus, gamacoronavírus e deltacoronavírus (Woo et al., 2010; Ashour et al., 2020; ICTV). Este grupo viral foi denominado como coronavírus (da palavra latina *corona*, que significa coroa) em virtude da morfologia esférica da partícula viral e das projeções da proteína "S" (do inglês, *spike protein*) na superfície do envelope que se assemelham a uma coroa ao microscópio eletrônico (Masters & Pearlman, 2013).

Os CoVs estão muito dispersos na população humana, assim como em outros mamíferos e em pássaros, sendo responsáveis por doenças respiratórias, entéricas, neurológicas e hepáticas (Weiss & Leibowitz, 2011). Dentre os CoVs, vale ressaltar as espécies que possuem capacidade de acometer os seres humanos (HCoVs) como o 229E, OC43, NL63 e HKU1, os quais geralmente causam doenças respiratórias leves em indivíduos imunocompetentes (Su et al., 2016), e as espécies de CoVs zoonóticas, o SARS-CoV (Coronavírus da Síndrome Respiratória Aguda Grave), o MERS-CoV (Coronavírus da Síndrome Respiratória do Oriente Médio) e o SARS-CoV-2 (Coronavírus 2 da Síndrome Respiratória Aguda Grave) (Ge et al., 2020).

A COVID-19 é a terceira epidemia de pneumonia causada por CoVs nas últimas duas décadas. A primeira foi em novembro de 2002, em que um novo betacoronavírus denominado SARS-CoV surgiu em Guandong, China, provocando mais de 8.000 infecções e 774 mortes em 37 países; A segunda ocorreu em 2012, causada pelo coronavírus MERS-CoV, notificado pela primeira vez na Arábia Saudita, infectando 2.494 e matando 858 indivíduos (Ge et al., 2020). E

mais recentemente, a pandemia causada pelo SARS-CoV-2, apresentando mais de 776 milhões de casos confirmados e mais de 2,9 milhões de mortes até janeiro de 2025 (WHO, 2025).

O surgimento periódico de novos coronavírus em surtos zoonóticos se deve, principalmente, à distribuição global e à grande diversidade genética desses vírus, assim como pelo aumento da ocupação humana em locais isolados (Cui, Li & Shi, 2019). O envelope dos CoVs é derivado da bicamada lipídica da membrana plasmática hospedeira, possuem genoma de RNA de fita simples (ssRNA), não segmentado, com polaridade positiva e se destacam pelos maiores genomas de RNA conhecidos **(**Hulswit et al., 2016). Esse genoma codifica dezesseis proteínas não estruturais e quatro proteínas estruturais. As proteínas estruturais são: proteína pico, *"Spike"* de superfície (S), proteína de membrana (M), proteína do envelope (E), fosfoproteína do nucleocapsídeo (N) encontrada no cerne ribonucleoprotéico e proteína hemaglutinina-esterase (HE) presente em alguns betacoronavírus (Hulswit et al., 2016; Ashour et al., 2020).

A proteína S é fortemente glicosilada, forma picos na superfície da partícula viral e está envolvida diretamente na interação vírus/hospedeiro ao mediar a adsorção do vírus às células (Ashour et al., 2020). A proteína M é uma das mais importantes e abundantes da estrutura viral, dando forma à partícula e sendo crucial, juntamente com a proteína E, na modulação da montagem do vírion (Ashour et al., 2020). A proteína E participa do processo de liberação de partículas virais das células hospedeiras (Siu et al., 2008). A proteína N interage com o RNA viral formando o nucleocapsídeo, o que a torna importante para o empacotamento do genoma durante a montagem do vírion (Hurst et al., 2009; Ashour et al., 2020). Presente em somente alguns betacoronavírus como já citado, a proteína HE se localiza na superfície dos vírus, é uma hemaglutinina semelhante à do vírus *Influenza* e possui atividade acetil-esterase (Klausegger et al., 1999). Os coronavírus portadores dessa proteína são mais virulentos e ela está envolvida no processo de adsorção desses vírus (Ashour et al., 2020). Já as proteínas não estruturais são regulatórias e imunomoduladoras, como as helicases e a RNA polimerase RNA-dependente (RdRp) responsável pela replicação do genoma (Wu te al., 2020). Os vírus de RNA são conhecidos por apresentarem taxas elevadas de mutações quando comparados aos de DNA e isso se deve à falta da atividade corretora da enzima RdRp durante a replicação do genoma, o que resulta na formação de partículas virais com ampla diversidade e eficientes na adaptação a diferentes hospedeiros (Vignuzzi et al., 2006).

A interação do SARS-CoV-2 com as células hospedeiras se dá, principalmente, pela ligação da proteína S do vírus à enzima conversora de angiotensina 2 (ECA-2) presente na superfície celular, que promove a entrada do vírus (Hoffmann et al., 2020). A ECA-2 é uma

molécula presente na superfície de diversos tipos celulares, o que explica parcialmente, o amplo tropismo viral e o extenso espectro clínico da COVID-19 (Kuba, et al., 2021). (Figura 1).

Figura 1: SARS-CoV-2 utiliza a ECA-2 como receptor para entrar na célula hospedeira e requer a protease celular TMPRSS2 para ativar a proteína *spike*. Adaptado de Mushebenge et al., 2023.

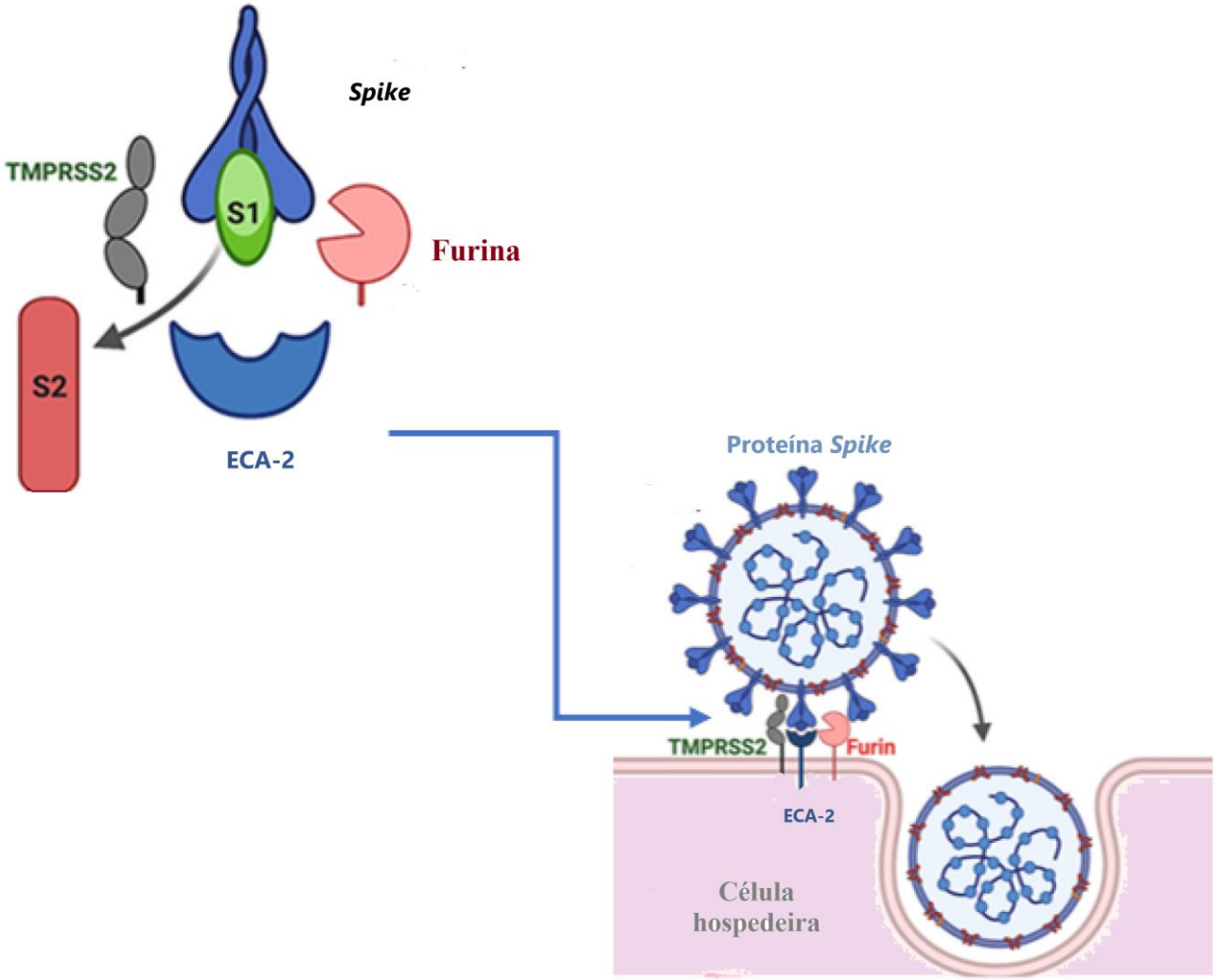

Já foi descrito que as células da glia e os neurônios expressam ECA-2, o que os torna alvo potencial do SARS-CoV-2 (Baig et al., 2020). Em concordância, *Netland* e colaboradores (2008) demonstraram que o SARS-CoV é capaz de induzir morte neuronal em camundongos ao acessar o cérebro através do epitélio olfatório.

1.2 COVID-19 e o Sistema Nervoso Central

A COVID-19 foi primeiramente caracterizada como uma doença respiratória. No entanto, à medida que os sintomas foram sendo compreendidos e mais estudos realizados, observou-se que a doença é multissistêmica, sendo o SNC um dos alvos **(**Bougakov et al., 2021). Curiosamente, os sinais neurológicos podem preceder os sintomas respiratórios ou ser os únicos sinais de infecção pelo SARS-CoV-2. As primeiras manifestações neurológicas decorrentes da COVID-19 são geralmente periféricas, como as disfunções gustativas e olfativas (Harapan & Yoo, 2021). Foram relatadas outras manifestações periféricas como a síndrome de Guillain-Barré, além de condições que indicam comprometimento do SNC, como acidente vascular encefálico, epilepsia, convulsões e encefalite (Harapan & Yoo, 2021).

A infecção aguda por SARS-CoV-2 pode estar relacionada a várias complicações neuropsiquiátricas (Boldrini et al., 2021; Bremner et al., 2025) que decorrem de eventos como, microinfartos associados à exacerbação da coagulação sanguínea, vasculite cerebral, comprometimento da seletividade da barreira hematoencefálica (BHE), assim como ativação de uma resposta inflamatória no cérebro e na periferia (Amruta et al., 2021). O material genético e as proteínas do SARS-CoV-2 foram identificados no tecido cerebral *post-mortem* e no líquido cefalorraquidiano (LCR) de pacientes afetados pela COVID-19 (Krasemann et al., 2022). Foram propostos mecanismos de entrada para explicar a presença do vírus no SNC (Figura 2), como:

I. Via neuronal

Devido à alta carga viral no epitélio nasal (Meinhardt et al., 2021) e à proximidade da cavidade nasal com o cérebro, a rota olfatória é considerada uma porta de entrada para o vírus atingir o SNC. Foram encontradas partículas intactas de CoV, assim como RNA de SARS-CoV-2 na mucosa olfatória e em áreas que recebem projeções do trato olfatório, o que sugere neuro invasão, via transporte axonal, pelo nervo olfatório (Meinhardt et al., 2021). No entanto, tem-se questionado essa via, pois os neurônios sensoriais olfatórios não expressam ECA-2 nem a protease TMPSSR-2 para serem infectados.

O SARS-CoV-2 infecta células não neuronais (células de sustentação e glandulares) e o epitélio olfativo, que expressam ECA-2 (Tsukahara et al., 2023). A infecção do epitélio causa alteração da arquitetura nuclear e regula negativamente a expressão de receptores olfativos, impactando indiretamente na função desses neurônios (Zazhytska et al., 2022). Foi sugerido que um pequeno número de neurônios olfatórios infectados poderia contribuir para a neuroinvasão,

porém constataram que a maioria dos exemplos mostrados são de neurônios imaturos, e esses são incapazes de transportar o vírus até o cérebro por ainda não possuírem as projeções axonais necessárias (Butowt et al., 2021).

O SARS-CoV-2 é um vírus que possui tropismo multissistêmico podendo infectar o Trato Gastrointestinal (TGI). O sistema nervoso entérico (SNE) interage com o SNC por meio de uma via de mão dupla, que se dá, principalmente, pelo nervo vago (Valdetaro et al., 2023). Os neurônios entéricos estão conectados trans-sinapticamente aos neurônios centrais, o que corrobora com a ideia de que o SNE além de ser um alvo potencial do SARS-CoV-2, é uma porta de entrada desse vírus para o SNC (Valdetaro et al., 2023). A infecção do TGI pelo coronavírus gera implicações clínicas como perda de apetite, náuseas, vômitos, diarreia e dores abdominais, e embora menos comuns, condições mais graves como isquemia mesentérica e sangramentos gastrointestinais podem ocorrer (Slabakova et al, 2023). Os sintomas gastrointestinais têm sido vinculados às infecções pelo SARS-CoV-2 desde o início da pandemia, embora a maioria dos indivíduos não relatasse. Durante a fase inicial, marcada pela predominância da variante G614, a diarreia foi o sintoma gastrointestinal mais reportado, com uma taxa de 28,2%. Porém a frequência reduziu nas fases seguintes dominadas por outras variantes: Alfa (19,4%), Delta (17,9%) e Ômicron (13,8%) (Schulze & Bayer, 2022).

II. Via hematogênica

A infecção e o dano às barreiras epiteliais permitem o acesso do vírus à corrente sanguínea e ao sistema linfático, e consequentemente a diversos órgãos, incluindo o cérebro (Pennisi et al., 2020). Nesse sentido, existem dois mecanismos propostos para a disseminação do SARS-CoV-2 pela via hematogênica (Zubair et al., 2020): a transcitose do vírus por meio das células endoteliais vasculares da BHE e a infecção de leucócitos capazes de atravessar a BHE, mecanismo denominado “cavalo de Tróia” (W.-K. Kim et al., 2003). Na primeira hipótese, o vírus presente na circulação sanguínea, ao chegar na microvasculatura da BHE, se liga ao receptor ECA-2 presente no endotélio capilar, e é transportado através da membrana basolateral para o interior do SNC (Baig et al., 2020). A segunda hipótese propõe um mecanismo semelhante ao “cavalo de Tróia”, onde leucócitos infectados pelo vírus, por expressarem a ECA-2, atuam como vetores, transportando o patógeno através da BHE até o SNC (Miner & Diamond, 2016). A resposta inflamatória sistêmica, caracterizada pela “tempestade de citocinas”, induzida pelo SARS-CoV-2, pode prejudicar a integridade da BHE possibilitando assim a entrada do vírus no SNC (Z. Li et al., 2020), corroborando o segundo mecanismo proposto. Contudo, ainda faltam

indícios que comprovem uma replicação viral ativa no SNC, o que sugere que os sintomas neurológicos que ocorrem durante ou após a COVID-19 são resultado, principalmente, da resposta inflamatória induzida pela infecção do que em consequência do neurotropismo de SARS-CoV-2 (Aschman et al., 2022). Portanto, a resposta inflamatória intensa, é atualmente considerada, o principal mecanismo responsável pelas alterações neuropsiquiátricas decorrentes da COVID-19 (Boldrini et al., 2021), em que vários mediadores produzidos na periferia durante a infecção aguda, são capazes de atingir o SNC e desencadear uma neuroinflamação.

Figura 2: Principais mecanismos utilizados pelo SARS-CoV-2 para alcançar o SNC. O vírus pode afetar o SNC, diretamente, chegando ao cérebro por várias vias, como: (1) via olfativa, pelo nervo trigêmeo ou nervo olfatório, (2) via nervo vago em conexão com os pulmões e (3) via eixo intestino-cérebro; ou indiretamente como consequência da resposta sistêmica, resultando em ruptura da BHE e aumento da inflamação e risco de infecções secundária. Adaptado de Sarubbo et al., 2022.

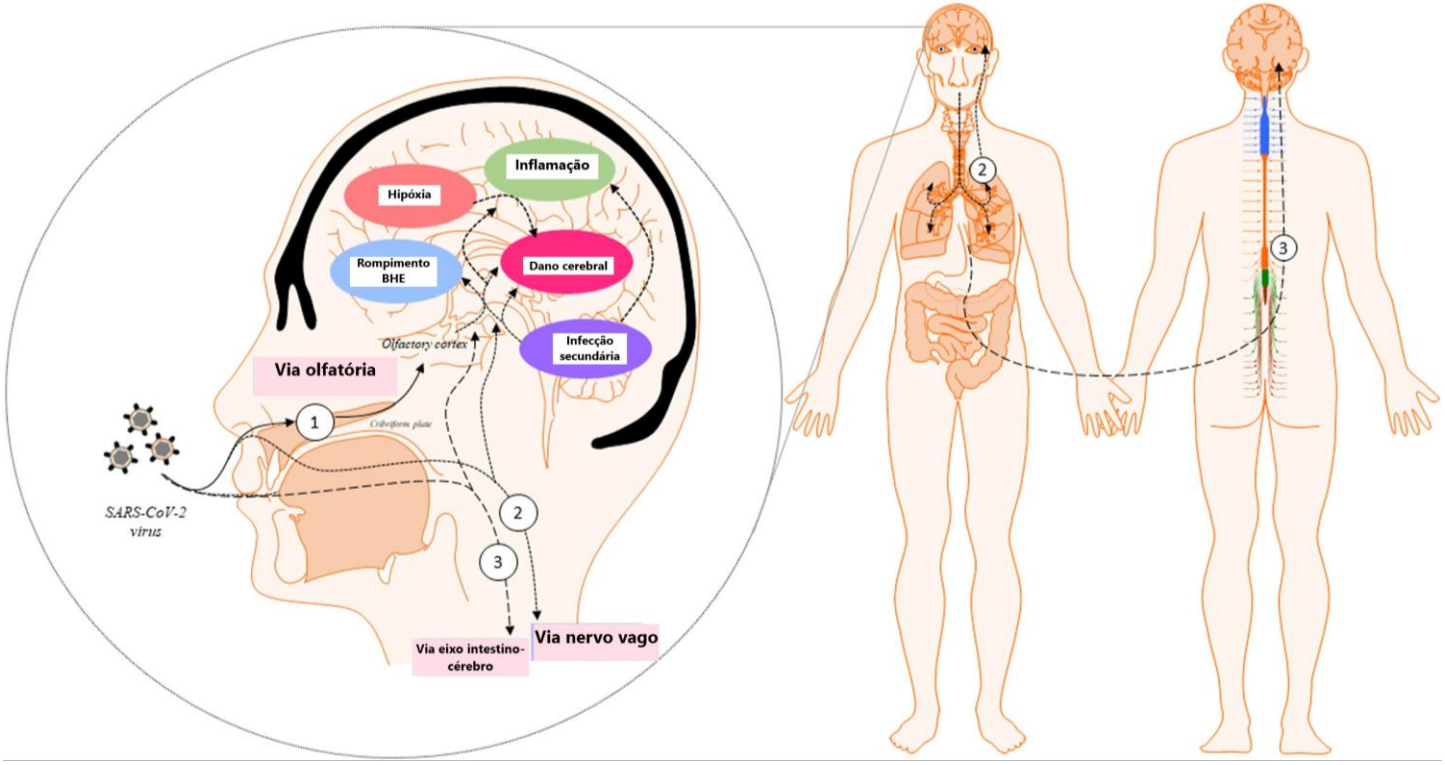

1.3 Neuroinflamação

A neuroinflamação, uma resposta inflamatória do SNC, é desencadeada por diversos estímulos nocivos, incluindo patógenos, isquemia e traumas (Diener et al. 2013). Esse fenômeno denominado neuroinflamação, constitui um processo complexo que envolve a interação dinâmica e a ativação coordenada de diferentes tipos celulares, incluindo neurônios, células da glia e células imunes periféricas (Gilhus & Deuschl, 2019). As respostas neuroinflamatórias são imprescindíveis para a comunicação adequada entre sistema imune e o cérebro, para remodelação tecidual pós-lesão, assim como para o pré-condicionamento imunológico (Almutairi et al., 2021). Todavia, uma neuroinflamação exacerbada e crônica está associada a um recrutamento excessivo de células imunes, ao estresse oxidativo, com consequente neurodegeneração e morte neuronal. O aumento de mediadores inflamatórios, óxido nítrico e a produção de radicais livres são mediados por células ativadas residentes no SNC, principalmente micróglia e astrócitos (Almutairi et al., 2021).

Nesse contexto, a micróglia desempenha um papel central na vigilância imunológica do SNC. Essas células residentes estão envolvidas na produção de mediadores inflamatórios e na execução de atividades que se assemelham às dos macrófagos (DiSabato et al., 2016). Sendo uma das primeiras células a colonizar o SNC, a micróglia se origina de precursores mieloides do saco vitelino durante a embriogênese e têm capacidade de autorrenovação, portanto, não são substituídas por células mieloides da medula óssea em estágios posteriores (Ginhoux et al., 2010). Essas células correspondem aproximadamente a 10% da população do SNC, são de longa duração, com baixa taxa de renovação, cuja reposição, quando necessária, provém de uma fonte progenitora intrínseca ao SNC (Ginhoux et al., 2010). Além de sua conhecida função imune, a micróglia exerce um papel multifacetado na fisiologia cerebral tanto durante o desenvolvimento quanto na vida adulta, pois atua como célula reguladora ao modular a neurogênese, ao interagir com astrócitos, oligodendrócitos e neurônios, ao influenciar a formação e a função das sinapses (Wright-Jin & Gutmann, 2019). A ativação da micróglia e suas atividades buscam manter a homeostase do SNC, no entanto uma ativação exacerbada e/ou crônica ou perda de sua função podem resultar em condições de doenças, como depressão e doenças neurodegenerativas (Norden & Godbout, 2013). Antes vista como um simples “agente” reagente à lesão cerebral, a micróglia é agora reconhecida como um participante ativo na iniciação e progressão de diversas doenças neurológicas, incluindo Alzheimer, tumores cerebrais e autismo (Wright-Jin & Gutmann, 2019).

Assim como a micróglia, os astrócitos são muito importantes para o equilíbrio do ambiente cerebral. São as células gliais mais numerosas do SNC, originando-se a partir da

diferenciação de células-tronco neurais (NSCs), desempenham funções essenciais para a homeostase e a proteção do SNC, como a reciclagem de neurotransmissores, a regulação do equilíbrio iônico, a modulação da sinaptogênese e da transmissão sináptica, além de contribuir para a manutenção da seletividade da barreira hematoencefálica (Volterra & Meldolesi,2005). Em situações patológicas, os astrócitos podem sofrer transformações adquirindo um fenótipo reativo que envolve aumento na expressão de várias moléculas, como a proteína fibrilar glial ácida (GFAP), e aumento do volume celular (T. Li et al., 2019). Ademais, a astrogliose está relacionada à progressão de doenças neurodegenerativas como a Esclerose Lateral Amiotrófica (ELA), Alzheimer e Parkinson, e à perda do controle dos níveis de glutamato, resultando em excitotoxicidade e dano neuronal (Valles et al., 2023). Portanto, os astrócitos com seu papel dual, podem tanto proteger quanto estar diretamente envolvidos na fisiopatologia de diversas doenças neurodegenerativas.

A resposta inflamatória sistêmica pode atingir o SNC por diferentes vias. Uma delas é por via neural, caracterizada pela ativação do nervo vago aferente, que por ter receptores de citocinas e receptores de reconhecimento de padrões (RRPs) reconhecem estímulos viscerais conduzindo-os até o SNC (Janig & Green, 2014). Outra via é a humoral, em que os órgãos circunventriculares e o plexo coróide, locais em que BHE é mais permeável, expressam receptores como o TLR (*Toll-like receptor)* e o CD14 (*cluster of differentiation 14*), assim como receptores de citocinas (Czura e Tracey, 2005) que respondem à insultos da periferia. Além das vias clássicas, Louveau e colaboradores (2015) revelaram a existência de um sistema glinfático no SNC, com vasos localizados nos seios durais que se conectam aos vasos sanguíneos. Essa descoberta sugere uma nova via de acesso ao SNC.

Nos últimos anos, a neuroinflamação emergiu como um dos focos centrais na pesquisa neurocientífica, pois os processos inflamatórios têm demonstrado ser um denominador comum na etiopatologia de uma ampla gama de distúrbios neuropsiquiátricos, tais como a depressão, a esquizofrenia e a doença de Alzheimer (Gilhus & Deuschl, 2019). Alterações neurológicas significativas podem ser diretamente atribuídas à inflamação do SNC, como a esclerose múltipla (EM). Além disso, muitos outros distúrbios cerebrais decorrem de insultos periféricos que alcançam o SNC por meio de intricados mecanismos de comunicação neuroimune, destacando a interconexão entre o sistema imune e o SNC (Gilhus & Deuschl, 2019).

De fato, já foi relatado mudanças na expressão gênica de astrócitos do córtex cerebral e comportamento de anedonia em camundongos após neuroinflamação induzida perifericamente pela endotoxina bacteriana, o lipopolissacarídeo (LPS) (Diaz-Castro et al., 2021). Outro estudo demonstrou que a infecção congênita pelo vírus Zika (ZIKV) estava associada a uma redução do

volume cerebral, ao aumento da neurodegeneração e à redução de neurônios em descendentes adultos nascidos de mães infectadas (Camargos et al., 2019). Por fim, foi demonstrado que o SARS-CoV-2 pode induzir a perda da homeostase do SNC tanto por ação direta quanto mediado pela resposta inflamatória sistêmica associada à infecção aguda (Reza-Zaldívar et al, 2021). A COVID-19 pode, portanto, comprometer a permeabilidade da BHE, visto que mediadores inflamatórios em excesso podem aumentar a permeabilidade da barreira. Tal fato, facilita tanto a entrada do vírus quanto a passagem de mediadores inflamatórios e células do sistema imune para o SNC e ambos os processos atuam na manutenção da neuroinflamação (Coperchini et al., 2020; Matschke et al., 2020).

Estudos recentes mostram que a infecção pelo SARS-CoV-2 pode impactar de forma significativa tanto a micróglia quanto os astrócitos. Evidências apontam que os astrócitos são suscetíveis à infecção pelo vírus e respondem a essa agressão alterando seu metabolismo, o que afeta a produção de metabólitos essenciais para a manutenção dos neurônios. Essa alteração no fenótipo secretor dos astrócitos infectados impacta diretamente a viabilidade neuronal, contribuindo para os danos observados nos cérebros de pacientes com COVID-19 (Crunfli et al., 2022). Também foi observado que o transcriptoma da micróglia no córtex de pacientes com COVID-19 apresentava semelhanças com padrões encontrados em doenças neurodegenerativas, como a Doença de Alzheimer (Mathys et al., 2019; Yang et al.,2021). Além disso, em um modelo murino de COVID-19 leve, demonstraram que a micróglia permanecia ativada mesmo após sete semanas do fim da infecção, sugerindo que essa ativação persistente pode contribuir para os sintomas neurológicos observados na COVID longa (Fernández-Castañeda et al., 2022).

1.4 COVID longa: um novo desafio

A COVID longa pode ser classificada como uma das síndromes de infecção pós-aguda (PAISs) e é frequentemente referida como Sequelas Pós-Agudas da COVID-19 (PASC) (Silva & Iwasaki, 2024). Até o momento, não há um consenso unânime sobre a definição de PASC.

O Centro de Controle e Prevenção de Doenças (CDC) dos Estados Unidos define a COVID longa como a presença de sintomas ou sequelas que persistem por mais de quatro semanas após a infecção inicial pelo SARS-CoV-2 (Datta et al., 2020). Já a OMS conceitua COVID longa como sintomas não atribuíveis a outras causas e estão presentes mais de três meses do início da COVID-19 e duram pelo menos dois meses (WHO, 2021).

Sequelas de longo prazo também foram observadas nas duas epidemias anteriores de CoVs, a SARS em 2003 (Ngai et al., 2010) e a MERS em 2012 (O'Sullivan et al., 2021). A

compreensão da fisiopatologia e dos fatores que predispõem o desenvolvimento das PASC diminuem os impactos socioeconômicos, portanto a OMS e o *Long COVID Forum Group* têm incentivado pesquisas que atuem na melhoria da caracterização clínica, assim como no desenvolvimento de estratégias terapêuticas para esses quadros (Carson, & *Long COVID Forum Group*, 2021).

Um estudo, realizado entre seis de setembro e 25 de novembro de 2020, disponibilizou um questionário em oito idiomas, além do inglês, e os dados foram coletados utilizando a *Qualtrics*, uma plataforma de pesquisa *on-line.* Avaliaram 3.762 participantes que tiveram COVID-19 demonstrando uma prevalência ainda maior de sintomas neurológicos após os primeiros seis meses pós-COVID-19 e os sintomas mais frequentemente relatados incluíram déficits sensório-motores (91%), disfunção cognitiva (85%), distúrbios de humor (88%), distúrbios de sono (79%), cefaleia (77%), comprometimento de memória (73%) e alterações do olfato e/ou paladar (58%). Além disso, desses pacientes 65% relataram persistência dos sintomas neurológicos por período superior a 6 meses, sendo os mais frequentes fadiga (80%), mal-estar pós-esforço (73%) e disfunção cognitiva (58%) (Davis et al., 2021). Outro estudo avaliou 1.733 pacientes após seis meses do diagnóstico laboratorial da COVID-19 e mostrou que 76% deles relataram pelo menos um sintoma neurológico, incluindo fadiga ou fraqueza muscular (63%), distúrbios de sono (26%), alteração do olfato ou paladar (11% e 7%, respectivamente), mialgias (2%) e dor de cabeça (2%), assim como transtornos psiquiátricos, em especial ansiedade e depressão (23%) (Huang et al., 2021). De fato, foi mostrado que as PASC atingem de 10% a 30% das pessoas e que as mulheres são mais suscetíveis (Thompson et al., 2022).

A COVID longa pode ser caracterizada como uma doença multissistêmica fundamentada por vários mecanismos que explicam as sequelas decorrentes da infecção por SARS-CoV-2 (Al-Aly & Topol, 2024). Apesar dos grandes esforços realizados para entender esse legado que a pandemia nos deixou, os potenciais mecanismos envolvidos no processo da PASC ainda são muito especulativos. Vale destacar as principais hipóteses apoiadas pela literatura para explicar as PASC (Figura 3):

Figura 3: Potenciais mecanismos fisiopatológicos relacionados à COVID longa. Os principais fatores hipotéticos envolvidos na fisiopatologia da PASC abrangem: (I) Reservatório viral, (II) Disfunção imune, (III) Coagulopatia/disfunção endotelial, (IV) Autoimunidade e (V) Alteração do microbioma intestinal. Modificado de J. Li et al., 2023.

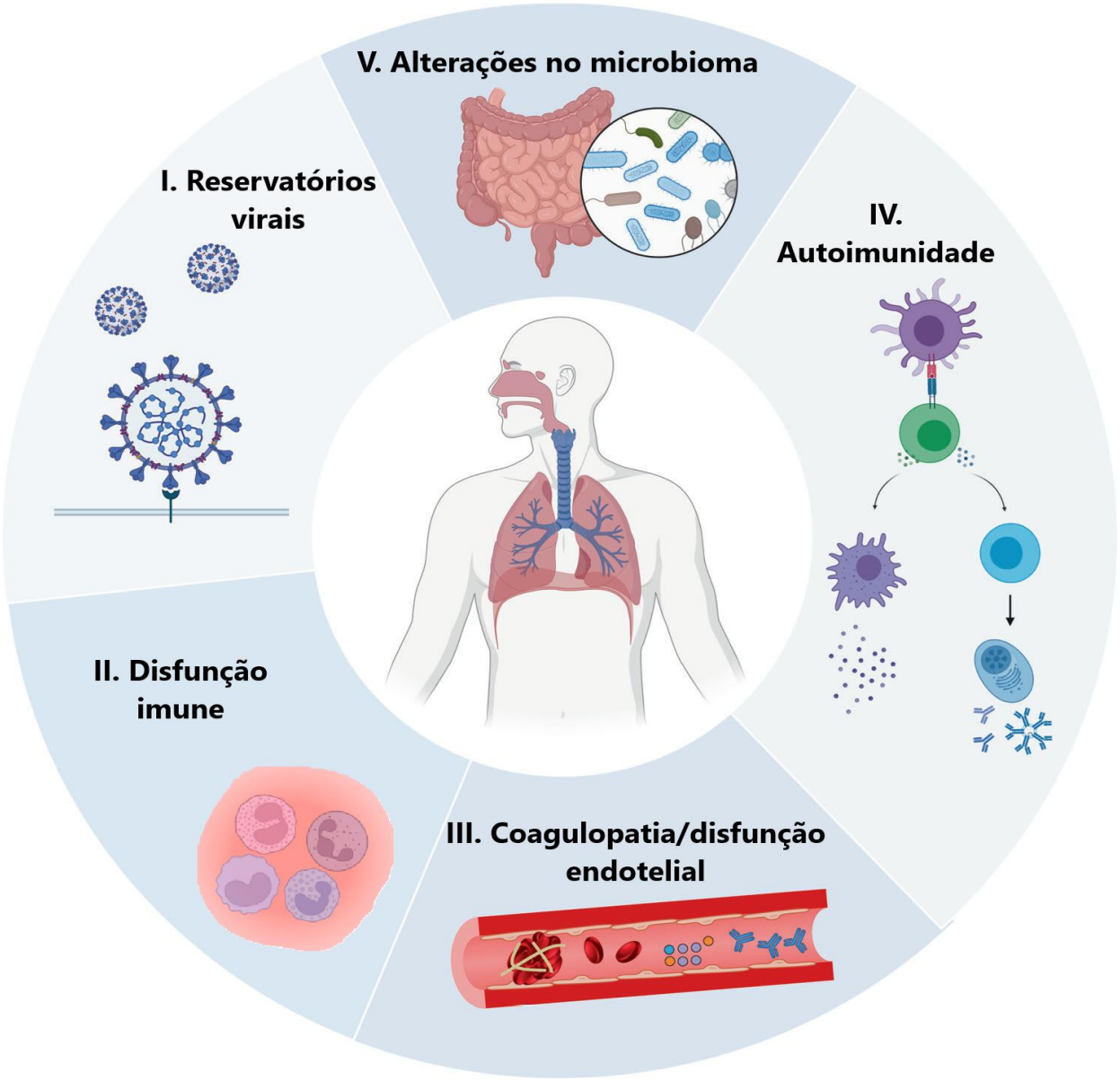

I. Reservatórios virais persistentes

Indivíduos com COVID longa podem não eliminar completamente o SARS-CoV-2 após a infecção inicial, ao contrário, o vírus replicante e/ou o RNA viral, com capacidade de produzir proteínas virais, podem persistir em reservatórios nos tecidos (Proal et al., 2023a). O SARS-CoV-2, um vírus de ssRNA de sentido positivo, compartilha características com outros vírus cuja persistência já foi observada, como o Ebola (Keita et al., 2019; Varkey et al., 2015) e o ZIKV (Paz-Bailey et al., 2017). Esses vírus persistentes têm sido associados ao desenvolvimento de doenças crônicas (Dokubo et al., 2018). Relatos indicam que novos surtos de Ebola foram causados por indivíduos que carregavam o vírus persistente anos após a recuperação (Keita et al., 2021) e o ZIKV pode ser transmitido por via sexual meses após a fase aguda da infecção (Russell et al., 2017).

Um estudo de autópsia identificou RNA e proteínas de SARS-CoV-2 em diversos tecidos, coletados entre 31 e 230 dias após o início dos sintomas da infecção. Mais de 50% dessas autópsias revelaram RNA viral persistente em linfonodos da cabeça, pescoço e tórax, além de tecido ocular, medula espinhal cervical, tronco cerebral e nervo olfatório (Stein et al., 2022). Outro estudo analisou biópsias intestinais de 46 indivíduos com doença inflamatória intestinal, dos quais apenas três haviam sido hospitalizados durante a COVID-19. Os resultados mostraram que 70% dos participantes apresentaram RNA do SARS-CoV-2 na mucosa intestinal sete meses após a infecção. Entre os 21 indivíduos com sintomas pós-COVID, todos tinham RNA viral no intestino, enquanto, dos 25 sem sintomas, 9 apresentaram RNA viral e os outros 14 não tiveram RNA viral detectável (Zollner et al., 2022).

A presença de RNA e/ou proteínas do SARS-CoV-2 em reservatórios no organismo pode desencadear doenças por meio de diversos mecanismos. Os componentes virais persistentes podem se ligar aos RRPs do hospedeiro, induzindo a produção de mediadores inflamatórios e promovendo inflamação; além disso, a ativação constante do sistema imunológico pode comprometer sua atividade efetora, levando à exaustão ou à diferenciação alterada das células imunes (Proal et al., 2023b). Essas alterações podem resultar em disfunções imunológicas e contribuir para o desenvolvimento de patologias associadas às PASC. A replicação viral nos reservatórios pode ter efeito citopático, visto que muitas células expressam receptores para entrada do vírus, o que resulta em danos diretos a diversos tecidos (Proal et al., 2023b).

A permanência do SARS-CoV-2 no SNC pode contribuir para a neuroinflamação e estar associada aos sintomas cognitivos, neurológicos ou psiquiátricos em pessoas com PASC. Um estudo de autópsia revelou aumento na deposição de placas de Aβ no cérebro de pacientes com

COVID-19 grave, com menos de 60 anos (Rhodes et al., 2022). A proteína Aβ, associada à doença de Alzheimer, atua como um peptídeo antimicrobiano na resposta imune inata contra patógenos no tecido cerebral (Proal et al., 2023b). Experimentos *in vitro* e em animais mostraram que a Aβ se acumula em resposta a patógenos, incluindo o vírus herpes simples tipo 1 (HSV-1) (Eimer et al., 2018). Portanto, a persistência de SARS-CoV-2 no SNC ou a reativação de outros patógenos, como herpesvírus, após a COVID-19 podem desencadear processos degenerativos como acúmulo de Aβ, aumentando o risco de Alzheimer (Proal et al., 2023b).

Por outro lado, as proteínas do SARS-CoV-2 podem modular negativamente a resposta imune inata do hospedeiro, desativando essas respostas em vez de induzi-las (Rashid et al., 2022). Além disso, essas proteínas podem desregular fatores metabólicos, epigenéticos e genéticos do hospedeiro, contribuindo para o surgimento de sintomas, mesmo na ausência de efeitos citopáticos diretos (Kee et al., 2022). Muitas são as evidências, no entanto há a necessidade de mais pesquisas para compreender os mecanismos subjacentes à persistência viral e sua relação com os sintomas de longo prazo.

II. Disfunção imune

Os indivíduos com COVID longa apresentam algumas diferenças imunológicas em relação às que se recuperaram completamente. Entre elas, destaca-se uma menor proporção de células T $CD8^+$ de memória específicas, produtoras de interferon gama (IFN-γ^+), em indivíduos com sintomas persistentes (Peluso et al., 2021). Schultheiß et al. (2022) identificaram que as PASC estão associadas a níveis elevados de citocinas inflamatórias, como IL-1β, IL-6 e TNF, sem relação direta com autoanticorpos (AABs). Além disso, Fernández-Castañeda et al. (2022) relataram níveis aumentados da quimiocina CCL11 (eotaxina) no sangue de indivíduos com comprometimento cognitivo relacionado à COVID longa, e esses níveis diminuíram conforme os sintomas cognitivos foram resolvidos.

Um estudo recente desenvolvido por Visvabharathy e colaboradores (2023) identificou um padrão distinto de ativação de células T em pacientes com Neuro-PASC. Demonstraram que pacientes com Neuro-PASC apresentam: (i): Respostas elevadas de IFN-γ ao domínio C-terminal da proteína N (região N3), enquanto os controles convalescentes mostraram pouca reatividade a essa região. Embora um aumento nas respostas de células T antivirais geralmente seja visto como protetor, estudos têm encontrado associações contraditórias entre essas respostas de células T e os desfechos clínicos da COVID-19; (ii): Resposta atenuada de células T $CD8^+$ de memória, o que prejudica a geração eficaz de respostas efetoras para proteger contra futuras reinfecções; (iii)

Maior expressão de IL-6, citocina que foi correlacionada com a dor relatadas pelos pacientes. De fato, níveis elevados de IL-6 sérica foram associados a piores prognósticos em pacientes com COVID-19 grave (Weiskopf et al., 2020). A IL-6 também esteve associada à fadiga e ao comprometimento cognitivo em uma coorte de pacientes com PASC que apresentaram infecção aguda leve (Schultheiß et al., 2022). (iv): Níveis significativamente elevados de ansiedade, depressão e dor foram observados em comparação aos controles convalescentes. A gravidade desses déficits correlacionou-se com respostas imunológicas adaptativas antivirais; Por fim, (v): assinaturas de resposta inflamatória e antiviral reduzidas em comparação com controles convalescentes, concomitantes à elevação de proteínas imunorreguladoras.

Ainda, outros estudos sugerem que a desregulação do sistema imune também pode estar associada à reativação de vírus que se encontram em estado latente no organismo. Um estudo reforça a associação entre a positividade de anticorpos contra o vírus Epstein-Barr (EBV) e os sintomas de COVID longa (Peluso et al., 2023). Também já foi demonstrado que mulheres com PASC apresentam, em sua maioria, níveis elevados de anticorpos contra herpesvírus, como EBV, CMV e HSV-2 (Klein et al., 2023). De forma semelhante, Silva e colaboradores (2024) observaram títulos elevados de IgG contra antígenos do EBV em mulheres com COVID longa, indicando uma possível reativação recente do vírus. O papel da reativação do EBV na PASC ainda não está completamente elucidado, entretanto foi sugerido que a replicação lítica do vírus pode aumentar a expressão de ECA-2 em células epiteliais, facilitando a entrada do SARS-CoV-2 nas células hospedeiras (Verma et al., 2021).

III. Coagulopatia/disfunção endotelial

Eventos trombóticos potencialmente fatais e consequentes manifestações neurológicas são frequentemente observados em pacientes com COVID-19, persistindo em muitos casos mesmo após a fase aguda da infecção (Tang et al., 2020). Apesar da ampla documentação clínica sobre esses fenômenos, os mecanismos responsáveis pela coagulopatia associada à COVID-19 e suas implicações na inflamação e na neuropatologia ainda não estão completamente elucidados.

Uma pesquisa envolvendo mais de 150 mil sobreviventes de COVID-19, incluindo casos não hospitalizados, hospitalizados e tratados em UTI, revelou que, após um ano, mesmo aqueles que não necessitaram de internação durante a fase aguda da doença apresentam um risco elevado de desenvolver distúrbios cardiovasculares. Além disso, sobreviventes que foram

hospitalizados enfrentam uma carga significativa após um ano, marcada por um aumento na incidência de trombose venosa profunda (TVP) e embolia pulmonar (EP) (Xie et al., 2022).

O fibrinogênio, uma proteína essencial na formação de coágulos sanguíneos, tem sido encontrado em grandes quantidades nos pulmões e no cérebro de pacientes infectados, apresentando uma forte correlação com a gravidade da doença; além disso, ele tem sido apontado como um biomarcador útil para prever déficits cognitivos pós-COVID-19 (J. K. Ryu et al., 2024). Nesse sentido, demonstraram que a fibrina derivada do fibrinogênio, interage diretamente com a proteína *spike* do SARS-CoV-2, resultando na formação de coágulos sanguíneos que contribuem para a tromboinflamação sistêmica, assim como desempenham um papel significativo na neuropatologia observada em pacientes com COVID-19 (J. K. Ryu et al., 2024). Após a infecção pelo SARS-CoV-2, a fibrina também intensifica a neuroinflamação e a perda neuronal, além de desencadear respostas imunes inatas tanto no cérebro quanto nos pulmões, mesmo na ausência de infecção ativa (J. K. Ryu et al., 2024). Interessantemente, nesse estudo utilizaram um anticorpo monoclonal que bloqueia o domínio inflamatório da fibrina, e este se mostrou eficaz em proteger contra a ativação da micróglia, danos neuronais e a tromboinflamação pulmonar após a infecção.

Um estudo adicional explorou os mecanismos subjacentes à disfunção vascular provocada pelos betacoronavírus MHV-3 e SARS-CoV-2. A pesquisa revelou uma redução da contratilidade em grandes artérias e veias, resultando em insuficiência circulatória e óbito. Esse processo foi associado à via TNF/iNOS/NO, destacando o papel crítico do endotélio vascular e do TNF na patogênese e na gravidade das infecções por coronavírus (Vieira-Alves et al., 2023). Diversas hipóteses foram sugeridas para explicar o estado de hipercoagulação persistente observado em sobreviventes da COVID-19. Entre elas, destacam-se a inflamação não resolvida, a geração de AABs e a possível presença de reservatórios virais ou fragmentos de RNA e proteínas virais, capazes de ativar leucócitos e plaquetas, perpetuando a resposta inflamatória. Independentemente do estímulo subjacente, indivíduos com PASC apresentam tromboinflamação persistente, sustentada pela ativação contínua de células endoteliais e plaquetas, além de uma formação exacerbada de coágulos de fibrina (Martins-Gonçalves et al., 2023).

IV. Autoimunidade

Os vírus possuem a notável capacidade de modular o sistema imunológico humano, como exemplificado pelo citomegalovírus (CMV) e pelo EBV, frequentemente associados ao

desenvolvimento de doenças autoimunes (Chang et al., 2023). O EBV é o agente etiológico da mononucleose infecciosa, pode estar associado a certos tipos de câncer e graves doenças linfoproliferativas, sendo capaz de estabelecer infecção permanente, geralmente assintomática, em mais de 90% da população adulta global (Fonseca et al., 2023). O EBV é considerado como um gatilho da esclerose múltipla (EM), visto que em uma ampla coorte de mais de 10 milhões de militares do exército dos EUA, foi identificado um aumento de 32 vezes de EM entre indivíduos que se tornaram soropositivos para o EBV, em comparação com aqueles que permaneceram soronegativos (Bjornevik et al., 2022). A EM é uma condição crônica do SNC, mediada pelo sistema imune, marcada por áreas de desmielinização e processos neurodegenerativos (Bellucci et al., 2021) e, nesse contexto, a contribuição do EBV é relacionada à reatividade cruzada entre seus antígenos e as proteínas do próprio organismo, envolvendo mecanismos tanto da imunidade celular quanto da imunidade humoral (Soldan & Lieberman, 2023). Na COVID-19 grave foram observadas algumas vias imunológicas desreguladas que coincidem com alterações típicas da EM, sugerindo que o SARS-CoV-2 pode representar um fator de risco para o surgimento ou a piora da EM em indivíduos suscetíveis (Fonseca et al., 2023).

A infecção pelo SARS-CoV-2 tem sido vinculada a um risco aumentado de outras condições autoimunes, incluindo diabetes mellitus tipo 1 (DM1), lúpus eritematoso sistêmico (LES), artrite reumatoide, diversas formas de vasculite e doenças inflamatórias intestinais (Antar & Cox, 2024). Os mecanismos exatos que sustentam a relação entre infecção viral e doenças autoimunes permanecem desconhecidos. Estudos sugerem que os vírus podem induzir autoimunidade por diversos processos, como mimetismo molecular (B. Kim et al., 2006), disseminação de epítopos (Getts et al., 2013) e ativação de células espectadoras (Fujinami et al., 2006). Supõe-se que a inflamação prolongada observada na COVID-19 possa ativar o sistema imunológico, levando à produção de anticorpos direcionados a antígenos virais estruturalmente semelhantes a autoantígenos, resultando em respostas cruzadas tanto contra autoantígenos quanto contra outros antígenos (Chang et al., 2023). Além disso, o surgimento de condições autoimunes após a COVID-19 pode ser associado à imunossupressão temporária, que compromete a auto tolerância, e a uma reconstituição imunológica inadequada em indivíduos predispostos à autoimunidade (Cañas, 2020).

A geração de AABs durante a infecção aguda por SARS-CoV-2 também está associado ao desenvolvimento de autoimunidade. A produção de anticorpos é uma mecanismos natural que ocorre em resposta às infecções, no entanto os AABs resultam da ativação de espectadores ou de mimetismo molecular (Zhao et al., 1998). Diversos AABs com potencial patológico foram

identificados durante a COVID-19 (Wang et al., 2021). mas, normalmente, os níveis de AAB tendem a diminuir conforme o sistema imune retorna à homeostase (Woodruff et al., 2022). Todavia, vários estudos retrospectivos demonstraram que pacientes com COVID-19 apresentam um risco de 20 a 40% maior de desenvolver diversas doenças autoimunes após a infecção (Peng et al., 2023; Syed et al., 2023; Tesch et al., 2023). Nesse contexto, uma pesquisa identificou a presença de anticorpos antinucleares (ANAs) relacionados a sintomas persistentes de COVID-19 até 12 meses após a infecção inicial (Son et al., 2023). Outro estudo constatou que AABs direcionados a diversos receptores acoplados à proteína G (GPCRs) estavam presentes em todos os 31 participantes diagnosticados com COVID longa, sendo que esses padrões de ABBs já foram observados em déficits neurológicos e em doenças cardiovasculares independentes da COVID-19 (Wallukat et al., 2021).

Um estudo recente revelou níveis elevados de AABs direcionados às proteínas do SNC em pacientes com COVID longa, correlacionando-os com os sintomas neurológicos e cognitivos observados nesses indivíduos. Além disso, os pesquisadores demonstraram que a injeção de IgG purificada desses pacientes em camundongos resultou em maior sensibilidade à dor, bem como em perda de equilíbrio e coordenação, reproduzindo os sintomas relatados pelos pacientes (Sa et al., 2024).

V. Alterações no microbioma

A COVID-19 pode causar alterações significativas e persistentes no microbioma intestinal, em parte devido à elevada expressão de ECA-2 no TGI, o que facilita a entrada do SARS-CoV-2 em células epiteliais intestinais, afetando organismos comensais benéficos (Yeoh et al., 2021). A infecção nessas células pode desencadear inflamação tecidual, morte celular e danos às barreiras intestinais, além de outros tecidos. Esses processos podem levar à translocação de microrganismos para a corrente sanguínea, resultando em uma resposta inflamatória sistêmica (Peluso & Deeks, 2024). Foram detectados níveis elevados de biomarcadores de translocação microbiana, como zonulina (proteína reguladora da permeabilidade do epitélio intestinal), beta-D-glucana (componente da parede celular de fungos) e proteína de ligação a LPS (componente da parede celular bacteriana) no sangue de indivíduos com COVID longa, em comparação com aqueles que se recuperaram completamente (Giron et al., 2022). Em Hong Kong, um ensaio clínico analisou o potencial da modulação do microbioma intestinal como tratamento para a COVID longa. Os participantes que utilizaram uma preparação simbiótica relataram melhorias significativas em sintomas associados à PASC, como redução da fadiga, melhora na

concentração e memória, alívio de distúrbios gastrointestinais e diminuição do mal-estar geral, quando comparados ao grupo placebo (Lau et al., 2024).

Um outro estudo revelou que a microbiota intestinal de indivíduos pós-COVID é dominada por bactérias da família *Enterobacteriaceae* com resistência a antibióticos, em comparação a controles saudáveis. O transplante fecal desses indivíduos para camundongos *germ-free* resultou em inflamação pulmonar e pior evolução na infecção por *Klebsiella pneumoniae* multirresistente. Além disso, os camundongos pós-COVID apresentaram déficits de memória em testes de reconhecimento e localização, acompanhados por níveis elevados de mRNA de *tnf* no hipocampo e redução de fatores neuroprotetores como *bdnf* e *psd-95*. Como prova de conceito, administraram um probiótico, o *Bifidobacterium longum*, em camundongos infectados pelo betacoronavírus MHV-3, e observaram que o tratamento preveniu o comprometimento de memória induzido pela infecção (Mendes de Almeida et al., 2023).

1.4.1 Sexo biológico e a relação com a COVID-19/COVID longa

Desde a epidemia de SARS-CoV em 2002–2003, ficou claro que os homens apresentam maior vulnerabilidade a doenças pulmonares agudas, uma tendência reforçada durante a pandemia de SARS-CoV-2, que revelou uma maior taxa de letalidade entre o público masculino (Scully et al., 2020). Por outro lado, as mulheres têm três vezes mais chance de desenvolver PASC em comparação aos homens, no entanto a gravidade da doença, assim como o tempo para resolução da fase viral aguda não foram associados à COVID longa (Bai et al., 2021). Esses padrões têm sido associados a diferenças na imunidade e influenciados pela produção de hormônios sexuais, além de variações na resposta imune relacionadas ao cromossomo X (Channappanavar et al., 2017).

De forma semelhante à PASC, outras síndromes de infecção pós-aguda (PAISs), como encefalomielite miálgica/síndrome da fadiga crônica (ME/CFS) e doença de Lyme longa, apresentam uma predominância feminina ainda mais acentuada, com até 80% dos casos ocorrendo em mulheres (Choutka et al., 2022). A análise da assinatura imunológica na COVID longa revelou um perfil distinto entre homens e mulheres. Em homens, essa assinatura se associou a um aumento significativo de sintomas como fadiga, distúrbios de humor, ansiedade, dor e comprometimento neurológico. Curiosamente, mulheres com uma assinatura imunológica mais similar à dos homens apresentaram uma menor carga sintomática (Silva et al., 2024). Esses resultados sugerem que a assinatura imunológica feminina, em particular, pode ser um fator

contribuinte para a maior intensidade e variedade de sintomas relatados por mulheres com COVID longa.

O sexo biológico afeta as respostas imunes inatas e adaptativas, conduzindo a diferenças sexuais na autoimunidade, assim como em respostas a infecções e vacinas (Klein & Flanagan, 2016). O estrógeno, em particular, desempenha um papel crucial na regulação do sistema imunológico, com diversos estudos destacando sua capacidade de suprimir respostas inflamatórias. No entanto, algumas pesquisas sugerem que os estrogênios podem exercer efeitos pró-inflamatórios ou até mesmo duplos (pró- e anti-inflamatórios), dependendo do tipo de citocina ou célula envolvida (Dragin et al., 2017). A ovariectomia, frequentemente utilizada em modelos murinos para modular a ação do estradiol produzido pelas gônadas, é um método eficaz para estudar esse hormônio, que também pode ser sintetizado em tecidos secundários, como cérebro, rim, osso, pele e tecido adiposo, ainda que em quantidades reduzidas (Harding & Heaton, 2022).

Em relação à COVID-19, Ding e colaboradores (2021) identificaram que o estradiol (E2) pode exercer um efeito protetor em mulheres, regulando citocinas associadas à gravidade da infecção (Ding et al., 2021). Além disso, níveis elevados do hormônio folículo estimulante (FSH) foram observados em mulheres durante a infecção por SARS-CoV-2 (Cai et al., 2022), porém os mecanismos que explicam a alteração do FSH na fase aguda e na COVID longa permanecem pouco explorados.

A testosterona, por sua vez, é outro hormônio de relevância devido às suas propriedades imunossupressoras. Em mulheres, níveis reduzidos de testosterona podem contribuir para uma maior predisposição a doenças autoimunes (Bupp & Jorgensen, 2018). Como os receptores de andrógenos são expressos em células do sistema imunológico, acredita-se que os níveis de testosterona desempenhem um papel direto na modulação dos perfis imunológicos individuais (Bupp & Jorgensen, 2018). Em homens, baixos níveis de testosterona têm sido associados a piores desfechos clínicos na COVID-19 (Schroeder et al., 2021). Paralelamente, as mulheres parecem mais suscetíveis à COVID longa devido à redução nos níveis de testosterona (Silva et al., 2024).

1.5 Coronavírus da hepatite murina (MHV) como potencial modelo para estudo da infecção pelo SARS-CoV-2

O gênero betacoronavírus é composto por quatro subgêneros. O subgênero *Embecovirus* abriga os MHV e o subgênero *Sarbecovirus* inclui os SARS-CoV e SARS-CoV-2 (ICTV, 2019).

Consistente com outros estudos (Yang et al., 2014; Andrade et al., 2021; S. Ryu et al., 2021; Lima et al., 2024), o MHV imita efetivamente a infecção pelo SARS-CoV-2, reproduzindo aspectos-chave da COVID-19 humana, como replicação viral, patogênese, respostas imunes pulmonares e extrapulmonares e o amplo espectro de manifestações clínicas (Figura 4) (Körner et al., 2020). A principal distinção entre MHV e SARS-CoV-2 está no receptor usado para entrada celular: as cepas de MHV utilizam a molécula de adesão CEACAM-1 (*Carcinoembryonic Antigen-Related Cell Adhesion Molecules 1*), enquanto o SARS-CoV-2 depende da enzima ECA-2 (Körner et al., 2020). Essa diferença pode representar desafios para estudar mecanismos de entrada viral e avaliar medicamentos direcionados a esse estágio do ciclo de replicação.

Várias cepas de CoVs que infectam camundongos induzem doenças hepáticas, respiratórias ou entéricas e são acompanhadas por alterações neurológicas (Cowley & Weiss, 2010). Por exemplo, o MHV-3 e o MHV-A59 se replicam inicialmente no epitélio nasal, com viremia subsequente e disseminação para os pulmões, fígado, medula óssea, cérebro, tecido linfoide e órgãos reprodutores (Homberger et al., 1998). No entanto, diferenças importantes em relação às manifestações da doença induzida por estas duas linhagens podem ocorrer. Enquanto o MHV-3 induz uma infecção inicialmente pulmonar seguida de disseminação sistêmica, com alto tropismo pelo fígado e elevada morbimortalidade dos animais, quadro semelhante a uma COVID-19 grave (Andrade et al., 2021), a infecção pelo MHV-A59 induz uma doença majoritariamente pulmonar e autolimitada (Yang et al., 2014). O MHV-A59 é uma cepa hepato-neurotrópica que causa hepatite aguda, meningoencefalomielite, neurite óptica e infecção persistente no SNC (Das Sarma et al., 2000). Outras cepas, como o MHV-2, também apresentam tropismo pelo fígado, entretanto é capaz de invadir o SNC de forma limitada, podendo induzir meningite sem causar encefalite (Das Sarma et al., 2010). Sobretudo o MHV-JHM é altamente neurotrópico, capaz de provocar encefalite grave e desmielinização, sem tropismo para o fígado (Bergmann et al. 2006).

Desde a descoberta do SARS-CoV, o MHV tem sido utilizado como modelo de infecção para entender a SARS e seus desdobramentos, já que sua manipulação requer contenção em nível de biossegurança 2 (NB-2), em contraste com a necessidade de contenção de nível de biossegurança 3 (NB-3) para SARS-CoV e SARS-CoV-2 (Körner et al., 2020). Este é um aspecto muito importante, pois muitos laboratórios de pesquisa não têm infraestrutura e recursos para manter instalações NB-3. Ryu et al. (2021) utilizaram o MHV-A59 para investigar a resposta imune relacionada ao envelhecimento durante a infecção por coronavírus e exploraram o impacto de uma dieta cetogênica pró-longevidade (KD) na vigilância imunológica. A inoculação

intranasal com MHV-A59 em camundongos idosos levou ao aumento da mortalidade e inflamação sistêmica, incluindo neutrofilia e depleção de células T γδ nos pulmões. A ativação da cetogênese expandiu as células T γδ protetoras do tecido, desativou o inflamassomao NLRP3 e reduziu os monócitos patogênicos nos pulmões de camundongos idosos infectados (Ryu et al., 2021)

Para mimetizar os sintomas da COVID-19, camundongos transgênicos expressando ECA-2 humana (hECA-2) sob vários promotores foram usados (Bao et al., 2020; Seo et al., 2022). No entanto, muitos desses modelos transgênicos falham em capturar o espectro completo da COVID-19, particularmente as manifestações extrapulmonares e seus sintomas persistentes (Knight et al., 2021). Isso acontece principalmente porque a expressão da ECA-2 é frequentemente restrita às células epiteliais nesses modelos, como visto com o promotor k18 (Fan et al., 2022; Knight et al., 2021). Nesse contexto, desenvolver modelos novos e diversos é fundamental para abordar essas limitações e progredir (Fan et al., 2022; Muñoz-Fontela et al., 2022).

Figura 4: Principais similaridades e diferenças na patogênese do vírus da hepatite murina (MHV) e o coronavírus da síndrome respiratória aguda grave 2 (SARS-CoV-2). Adaptado de (Körner et al., 2020).

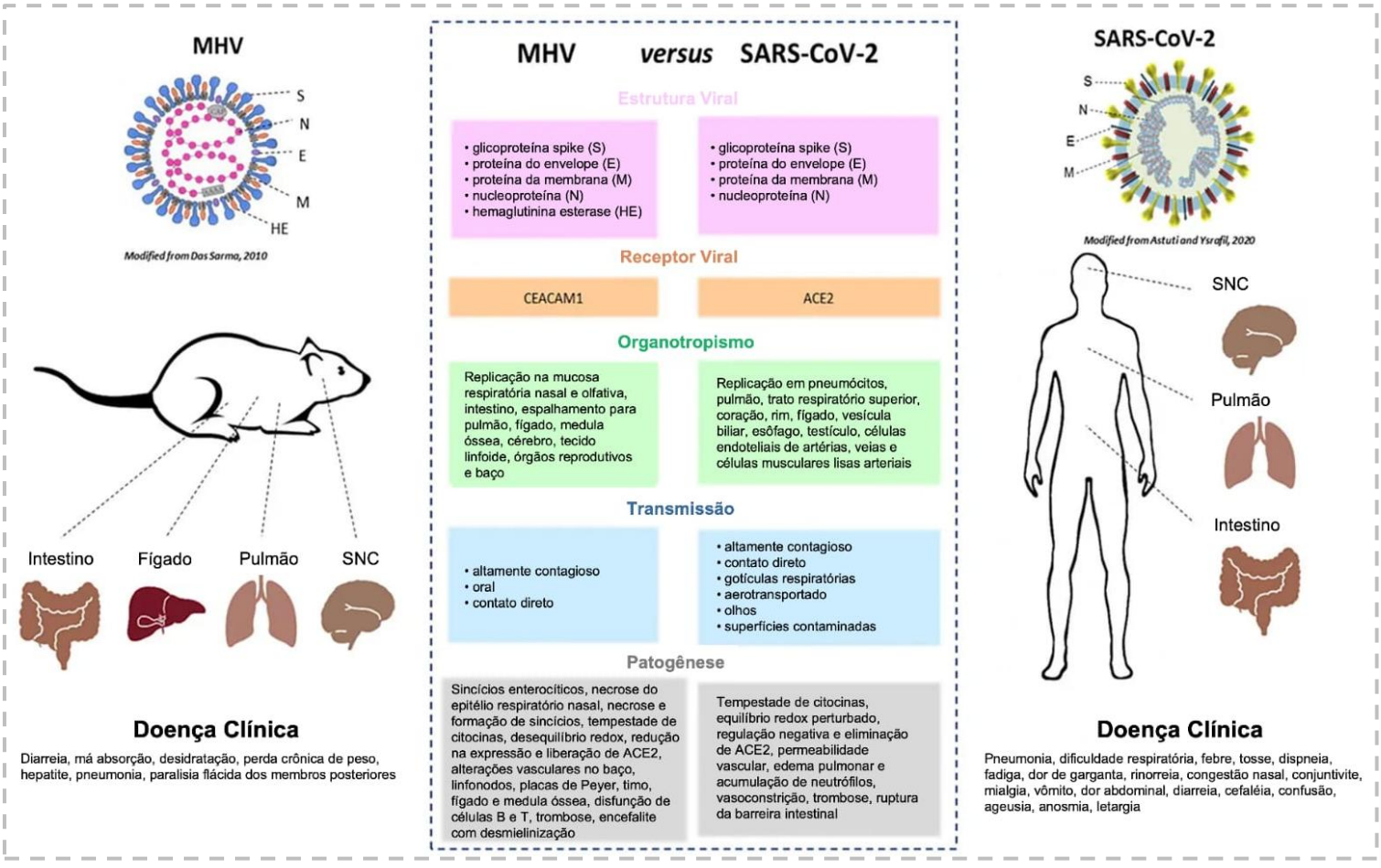

1.6 Intervenções farmacológicas

A fase aguda da COVID-19, especialmente a doença grave, é caracterizada por alta replicação viral e uma resposta inflamatória exacerbada (Merad et al., 2022). Antivirais, anti-inflamatórios e anticoagulantes são usados para controlar a COVID-19 aguda grave (Braz-de-Melo et al., 2021). Até o momento, alguns antivirais de moléculas pequenas, como nirmatrelvir-ritonavir, remdesivir e molnupiravir, além de 11 anticorpos monoclonais, foram aprovados para o tratamento da COVID-19(G. Li et al., 2023). Pacientes hospitalizados com COVID-19 grave também podem ser tratados com agentes imunomoduladores previamente aprovadas, como glicocorticoides (ex.: dexametasona), antagonistas de citocinas (ex.: tocilizumabe) e inibidores da Janus quinase (ex.: baricitinibe) (G. Li et al., 2023).

Dexametasona e hidrocortisona, ambos glicocorticoides, são corticosteroides recomendados principalmente para pacientes hospitalizados com COVID-19 que requerem suporte de oxigênio (Bhimraj et al., 2020). A dexametasona foi o primeiro glicocorticoide a apresentar benefícios clínicos em casos graves da doença. Nos estágios iniciais da pandemia, o estudo RECOVERY demonstrou que esse medicamento reduziu significativamente a mortalidade em pacientes que necessitavam de suporte respiratório (RECOVERY Collaborative Group, 2021). Além disso, a dexametasona, isoladamente ou em combinação com tocilizumabe e antivirais, mostrou-se eficaz no tratamento de formas moderadas a graves de COVID-19 (Alunno et al., 2022). Contudo, não foram observados benefícios em pacientes internados que não precisavam de suporte respiratório (RECOVERY Collaborative Group, 2021), e seu uso pode aumentar o risco de eventos adversos graves relacionados ao medicamento em casos de COVID-19 grave (Wolfe et al., 2022).

A rápida resposta global com o desenvolvimento de vacinas contra a COVID-19 e o reposicionamento de fármacos foi um avanço sem precedentes. No entanto, a identificação de tratamentos eficazes para a Covid Longa tem sido um processo mais lento. Já existem relatos que apontam para um possível alívio dos sintomas pós-COVID após a vacinação contra o SARS-CoV-2 (Arnold et al., 2021), mas um número significativo de pessoas não observou nenhuma mudança (Nakagawara et al., 2023).

A hipótese de que a replicação viral contínua seja um fator causal da Covid Longa tem sido investigada em ensaios clínicos com medicamentos antivirais em pacientes com a doença em estágio crônico. O ensaio clínico controlado randomizado, duplo-cego, STOP-PASC avaliou a eficácia do nirmatrelvir-ritonavir, no qual 155 adultos com pelo menos dois sintomas moderados a graves autorrelatados foram randomizados para utilizar 15 dias de nirmatrelvir-

ritonavir oral (Paxlovid) ou placebo-ritonavir (100 mg) duas vezes ao dia. Os resultados demonstraram que o tratamento, embora seguro, não foi capaz de melhorar significativamente os sintomas de longo prazo, apesar de um leve alívio durante as 15 semanas em que as pessoas foram acompanhadas (Geng et al., 2024).

A escassez de estudos relacionados a terapias para COVID Longa é uma lacuna significativa na pesquisa. Um estudo recente, randomizado e duplo-cego, avaliou a eficácia do probiótico SIM01 em reduzir os sintomas da PASC. Os resultados indicaram que os participantes que receberam SIM01 apresentaram menor frequência de fadiga, dificuldades cognitivas, dor, insônia e problemas gastrointestinais em comparação ao grupo placebo (Lau et al., 2024). Em um pequeno ensaio clínico randomizado e controlado, 41 pacientes com Covid Longa foram tratados com AXA1125, um modulador metabólico endógeno que visa melhorar a função mitocondrial e reduzir o stress oxidativo. Embora tenha sido observado um número moderado de eventos adversos leves, os participantes do grupo de tratamento apresentaram uma melhora estatisticamente significativa nos sintomas de fadiga em comparação com o grupo placebo (Finnigan et al., 2023). Em contrapartida, dois ensaios clínicos controlados não demonstraram eficácia na redução dos sintomas da Covid Longa após o uso de coenzima Q10 por 6 semanas (Hansen et al., 2022) ou da estimulação transcraniana do córtex pré-frontal (Klírová et al., 2024). Nesse contexto, busca-se compreender se o manejo clínico precoce da COVID-19 pode influenciar o surgimento e a gravidade dos sintomas de longo prazo, característicos da PASC.

O Sistema Renina-Angiotensina (SRA) está presente no SNC e desempenha funções importantes que vão além do sistema renal e cardiovascular (Paul et al., 2006). O SRA é composto por dois eixos principais, sendo a Angiotensina (1-7) [Ang-(1-7)] componente do eixo contrarregulador que inclui a ECA-2 e o receptor Mas. Evidências de estudos clínicos e experimentais indicam que desequilíbrios no SRA cerebral estão associados ao desenvolvimento e à progressão de doenças neurodegenerativas (Kangussu et al., 2022).

A literatura já vem mostrando que a Angio (1-7) pode atuar como neuroprotetor em vários processos patológicos do SNC. Janatpour e colaboradores (2019) mostraram que administração subcutânea de Angio (1-7) melhora a recuperação de camundongos após lesão cerebral., visto que atenuou os déficits motores e a histologia cerebral juntamente com a ressonância magnética indicaram que os camundongos tratados apresentaram volumes menores nas lesões. Além disso, observaram que o tratamento reduziu a microgliose, a astrogliose e reduziu a perda neuronal (Janatpour et al., 2019). Outro estudo investigou o papel da Angio (1-7) na doença de Parkinson, em que o tratamento com esse peptídeo amenizou as alterações comportamentais, evidenciado pelo aumento da atividade locomotora no teste de campo aberto e aumento da latência no teste

de Rotarod, em comparação ao grupo que não recebeu o tratamento. Além disso, a intervenção demonstrou efeitos neuroprotetores, como a preservação de neurônios dopaminérgicos e a redução da expressão de α-sinucleína na substância negra de camundongos com Parkinson (Gao et al., 2024)

O peptídeo endógeno Angio (1-7) e os agonistas de seu receptor Mas foram sugeridos como moléculas promissoras para limitar a inflamação induzida por SARS-CoV-2 (Lobo et al., 2024; Sousa et al., 2020). Durante a infecção pelo SARS-CoV-2 os níveis de Ang (1-7) são reduzidos, uma vez que a ECA-2, responsável pela conversão da angiotensina II em Angio (1-7), é regulada negativamente após a entrada do vírus (Issa et al., 2021). Portanto, lesão pulmonar grave e alta carga viral em pacientes com COVID-19 têm sido associadas a altos níveis de angiotensina II e redução de Angio (1-7), uma molécula anti-inflamatória e vasodilatadora (Miesbach, 2020).

2. OBJETIVO GERAL

Avaliar as possíveis alterações neuroquímicas e comportamentais resultantes da infecção por coronavírus.

2.1 OBJETIVOS ESPECÍFICOS

I. Caracterizar as alterações celulares e morfológicas agudas no SNC decorrentes da infecção pelo MHV-3;

II. Investigar as alterações neuroquímicas e inflamatórias agudas no SNC induzidas pela infecção pelo MHV-3;

III. Investigar a ocorrência de alterações comportamentais durante a fase aguda da infecção pelo MHV-3;

IV. Implementar um modelo de COVID longa utilizando o coronavírus murino MHV-A59 como plataforma para investigar as alterações/sequelas neuropsiquiátricas de longo prazo decorrentes da infecção;

V. Avaliar como intervenções terapêuticas (antiviral e anti-inflamatória) na fase aguda da infecção podem repercutir nas sequelas neuropsiquiátricas no modelo de COVID longa.

3. ARTIGOS RESULTANTES DA TESE

3.1 Trabalho científico I:

"A suitable model to investigate acute neurological consequences of coronavirus infection"

O presente artigo explora os impactos neurológicos agudos desencadeados pela infecção por coronavírus, utilizando um modelo experimental murino. A pesquisa teve como objetivo avaliar os efeitos neuroquímicos, comportamentais e histológicos associados à infecção aguda pelo vírus MHV-3, um betacoronavírus. Para tanto, foram utilizados camundongos C57BL/6, machos e fêmeas, infectados por via intranasal com o MHV-3, sendo todas as análises realizadas até o 5° dpi.

O estudo empregou uma abordagem integrada que incluiu testes comportamentais, análises histológicas e ensaios bioquímicos. Entre as análises destacam-se a quantificação de mediadores inflamatórios e neuroprotetores (IL-6, IFN-γ, TNF, BDNF e CX3CL1) por ELISA, a análise de sinaptossomas para avaliar a liberação de glutamato e os níveis intracelulares de cálcio, bem como testes comportamentais, como campo aberto, labirinto em cruz elevado e teste de nado forçado.

Os resultados revelaram alterações neuroquímicas significativas, incluindo aumento nos níveis de glutamato e cálcio intracelular. Paralelamente, observou-se elevação de citocinas pró-inflamatórias (IL-6 e IFN-γ) no córtex cerebral, especialmente em fêmeas, e redução de mediadores neuroprotetores como BDNF e CX3CL1 em camundongos infectados. As análises histológicas demonstraram sinais de degeneração neuronal no córtex cerebral e alterações celulares, conforme indicaram os marcadores NeuN, IBA-1 (*Ionized calcium binding adaptor molecules 1)* e S100B (*Calcium binding protein B).* Nos testes comportamentais, os animais infectados exibiram comportamento de anedonia, do tipo ansioso e déficits motores.

Os achados reforçam a utilidade do modelo murino de MHV-3 para o estudo da fisiopatologia das manifestações neurológicas agudas observadas em casos graves de COVID-19. Contudo, o modelo apresenta limitações importantes, como a ausência de interação direta do vírus com o receptor ECA-2, utilizado pelo SARS-CoV-2, e a natureza altamente aguda e letal da infecção pelo MHV-3, o que dificulta a análise de sequelas tardias.

Inflammation Research (2023) 72:2073–2088
https://doi.org/10.1007/s00011-023-01798-w

Inflammation Research

ORIGINAL RESEARCH PAPER

A suitable model to investigate acute neurological consequences of coronavirus infection

Jordane Pimenta[1] · Bruna Da Silva Oliveira[1] · Anna Luiza Diniz Lima[3] · Caroline Amaral Machado[1] · Larisse De Souza Barbosa Lacerda[1] · Leonardo Rossi[1] · Celso Martins Queiroz-Junior[1] · Luiz Pedro De Souza-Costa[5] · Ana Claudia Santos Pereira Andrade[1] · Matheus Rodrigues Gonçalves[6] · Bárbara Mota[1] · Fernanda Martins Marim[2] · Renato Santana Aguiar[2] · Pedro Pires Goulart Guimarães[3] · Antônio Lúcio Teixeira[4] · Luciene Bruno Vieira[3] · Cristina Guatimosim[1] · Mauro Martins Teixeira[5] · Aline Silva De Miranda[1] · Vivian Vasconcelos Costa[1]

Received: 2 June 2023 / Revised: 6 September 2023 / Accepted: 13 September 2023 / Published online: 14 October 2023

Abstract

Objective and design The present study aimed to investigate the neurochemical and behavioral effects of the acute consequences after coronavirus infection through a murine model.

Material Wild-type C57BL/6 mice were infected intranasally (i.n) with the murine coronavirus 3 (MHV-3). Methods: Mice underwent behavioral tests. Euthanasia was performed on the fifth day after infection (5 dpi), and the brain tissue was subjected to plaque assays for viral titration, ELISA, histopathological, immunohistochemical and synaptosome analysis. Results: Increased viral titers and mild histological changes, including signs of neuronal degeneration, were observed in the cerebral cortex of infected mice. Importantly, MHV-3 infection induced an increase in cortical levels of glutamate and calcium, which is indicative of excitotoxicity, as well as increased levels of pro-inflammatory cytokines (IL-6, IFN-γ) and reduced levels of neuroprotective mediators (BDNF and CX3CL1) in the mice brain. Finally, behavioral analysis showed impaired motor, anhedonia-like and anxiety-like behaviors in animals infected with MHV-3.

Conclusions In conclusion, the data presented emulate many aspects of the acute neurological outcomes seen in patients with COVID-19. Therefore, this model may provide a preclinical platform to study acute neurological sequelae induced by coronavirus infection and test possible therapies.

Keywords MHV · SARS-CoV-2 · Acute neurological outcomes · Glutamatergic levels · COVID-19 · Animal behavior

Responsible Editor: Anatolii Kubyshkin.

Jordane Pimenta and Bruna Da Silva Oliveira authors contributed equally to this work.

✉ Aline Silva De Miranda
mirandas.aline@gmail.com

✉ Vivian Vasconcelos Costa
vivianvcosta@gmail.com

[1] Department of Morphology, Institute of Biological Sciences, Universidade Federal de Minas Gerais, Avenida Presidente Antônio Carlos, 6627, Belo Horizonte, MG 31270-901, Brazil

[2] Department of Genetics, Ecology and Evolution, Institute of Biological Sciences, Universidade Federal de Minas Gerais, Belo Horizonte, MG, Brazil

[3] Department of Physiology and Biophysics, Institute of Biological Sciences, Universidade Federal de Minas Gerais, Belo Horizonte, MG, Brazil

[4] Department of Psychiatry and Behavioral Sciences, McGovern Medical Houston, The University of Texas Health Science Center at Houston, Houston, TX, USA

[5] Department of Biochemistry and Immunology, Institute of Biological Sciences, Universidade Federal de Minas Gerais, Belo Horizonte, MG, Brazil

[6] Department of Microbiology, Institute of Biological Sciences, Universidade Federal de Minas Gerais, Belo Horizonte, MG, Brazil

Introduction

COVID-19 has resulted in more than 769 million cases and 6,9 million deaths worldwide [31]. Initially, COVID-19 was considered a respiratory disease, however, soon after it has been observed that the disease affects several organs and tissues, including the central nervous system (CNS) [1].

The first neurological symptom resulting from COVID-19 is typically gustatory and/or olfactory dysfunction [2]. In the most severe cases, peripheral neurological conditions such as Guillain–Barré syndrome, as well as conditions that indicate CNS involvement such as stroke, epilepsy/seizures, encephalitis, and others have been reported [2]. The GCS-NeuroCOVID study, which involved more than 3.500 patients, found that 80% of them reported neurological manifestations during COVID-19, with encephalopathy being the most prevalent [51].

Viral genetic material and SARS-CoV-2 (severe acute respiratory syndrome coronavirus-2) proteins have been identified in post-mortem brain tissue and cerebrospinal fluid (CSF) of patients affected by COVID-19 [3–7]. It is assumed that the olfactory nerve and olfactory bulb serve as a gateway to the CNS. Several viruses, including murine hepatitis coronavirus (MHV) [9, 10], have been shown to use this route to reach the CNS. SARS-CoV-2 RNA found in the CSF or CNS parenchyma of patients with COVID-19 may originate from the blood due to compromised blood–brain barrier (BBB) permeability [7], as well as from the migration of peripheral immune cells carrying the virus or viral fragments. COVID-19-related neurological symptoms are likely due to immune responses instead of a consequence of SARS-CoV-2 neurotropism [30]. The most accepted mechanism involved in the neurological and neuropsychiatric changes resulting from COVID-19 is the "cytokine storm", in which various mediators that are peripherally produced can reach the CNS, triggering neuroinflammation [8]. Thus, SARS-CoV-2 may induce a loss of central homeostasis both through direct action and by a systemic inflammatory response [14]. Hypoxia resulting from SARS is also associated with disturbances in brain metabolism that can result in neurological manifestations [12].

Different mouse strains of CoVs induce hepatic, respiratory, and enteric diseases that are followed by neurological alterations [11]. Given the inherent limits of human studies on the kinetics and mechanisms related to the disease [7], experimental models may provide a better understanding of the disease and the development of therapeutic strategies. Recently, our research group standardized a murine model to study the acute lung injury and systemic manifestation induced by a betacoronavirus, the MHV-3, which has the *Mus musculus* species as a natural host [13, 15]. When inoculated intranasally, infections induce severe lung inflammation which peaks at day 3 post-infection. This is followed by subsequent viral dissemination and systemic disease manifestations, which peak at day 5, when animals start to perish [13]. Recognizing the relationship between COVID-19 and the CNS, our objective was to investigate and characterize the effect of betacoronavirus infection in the CNS, using the intranasal route. We found that the MHV-3 infected mice displayed important inflammatory, neurochemical, and behavioral changes. Overall, this model may serve as a platform for studying possible acute neuropsychiatric alterations resulting from betacoronavirus infection, as well as for testing the efficacy of potential therapeutic strategies.

Materials and methods

Assay of cells, viruses, and plates

The cells used for viral propagation were L929 (ATCC CCL-1), a fibroblast cell line derived from a clone of normal subcutaneous connective tissue, areolar and adipose tissue of a male C3H/An mouse [65]. The cells were kept under a controlled atmosphere (37 °C and 5% CO_2) in Dulbecco's modified Eagle's medium (DMEM) with high content glucose content. The MHV-3 strain was granted by Clarice Weis Arns and Ricardo Durães-Carvalho of the State University of Campinas [(UNICAMP, Brazil; GenBank accession nº. MW620427.1; see reference [16])]. The propagated virus was titrated on L929 cells to determine the viral stock titer, which was found to be 1×10^6 PFU/mL. From the viral stock containing 1×10^6 PFU/mL, 100 uL of the viral stock was mixed with 900 uL of sterile saline solution to obtain 3×10^3 PFU in 30 uL. For viable virus detection, viral titration was performed from brain homogenates (1:9 tissue for DMEM). Cells were grown in 24-well plates and each well with a confluent monolayer of cells was inoculated with 100 µL of this homogenate. These plates were gently rotated for 1 h (4×15 min) to ensure effective viral adsorption. After 1 h the samples were removed from the wells, the overlay medium was added (DMEM containing 0,8% carboxymethylcellulose, 2% FBS and 1% penicillin–streptomycin–glutamine) and the plates were placed for 48 h at 37 °C and 5% CO_2. Subsequently, 10% neutral buffered formalin (NBF) was added for 1 h for cell fixation and 0,1% crystal violet was used for staining. The viral titer was expressed by counting the number of plaque forming units per gram of tissue (PFU/g tissue).

Mice

Animal experiments were carried out in WT C57BL/6, male and female, aged between 6 and 8 weeks, with approval from the Ethics Committee on Animal Experimentation of the UFMG (process nº 253/2020). The WT animals were obtained from the Central Animal Facility of UFMG maintained in micro-isolator cages at ABSL-2 under controlled conditions (24 °C ± 2 °C; on a 12-h light/12-h dark cycle), with ad libitum access to water and food.

MHV-3 infection

Mice were smoothly anesthetized (ketamine solution [50 mg/kg] and xylazine [5 mg/kg], [ip]) and then inoculated i.n with 30 µL of sterile saline (mock), with MHV-3 at a concentration of 3×10^3 PFU/mL. Manifestations of morbidity, such as weight loss, dorsal arching, facial swelling, ruffled hair and prostration were monitored daily until the 5th dpi and the survival until the 14th dpi.

Sample

For sample collection, the simulated and infected animals were previously anesthetized (ketamine solution [50 mg/kg] and xylazine [5 mg/kg], ip) and after sedation they were euthanized by cervical dislocation, on the 5th dpi. Cervical dislocation without anesthesia was used only in experiments in which drug interference in the analyses is proven. The brain was harvested, the left hemisphere was placed in 10% formalin buffer, and the other hemisphere was frozen. Other tissues were collected and frozen for further analysis.

Histopathological analysis

Brains from mock and infected mice with MHV-3 were removed and processed for hematoxylin and eosin (H&E) staining according to the following works [17, 18]. The histopathological score was adapted from the cited works and the analyses performed by a pathologist in a blinded manner. The evaluation was performed in the cerebral cortex and in the hippocampus, following a point scale: 0, no lesion; 1 mild tissue injury and/or mild inflammation; 2 mild tissue injury and/or inflammation moderate; 3, definitive tissue damage (neuronal loss and parenchymal damage) and intense inflammation; 4, necrosis (complete loss of all tissue elements with the presence of cellular debris). Meningeal inflammation was assessed using a point scale (0 to 4) with 0 representing no inflammation and 1 to 4 corresponding to 1 to 4 layers affected by inflammation. The final score was the sum of the cerebral cortex and hippocampus scores plus the meningitis score, totaling 12 points.

Measurement of cytokine and chemokine concentration

Cerebral cortex homogenates were obtained by homogenizing frozen tissue in refrigerated cytokine extraction buffer (100 mM Tris [pH 7,4], 150 MM NaCl, 1 mM EGTA, 1 mM EDTA, 1% Triton X -100, 0,5% sodium deoxycholate and 1% protease inhibitor). This homogenate was subjected to centrifugation (14.000 *g*, 15 min, 4 °C) and then the supernatant was collected for the determination of TNF, IFN-γ, IL-10, IL-6, BNDF and CX3CL1 using the immunosorbent assay system limited by mouse DuoSet enzymes (ELISA) (R&D Systems). According to the manufacturer, the sensitivity of the kit for each mediator: TNF (7,21 pg/mL), IFN-γ (2 pg/mL), IL-10 (5,22 pg/mL), IL-6 (1,8 pg/mL), BDNF (1,35 pg/mL) e CX3CL1 (0,32 ng/mL).

Immunohistochemistry IBA1, S100B, NeuN and cleaved Caspase-3

Sections of mouse cortex were evaluated for quantitative alteration of microglia, IBA1 (ionized calcium-binding adaptor molecule 1; antibody PA5-21,274, Invitrogen; 1:150), astrocytes (Anti-S100 beta antibody; ab41548, Abcam; 1:75), neurons (Anti-NeuN, MAB377, EMD Millipore; 1:200) and apoptosis (Anti-cleaved caspase-3; Asp175, Cell Signaling; 1:100,) according to the manufacturer's instructions (Vector Elite kit). Two independent experiments were carried out, each with $n = 5$ mice and both presented similar results. Representative photos of one of these experiments were used.

Transmission electron microscopy (TEM)

For ultrastructural analyzes, we used the protocol described by Rodrigues et al. [see reference [22]]. Briefly, mice were anesthetized with ketamine/xilazine and transcardially perfused with ice-cold modified Karnovsky fixative and maintained in this solution overnight at 4 °C. The brain was removed, and the cortex was isolated were washed with cacodylate buffer (0,1 M), cut into several pieces, post-fixed in reduced osmium (1% osmium tetroxide containing 1,6% potassium ferrocyanide) and contrasted en bloc with uranyl acetate (2% uranyl acetate in deionized water). The samples were then dehydrated through an ascending series of ethanol solutions and embedded in EPON resin. Blocks were sectioned (50 nm) and collected on 200 or 300 mesh copper grids 8 and contrasted with lead citrate. Sections

were viewed with a Tecnai- G2-SpiritFEI/Quanta electron microscope (120 kV Philips) located at Microscopy Center – UFMG.

Purification of synaptosomes

Immediately after euthanasia, the cortex was removed and homogenized in a gradient solution containing: 320 mM sucrose, 0,25 mM dithiothreitol, 1 mM EDTA. Then, the homogenate was exposed to a low-speed centrifugation (1000 × *g* × 10 min). Synaptosomes were isolated from the supernatant by discontinuous Percoll density gradient centrifugation [according to reference [19]]. Isolated nerve terminals were resuspended in Krebs–Ringer-HEPES (KRH) solution containing: 124 mM NaCl, 4 mM KCl, 1,2 mM MgSO4, 10 mM glucose, 25 mM HEPES, with pH 7,4 and without addition of $CaCl_2$, at a concentration of approximately 10 mg/mL. For measurement of glutamate release and intrasynaptosomal calcium concentration, aliquots of 30 µL were prepared and kept on ice until use.

Measurements of glutamate release

To measure continuous glutamate release, a fluorimetric assay was performed in a fluorimeter (Synergy TM2, Biotek®). Fluorescence emission was registered using an excitation wavelength of 360 nm and emission of 450 nm. Glutamate release was measured indirectly by following the increase in the fluorescence due to the production of NADPH in the presence of glutamate dehydrogenase type II and $NADP^+$. In brief, synaptosomes were incubated with 1 Mm $CaCl_2$, 1 mM $NADP^+$ in KRH medium for 5 min. Glutamate dehydrogenase (50 units per well) was added to each well after 5 min. For depolarization, we used 33 mM KCl. Calibration curve was achieved by the addition of glutamate (5 nM/µL) to the reaction medium. Glutamate levels were normalized to the total amount of protein per well.

Measurements of intrasynaptosomal free calcium concentration

To measure intrasynaptosomal free calcium concentration**,** synaptosomes were preincubated with 5 µmol/L of Fura-2 pentakis (acetoxymethyl) Ester (FURA2-AM) probe for 30 min at 35,5 °C. Next, synaptosome was centrifuged (3000 × *g* × 60 s), resuspended in KRH without $CaCl_2$, and reincubated again during 30 min. After washout with KRH without $CaCl_2$ synaptosomes were immediately used for quantification of intracellular free calcium ($[Ca^{2+}]_i$). Fluorescence was recorded with an excitation wavelength of 340/380 nm and an emission of 510 nm. $CaCl_2$ (1 mmol/L, final concentration) was added in synaptosomal suspension before reading and 33 mM of KCl was added to evoke calcium influx. Finally, we added 10% SDS to obtain Rmax and tris-EGTA (3 mol/L Tris, 400 mmol/L EGTA, pH 8,6) to obtain Rmin [as described in references 20 and 21].

Open field test

Locomotor activity and anxiety-like behavior were evaluated by the Open field test on the 3rd, 4th and 5th dpi [28]. Briefly, animals were videotaped by the Phenotyper apparatus (Noldus, Information Technology, Leesburg, VA, USA). There were four analysis cages in the room, which allowed for observation individually at the same time. Each cage (30 × 30 cm) contained a top unit with a digital video camera and infrared lights. Mice were placed in the center of the open field arena and were allowed to freely move and explore the environment for thirty minutes. Parameters such as locomotion activity and percentage of time spent at the center area (anxiety measure) were recorded and analyzed by a tracking software (EthoVision XT, Noldus Information Technology, Leesburg, VA, USA).

Marble buried test

Mice at 4th day post-MHV-3 infection were tested in the Marble buried test, which evaluates compulsive-like behavior. The test was previously described [see reference [26]]. Mice were tested in a rectangular cage (30 × 30 × 50cm) with 20 cm of fresh beddings. 25 marbles were placed equidistant to each other. Briefly, the animal was placed in the middle of the cage and allowed to explore and bury for 30 min. At the end of the section, the animals were removed and measured the number of marbles buried. Only the balls buried by more than 2 cm were considered.

Forced swim test

Mice at 4th day post-MHV-3 infection were tested in the forced swimming test, which evaluates the depressive-like behavior. The test was performed as previously described [see reference [27]]. Mice were placed in a cylindrical tank (30 cm height × 20 cm diameters) and recorded for 6 min. The duration of immobility time was recorded during the last 4 min of the 6 min testing period, after a 2 min habituation period by the EthoVision XT (Noldus, Technology, Leesburg, VA, USA).

Elevated plus maze test

Mice at 4th day post-MHV-3 infection were tested in the elevated plus-maze test (EPM), which evaluates mice anxiety-like behavior. The EPM test was performed as previously described [see reference [30]]. Mice were placed in the EPM apparatus consisting of two open and two closed

arms, crossed in the middle perpendicularly to each other creating a center area. Briefly, mice were placed in the center of the apparatus and allowed to freely explore for 5 min. The apparatus was wiped clean with 70% alcohol and dried with paper towels between each trial. The percentage (%) of open arm entries and % of time spent on the open arms (anxiety-like behavior measure) were recorded and analyzed by EthoVision XT (Noldus, Technology, Leesburg, VA, USA).

Sucrose preference test

The sucrose preference test was employed to assess anhedonic-like behavior in mice at 3rd,4th and 5th day post-MHV-3 infection as described elsewhere [29]. Briefly, at day 1 and 2 after MHV infection, i.e., the first two days of the test, the animals were habituated to two bottles of freshwater. On the following three days, corresponding to the 3rd, 4th, and 5th day post-MHV infection, the previous bottles were removed and replaced with a bottle filled with water and another one filled with 1% sucrose solution. The percentage of sucrose preference was calculated for each of the last three days of experiment.

Statistical analyses

All statistical analyses were performed, and all graphs were created in GraphPad Prism 8 (GraphPad Software). Data distribution was assessed by the Shapiro–Wilk test. Parametric comparisons between groups were performed using Student's *t*-test. The Mann–Whitney test was used to assess differences between nonparametric data. Data were presented as mean ± Standard Deviation (SD). Differences with a p-value < 0.05 were considered statistically significant.

Results

Characterization of cellular and histopathological alterations in the brain of mice infected with MHV-3

To evaluate potential brain alterations induced by the coronavirus, male and female C57BL/6 J mice, 6–8 weeks of age, were infected i.n. with 3×10^3 PFU/mL of MHV-3 (Fig. 1a). Analyses were performed on the fifth day after infection (5th dpi) when systemic manifestations peaked, as previously described [13]. Upon infection, MHV-3 replicates in the brain of female (Fig. 1b) and male mice (Fig. S1b). Histopathological analysis (H&E) of the cerebral cortex revealed the presence of hyperemic blood vessels, surrounded by few leukocytes, which translated to a mild histopathological score in a similar way in both sexes (Fig. 1c–d and S1 c–d). Subsequently, we investigated whether this mild CNS damage was related to changes in the number of cells as well as in the process of apoptosis. According to H&E data, no significant differences were found in the number of cells stained for NeuN (Fig. 1e), IBA1 (Fig. 1f), S100B (Fig. 1g), and caspase 3 (Fig. S1h) in the cerebral cortex of female MHV3-infected mice compared with mock animals. Similar results were also found in male C57BL/6 mice (Fig. S1e–g, i). Overall, the presented data suggest that the mild histopathological damage induced by MHV-3 was not associated with neuronal or glial death.

Signs of neuronal degeneration were observed in the cerebral cortex of mice infected with MHV-3

To evaluate potential neurodegenerative signs caused by MHV-3 infection, we performed a qualitative ultrastructure analysis of female mouse cerebral cortex samples from infected and non-infected mice (Fig. 2). Our data showed signs of degeneration in neuronal cell bodies. For example, Fig. 2a (red arrowhead) shows a dark degenerating neuron with a shrunk cell body, darker staining (increased electron density), Golgi and endoplasmic reticulum dilation (Fig. 2a', arrows) and mitochondria with disrupted cristae (Fig. 2a'' and c'', arrows). We also observed typical neuronal cell bodies such as the profile shown in Fig. 2b but with prominent and complex lipofuscin granules (Fig. 2b', c' and C'' arrowheads). Both in control and infected mice (in addition to the ones described above), there were neuronal cell bodies with typical morphological features such normal cell size, typical nucleus with normal chromatin (Fig. 2d) and mitochondria with conserved cristae (Fig. 2d'). Eventually, we noticed occasional lipofuscin granules in control mice, such as the one on Fig. 2d, (blue arrowhead) but they were less complex than the ones observed in MHV-3 infected cerebral cortex.

MHV-3 infection induces glutamate release, intracellular calcium levels elevation and production of inflammatory mediators in the cortical brain of mice

Glutamate is an important excitatory neurotransmitter, and numerous studies have indicated that overstimulation of the glutamatergic system through activation of ionotropic glutamate receptors can lead to excitotoxicity, which may result in neuronal calcium overload and consequent neurodegeneration [18, 23, 24]. To investigate whether coronavirus has the potential to induce neurochemical changes in the cerebral cortex, we measured glutamate levels and intracellular calcium in cortical synaptosomes of female and male mice [25–27]. Indeed, MHV-3 infection induced a greater release of glutamate, as well as an increase in intracellular calcium levels, in the cerebral cortex of both male and female infected animals (Fig. 3b–e).

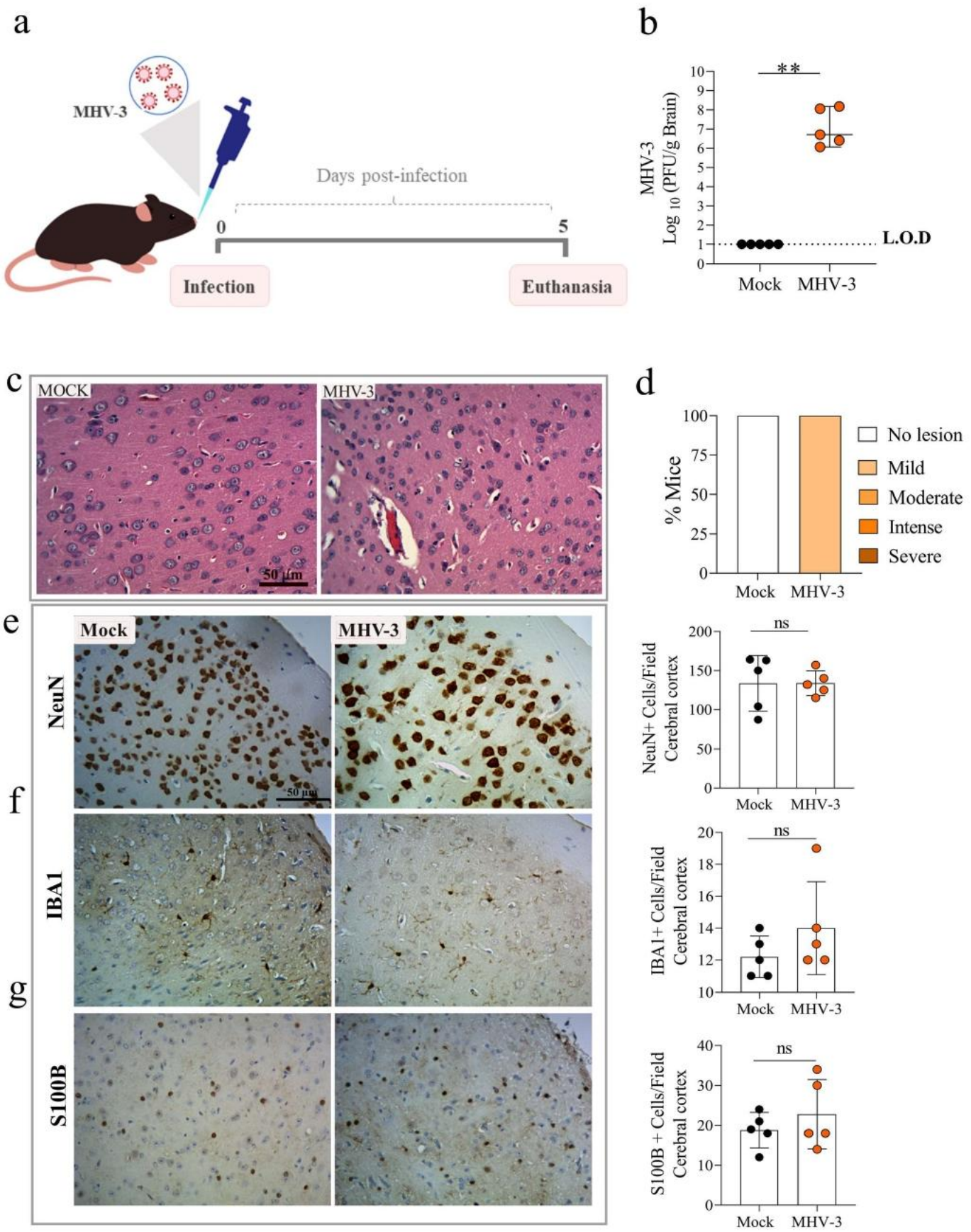
a
MHV-3
Days post-infection
0
5
Infection
Euthanasia
b
**
MHV-3
Log 10 (PFU/g Brain)
L.O.D
Mock
MHV-3
c
MOCK
MHV-3
50 µm
d
% Mice
No lesion
Mild
Moderate
Intense
Severe
Mock
MHV-3
e
Mock
MHV-3
NeuN
50 µm
f
IBA1
g
S100B
NeuN+ Cells/Field Cerebral cortex
IBA1+ Cells/Field Cerebral cortex
S100B + Cells/Field Cerebral cortex
ns

◂**Fig. 1** Intranasal MHV-3 infection induces mild alterations in the cerebral cortex of mice. Female C57BL/6 mice ($n=5$/group) were infected i.n. with 3×10^3 PFU/mL of MHV-3. Euthanasia was performed at 5 dpi. **a** Experimental design. **b** Viral titers quantified in brain extracts of MHV-3 infected mice by plaque assay. Results are demonstrated as $\log_{10}$ PFU per gram of tissue. Statistical comparison among groups were made using the Mann–Whitney test (median with 95% CI). LOD, limit of detection. **, $p<0.01$. **c** Hematoxylin and eosin (H&E) staining of sections of the cerebral cortex showed mild histological damage in infected mice, 50 µm bars. **d** Percentages of mice according to the degree of tissue damage in the brain. **e** Immunohistochemistry using antibodies anti-NeuN (count of neurons), **f** anti-IBA1 (microglia/macrophages count), **g** anti-S100B (astrocyte count). Representative images are on the left panels and the quantification of positive cells (ImageJ software) is presented on the right panels. Results are expressed as the mean of all cells counts per group and statistical comparison among groups was made using unpaired Student *t*-test (mean ± SD); ns, not significant ($p>0.05$)

Next, we evaluated the levels of certain molecules involved in the host response induced by infections, such as cytokines (interleukin-6 [IL-6], interferon-gamma [IFN-γ], tumor necrosis factor [TNF], interleukin-10 [IL-10], brain-derived neurotrophic factor [BDNF]), and the chemokine CX3CL1 (fractalkine) in distinct brain areas of mice infected with MHV-3 and their control littermates. Cytokines IL-6 and IFN-γ showed an increase in the prefrontal cortex (PFC) of female mice infected with MHV-3 compared to mock animals (Fig. 4a and b). In male mice infected with MHV-3, there was an increase in IFN-γ levels in the PFC, while IL-6 was not altered (Fig. 4g and h). No significant differences were found in the concentration of TNF and IL-10 in both sexes (Fig. 4c–d and i–j). Interestingly, female mice infected with MHV-3 had a reduction in BDNF and CX3CL1 levels in the PFC compared with control mice, while male mice responded to the infection with an increase in CX3CL1 levels and no significant changes in BDNF concentrations in the PFC compared with control littermates (Fig. 4e–f and k–l, respectively). We measured the same mediators in the hippocampus and striatum of both sexes. Regarding the concentrations of IL-10, TNF, IFN-γ and CX3CL1, there were no significant changes in these regions in both sex (Figs. S2 and S3). IL-6, on the other hand, had its concentration increased in the hippocampus and striatum of females infected with MHV-3 compared with their controls, while no change was observed in males (Fig. S2a and S2g; S3a and S3g, respectively). Levels of the neurotrophic factor BDNF did not change in the hippocampus and striatum of infected female mice (Fig. S2e and S2k) but were increased in the hippocampus of male MHV-3 mice (Fig. S3e).

Overall, our results show that MHV-3 infection induces acute neurochemical alterations in the brain of mice, as demonstrated by increased levels of glutamate/calcium, suggesting the occurrence of excitotoxicity, and changes in the levels of inflammatory mediators. Furthermore, we observed that female mice seem to be more susceptible to MHV-3 infection and to the reduction of neuroprotective mediators compared to male mice.

MHV-3 infection promotes anxiety-like and anhedonia-like behaviors alongside motor dysfunction in mice

We evaluated whether MHV-3 infection is associated with acute behavioral changes in mice. No significant differences were observed in the total distance traveled in the Open Field Test (OFT) on days 3 (Fig. 5b and S4a) and 4 (Fig. 5c) post-infection. However, on day 5, when systemic disease symptoms peaked, MHV-3-infected female mice (Fig. 5d) but not male mice (Fig. S4b) showed a significant decrease in the total distance traveled compared to non-infected controls, indicating locomotor impairment in females. At 4 days post-infection, female infected mice displayed anxiety-like behavior, as indicated by a significant decrease in the percentage of time spent in the open arms of the elevated plus maze (EPM) (Fig. 5e), which was not observed in male mice (Fig. S4c). Both female and male infected mice displayed an anhedonic-like behavior in the Marble Burying test (MBT) at 4 days post-infection, as indicated by a significant reduction in the number of marbles buried (Fig. 5f and S4d). In addition, infected male mice had an increase in immobility time in the Forced Swimming Test (FST) (Fig S4e), but no change in the frequency of immobility (Fig S4f). Infected females, on the other hand, did not present significant differences in the time or frequency of immobility in the FST when compared to their control group (Fig. 5g–h). When performing the sucrose preference test (SPT), females infected with MHV-3 showed an anhedonic behavior on the third and fifth dpi. In summary, these results suggest that MHV-3 infection induces acute behavioral changes in mice, especially in females, including locomotor impairment, anxiety-like and anhedonic-like behavior.

Discussion

COVID-19 has been associated with a wide range of clinical manifestations, including neurological and psychiatric alterations. In this study, we investigated whether MHV-3 can directly affect the CNS and serve as a suitable platform to study COVID-19-related neurobiological mechanisms and identify novel therapeutic targets. The main findings of this study are: (i) MHV-3 delivered intranasally is capable of infecting and replicating in the CNS, causing mild histopathological alterations; (ii) MHV-3 infection results in increased glutamate release, intracellular calcium levels and pro-inflammatory mediators in the cortex; (iii) MHV-3 infection decreases the production of neuroprotective mediators such as BDNF and CX3CL1 in the brain; and (iv)

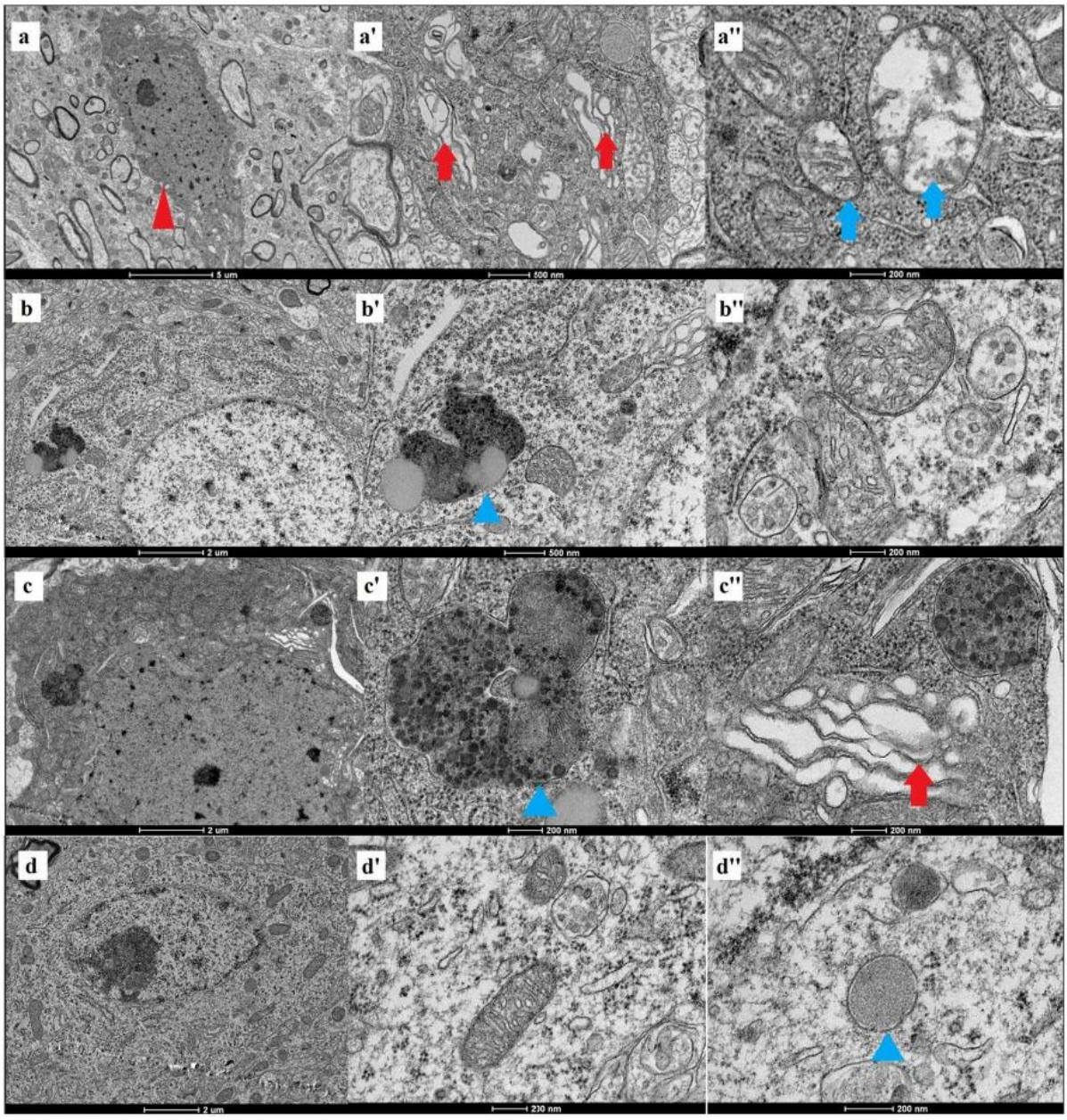

Fig. 2 Cerebral cortex neurons from MHV-3 infected mice show signs of degeneration at the ultrastructure level. a–a"- Female C57BL/6 mice were infected intranasally with 3×10^3 PFU/mL of MHV-3. A dark degenerating neuron profile from cerebral cortex of MHV-3 infected mouse (red arrowhead) with enlarged Golgi cisternae (a' red arrows) and mitochondria with disrupted cisternae (a" blue arrows). **b–b" and c–c"** cerebral cortex neurons from two distinct MHV-3 infected mice presenting complex lipofuscin granules (b' and c' blue arrowheads) and enlarged Golgi cisternae (red arrow c"). **d–d"-** A neuron profile from a mock mouse cerebral cortex with regular features

Animals infected with MHV-3 showed signs of anxiety-like and anhedonic-like behaviors and motor dysfunction, especially female mice.

Models that assess behavioral changes in the context of betacoronavirus infections in the CNS are still scarce. We have demonstrated the applicability of a murine betacoronavirus model as a platform to recapitulate the acute neurological and psychiatric symptoms observed in patients with COVID-19. All analyses were performed up to the 5th day post infection, i.e., at the peak of systemic disease [13]. First, the neurotropism of MHV-3 was confirmed by recovering viable virus particles in the brain of mice. In addition, histopathological analysis of the brain of MHV-3-infected mice revealed mild changes, such as dilated blood vessels in the meninges, an inflammatory infiltrate, and hyperemic vessels in the cerebral cortex. These findings support human studies showing that SARS-CoV-2 was detected in the post-mortem brain of half of COVID-19 patients along with mild

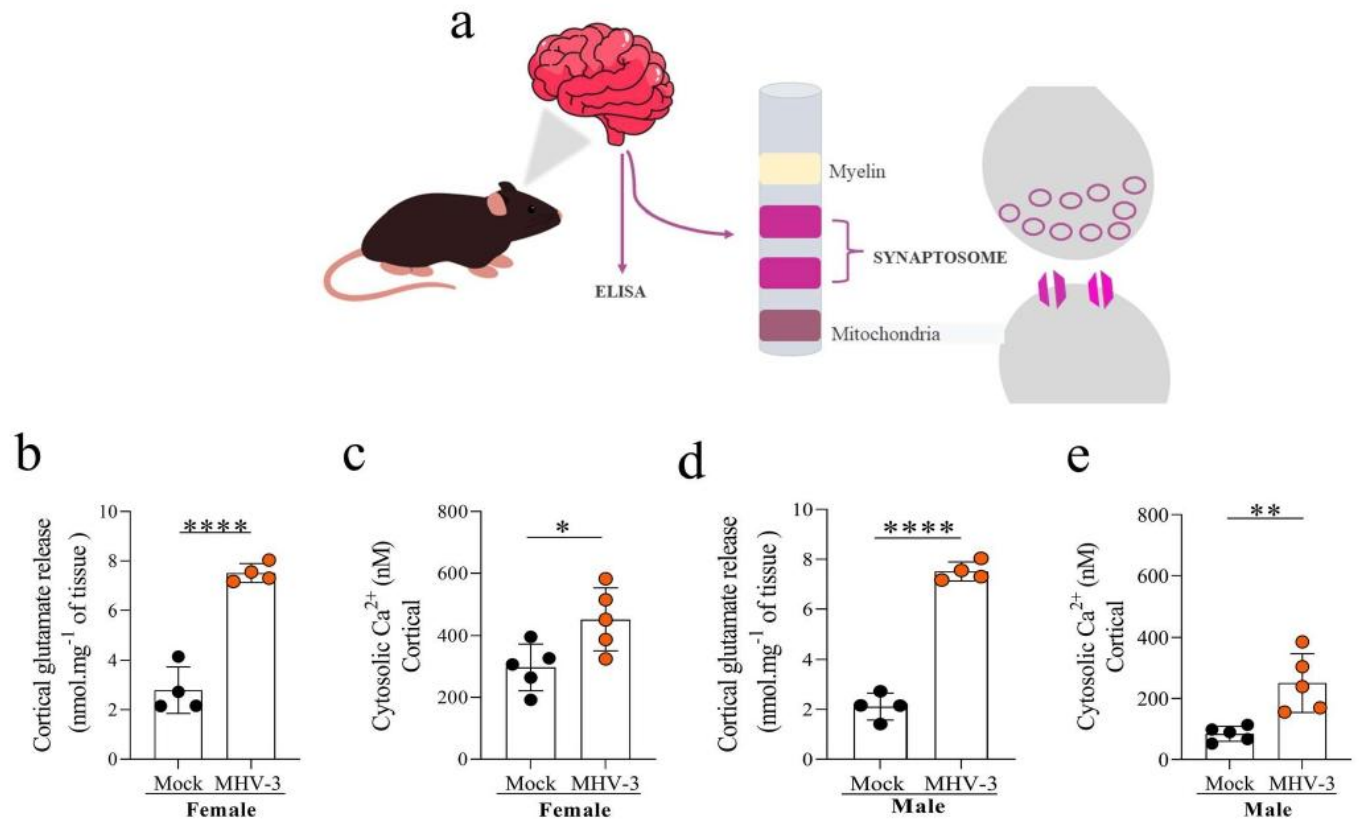

Fig. 3 MHV-3 infection induces increased cortical glutamate levels and intrasynaptosomal calcium levels in mice female and male C57BL/6 mice infected i.n. with 3×10^3 PFU/mL of MHV-3. **a** Schematic figure of cortical synaptosome preparation. **b** Cortical glutamate levels and (**c**) cortical intrasynaptosomal calcium levels were measured in female mice infected with MHV-3 and control group. **d** and **e** Cortical glutamate levels and cortical intrasynaptosomal calcium levels were also measured in male mice infected with MHV-3 and mock group, respectively. Statistical analysis was performed using unpaired Student *t*-test (mean ± SD) or Mann–Whitney test (median with 95% CI); $n = 4$ to 5/group. $^*p < 0.05$; $^{**}p < 0.01$, $^{****}p < 0.001$

neuropathological lesions [3]. Although many studies have not found SARS-CoV-2 in the brain, it is already known that the immune response triggered by the virus can culminate in a "cytokine storm", which reaches and compromises the homeostasis of the CNS, as well as other tissues [8].

In addition, we conducted a quantitative analysis of neurons (NeuN), microglia/macrophage (IBA1), and astrocytes (S100B), as well as evaluated apoptosis (cleaved caspase 3). None of these markers were found to be altered in the cortex of infected animals when compared to mock. However, this finding does not necessarily indicate that glia and neurons were not affected. In fact, brain tissues from individuals who died with COVID-19 showed that microglia abundantly expressed the lysosomal marker CD68, which is a marker of phagocytic activity, especially in the olfactory bulb and cerebellum [52]. Boroujeni et al. 53 also demonstrated that the inflammatory response in COVID-19 caused neuronal death in the cerebral cortex (post-mortem) of critically ill patients [53]. NeuN quantification revealed a similar number of marker-positive neurons when we compared the infected and control groups. Nonetheless, the analysis of the ultrastructure of cerebral cortex samples from animals infected with MHV-3 revealed the presence of darkened neurons, known as Dark Neurons (DNs), indicating ongoing degeneration. Golgi complexes and dilated endoplasmic reticulum and mitochondria with ruptured cristae were also observed in these cases. Although the NeuN quantification showed no change, about 90–99% of DNs recover with time, while a small number of neurons die [54]. Electron microscopy studies have shown that these DNs have low functional activity. However, the origin and mechanism of the emergence of these dark neurons remain undefined [54].

In the present study, we also measured the levels of the excitatory neurotransmitter glutamate and calcium (Ca^{2+}) released at presynaptic terminals in the cerebral cortex [55–59]. Our results showed that MHV-3 infection led to massive glutamate release and increased intracellular Ca^{2+} levels. Other viruses such as HIV, ZIKV, and H1N1 have been reported to impair glutamatergic transmission, which can result in excitotoxicity and impaired cell signaling [18, 32, 60, 61]. Additionally, HCoV-OC43, a human coronavirus, can infect human CNS neuronal and glial cells and

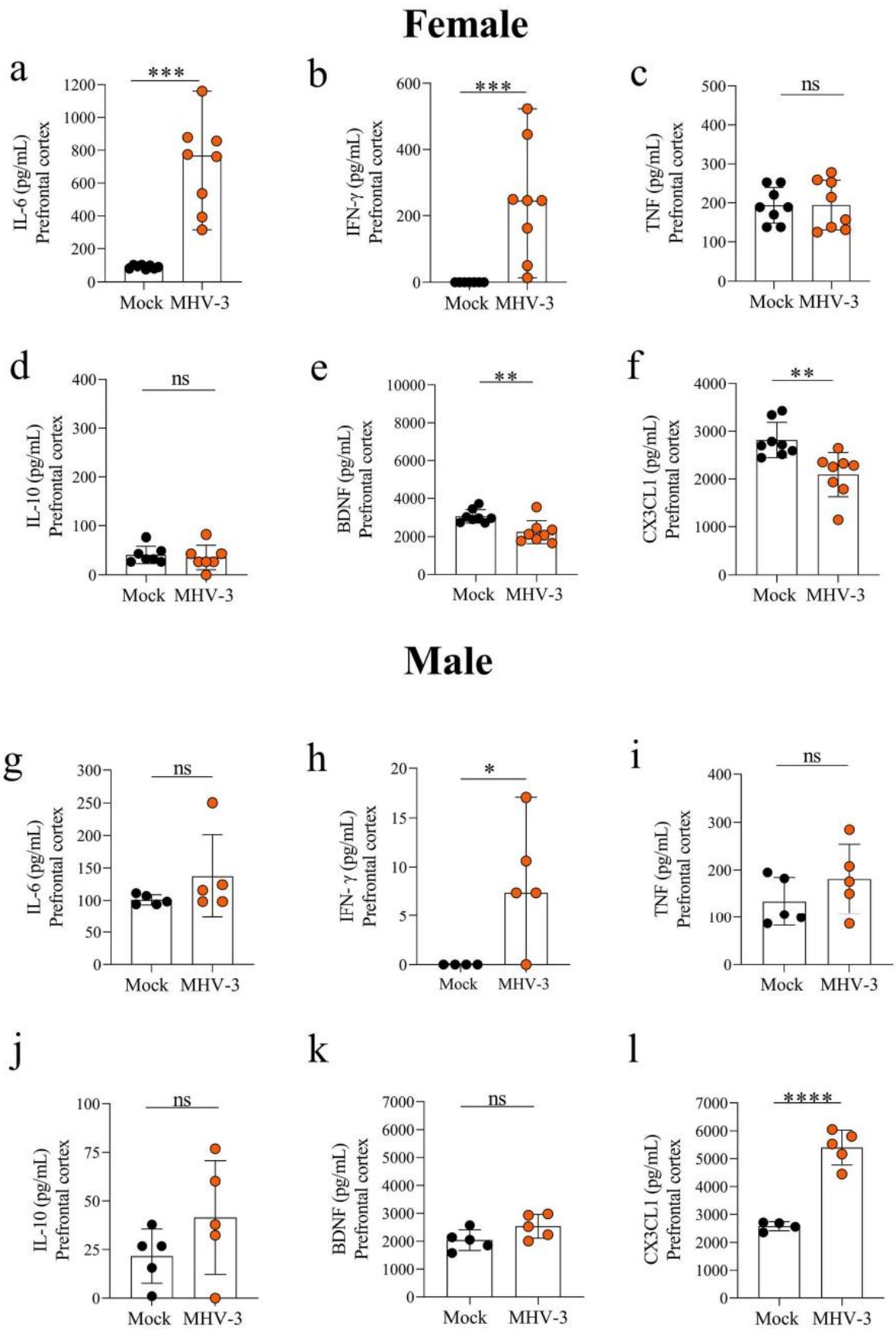
Female
a
IL-6 (pg/mL) Prefrontal cortex
***
Mock MHV-3
b
IFN-γ (pg/mL) Prefrontal cortex
***
Mock MHV-3
c
TNF (pg/mL) Prefrontal cortex
ns
Mock MHV-3
d
IL-10 (pg/mL) Prefrontal cortex
ns
Mock MHV-3
e
BDNF (pg/mL) Prefrontal cortex
**
Mock MHV-3
f
CX3CL1 (pg/mL) Prefrontal cortex
**
Mock MHV-3
Male
g
IL-6 (pg/mL) Prefrontal cortex
ns
Mock MHV-3
h
IFN- γ (pg/mL) Prefrontal cortex
*
Mock MHV-3
i
TNF (pg/mL) Prefrontal cortex
ns
Mock MHV-3
j
IL-10 (pg/mL) Prefrontal cortex
ns
Mock MHV-3
k
BDNF (pg/mL) Prefrontal cortex
ns
Mock MHV-3
l
CX3CL1 (pg/mL) Prefrontal cortex
****
Mock MHV-3

◂**Fig. 4** Inflammatory mediator levels in the cortex of female and male mice upon MHV-3 infection. Female and male C57BL/6 mice were infected i.n. with 3×10^3 PFU/mL of MHV-3. Levels of IL-6, IFN-γ, TNF, IL-10, BDNF and CX3CL1 (fractalkine) (a - l) were quantified by enzyme-limited immunosorbent assay (ELISA) in the prefrontal cortex of control and MHV-3-infected mice. Statistical analysis was performed using unpaired Student *t*-test (mean ± SD) or Mann–Whitney test (median with 95% CI); $n = 7$ to 8/group (female) and $n = 4$ to 5/group (male). *ns* not significant ($p > 0.05$); *$p < 0.05$; **$p < 0.01$; ***$p < 0.001$; ****$p < 0.0001$

activate neuroinflammatory mechanisms [33]. Infection of mice with HCoV-OC43 has been shown to induce neuronal dysfunction and decrease the expression of the glutamate transporter GLT-1 in astrocytes, potentially leading to increased central glutamate levels [34]. We also observed an increase in IL-6 levels in the PFC of animals after MHV-3 infection. IL-6 can be produced within the CNS by various cell types and infiltrating inflammatory cells under neuroinflammatory conditions [35]. It has been reported that membrane depolarization is one of the primary mechanisms for the upregulation of IL-6 in neurons, which is dependent on glutamatergic activation of N-methyl-D-aspartate receptors (NMDA-R), an increase in Ca^{2+} levels, and activation of Ca^{2+}/dependent kinases, such as calmodulin [36]. In a ZIKV infection model, we demonstrated that neuronal cell death could be prevented when infected animals were treated with an NMDA-R non-competitive inhibitor. Neurodegeneration and microgliosis induced by the infection were also inhibited in vitro and in vivo [8, 61].

It is interesting to note that increased levels of IL-6 have been associated with anxiety and depressive symptoms [37, 38], and play a role in neurogenesis [39]. Additionally, mounting evidence suggests that inflammation and alterations in glutamate neurotransmission may contribute to the pathophysiology of mood disorders [40]. There is evidence indicating that fractalkine has protective effects against glutamate-mediated excitotoxicity, as fractalkine increases BDNF levels and TrkB phosphorylation [41]. In our study, we observed a decrease in cortical levels of fractalkine and BDNF, which leads us to speculate that neuroprotection mechanisms are reduced, contributing to depressive-like behaviors in mice [62]. While IFN-γ contributes to virus clearance [42], we observed a decrease in IFN-γ levels after MHV-3 infection. Interestingly, at low physiological glutamate concentrations, glutamate can directly activate naïve T cells via AMPA-R. However, when glutamate concentration markedly increases, this neurotransmitter usually inhibits T cell function [43].

To evaluate the behavioral consequences of MHV-3 infection, we conducted several specific tests. In the elevated plus maze test, we observed anxiety-like behavior in the infected animals. This finding is consistent with a previous study on DENV-3 encephalitis, which showed that infected mice also displayed anxiety-like behavior and increased mRNA expression of pro-inflammatory cytokines in the hippocampus associated with neuronal loss [55]. BDNF has been shown to have an antidepressant function in the PFC [45] and hippocampus [46]. In addition, another study demonstrated that administration of BDNF into the hippocampus of rats reduced anxiety-like behavior in the elevated plus maze test [47], suggesting that the reduction in BDNF levels may be associated with the development of anxiety disorders. Moreover, impaired neuron-microglia communication, specifically the CX3CL1/CX3CR1 pathways, has been increasingly linked to the development of psychiatric conditions [48].

Studies performed in transgenic mice (K18-hACE2) that overexpress human ACE-2 and are infected with SARS-CoV-2 strongly support the acute CNS effects observed in our MHV-3 model. Kumari and colleagues [58] reported that intranasal inoculation of SARS-CoV-2 in K18-hACE2 mice was associated with neuroinvasion and encephalitis. These findings were corroborated by Oladunni et al. [62], who demonstrated that intranasal infection of K18-hACE2 mice resulted in viable viral titers in various organs, including the nostril, lungs, and brain. Moreover, the infection was linked to local and systemic chemokine storms, with increased levels of CXCL-2, CXCL-10, and CCL-3 in the brain of SARS-CoV-2-infected mice. Finally, another recent study showed that primary neurons isolated from K18-hACE2 mice are susceptible to SARS-CoV-2 infection, and that the infection upregulates the expression of genes involved in innate immunity and inflammation, including IFN-α, ISG-15, CXCL-10, CCL-2, IL-6, and TNF, in the neurons [63].

According to Andrade et al. [13], there are no sexes difference in the lung disease caused by MHV-3 in mice. This finding is supported by Oladunni et al. (2020) who found no significant difference in chemokine levels in the lung between male and female K18-hACE2 transgenic-infected mice, except for CXCL-10 at early time points of infection, which was significantly higher in female K18-hACE2 mice. However, our results indicate significant sex differences in the central nervous system (CNS) of MHV-3 infected mice, particularly in terms of the inflammatory response. Female mice infected with MHV-3 had increased levels of IL-6 in the analyzed brain regions (PFC, hippocampus, and striatum), while this cytokine did not change in male mice. On the other hand, infected male mice showed an increase in CX3CL1 in the PFC and BDNF in the hippocampus compared to the control group, while females infected had reduced levels of these mediators in the PFC. Previous studies have also reported the role of BDNF in the pathogenesis of depression, and its action is directly related to the brain region [44].

The Brazilian COVID Registry Project, a multicenter study that collected data from 39 Brazilian hospitals in 17

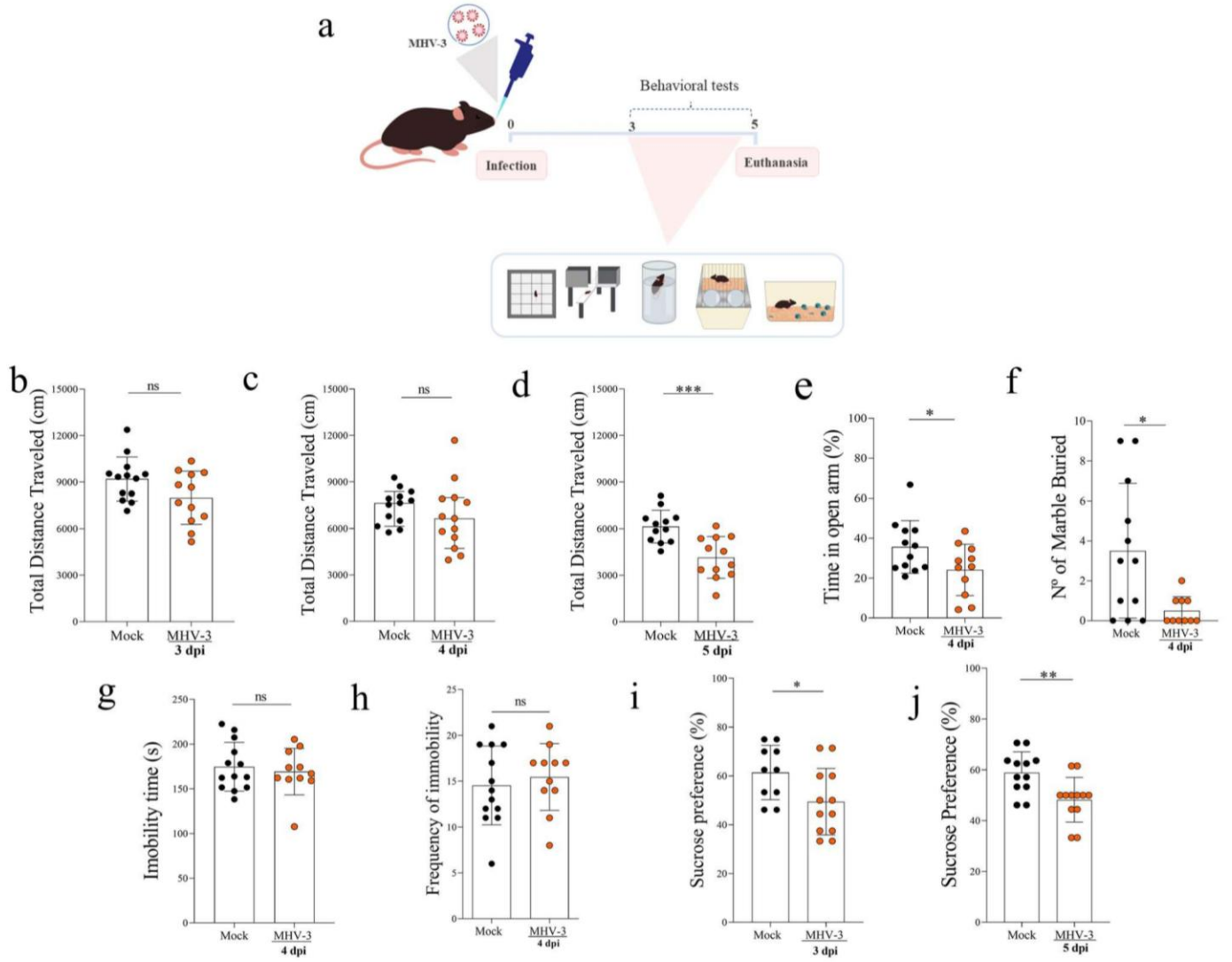

Fig. 5 MHV-3 infection induces behavioral alterations in female C57BL/6 mice. **a** Experimental design. **b–d** Locomotor activity was assessed using the open field test. **e** Anxiety-like behavior was assessed by calculating the percentage of time the animals remained in the open arms of the elevated plus maze. **f** Anhedonic-like behavior was assessed by the Marble Buried test, (**g**, **h**) Forced Swimming test and (**i**, **j**) Sucrose preference test. Statistical analysis was performed using unpaired Student *t*-test (mean ± SD) or Mann–Whitney test (median with 95% CI); $n = 12$ to 13/group. *ns* not significant ($p > 0.05$); *$p < 0.05$; **$p < 0.01$; ***$p < 0.001$

cities, observed that patients admitted with COVID-19 and clinically diagnosed with neurological syndromes had a higher incidence of septic shock, ICU admission and death compared to controls [49]. Furthermore, the study analyzed the incidence of neurological manifestations at hospital admission by gender and age group and found that women were more likely to experience headaches and less likely to have seizures [50]. In MHV-3 infection in females, there was a reduction of BDNF and CX3CL1, which may result in behavioral changes and loss of protection mechanisms. On the other hand, infected males show an increase in CX3CL1 and maintain homeostatic BDNF levels, which may help to mitigate possible behavioral repercussions.

The MHV-3 model, like other models used to study the neurological effects of COVID-19, has several limitations. First, it is not suitable for investigating the viral entry step, as SARS-CoV-2 uses a different receptor, ACE-2, while MHV-3 enters the cell through the CEACAM-1 adhesion molecule. This limits the usefulness of the model in studying drugs that target viral entry. Additionally, the MHV-3 model is very acute and lethal, with mice succumbing to the infection within a short period of time (around 6–7 dpi). As a result, it may be challenging to detect tissue damage in refractory organs such as the brain and heart [64] using regular techniques. In addition, future studies should be performed on the third and fourth day after infection to better understand the early inflammatory and biochemical mechanisms of infection related to neuropsychiatric symptoms. Another limitation of this work is the evaluation of a single protein (cleaved caspase 3)

involved in the apoptotic pathway, so there is a need to explore other caspases/pathways related to programmed cell death. We found some differences between males and females in some experiments, while the sex differences are intriguing and warrant further investigation, such an exploration would require dedicated research and analysis and are beyond the scope of this study.

In fact, fatigue is a very common symptom in cases of COVID and, above all, post-COVID. The frequency of immobility can be considered as an indication of motor activity in the forced swimming test [66, 67]. In the present study, no significant differences were found in the frequency of immobility when comparing mice infected with MHV-3 and controls, regardless of sex. These results, along with the open field data, suggest that the observed depressive-like behavior in males may not be solely attributed to fatigue. However, we acknowledge that further comprehensive investigations are warranted to systematically explore the role of fatigue during MHV-3 infection. Nevertheless, despite these limitations, the MHV-3 model can still be valuable in mimicking a severe betacoronavirus infection and may serve as a useful platform for further studies on acute neuropsychiatric changes caused by COVID-19, as well as testing potential novel therapeutic strategies against severe disease.

Supplementary Information The online version contains supplementary material available at https://doi.org/10.1007/s00011-023-01798-w.

Author contributions J.C. Pimenta: Conceptualization, Methodology, Investigation, Writing – Original Draft, Writing – Review & Editing, Project administration. B. D. S Oliveira: Investigation, Writing – Original Draft; A.L.D. Lima: Investigation, Methodology. C.A. Machado: Investigation. L. Rossi: Investigation, Writing – Original Draft- Review & Editing. L.D.S.B. Lacerda: Investigation. C.M. Queiroz-Junior: Investigation, Writing – Original Draft- Review & Editing. A.C. D. S. P. Andrade: S.R. Oliveira: Conceptualization, Methodology. M.R. Gonçalves: Investigation. B. Mota: Investigator. F. M. Marim: Investigator- Review & Editing. R. Santana: Review & Editing. P. Pires: Resources. A. L. Teixeira: Writing -Review & Editing. L.B. Vieira: Writing - Review & Editing, Resources. C. Guatimosim: Writing – Review & Editing, Resources. M.M. Teixeira: Writing – Review & Editing, Resources, Project administration, Funding acquisition. A.S.D Miranda: Conceptualization, Methodology, Resources, Writing – Review & Editing, Project administration. V.V. Costa: Conceptualization, Methodology, Resources, Writing – Review & Editing, Supervision, Project administration, Funding acquisition.

Funding This study was funded by the Coordenação de Aperfeiçoamento de Pessoal de Nível Superior,88881.507175 /2020 -01, Fundação de Amparo à Pesquisa do Estado de Minas Gerais,APQ 02281-18,APQ 02281-18, Conselho Nacional de Desenvolvimento Científico e Tecnológico,465425 /2014-3

Data availability The data that support the findings of this study are included within the article and available if required.

Declarations

Competing interests The authors declare no competing interests.

References

1. Bougakov D, Podell K, Goldberg E. Multiple neuroinvasive pathways in COVID-19. Mol Neurobiol. 2021;58(2):564–75. https://doi.org/10.1007/s12035-020-02152-5.
2. Harapan BN, Yoo HJ. Neurological symptoms, manifestations, and complications associated with severe acute respiratory syndrome coronavirus 2 (SARS-CoV-2) and coronavirus disease 19 (COVID-19). J Neurol. 2021;268(9):3059–71. https://doi.org/10.1007/s00415-021-10406-y.
3. Matschke J, Lütgehetmann M, Hagel C, Sperhake JP, Schröder AS, Edler C, Mushumba H, Fitzek A, Allweiss L, Dandri M, Dottermusch M, Heinemann A, Pfefferle S, Schwabenland M, Sumner Magruder D, Bonn S, Prinz M, Gerloff C, Püschel K, Glatzel M. Neuropathology of patients with COVID-19 in Germany: a post-mortem case series. Lancet Neurol. 2020;19(11):919–29. https://doi.org/10.1016/S1474-4422(20)30308-2.
4. Meinhardt J, Radke J, Dittmayer C, Franz J, Thomas C, Mothes R, Laue M, Schneider J, Brünink S, Greuel S, Lehmann M, Hassan O, Aschman T, Schumann E, Chua RL, Conrad C, Eils R, Stenzel W, Windgassen M, Heppner FL. Olfactory transmucosal SARS-CoV-2 invasion as a port of central nervous system entry in individuals with COVID-19. Nat Neurosci. 2021;24(2):168–75. https://doi.org/10.1038/s41593-020-00758-5.
5. Puelles VG, Lütgehetmann M, Lindenmeyer MT, Sperhake JP, Wong MN, Allweiss L, Chilla S, Heinemann A, Wanner N, Liu S, Braun F, Lu S, Pfefferle S, Schröder AS, Edler C, Gross O, Glatzel M, Wichmann D, Wiech T, Huber TB. Multiorgan and renal tropism of SARS-CoV-2. New Engld J Med. 2020;383(6):590–2. https://doi.org/10.1056/NEJMc2011400.
6. Song E, Zhang C, Israelow B, Lu-Culligan A, Prado AV, Skriabine S, Lu P, Weizman O-E, Liu F, Dai Y, Szigeti-Buck K, Yasumoto Y, Wang G, Castaldi C, Heltke J, Ng E, Wheeler J, Alfajaro MM, Levavasseur E, Iwasaki A. Neuroinvasion of SARS-CoV-2 in human and mouse brain. J Experim Med. 2021. https://doi.org/10.1084/jem.20202135.
7. Krasemann S, Haferkamp U, Pfefferle S, Woo MS, Heinrich F, Schweizer M, Appelt-Menzel A, Cubukova A, Barenberg J, Leu J, Hartmann K, Thies E, Littau JL, Sepulveda-Falla D, Zhang L, Ton K, Liang Y, Matschke J, Ricklefs F, Pless O. The blood-brain barrier is dysregulated in COVID-19 and serves as a CNS entry route for SARS-CoV-2. Stem Cell Rep. 2022;17(2):307–20. https://doi.org/10.1016/j.stemcr.2021.12.011.
8. Boldrini M, Canoll PD, Klein RS. How COVID-19 affects the brain. JAMA Psychiat. 2021;78(6):682. https://doi.org/10.1001/jamapsychiatry.2021.0500.
9. Burks SM, Rosas-Hernandez H, Alejandro Ramirez-Lee M, Cuevas E, Talpos JC. Can SARS-CoV-2 infect the central nervous system via the olfactory bulb or the blood-brain barrier? Brain Behav Immun. 2021;95:7–14. https://doi.org/10.1016/j.bbi.2020.12.031.
10. Perlman S, Evans G, Afifi A. Effect of olfactory bulb ablation on spread of a neurotropic coronavirus into the mouse brain. J Exp Med. 1990;172(4):1127–32. https://doi.org/10.1084/jem.172.4.1127.
11. Cowley TJ, Weiss SR. Murine coronavirus neuropathogenesis: determinants of virulence. J Neurovirol. 2010;16(6):427–34. https://doi.org/10.1007/BF03210848.
12. Cheng Q, Yang Y, Gao J. Infectivity of human coronavirus in the brain. EBioMedicine. 2020;56:102799. https://doi.org/10.1016/j.ebiom.2020.102799.
13. Andrade AC, dos SP, Campolina-Silva GH, Queiroz-Junior CM, de Oliveira LC, Lacerda L de SB, Gaggino JCP, de Souza FRO, de Meira Chaves I, Passos IB, Teixeira DC, Bittencourt-Silva PG, Valadão PAC, Rossi-Oliveira L, Antunes MM, Figueiredo

AFA, Wnuk NT, Temerozo JR, Ferreira AC, Cramer A, Costa VV (2021) A biosafety level 2 mouse model for studying betacoronavirus-induced acute lung damage and systemic manifestations. J Virol https://doi.org/10.1128/JVI.01276-21

14. Reza-Zaldívar EE, Hernández-Sapiéns MA, Minjarez B, Gómez-Pinedo U, Márquez-Aguirre AL, Mateos-Díaz JC, Matias-Guiu J, Canales-Aguirre AA. Infection mechanism of SARS-COV-2 and its implication on the nervous system. Front Immunol. 2021. https://doi.org/10.3389/fimmu.2020.621735.
15. Weiss SR, Leibowitz JL (2011) Coronavirus Pathogenesis (pp. 85–164). https://doi.org/10.1016/B978-0-12-385885-6.00009-2
16. Garcia AB, de Moraes AP, Rodrigues DM, Gilioli R, de Oliveira-Filho EF, Durães-Carvalho R, Arns CW. Coding-complete genome sequence of murine hepatitis virus strain 3 from Brazil. Microbiol Resour Announc. 2021. https://doi.org/10.1128/MRA.00248-21.
17. Amaral DC, Rachid MA, Vilela MC, Campos RD, Ferreira GP, Rodrigues DH, Lacerda-Queiroz N, Miranda AS, Costa VV, Campos MA, Kroon EG, Teixeira MM, Teixeira AL. Intracerebral infection with dengue-3 virus induces meningoencephalitis and behavioral changes that precede lethality in mice. J Neuroinflamm. 2011;8(1):23. https://doi.org/10.1186/1742-2094-8-23.
18. Costa VV, Del Sarto JL, Rocha RF, Silva FR, Doria JG, Olmo IG, Marques RE, Queiroz-Junior CM, Foureaux G, Araújo JMS, Cramer A, Real ALCV, Ribeiro LS, Sardi SI, Ferreira AJ, Machado FS, de Oliveira AC, Teixeira AL, Nakaya HI, Teixeira MM. N -Methyl-d-Aspartate (NMDA) receptor blockade prevents neuronal death induced by Zika virus infection. MBio. 2017. https://doi.org/10.1128/mBio.00350-17.
19. Dunkley PR, Heath JW, Harrison SM, Jarvie PE, Glenfield PJ, Rostas JAP. A rapid Percoll gradient procedure for isolation of synaptosomes directly from an S1 fraction: homogeneity and morphology of subcellular fractions. Brain Res. 1988;441(1–2):59–71. https://doi.org/10.1016/0006-8993(88)91383-2.
20. Grynkiewicz G, Poenie M, Tsien RY. A new generation of Ca2+ indicators with greatly improved fluorescence properties. J Biol Chem. 1985;260(6):3440–50.
21. Nicholls DG, Sihra TS, Sanchez-Prieto J. Calcium-dependent and -independent release of glutamate from synaptosomes monitored by continuous fluorometry. J Neurochem. 1987;49(1):50–7. https://doi.org/10.1111/j.1471-4159.1987.tb03393.x.
22. Rodrigues HA, de Fonseca MC, Camargo WL, Lima PMA, Martinelli PM, Naves LA, Prado VF, Prado MAM, Guatimosim C. Reduced expression of the vesicular acetylcholine transporter and neurotransmitter content affects synaptic vesicle distribution and shape in mouse neuromuscular junction. PLoS One. 2013;8(11):e78342. https://doi.org/10.1371/journal.pone.0078342.
23. Esposito Z, Belli L, Toniolo S, Sancesario G, Bianconi C, Martorana A. Amyloid β, glutamate, excitotoxicity in Alzheimer's Disease: are we on the right track? CNS Neurosci Ther. 2013;19(8):549–55. https://doi.org/10.1111/cns.12095.
24. Mody I. NMDA receptor-dependent excitotoxicity: the role of intracellular Ca2+ release. Trends Pharmacol Sci. 1995;16(10):356–9. https://doi.org/10.1016/S0165-6147(00)89070-7.
25. Prediger RDS, Aguiar AS, Rojas-Mayorquin AE, Figueiredo CP, Matheus FC, Ginestet L, Chevarin C, Bel ED, Mongeau R, Hamon M, Lanfumey L, Raisman-Vozari R. Single intranasal administration of 1-methyl-4-phenyl-1,2,3,6-tetrahydropyridine in C57BL/6 mice models early preclinical phase of Parkinson's disease. Neurotox Res. 2010;17(2):114–29. https://doi.org/10.1007/s12640-009-9087-0.
26. Oliveira TPD, Gonçalves BDC, Oliveira BS, de Oliveira ACP, Reis HJ, Ferreira CN, Aguiar DC, de Miranda AS, Ribeiro FM, Vieira EML, Palotás A, Vieira LB. Negative modulation of the metabotropic glutamate receptor type 5 as a potential therapeutic strategy in obesity and binge-like eating behavior. Front Neurosci. 2021. https://doi.org/10.3389/fnins.2021.631311.
27. Camargos QM, Silva BC, Silva DG, Toscano ECB, Oliveira BS, Bellozi PMQ, Jardim BLO, Vieira ÉLM, de Oliveira ACP, Sousa LP, Teixeira AL, de Miranda AS, Rachid MA. Minocycline treatment prevents depression and anxiety-like behaviors and promotes neuroprotection after experimental ischemic stroke. Brain Res Bull. 2020;155:1–10. https://doi.org/10.1016/j.brainresbull.2019.11.009.
28. de Miranda AS, Brant F, Vieira LB, Rocha NP, Vieira ÉLM, Rezende GHS, de Oliveira Pimentel PM, Moraes MFD, Ribeiro FM, Ransohoff RM, Teixeira MM, Machado FS, Rachid MA, Teixeira AL. A neuroprotective effect of the glutamate receptor antagonist MK801 on long-term cognitive and behavioral outcomes secondary to experimental cerebral malaria. Mol Neurobiol. 2017;54(9):7063–82. https://doi.org/10.1007/s12035-016-0226-3.
29. Eltokhi A, Kurpiers B, Pitzer C. Baseline depression-like behaviors in wild-type adolescent mice are strain and age but not sex dependent. Front Behav Neurosci. 2021. https://doi.org/10.3389/fnbeh.2021.759574.
30. Davis HE, Assaf GS, McCorkell L, Wei H, Low RJ, Re'em Y, Redfield S, Austin JP, Akrami A. Characterizing long COVID in an international cohort: 7 months of symptoms and their impact. EClinicalMedicine. 2021. https://doi.org/10.1016/j.eclinm.2021.101019.
31. WHO Coronavirus (COVID-19) Dashboard. Available from: https://covid19.who.int/.
32. Gorska AM, Eugenin EA. The glutamate system as a crucial regulator of CNS toxicity and survival of HIV reservoirs. Front Cell Infect Microbiol. 2020. https://doi.org/10.3389/fcimb.2020.00261.
33. Brison E, Jacomy H, Desforges M, Talbot PJ. Glutamate excitotoxicity is involved in the induction of paralysis in mice after infection by a human coronavirus with a single point mutation in its spike protein. J Virol. 2011;85(23):12464–73. https://doi.org/10.1128/JVI.05576-11.
34. Liu GJ, Nagarajah R, Banati RB, Bennett MR. Glutamate induces directed chemotaxis of microglia. Eur J Neurosci. 2009;29(6):1108–18. https://doi.org/10.1111/j.1460-9568.2009.06659.x.
35. Sanchis P, Fernández-Gayol O, Comes G, Escrig A, Giralt M, Palmiter RD, Hidalgo J. Interleukin-6 derived from the central nervous system may influence the pathogenesis of experimental autoimmune encephalomyelitis in a cell-dependent manner. Cells. 2020;9(2):330. https://doi.org/10.3390/cells9020330.
36. Sallmann S, Jüttler E, Prinz S, Petersen N, Knopf U, Weiser T, Schwaninger M. Induction of interleukin-6 by depolarization of neurons. J Neurosci. 2000;20(23):8637–42. https://doi.org/10.1523/JNEUROSCI.20-23-08637.2000.
37. Lotrich FE. Inflammatory cytokine-associated depression. Brain Res. 2015;1617:113–25. https://doi.org/10.1016/j.brainres.2014.06.032.
38. Dowlati Y, Herrmann N, Swardfager W, Liu H, Sham L, Reim EK, Lanctôt KL. A meta-analysis of cytokines in major depression. Biol Psychiat. 2010;67(5):446–57. https://doi.org/10.1016/j.biopsych.2009.09.033.
39. Bauer S, Kerr BJ, Patterson PH. The neuropoietic cytokine family in development, plasticity, disease and injury. Nat Rev Neurosci. 2007;8(3):221–32. https://doi.org/10.1038/nrn2054.
40. Haroon E, Miller AH, Sanacora G. Inflammation, glutamate, and glia: a trio of trouble in mood disorders. Neuropsychopharmacology. 2017;42(1):193–215. https://doi.org/10.1038/npp.2016.199.
41. Lauro C, Catalano M, Di Paolo E, Chece G, de Costanzo I, Trettel F, Limatola C. Fractalkine/CX3CL1 engages different neuroprotective responses upon selective glutamate receptor overactivation.

Front Cell Neurosci. 2015. https://doi.org/10.3389/fncel.2014.00472.
42. Binder GK, Griffin DE. Interferon-γ-mediated site-specific clearance of alphavirus from CNS neurons. Science. 2001;293(5528):303–6. https://doi.org/10.1126/science.1059742.
43. Ganor Y, Besser M, Ben-Zakay N, Unger T, Levite M. Human T cells express a functional ionotropic glutamate receptor GluR3, and glutamate by itself triggers integrin-mediated adhesion to laminin and fibronectin and chemotactic migration. J Immunol. 2003;170(8):4362–72. https://doi.org/10.4049/jimmunol.170.8.4362.
44. Miyanishi H, Nitta A. A role of BDNF in the depression pathogenesis and a potential target as antidepressant: The modulator of stress sensitivity "Shati/Nat8l-BDNF system" in the dorsal striatum. Pharmaceuticals. 2021;14(9):889. https://doi.org/10.3390/ph14090889.
45. Li H, Wang T, Shi C, Yang Y, Li X, Wu Y, Xu Z-QD. Inhibition of GALR1 in PFC alleviates depressive-like behaviors in postpartum depression rat model by upregulating CREB-BNDF and 5-HT levels. Front Psychiatry. 2018. https://doi.org/10.3389/fpsyt.2018.00588.
46. Li M, Li C, Yu H, Cai X, Shen X, Sun X, Wang J, Zhang Y, Wang C. Lentivirus-mediated interleukin-1β (IL-1β) knock-down in the hippocampus alleviates lipopolysaccharide (LPS)-induced memory deficits and anxiety- and depression-like behaviors in mice. J Neuroinflammation. 2017;14(1):190. https://doi.org/10.1186/s12974-017-0964-9.
47. Cirulli F, Berry A, Chiarotti F, Alleva E. Intrahippocampal administration of BDNF in adult rats affects short-term behavioral plasticity in the Morris water maze and performance in the elevated plus-maze. Hippocampus. 2004;14(7):802–7. https://doi.org/10.1002/hipo.10220.
48. Chamera K, Trojan E, Szuster-Głuszczak M, Basta-Kaim A. The potential role of dysfunctions in neuron-microglia communication in the pathogenesis of brain disorders. Curr Neuropharmacol. 2020;18(5):408–30. https://doi.org/10.2174/1570159X17666191113101629.
49. Marcolino MS, Anschau F, Kopittke L, Pires MC, Barbosa IG, Pereira DN, Ramos LEF, Assunção LFI, Costa ASM, Nogueira MCA, Duani H, Martins KPMP, Moreira LB, Silva CTCA, Oliveira NR, de Ziegelmann PK, Guimarães-Júnior MH, Lima MOSS, Aguiar RLO, Teixeira AL. Frequency and burden of neurological manifestations upon hospital presentation in COVID-19 patients: Findings from a large Brazilian cohort. J Neurol Sci. 2022. https://doi.org/10.1016/j.jns.2022.120485.
50. Pereira DN, Bicalho MAC, Jorge AO, Gomes AGR, Schwarzbold AV, Araújo ALH, Cimini CCR, Ponce D, Rios DRA, Grizende GMS, Manenti ERF, Anschau F, Aranha FG, Bartolazzi F, Batista JL, Tupinambás JT, Ruschel KB, Ferreira MAP, Paraíso PG, Marcolino MS. Neurological manifestations by sex and age group in COVID-19 inhospital patients. ENeurologicalSci. 2022;28:100419. https://doi.org/10.1016/j.ensci.2022.100419.
51. Chou SH-Y, Beghi E, Helbok R, Moro E, Sampson J, Altamirano V, Mainali S, Bassetti C, Suarez JI, McNett M, Nolan L, Temro K, Cervantes-Arslanian AM, Anand P, Mukerji S, Alabasi H, Westover MB, Kavi T, John S, David K. Global incidence of neurological manifestations among patients hospitalized with COVID-19—a report for the GCS-NeuroCOVID Consortium and the ENERGY Consortium. JAMA Network Open. 2021;4(5):e2112131. https://doi.org/10.1001/jamanetworkopen.2021.12131.
52. Solomon IH, Normandin E, Bhattacharyya S, Mukerji SS, Keller K, Ali AS, Adams G, Hornick JL, Padera RF, Sabeti P. Neuropathological features of Covid-19. N Engl J Med. 2020;383(10):989–92. https://doi.org/10.1056/NEJMc2019373.
53. Boroujeni ME, Simani L, Bluyssen HAR, Samadikhah HR, Zamanlui Benisi S, Hassani S, Akbari Dilmaghani N, Fathi M, Vakili K, Mahmoudiasl G-R, Abbaszadeh HA, Hassani Moghaddam M, Abdollahifar M-A, Aliaghaei A. Inflammatory response leads to neuronal death in human post-mortem cerebral cortex in patients with COVID-19. ACS Chem Neurosci. 2021;12(12):2143–50. https://doi.org/10.1021/acschemneuro.1c00111.
54. Csordás A, Mázló M, Gallyas F. Recovery versus death of "dark" (compacted) neurons in non-impaired parenchymal environment: light and electron microscopic observations. Acta Neuropathol. 2003;106(1):37–49. https://doi.org/10.1007/s00401-003-0694-1.
55. de Miranda AS, Rodrigues DH, Amaral DCG, de Lima Campos RD, Cisalpino D, Vilela MC, Lacerda-Queiroz N, de Souza KPR, Vago JP, Campos MA, Kroon EG. Dengue-3 encephalitis promotes anxiety-like behavior in mice. Behav Brain Res. 2012;230(1):237–42. https://doi.org/10.1016/j.bbr.2012.02.020.
56. Andrews MG, Mukhtar T, Eze UC, Simoneau CR, Ross J, Parikshak N, Wang S, Zhou L, Koontz M, Velmeshev D, Siebert C-V, Gemenes KM, Tabata T, Perez Y, Wang L, Mostajo-Radji MA, de Majo M, Donohue KC, Shin D, Kriegstein AR. Tropism of SARS-CoV-2 for human cortical astrocytes. Proc Natl Acad Sci. 2022. https://doi.org/10.1073/pnas.2122236119.
57. Winkler ES, Bailey AL, Kafai NM, Nair S, McCune BT, Yu J, Fox JM, Chen RE, Earnest JT, Keeler SP, Ritter JH, Kang L-I, Dort S, Robichaud A, Head R, Holtzman MJ, Diamond MS. SARS-CoV-2 infection of human ACE2-transgenic mice causes severe lung inflammation and impaired function. Nat Immunol. 2020;21(11):1327–35. https://doi.org/10.1038/s41590-020-0778-2.
58. Kumari P, Rothan HA, Natekar JP, Stone S, Pathak H, Strate PG, Arora K, Brinton MA, Kumar M. Neuroinvasion and encephalitis following intranasal inoculation of SARS-CoV-2 in K18-hACE2 mice. Viruses. 2021;13(1):132. https://doi.org/10.3390/v13010132.
59. Hoffmann M, Kleine-Weber H, Schroeder S, Krüger N, Herrler T, Erichsen S, Schiergens TS, Herrler G, Wu N-H, Nitsche A, Müller MA, Drosten C, Pöhlmann S. SARS-CoV-2 cell entry depends on ACE2 and TMPRSS2 and is blocked by a clinically proven protease inhibitor. Cell. 2020;181(2):271-280.e8. https://doi.org/10.1016/j.cell.2020.02.052.
60. Düsedau HP, Steffen J, Figueiredo CA, Boehme JD, Schultz K, Erck C, Korte M, Faber-Zuschratter H, Smalla K-H, Dieterich D, Kröger A, Bruder D, Dunay IR. Influenza A Virus (H1N1) infection induces microglial activation and temporal dysbalance in glutamatergic synaptic transmission. MBio. 2021. https://doi.org/10.1128/mBio.01776-21.
61. Olmo IG, Carvalho TG, Costa VV, Alves-Silva J, Ferrari CZ, Izidoro-Toledo TC, da Silva JF, Teixeira AL, Souza DG, Marques JT, Teixeira MM, Vieira LB, Ribeiro FM. Zika virus promotes neuronal cell death in a non-cell autonomous manner by triggering the release of neurotoxic factors. Front Immunol. 2017. https://doi.org/10.3389/fimmu.2017.01016.
62. Oladunni FS, Park JG, Pino PA, Gonzalez O, Akhter A, Allué-Guardia A, Olmo-Fontánez A, Gautam S, Garcia-Vilanova A, Ye C, Chiem K, Headley C, Dwivedi V, Parodi LM, Alfson KJ, Staples HM, Schami A, Garcia JI, Whigham A, Torrelles JB. Lethality of SARS-CoV-2 infection in K18 human angiotensin-converting enzyme 2 transgenic mice. Nat Commun. 2020;11(1):6122. https://doi.org/10.1038/s41467-020-19891-7.
63. Rothan H, Kumari P, Stone S, Natekar J, Arora K, Auroni T, Kumar M. SARS-CoV-2 infects primary neurons from human ACE2 expressing mice and upregulates genes involved in the inflammatory and necroptotic pathways. Pathogens. 2022;11(2):257. https://doi.org/10.3390/pathogens11020257.

64. Vieira-Alves I, Alves ARP, Souza NMV, Melo TL, Coimbra Campos LMC, Lacerda LSB, Queiroz-Junior CM, Andrade ACSP, Barcelos LS, Teixeira MM, Costa VV, Cortes SF, Lemos VS. TNF/iNOS/NO pathway mediates host susceptibility to endothelial-dependent circulatory failure and death induced by betacoronavirus infection. Clin Sci. 2023;137(7):543–59. https://doi.org/10.1042/CS20220663.
65. Heap RE, Marín-Rubio JL, Peltier J, Heunis T, Dannoura A, Moore A, Trost M (2021) Proteomics characterisation of the L929 cell supernatant and its role in BMDM differentiation. Life Sci Alliance 4(6): e202000957. https://doi.org/10.26508/lsa.202000957
66. Costa AP, Vieira C, Bohner LO, Silva CF, Santos EC, De Lima TC, Lino-de-Oliveira C. A proposal for refining the forced swim test in Swiss mice. Prog Neuropsychopharmacol Biol Psychiatry. 2013;45:150–5. https://doi.org/10.1016/j.pnpbp.2013.05.002.
67. Suman P, Zerbinatti N, Theindl L, Domingues K, Lino de Oliveira C. Failure to detect the action of antidepressants in the forced swim test in Swiss mice. Acta Neuropsychiatrica. 2018;30(3):158–67. https://doi.org/10.1017/neu.2017.33.

SUPPLEMENTARY MATERIAL

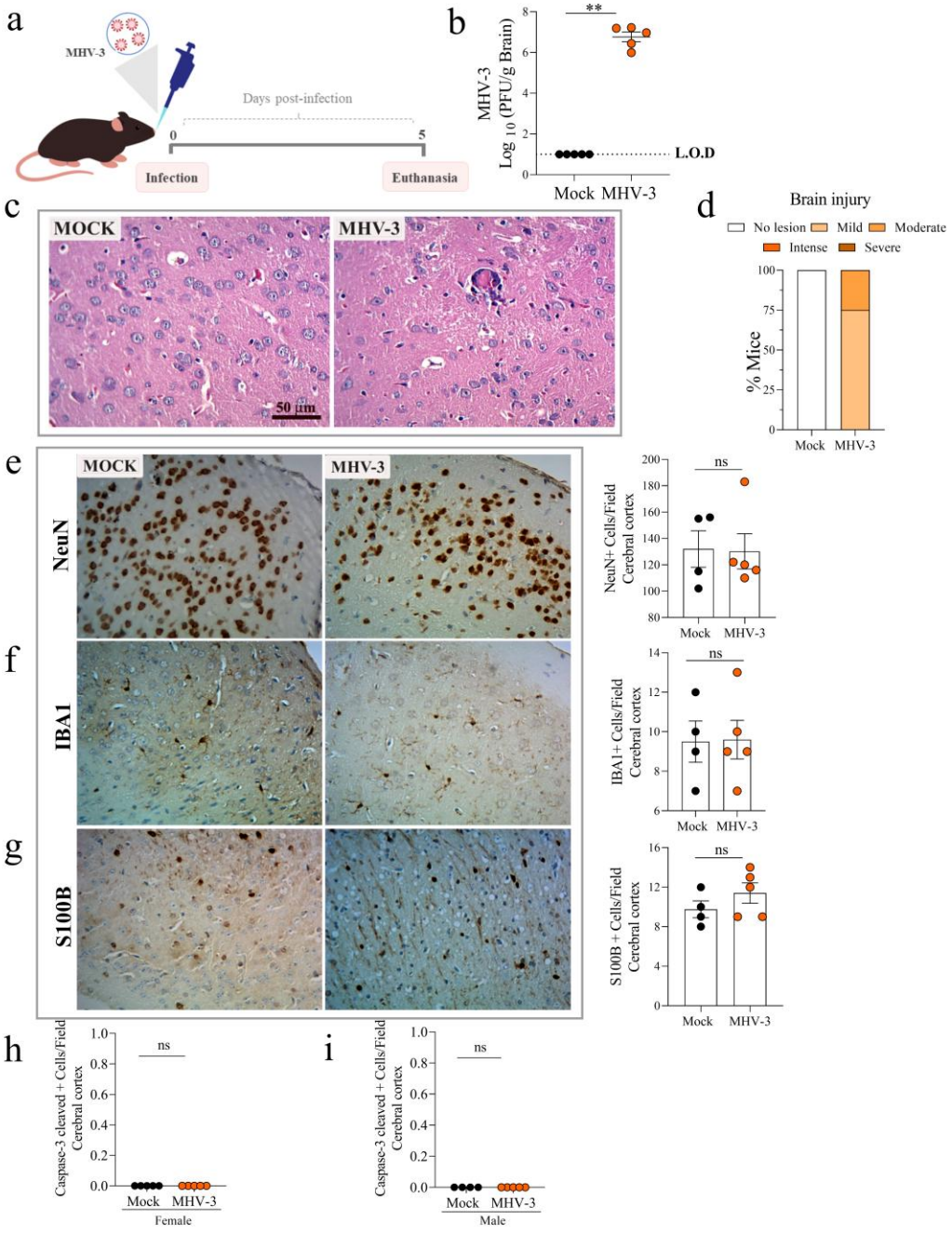

Fig. S1 Intranasal MHV-3 infection in C57BL/6 male mice at 5dpi. (a) Experimental design. (b) Viral titters quantified in brain extracts of MHV-3 infected mice by plaque assay. Results are demonstrated as log10 PFU per gram of tissue. Statistical comparison among groups were made using the t test [unpaired t test; mean (SD), n = 5]. LOD, limit of detection. ns, not significant ($P > 0.05$); *, $P < 0.05$; **, $P < 0.01$. (c) Hematoxylin and eosin (H&E) staining of sections of the cerebral cortex showed mild histological damage in infected mice, 50 µm bars. (d) Percentages of mice according to the degree of tissue damage in the brain. (e) Immunohistochemistry using antibodies against anti-NeuN (count of neurons), (f) anti-

IBA1 (microglia/macrophages count), (g) anti-S100B (astrocyte count). On the right of each graph are representative images and cells were quantified using ImageJ software. (h, i) anti-caspase-3 cleaved, female and male, respectively. Results are expressed as the mean of all cells counts per group and statistical comparison among groups were made using t test [unpaired t test; mean (SD), n =4 to 5].

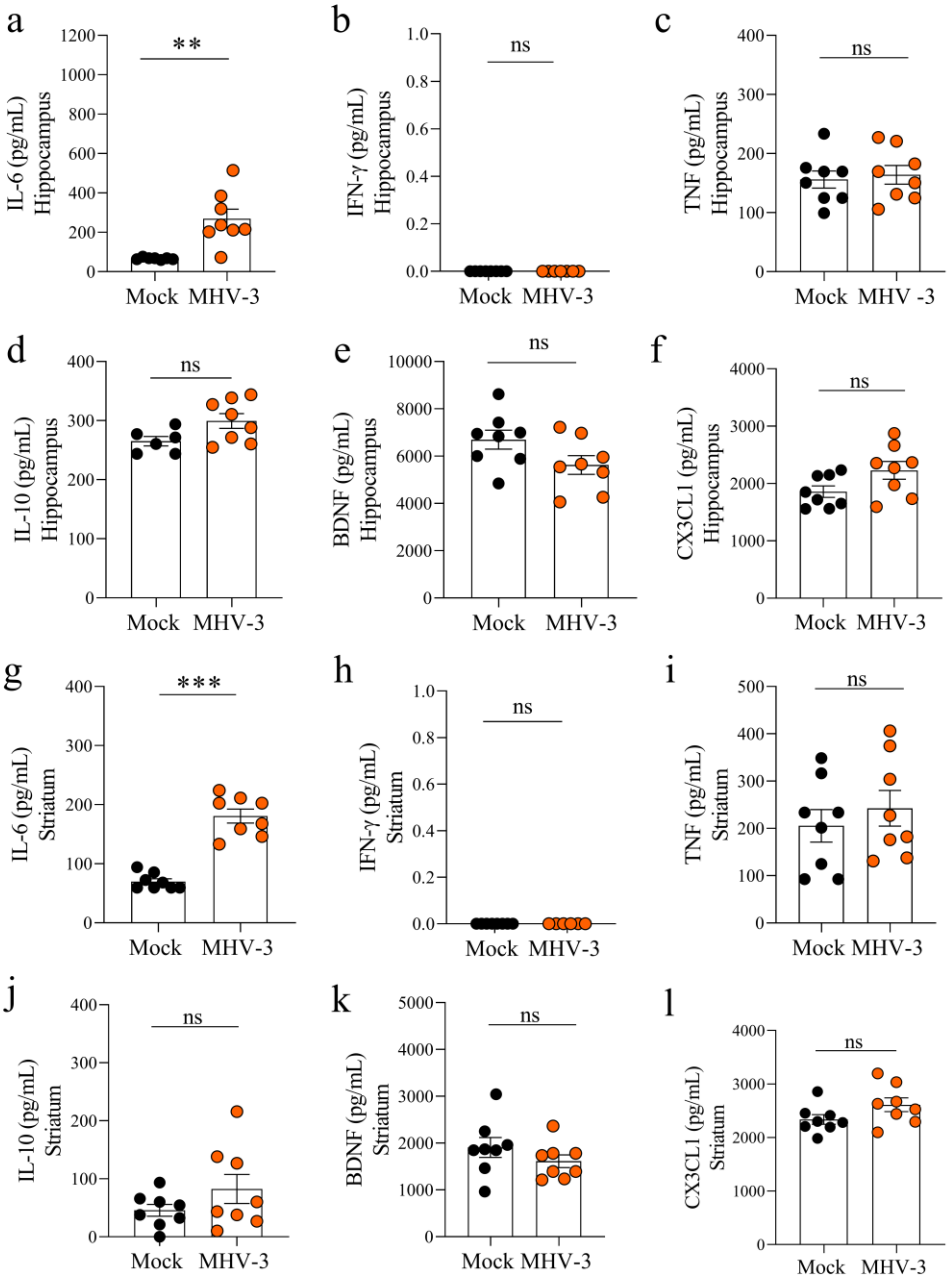

Fig. S2 Level of inflammatory mediators in the hippocampus and striatum of C57BL/6 female mice at 5 dpi. (a-f) Concentrations of mediators IL-6, IFN-γ, TNF, IL-10, BDNF and CX3CL1 (fractalkine) in hippocampus and striatum (g-l), quantified by ELISA in the of mock controls and MHV-3-infected mice

[unpaired t test; mean (SD); n= 6 to 8]. ns, not significant (P > 0.05); *, P< 0.05; **, P < 0.01; ***, P <0.001

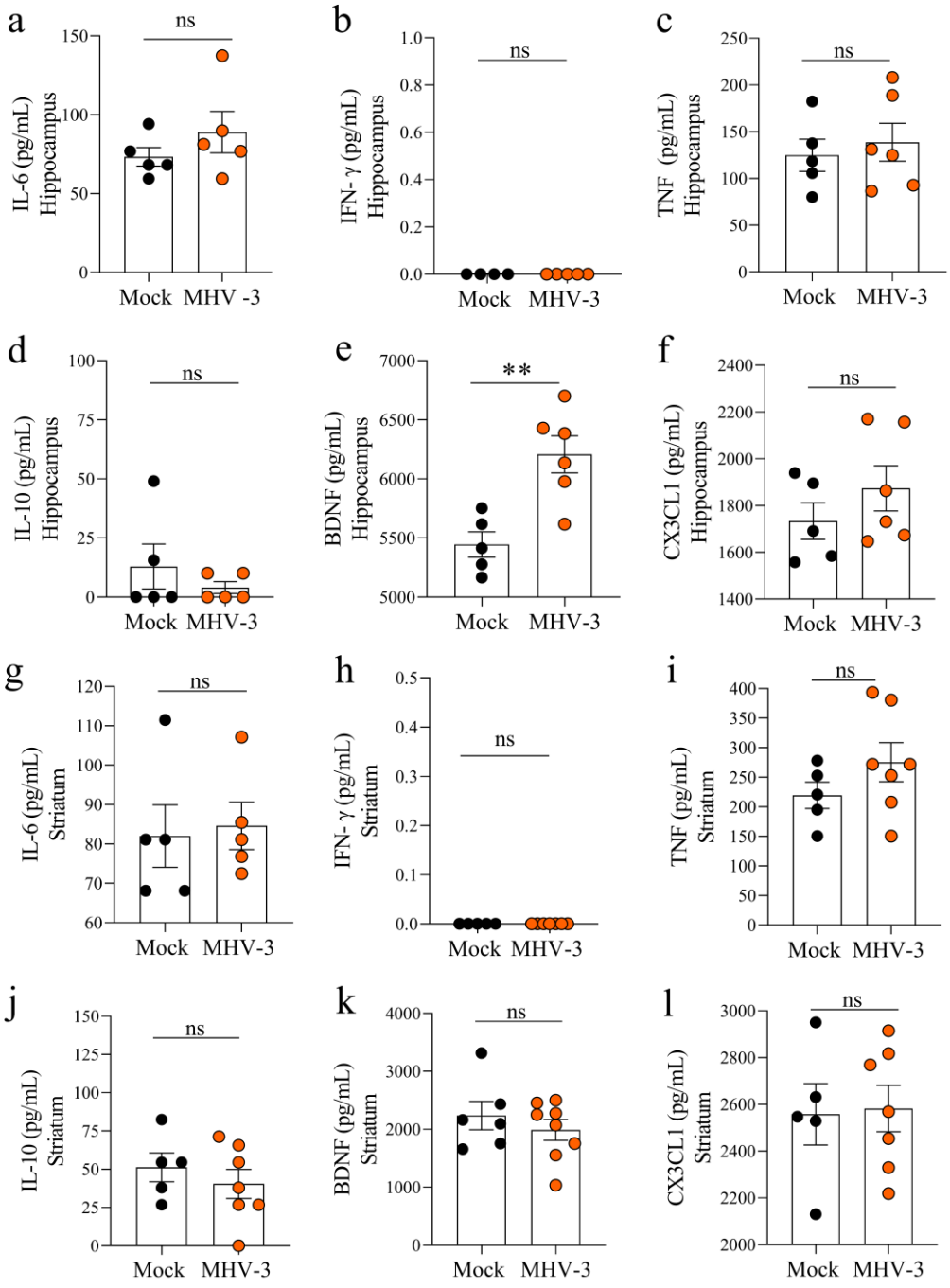

Fig. S3 Level of inflammatory mediators in the hippocampus and striatum of C57BL/6 male mice at 5 dpi. (a-f) Concentrations of mediators IL-6, IFN-γ, TNF, IL-10, BDNF and CX3CL1 in hippocampus and striatum (g-l), quantified by ELISA in the of mock controls and MHV-3-infected mice [unpaired t test; mean (SD); n= 4 to 5]. ns, not significant (P > 0.05); **, P < 0.01

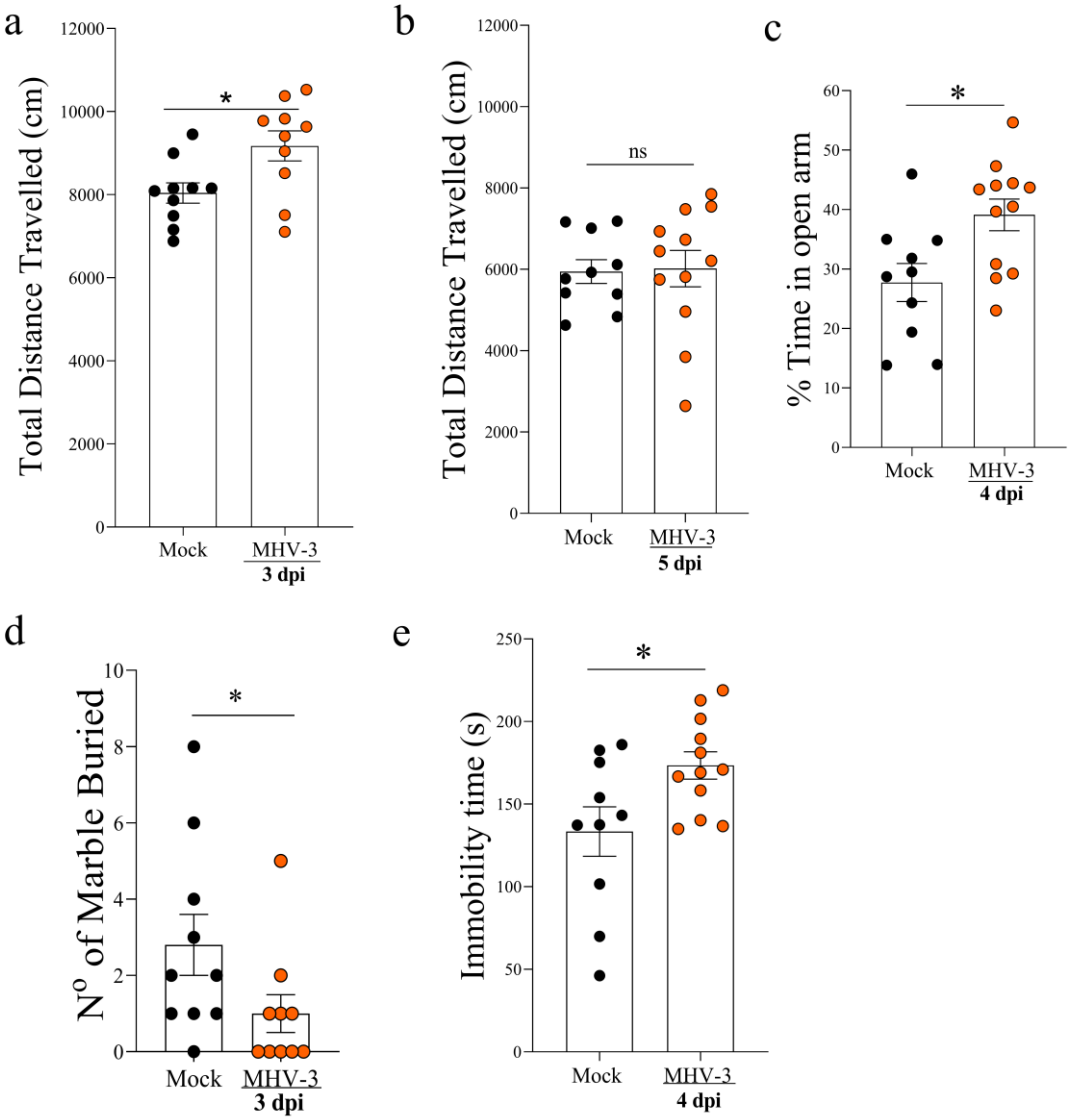

Fig. S4 MHV-3 infection induced anhedonia behavior in C57BL/6 male mice. (a, b) Locomotor activity on the 3rd and 5th day after infection, respectively (Open field test)**.** (c) Anxiety-like behavior on the 4th day after infection (Elevated plus maze). (d) Anhedonia behavior on the 3rd day after infection (Marble Buried test). (e) Depressive-like behavior on the 4th day after infection (Forced Swimming test). Statistical comparison among groups were made using Studen't t test [unpaired t test; mean (SD), n = 10 to 12]. ns, not significant ($P > 0.05$); *, $P < 0.05$

3.2 Trabalho científico II:

“Neuropsychiatric sequelae in an experimental model of post-covid syndrome in mice”

Este artigo apresenta uma análise abrangente da doença pulmonar e das sequelas neuropsiquiátricas em um modelo murino de síndrome pós-COVID-19, utilizando o betacoronavírus MHV-A59. A investigação abrangeu os efeitos agudos e crônicos da infecção com o objetivo de explorar alterações pulmonares, musculoesqueléticas e neuropsiquiátricas, além de avaliar respostas diferenciadas entre os sexos em camundongos C57BL/6 infectados.

Os resultados demonstraram uma infecção pulmonar transitória caracterizada por aumento de citocinas inflamatórias, alterações histológicas leves e recuperação funcional sem fibrose. Contudo, o impacto mais relevante foi observado nas sequelas neuropsiquiátricas. Camundongos fêmeas apresentaram comprometimentos comportamentais significativos, incluindo perda de memória espacial e anedonia, enquanto ambos os sexos experimentaram disfunção motora transitória. No contexto neuroinflamatório, fêmeas infectadas exibiram aumento no número de células IBA-1^{+} e S100B^{+}, acompanhado por níveis elevados de glutamato e cálcio intracelular no hipocampo, sugerindo um mecanismo de excitotoxicidade.

Um ponto crucial do estudo foi a identificação da influência hormonal nas sequelas neuropsiquiátricas, particularmente em fêmeas. A ovariectomia reverteu os déficits comportamentais observados, reforçando o papel dos hormônios sexuais nesse contexto. Importante notar que este procedimento não alterou a evolução da infecção pulmonar, mostrando que os camundongos não apresentaram comprometimento na capacidade em lidar com a infecção. Além disso, foram avaliados níveis de alguns hormônios no plasma, revelando que os camundongos fêmeas infectados apresentaram um pico de estradiol aos 60 dpi, níveis reduzidos de testosterona ao longo de todo o período observado e níveis de FSH elevados na maioria dos pontos de infecção avaliados. De fato, as sequelas neuropsiquiátricas estão associadas à mecanismos relacionados aos hormônios sexuais, principalmente a níveis reduzidos de testosterona. Em conclusão, o modelo implementado mimetiza muitas características clínicas da síndrome pós-COVID, evidenciando uma maior susceptibilidade de fêmeas a desenvolverem esta condição. Além disso, fornece uma plataforma promissora para explorar mecanismos subjacentes e para o desenvolvimento de estratégias terapêuticas.

Brain Behavior and Immunity

Neuropsychiatric sequelae in an experimental model of post-COVID syndrome in mice.

--Manuscript Draft--

Manuscript Number:	BBI-D-23-01808R2
Article Type:	Full Length Article
Section/Category:	Immunology
Keywords:	COVID-19; MHV-A59; Post-COVID syndrome; Long COVID; neuropsychiatric sequelae; Ovariectomy
Corresponding Author:	Vivian Costa, Ph.D Federal University of Minas Gerais BRAZIL
First Author:	Jordane Clarisse Pimenta

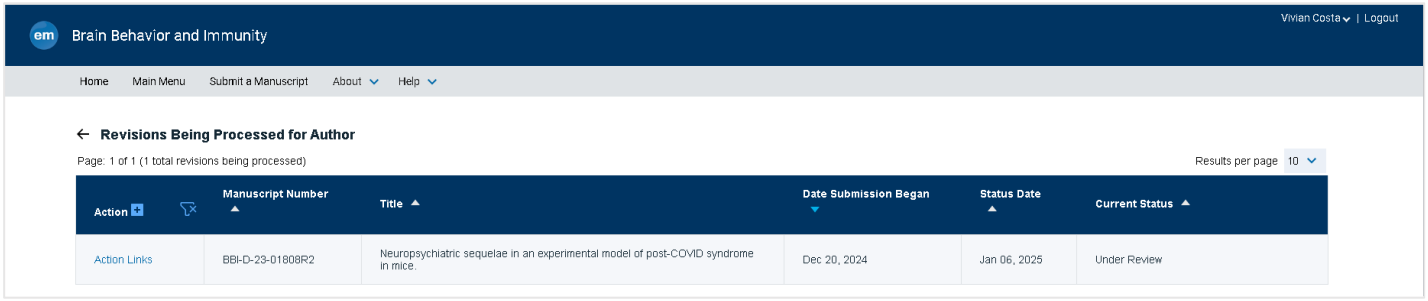

Neuropsychiatric sequelae in an experimental model of post-COVID syndrome in mice

Jordane Clarisse Pimenta[1#], Vinícius Amorim Beltrami[1#], Bruna Da Silva Oliveira[1#], Celso Martins Queiroz-Junior[1], Jéssica Barsalini[1], Danielle Cunha Teixeira[1], Luiz Pedro de Souza-Costa[4], Anna Luiza Diniz Lima[2], Caroline Amaral Machado[1], Bárbara Zuccolotto Schneider Guimarães Parreira[1], Felipe Rocha da Silva Santos[4], Pedro Augusto Carvalho Costa[6], Larisse De Souza Barbosa Lacerda[1], Matheus Rodrigues Gonçalves[5], Ian de Meira Chaves[1] , Manoela Gonzaga Gontijo Do Couto[1],Victor Rodrigues de Melo Costa[5] , Natália Ribeiro Cabacinha Nóbrega[1], Bárbara Luísa Silva[1], Talita Fonseca[1], Filipe Resende[1], Natália Teixeira Wnuk[1], Fernanda Martins Marim[9], Felipe Emanuel Oliveira Rocha[1], Hanna L. Umezu[6], Gabriel Campolina-Silva[1,7], Ana Cláudia dos Santos Pereira Andrade[1,8], Renato Santana de Aguiar[9], Guilherme Mattos Jardim Costa[1] , Pedro Pires Goulart Guimarães[6], Glauber Santos Ferreira da Silva[6] , Milene Alvarenga Rachid[10], Luciene Bruno Vieira[2], Vanessa Pinho[1], Antônio Lúcio Teixeira[3], Mauro Martins Teixeira[4], Aline Silva De Miranda[1*, a], Vivian Vasconcelos Costa[1*,a] .

[1]Department of Morphology, Institute of Biological Sciences, Universidade Federal de Minas Gerais, Belo Horizonte, MG, Brazil.

[2]Department of Pharmacology, Institute of Biological Sciences, Universidade Federal de Minas Gerais, Belo Horizonte, MG, Brazil.

[3]Biggs Institute, The University of Texas Health Science Center at San Antonio, San Antonio, TX, United States.

[4]Department of Biochemistry and Immunology, Institute of Biological Sciences, Universidade Federal de Minas Gerais, Belo Horizonte, MG, Brazil.

[5]Department of Microbiology, Institute of Biological Sciences, Universidade Federal de Minas Gerais, Belo Horizonte, MG, Brazil.

[6]Department of Physiology and Biophysics, Institute of Biological Sciences, Universidade Federal de Minas Gerais, Belo Horizonte, MG, Brazil.

[7]Department of Obstetrics, Gynecology and Reproduction, Faculty of Medicine, Université Laval, Quebec, Canada

[8]Department of Microbiology and Immunology, Université Laval, Quebec, Canada

[9]Department of Genetics, Ecology and Evolution, Institute of Biological Sciences, Universidade Federal de Minas Gerais, Belo Horizonte, MG, Brazil.

[10] Department of General Pathology, Institute of Biological Sciences, Universidade Federal de Minas Gerais, Belo Horizonte, MG, Brazil.

# These authors contributed equally

*Both are corresponding authors

[a]Corresponding authors at: Departamento de Morfologia, Instituto de Ciências Biológicas, Universidade Federal de Minas Gerais, Avenida Antônio Carlos, 6.627, Pampulha, CEP 31270-901, Belo Horizonte, MG, Brasil. E-mail addresses: vivianvcosta@gmail.com (V.V. Costa); mirandas.aline@gmail.com (A. S. Miranda).

Word Count: 19.301

Abstract

The global impact of the COVID-19 pandemic has been unprecedented, and presently, the world is facing a new challenge known as post-COVID syndrome (PCS). Current estimates suggest that more than 65 million people are grappling with PCS, encompassing several manifestations, including pulmonary, musculoskeletal, metabolic, and neuropsychiatric sequelae (cognitive and behavioral). The mechanisms underlying PCS remain unclear. The present study aimed to: (i) comprehensively characterize the acute effects of pulmonary inoculation of the betacoronavirus MHV-A59 in immunocompetent mice at clinical, cellular, and molecular levels; (ii) examine potential acute and long-term pulmonary, musculoskeletal, and neuropsychiatric sequelae induced by the betacoronavirus MHV-A59; and to (iii) assess sex-specific differences. Male and female C57Bl/6 mice were initially inoculated with varying viral titers ($3x10^3$ to $3x10^5$ PFU/30 μL) of the betacoronavirus MHV-A59 via the intranasal route to define the highest inoculum capable of inducing disease without causing mortality. Further experiments were conducted with the $3x10^4$ PFU inoculum. Mice exhibited an altered neutrophil/lymphocyte ratio in the blood in the 2nd and 5th day post-infection (dpi). Marked lung lesions were characterized by hyperplasia of the alveolar walls, infiltration of polymorphonuclear leukocytes (PMN) and mononuclear leukocytes, hemorrhage, increased concentrations of CCL2, CCL3, CCL5, and CXCL1 chemokines, as well as high viral titters until the 5th dpi. While these lung inflammatory signs resolved, other manifestations were observed up to the 60 dpi, including mild brain lesions with gliosis and hyperemic blood vessels, neuromuscular dysfunctions, anhedonic-like behavior, deficits in spatial working memory, and short-term aversive memory. These musculoskeletal and neuropsychiatric complications were exclusive to female mice and were prevented after ovariectomy. In summary, our study describes for the first time a novel sex-dependent model of PCS focused on neuropsychiatric and musculoskeletal disorders. This model provides a unique

platform for future investigations regarding the effects of acute therapeutic interventions on the long-term sequelae unleashed by betacoronavirus infection.

Keywords: COVID-19, MHV-A59, post-COVID syndrome, long COVID, neuropsychiatric sequelae, ovariectomy.

1. Introduction

The global impact of the COVID-19 pandemic caused by the betacoronavirus SARS-CoV-2 has been unprecedented. It has affected over 777 million people, resulting in more than 7 million deaths worldwide (WHO, 2024). The peak of the pandemic overwhelmed the healthcare systems globally (Huang et al., 2020). Despite the subsequent development and approval of vaccines, our understanding of the enduring effects of COVID-19, particularly the long-term consequences known as long-COVID or Post-COVID syndrome (PCS), remains incomplete (Phillips and Williams, 2021).

Post-COVID syndrome (Proal et al., 2023; WHO, 2024) is a condition marked by the persistence of symptoms for months or even years after confirmed acute infection by SARS-CoV-2 (Proal and VanElzakker, 2021; WHO, 2024). Current estimates suggest that more than 65 million people are grappling with PCS (Ballering et al., 2022). The condition seems to affect approximately 10-30% of non-hospitalized individuals, 50-70% hospitalized individuals, and around 10-12% of vaccinated individuals (Davis et al., 2023). Post-COVID syndrome may affect any age group and is not necessarily associated with the severity of the acute phase of the disease (Davis et al., 2023; Mao et al., 2020a; Mao et al., 2020b; Zheng et al., 2020).

Clinically, PCS encompasses a broad spectrum of manifestations attributed to the widespread viral tropism associated with the expression of the ACE-2 receptor across various cell types (Hikmet et al., 2020). Symptoms of PCS include fatigue, impaired breathing (Tsuchida et al., 2023), arthralgia and myalgia (Romero et al., 2023), bone pain (Davis et al., 2021), cardiac symptoms as palpitations (Jiang et al., 2023), gastrointestinal changes including altered bowel habits and bloating (Comelli et al., 2022), as well as neuropsychiatric impairment, such as cognitive complaints (often referred to as “brain fog”), anxiety and depression (reviewed in Badenoch et al., 2022). These neuropsychiatric sequelae constitute a major concern since they may be associated with an increased risk of developing long-term cognitive impairment and

dementia (García-González et al., 2023). A systematic review and meta-analysis examining persistent neuropsychiatric symptoms following COVID-19 revealed that among nearly 19,000 patients, 27.4% reported sleep disorder, 24.4% experienced fatigue, and 15.7% exhibited symptoms consistent with post-traumatic stress disorder (PTSD) (Simani et al., 2021), 35,5% cognitive dysfunction, 19.1% anxiety, 12.9% depression, 11.4% dysosmia, 7.4% dysgeusia, 6.6% headache, 5.5% disorder sensorimotor and 2.9% dizziness (Badenoch et al., 2022). Another comprehensive meta-analysis of 151 studies involving 1,285,407 participants across 32 countries examined the long-term physical and mental effects of COVID-19. Among the 659,454 survivors studied up to 12 months post-infection, 28.7% reported fatigue, 18.3% experienced depression, 17.9% showed symptoms of PTSD, and 19.7% displayed cognitive deficits (Zeng et al., 2023). Importantly, a study has shown that the risk of neuropsychiatric symptoms may be higher in COVID-19 than in other conditions, such as sepsis (Stallmach et al., 2022). Several hypotheses have been proposed to explain the development of neuropsychiatric and other non-pulmonary symptoms during the PCS, but the underlying mechanisms remain elusive. These hypotheses encompass: (i) the systemic acute inflammatory process and dysregulation of the immune response (Frere et al., 2022); (ii) the persistence of SARS-CoV-2 in immune privileged reservoirs (Stein et al., 2022); (iii) autoimmunity triggered by infection (Woodruff et al., 2022); (iv) microbiome dysbiosis (Mendes de Almeida et al., 2023); (v) reactivation of latent viruses such as Epstein-Barr (EBV) (Chen et al., 2021); (vi) dysfunctional neuronal signaling (Spudich and Nath, 2022); and/or (vii) sex-related susceptibility (Bai et al., 2022). Given the societal impact of the disease, there is a great need to understand the pathogenesis of PCS, which would allow the development of specific therapeutic strategies. Currently, the available approaches have focused on symptom management and rehabilitation measures (Möller et al., 2023).

Wild-type mice have shown resistance to SARS-CoV-2 infection (Dinnon et al., 2020; Gu et al., 2020). To study coronavirus infections in mice, researchers commonly use

betacoronaviruses such as Murine Hepatitis Viruses (MHV-1, MHV-3, MHV-A59, and MHV-S strains), which naturally infect mice. They are associated with pulmonary infection and disease, effectively mimicking several aspects of human coronavirus infections (Andrade et al., 2021a; De Albuquerque et al., 2006; Yang et al., 2014). In this study, we thoroughly examined the acute effects of the intranasal inoculation of the betacoronavirus MHV-A59 and the potential long-term pulmonary and neuropsychiatric sequelae. Our findings revealed that MHV-A59 intranasal inoculation leads to transient lung infection and female hormone-dependent brain inflammation, followed by long-term cognitive and behavioral changes mimicking several aspects of long-COVID syndrome. This model provides a unique platform for investigating the pathogenesis of long-COVID and the therapeutic impact of antiviral, anti-inflammatory, or neuroprotective strategies.

2.Material and Methods

2.1 Mice

Animal experimental procedures were approved by the Ethical Committee for Animal Experimentation of the Universidade Federal de Minas Gerais (UFMG) (process number 140/2023). Experiments were carried out with male and/or female wild-type 5 and 6-weeks-old C57BL/6 mice (Central Animal House of the UFMG), as described in figure legends. Mice were housed in individually ventilated cages placed in an animal care facility at 24°C ± 2°C on a 12-h light/12-h dark cycle, receiving *ad libitum* access to water and food.

2.2 Cells and virus

L929 cells were cultured under a controlled atmosphere (37°C and 5% CO_2) in high-glucose Dulbecco's modified Eagle's medium (DMEM) supplemented with 7% fetal bovine

serum (FBS), 100 μg/mL streptomycin and 100 U/mL penicillin. The MHV-A59 strain was purchased from ATCC (Manassas, Virginia, USA) and propagated in L929 cells.

2.3 MHV-A59 infection

Mice were anesthetized intraperitoneally with ketamine (80 mg/kg) and xylazine (15 mg/kg) and intranasally inoculated with 30 μL of sterile saline containing *or not* (Mock control) MHV-A59. The experimental designs varied based on the objectives:

Figure 1: Male and female C57BL/6 mice were infected with 3×10^3 to 3×10^5 PFU of MHV-A59. Weight loss and survival were monitored daily for 14 days post-infection (dpi). In a separate cohort (3×10^4 PFU), mice were euthanized at 2, 5, 8, 16, 30, and 60 dpi to assess circulating neutrophils, lymphocytes, organ-specific viral titters (lung, liver, spleen, plasma), and lung histopathology and function.

Figure 2: Mice infected with 3×10^4 PFU were euthanized at 2, 5, and 8 dpi to evaluate lung immune populations, including neutrophils, dendritic cells, $CD4^+$ and $CD8^+$ T cells, and natural killer cells.

Figure 3: Behavioral tests (open field, marble burying, sucrose preference, Y-maze, grip-force, step-down inhibitory avoidance, olfactory discrimination) were conducted from 5 to 60 dpi in mice infected with 3×10^4 PFU.

Figure 4: Mice infected with 3×10^4 PFU were euthanized at 2, 5, 8, 16, 30, and 60 dpi to measure viral load and markers of macrophages/microglia (IBA-1) and astrocytes (S100B) in brain samples. Brain glutamate and synaptosomal calcium levels were analyzed at 5 and 30 dpi.

Figure 5: Mice were euthanized at 2, 5, and 8 dpi to evaluate brain neutrophils, microglia, and $CD4^+$/$CD8^+$ T-cell populations. At 2, 5, 8, 16, 30, and 60 dpi, hippocampal and prefrontal cortex levels of CX3CL1, BDNF, and IL-6 were quantified.

Figure 6: Female mice were infected with 3×10^4 PFU and euthanized at 2, 5, 8, 16, 30, and 60 dpi to measure plasma estradiol, FSH, and testosterone. In an additional group (ovariectomized/non-ovariectomized), lung and brain viral loads, histopathology, and behavioral changes (marble burying, Y-maze, grip-force) were assessed from 5 to 60 dpi.

2.4 Sample collection

Mice were intraperitoneally anesthetized with ketamine (80 mg/kg) and xylazine (15 mg/kg), and blood samples were collected from the abdominal vena cava for cell count (neutrophil to lymphocyte ratio (NLR) analyses determined with a Celltac MEK-6500K hemocytometer (Nihon Kohden) and euthanized by cervical dislocation. The lungs were collected, and the left lobe was fixed in 4% formaldehyde-buffered solution for histological analyses. The right lung lobes, brain, liver, and spleen were snap-frozen in liquid nitrogen and stored at -80 °C for viral titration, ELISA, and PCR assays. In another set of experiments whole lung and brain samples were collected for flow cytometry assays.

2.5 Viral titration

To evaluate viral titters, serially diluted virus suspension of plasma samples, lung, liver, spleen, and brain tissue homogenates (1:9 tissue to DMEM) were inoculated onto a confluent monolayer of L929 cells grown in 24-well plates. After gentle shaking for 1 h, samples were removed and replaced with DMEM containing 0.8% carboxymethylcellulose, 2% FBS, and 1% penicillin-streptomycin-glutamine and kept for 3 days at 37 °C and 5% CO_2. Then, cells were fixed with 10% neutral buffered formalin solution for 2h and stained with 0.1% crystal violet. Virus titters were determined as PFU/mL or PFU/mg of tissue.

2.6 Histopathology

To evaluate lung and brain inflammatory scores, formaldehyde-fixed and paraffin-embedded lung and brain tissues were sectioned into 5-μm-thickness slices and stained with hematoxylin and eosin (H&E) or Masson's trichrome stain. The inflammatory score in the lungs and brain of mice was determined blindly by two pathologists and the result was expressed as the average of the two analyses (C.M.Q.J.) and (M.A.R). Lung inflammatory score encompasses (1) airway (0 to 4 points), (2) vascular (0 to 4 points), (3) parenchyma damage (0 to 5 points), and (4) general neutrophil infiltration (0 to 5 points). In the brain, the evaluation was carried out in the cortex and hippocampus following a point scale: 0, no lesion; 1, mild tissue injury and/or mild inflammation; 2, mild tissue injury and/or moderate inflammation; 3, definitive tissue damage (neuronal loss and parenchymal damage) and intense inflammation; 4, necrosis (complete loss of all tissue elements with the presence of cellular debris). Meningeal inflammation was assessed using a point scale (0 to 4), with 0 representing no inflammation and 1 to 4 corresponding to 1 to 4 layers affected by inflammation. The final score was the sum of the cerebral cortex and hippocampus scores plus the meningitis score, totaling 12 points (Pimenta et al, 2023).

2.7 Mechanics of the respiratory system

To measure the compliance of the respiratory system, full-range pressure-volume (PV) curves were completed like those described in previous studies of our group (Pereira et al., 2023; Andrade et al., 2021) and adapted from Limjunyawong et al., 2015 and Robichaud et al., 2017. Briefly, mice were divided into three groups: control (mock), 5- and 30-dpi. The animals were deeply anesthetized, and a polyethylene tube (P50) was inserted into the mouse’s trachea. The PV curve was generated by injecting air volume continuously using a 3 mL syringe and an automated syringe pump (Bonther, Ribeirão Preto, SP, Brazil) at a rate of 3 mL/min until the

intratracheal pressure peaked at approximately 35 cm H_2O. At peak pressure, the syringe pump was manually switched for the deflation limb, deflated at the same rate until the pressure reached approximately -15 cm H_2O, and finally inflated again to the resting lung volume. Both volume and pressure signals were acquired and recorded using PowerLab software (LabChart v7, AdInstruments, Sydney, Australia). Inflation and deflation were repeated at least twice to obtain accurate curves, and full-range PV curves for each animal were obtained. If leaks or high pressures were detected, the data for that animal were not included in the analysis. Vital capacity was determined by maximum insufflation (lung volume at 35 cm H_2O), and static compliance of the respiratory system (expressed in mL/cmH2O) was measured at the steepest point of the deflation limb of the PV curve (Andrade et al., 2021; Limjunyawong et al., 2015; Robichaud et al., 2017).

2.8 Cytokine and chemokine measurement

For the determination of inflammatory mediators in the lung and brain tissues, the samples were homogenized in chilled cytokine extraction buffer (100 mM Tris [pH 7.4], 150 MM NaCl, 1 mM EGTA, 1 mM EDTA, 1% Triton X-100, 0.5% sodium deoxycholate and 1% protease inhibitor cocktail). After centrifugation (10,000 rpm, 10 min, 4 °C), the supernatant was collected and used to measure inflammatory mediators using the DuoSet enzyme-limited immunosorbent assay (ELISA) system (R&D Systems). The concentrations of CXCL1, CCL2, CCL3, CCL5, TNF, IL-1β, IL-6, IFN-γ, IL-10 and TGF-β were measured in the lung supernatant. IL-6, IFN-γ, BDNF (brain-derived neurotrophic factor), and CX3CL1 (fractalkine) were measured in the prefrontal cortex (PFC) and hippocampus.

To perform plasma estradiol measurement, 0.3 mL blood was collected and centrifuged at 2,000 rpm for 10 min to separate the plasma, which was subsequently stored at -20°C. Plasma estradiol levels were measured using enzyme-linked immunosorbent assay (ELISA) with the

commercial AccuBind kit (Monobind Inc., USA). To determine the estradiol concentration, a curve graph was constructed using the absorbance of each duplicate serum reference and the corresponding concentration of the estradiol standard in pg/mL.

The quantification of anti-MHV-A59 IgG/IgM antibodies followed the methodology outlined by Costa et al. (2014). In brief, 96-well plates were initially coated with the MHV-A59 isolate at 10^6 PFU/well. Subsequently, the plates underwent a one-hour exposure to UV-C light to render the virus inactive, followed by an overnight incubation at 4°C and 1% bovine albumin PBS solution blocking for a duration of 2 hours. Then, serum samples diluted at 1:200 for IgG and 1:20 for IgM were applied and allowed to incubate for 3 hours at 37 °C. Post-incubation, a peroxidase-Anti-IgG or anti-IgM antibody was applied and incubated for an additional 2 hours. Results were quantified in abstract units, derived from the detected absorbance readings in conjunction with the respective dilutions. Measurements of the absorbance were conducted using an ELISA reader (Status-labsystems, Multiskan RC, Uniscience do Brasil) set at 490 nm. The antibodies used are listed in Table 1.

2.9 Estradiol, FSH (Follicle Stimulating Hormone) e testosterone measurement

We performed hormone assays using the AccuBind® ELISA Test System to measure testosterone, follicle-stimulating hormone (FSH), and estradiol levels. This system utilizes a microplate enzyme immunoassay with colorimetric detection to quantitatively determine hormone concentrations. We collected 0.3 mL blood samples from anesthetized animals to carry out these analyses. The blood samples were centrifuged at 10,000 RPM for 10 minutes to separate the plasma and stored at -20°C.

For the testosterone assay (Product Code: 3725-300), we used a competitive enzyme immunoassay method. We used a sample volume of 0.010 mL, and the final concentration was expressed in nanograms per milliliter (ng/mL). Testosterone in the sample competed with an

enzyme-antigen combination for antibody binding sites. As testosterone levels increased, enzyme activity decreased. After adding the enzyme and biotin reagents, samples were incubated for 60 minutes at room temperature (20-27°C). After the incubation period, absorbance was measured at 450nm with a reference wavelength of 620-630nm using a microplate reader.

For the follicle-stimulating hormone (FSH) assay (Product Code: 425-300), we utilized an immuno-enzymometric method. We used a sample volume of 0.050 mL, and the final concentration was expressed in milli-international units per milliliter (mIU/mL). This method involved forming a sandwich complex with high-affinity antibodies, where enzyme activity was directly correlated with antigen concentration. After adding the enzyme reagent, the samples were incubated for 60 minutes at room temperature. Using a microplate reader, the absorbance was then measured at 450nm with a reference wavelength of 620-630nm.

For the estradiol assay (Product Code: 4925-300), a delayed competitive enzyme immunoassay approach was employed. We used a sample volume of 0.025 mL, and the final concentration was expressed in picograms per milliliter (pg/mL). Native estradiol in the sample competed with an enzyme-labeled analog for antibody binding, with the enzyme activity inversely proportional to the estradiol concentration. The assay required a two-step incubation process: an initial 30-minute incubation at room temperature after adding the biotin reagent, followed by a 90-minute incubation after adding the enzyme reagent. After incubation, absorbance was measured at 450nm with a reference wavelength of 620-630nm using a microplate reader.

For all assays, we plotted a dose-response curve with the absorbance of each serum reference against hormone concentration to determine unknown sample concentrations by locating their average absorbance on the curve. The assays required that reagents, serum calibrators, and controls be brought to room temperature (20-27°C) before use.

2.10 Flow cytometry

To assess infiltrating cell immunophenotyping and intracellular cytokines, brain and lung tissues were collected, processed, and enriched. Brain tissues underwent maceration, Percoll gradient separation, and filtration. Lung tissues were dissected, digested with Collagenase I, dissociated, and filtered. Cells were washed in the FACS buffer, and dead cells were excluded. Extracellular and intracellular antigens were labeled after fixation and permeabilization. The LSR-FORTESSA equipment was used for acquisition, and data were analyzed using singlets with FSC-A versus FSC-H gate. In the lung, live leukocytes (neutrophils, T $CD4^+$, $CD8^+$, NK cells, and dendritic cells) were characterized. In the brain, infiltrated T subsets and neutrophils were evaluated, along with activated microglia. IFN-γ, IL-10, and iNOS production were measured in each cell subset in the brain and lung microenvironment using intracellular staining. Isolated cells were maintained for 4 hours in RPMI with supplements, and Brefeldin A. FlowJo V10.4.11 was used for data analysis, and the antibodies used are listed in Table 1.

2.11 IBA-1 and S100B Immunohistochemistry in brain samples

Sections of the cerebral cortex and hippocampus from MHV-A59-infected mice and the control group (mock) were quantitatively analyzed for microglia, IBA-1 (ionized calcium-binding adapter molecule 1; antibody PA5-21274, Invitrogen; 1:150) and astrocytes (anti-S100 beta antibody; ab41548, Abcam; 1:75), according to the manufacturer's instructions (Vector Elite kit). The quantification of IBA-1, for microglial cells, and S100B, for astrocytes, was carried out from 10 random sections of the histological section of the brain areas using the Image J® software (National Institute of Health, USA).

2.12 Purification of synaptosomes

Mice infected with MHV-A59, and control mice were euthanized by cervical dislocation, since experiments involving the evaluation of neurotransmitters are subject to interference from drugs, such as anesthetics (Hao et al., 2020). The cortex and/or hippocampus were promptly dissected and homogenized in a gradient solution composed of 320 mM sucrose, 0.25 mM dithiothreitol, and 1 mM EDTA. Subsequently, the homogenate underwent low-speed centrifugation (1000 *g* × 10 min). Synaptosomes were then isolated from the supernatant through discontinuous Percoll density gradient centrifugation, as detailed by Dunkley et al. (1988). The isolated nerve terminals were resuspended in Krebs–Ringer-HEPES (KRH) solution, which included 124 mM NaCl, 4 mM KCl, 1.2 mM $MgSO_4$, 10 mM glucose, 25 mM HEPES, with pH adjusted to 7.4 and devoid of additional $CaCl_2$, achieving a concentration of approximately 10 mg/mL. For the assessment of glutamate release and intrasynaptosomal calcium concentration, 30 μL aliquots were prepared and maintained on ice until further use.

2.13 Glutamate measurements

To assess continuous glutamate release, a fluorometric assay was conducted using a Synergy TM2 fluorimeter (Biotek®). Fluorescence emission was recorded with an excitation wavelength of 360 nm and emission at 450 nm. Glutamate release was indirectly quantified by monitoring the fluorescence increase resulting from NADPH production in the presence of glutamate dehydrogenase type II and $NADP^+$ (according to Nicholls et al., 1987). In brief, synaptosomes were incubated with 1 mM $CaCl_2$ and 1 mM $NADP^+$ in KRH medium for 5 minutes. Glutamate dehydrogenase (50 units per well) was introduced after 5 minutes. Depolarization was induced using 33 mM KCl. A calibration curve was established by adding glutamate (5 nM/μL) to the reaction medium. Glutamate levels were normalized to the total protein content per well.

2.14 Intrasynaptosomal free calcium measurements

For the determination of intrasynaptosomal free calcium concentration, synaptosomes were preincubated with 5 μmol/L of Fura-2 pentakis (acetoxymethyl) Ester (FURA2-AM) probe for 30 minutes at 35.5 °C. Subsequently, the synaptosomes were centrifuged (3,000 *g* × 60 s), resuspended in KRH without $CaCl_2$, and reincubated for 30 minutes. Following washout with $CaCl_2$-free KRH, synaptosomes were promptly employed for the quantification of intracellular free calcium ($[Ca^{2+}]i$). Fluorescence was recorded at an excitation wavelength of 340/380 nm and an emission of 510 nm. $CaCl_2$ (1 mmol/L, final concentration) was introduced into the synaptosomal suspension before reading, and 33 mM of KCl was added to induce calcium influx. Finally, 10% SDS was added to establish Rmax, and tris-EGTA (3 mol/L Tris, 400 mmol/L EGTA, pH 8.6) was introduced to establish Rmin, following the procedures outlined by Grynkiewicz et al., 1985; Nicholls et al., 1987.

2.15 Ovariectomy (OVX)

To study the effect of female sex hormones in MHV-A59-induced sequelae, 6-week-old female C57BL/6 mice were anesthetized (ketamine 80 mg/kg, xylazine 15mg/kg, i.p.) and ovariectomized bilaterally (group OVX). Sham-operated mice were subjected to the same experimental procedure but without ovariectomy (group SHAM). Fourteen days after the surgery, groups of Sham or OVX mice were inoculated with MHV-A59 (3×10^4 PFU in 30 μL) or sterile saline (30 μL) intranasally. Mice were evaluated for neuropsychiatric sequelae along 60 dpi or euthanized at 2, 5, or 60 dpi for lung, brain, uterus, and plasma collection. The uterus weight was determined to detect uterus atrophy induced by female hormones' deficiency.

2.16 Open field test

The open field test was employed 5, 16, and 28 days after MHV-A59 infection to measure spontaneous locomotor activity as described elsewhere (Hefner and Holmes, 2007). Briefly, mice were gently placed in an arena (30 cm × 30 cm × 50 cm square), and then they were allowed to explore the arena for 30 min freely. Key parameters were recorded, such as spontaneous locomotor activity and the percentage of time spent in the center of the arena (a measure of anxiety-like behavior). The test was conducted using the Phenotyper apparatus (Noldus, Information Technology, Leesburg, VA, USA), containing a digital video camera and infrared lights in each arena. The EthoVision video tracking software (EthoVision XT, Noldus Information Technology, Leesburg, VA, USA) was used for data recording and analysis.

2.17 Marble burying

The marble burying test was performed 34 days after MHV-A59 infection to evaluate compulsive-like behavior as described by Kalueff et al., 2006. Briefly, mice were placed in a rectangular cage (30 × 30 × 50 cm) with 20 cm of fresh bedding and 25 marbles placed equidistant to each other. The animals were allowed to explore and bury the marbles freely for 30 minutes. At the end of the session, we removed the mouse and measured the number of marbles buried. We considered only the balls buried by more than 2.5 cm. A significant increase in the number of balls buried indicates compulsive-like behavior. However, associated with tests like the sucrose preference, a decrease in the number of balls buried reinforces an anhedonic-like behavior.

2.18 Sucrose preference test

The sucrose preference test (SPT) was performed to measure anhedonia-like behavior as described elsewhere (De Bundel et al., 2013). Anhedonia is conceived as the reduction or loss of

interest in pleasurable feelings or enjoyable activities. The SPT is based on a two-bottle choice test that measures the preference of mice to intake a sweet solution, being the reduced interest indicative of anhedonia-like behavior. Double-housing mice were initially habituated for 2 days with two water bottles. During the next 3 days, one water bottle was replaced with a bottle with sucrose solution (1%). The percentage of sucrose consummation was recorded, and a significant decrease in this parameter indicates an anhedonic-like behavior.

2.19 Y maze test

The Y maze test was conducted 60 days after the MHV-59 infection to evaluate spatial working memory as described by (Rice et al., 2019). The Y-maze is composed of three arms intersecting at an angle of 120°. Mice were gently placed in the apparatus and allowed to explore the maze freely for 5 minutes. Following each trial, the maze was meticulously cleaned with a 70% alcohol solution and dried using paper towels. The percentage of spontaneous alternations between arms for 5 minutes was obtained through the index: [alternate total/ (total of entries in arms -2) × 100]. A significant decrease in spontaneous alternation indicates an impairment in spatial working memory.

2.20 Grip-force test

Grip-force in the forelimbs and all limbs was measured using Grip Strength Meter (Insight Equipamentos, Ribeirão Preto, SP) as previously described (Kolisnyk et al., 2013; Rossi et al., 2023). Mice were allowed to grasp the smooth pull bar with forelimbs and all limbs by holding their tails. Mice were then pulled backward in the horizontal plane, and the peak force (*g*) applied to the bar was recorded. Three trials were performed per mouse within the same session, and the average of the three trials was recorded. The average of these three trials was

then converted into force using the formula F = m × g, where "F" represents force, "m" is the mass, and "*g*" is the acceleration due to gravity.

2.21 Step-down inhibitory avoidance test

The step-down inhibitory avoidance test was performed to assess short and long-term aversive memory 60 days after MHV-A59 infection, as previously described by Liu et al., 2019. Briefly, in the training trial, mice were placed on the platform, and their latency to step down on the grid with all four paws was measured. Immediately after stepping down on the grid with the four paws, the animals received a single mild foot shock (0.2 mA, 2.0 s). A retention test trial was performed at 1.5 h (short-term aversive memory) and 24 h (long-term aversive memory) after the training session. In retention tests, each animal was placed on the platform again, and no shock was applied when the animal stepped down on the grid. The results were expressed as a latency period to step down the platform, with a cutoff of 180 seconds.

2.22 Olfactory discrimination test

Olfactory memory was assessed by the olfactory discrimination test at 6 and 38 days after MHV-A59 infection, as previously described by Prediger et al., 2010. The apparatus used for this test was an acrylic box divided into two equal compartments by an open door (7.0 cm^2) in the center, enabling the animal to select between two compartments. One compartment, known as the familiar compartment, contained sawdust that had remained unchanged for a minimum of 3 days. Conversely, the other compartment, considered non-familiar, was filled with fresh sawdust. The animals were allowed to explore the environment freely for five minutes. The time spent in each compartment was recorded and subsequently analyzed using the EthoVision XT software (Noldus, Technology, Leesburg, VA, USA). The olfactory discriminative memory impairment was indicated by a significant decrease in the time spent in the familiar compartment.

2.23 PCR

RNA extraction from tissues was carried out using QIAamp® Viral RNA kits, in accordance with the manufacturer's instructions with specific adaptations. Tissue homogenization was performed in conjunction with the lysis buffer. The quantification of the extracted RNA was conducted using a spectrophotometer (NanoDrop™, Thermo Scientific). For cDNA synthesis, the iScript™ gDNA Clear cDNA Synthesis Kit (BIO-RAD) was employed. The initiation of cDNA synthesis utilized 500 ng of total RNA, following the manufacturer's protocols. The resulting total cDNA was previously diluted at a ratio of 1:10 for subsequent use in the qPCR assay. Fast SYBR™ Green Master Mix (Applied Biosystems™) was employed along with primers at a concentration of 5nM. The forward primer sequence was 5′-CAGATCCTTGATGATGGCGTAGT-3′, and the reverse primer sequence was 5′-AGAGTGTCCTATCCCGACTTTCTC-3′. Additionally, RNA extraction was performed on a known PFU quantity of MHV-A59 to establish the standard, and the results were expressed in Arbitrary Units.

2.24 Statistical analyses

GraphPad Prism software (v.9.3.0) was used for statistical analyzes. Significant outliers identified by the ROUT test (Q = 1%) were excluded from the data prior to subsequent analyses. The data were tested for normality using the Shapiro-Wilk test. For data that passed the normality test, a confidence interval of 95% was assumed. Two-way ANOVA and Dunnet’s multiple comparison test were used to analyze differences in weight changes. Simple Kaplan-Meier survival analysis was used to analyze the differences in survival probability. Student's t-test (for normal distribution) or Mann–Whitney test (for non-normal distribution) was used to analyze the differences between the mock controls and the infected mice at a single time point. Two-way ANOVA and Dunnet’s multiple comparison test were used to analyze differences between mock

controls and infected mice of respective sex at different time points. Two-way ANOVA and the Šídák multiple comparison test were used to analyze the differences between the sexes at the respective infection time points. For data that did not pass the normality test, a confidence interval of 99% was assumed for Dunnet's multiple comparison test or the Šídák multiple comparison. Three-way ANOVA and Tukey's multiple comparison tests were used to analyze the differences between sham or ovariectomized (OVX) mock or infected mice at different time points. For data that did not pass the normality test, a confidence interval of 99% was assumed for the Tukey multiple comparison test. Data are shown as mean values ± standard error of the mean.

3. Results

3.1 Intranasal instillation of MHV-A59 induces a transient pulmonary infection and an inflammatory state.

Intranasal MHV-A59 infection induces acute pneumonia and severe lung injuries in C57BL/6 wild-type mice (Yang et al., 2014). However, comprehensive analyses of the chronic and systemic consequences associated with MHV-A59 infection have not been conducted. Here, we intranasally inoculated 5-week-old C57BL/6 mice with MHV-A59 at different viral loads (3×10^3, 3×10^4, or 3×10^5 PFU/30 μL) (Fig. 1A). Infection with MHV-A59 reduced the body weight of mice in an inoculum-dependent manner (Fig. 1B), whereas only the 3×10^5 PFU inoculum was lethal to infected mice (Fig. 1C). To investigate the systemic, pulmonary, and cerebral changes induced by MHV-A59 infection, we opted for a higher, non-lethal inoculum of 3×10^4 PFU to proceed with the experiments. Mice were euthanized at intervals of 2, 5, 8-, 16-, 30-, and 60-days post-infection (dpi), and samples of lung, liver, spleen, and blood were subsequently collected (Fig. 1A).

Coronavirus infection can lead to an imbalance in the neutrophil-to-lymphocyte ratio (NLR), a potential indicator of the severity and mortality of the disease (Henry et al., 2020; Liao et al., 2020; Ponti et al., 2020). Mice infected with MHV-A59 exhibited increased NLR in the blood at 2 and 5-dpi (Fig. 1D). As MHV-A59 and SARS-CoV–2 have been shown to spread to extrapulmonary sites (Körner et al., 2020; Synowiec et al., 2021), our investigation assessed viral titers not only in lung samples but also in plasma, liver, and spleen obtained from MHV-A59-infected mice. The intranasal inoculation of MHV-A59 resulted in a transient lung infection, with the peak viral titter at 2 dpi. The titter decreased by 5 dpi and remained undetectable after that (Fig. 1E). Replicating virus was also detected in the liver (Fig. 1E), with mild histopathological alterations (Figure S1 A-B).

As shown by the H&E-stained slides, intranasal infection with MHV-A59 resulted in transient mild lung inflammation characterized by perivascular and peribronchiolar leukocyte infiltrate, desquamation of bronchiolar cells, hyperplasia of the alveolar walls and points of hemorrhage in some samples (Fig. 1H). In addition, infected mice presented impaired lung function, with a significant reduction in both vital capacity (Fig. 1I) and compliance of the respiratory system (Fig. 1J) at 5dpi. This stiff behavior of the respiratory system is consistent with pulmonary restrictive disease (Mortola 2019) and can be associated with fibrosis (Schaller et al., 2020). As TGF-β is a pivotal regulator of collagen deposition (Meng et al., 2016), we investigated the concentration of this cytokine in the lungs of MHV-A59-infected mice. Infection with MHV-A59 increased the TGF-β levels in the lung at 8, 16, and 30 dpi (Fig. 1K). Despite the elevated TGF-β levels, there was no accumulation of collagen in the lungs of the mice throughout the infection, as evidenced by Masson's trichrome-stained slides (Fig. 1G).

3.2 MHV-A59 intranasal infection promotes differential accumulation of pulmonary chemokines and leukocytes.

Next, we evaluated the molecular and cellular profiles involved in MHV-A59-induced lung inflammation (Fig. 2). Considering that biological sex has an impact on both immune response and COVID-19 outcomes (Scully et al., 2020; Takahashi et al., 2020), we stratified the sexes in our analyses to elucidate potential mechanisms contributing to the disease phenotype. Both male and female MHV-A59-infected mice showed elevated levels of CCL2, CCL3, and CCL5 in lung tissue, while only male-infected mice showed elevated levels of CXCL1 (Fig. 2A). Additionally, we assessed the levels of the pro-inflammatory cytokines TNF, IFN-γ, IL-6, and the anti-inflammatory cytokine IL-10 in the lung tissue of MHV-A59-infected mice. However, these levels were not statistically different between non-infected and infected mice (data not shown). At 5 dpi, both female and male MHV-A59-infected mice displayed increased leukocyte accumulation in lung tissue (Fig. 2B and S2). While the levels of CXCL-1 were elevated in the lung tissue of male MHV-A59-infected mice, there was no alteration in neutrophil accumulation throughout the course of the disease in both female and male mice (Fig. 2C).

Subsequently, at 5 dpi, a distinct subset of anti-inflammatory dendritic cells, marked by elevated IL-10 levels, aggregated in the lung tissue of MHV-A59-infected mice. Notably, this particular population was more abundant in male mice compared to their female counterparts (Fig. 2D-E). MHV-A59 induced a lymphocytic response in lung tissue, particularly notable in female animals. At 5 dpi, female infected mice showed an increased number of T $CD4^+$ lymphocytes in the lungs (Fig. 2F). At 8 dpi, a pro-inflammatory subset of these cells, characterized by elevated levels of IFN-γ, accumulated in female infected mice but not in males (Fig. 2G). The T CD4-$^+$ lymphocytes were characterized by high levels of the cell proliferation marker $Ki67^+$ (Fig. 2H). Both female and male MHV-A59-infected mice exhibited an accumulation of T $CD8^+$ lymphocytes in lung tissue (Fig. 2I). However, only female infected

mice demonstrated an increase in the IFN-γ^+ secreting $CD8^+$ T lymphocyte subset in the lungs (Fig. 2J). While the overall number of pulmonary NK cells remained consistent between female and male mice throughout the disease (data not shown), a subpopulation of NK cells with high IFN-γ levels increased solely in the lung tissue of female infected mice (Fig. 2K) Protective humoral immunity against SARS-CoV-2 is a crucial determinant in COVID-19, correlating with clinical outcomes (Carrillo et al., 2021). Thus, we subsequently examined IgM and IgG levels against MHV-A59 in the plasma of infected mice. Plasma IgM and IgG levels were elevated in both female and male infected mice. Notably, males exhibited prolonged IgM plasma levels compared to females, whereas females demonstrated faster IgG production compared to male infected mice (Fig. 2L-M).

In sum, both female and male infected mice displayed the production of inflammatory mediators and the accumulation of cells in lung tissue following MHV-A59 infection. However, males exhibited increased chemokine production, while females demonstrated higher T lymphocyte activation.

3.3 MHV-A59-infected mice display behavioral and cognitive alterations in a time and sex-dependent manner.

Following the characterization of lung effects induced by MHV-A59, we explored potential neuropsychiatric sequelae associated with post-COVID syndrome (Xu et al., 2022). We analyzed behavioral and cognitive changes in male and female mice infected with MHV-A59 (Fig. 3A). In the open field test, no significant difference was found at 5 dpi (peak of lung disease) regardless of sex. Meanwhile, female MHV-A59 mice exhibited a significant decrease in spontaneous locomotor activity at 16 dpi. Notably, female mice exhibited complete recovery at 28 dpi, as evidenced by the total distance traveled in the open field. MHV-A59 infection did not result in locomotor activity impairment in male mice (Fig. 3B-D).

As olfactory loss is a core symptom of COVID-19 (Harapan and Yoo, 2021), we investigated olfactory discrimination memory at early and later time points after MHV-A59 infection. Male-infected mice had no disturbance in the olfactory discrimination memory, while at 6 dpi female-infected mice presented a significant dysfunction compared to mock groups (Fig. 3E). Olfactory discrimination memory dysfunction was completely resolved by 38 dpi (Fig. 3F). However, from this test alone we cannot state that infected female mice exhibit anosmia. Neuromuscular dysfunction is also an important symptom related to COVID-19 (Rossi et al., 2023). At 16 dpi, both female MHV-A59-infected mice displayed a significant decrease in the forelimb and for all limbs grip force compared with mock controls (Fig. 3G). Grip strength impairments were not observed for forelimbs and all limbs at 28 dpi regardless of sex (Fig. 3H). Male MHV-A59-infected mice displayed an anhedonic-like behavior, as indicated by a significant decrease in the percentage of sucrose preference at 17 dpi (Fig. 3I). A reduction in the percentage of sucrose preference was also observed in infected female mice (Fig. 3I), however it did not reach statistical significance ($p= 0.056$). Interestingly, female animals presented a decrease in the number of buried marbles at 34 dpi, also suggesting an anhedonic-like behavior (Fig. 3J).

Importantly, only female mice showed significant cognitive dysfunctions at 60 dpi MHV-A59 infection. There was a significant decrease in the percentage of spontaneous alternations in the Y maze, indicating an impairment in spatial working memory. No significant differences were found between MHV-A59 infected male mice and mock controls (Fig. 3K). Regarding aversive memory, mock and infected mice displayed similar step-down latency in the training session regardless of sex (Fig. 3L). MHV-A59 female mice showed impairment in short-term but not long-term aversive memory compared with mocks, as indicated by a decrease in the step-down latency 1.5 h but not 24 h after the training session. No significant changes in aversive memory were observed in male mice after MHV-A59 infection (Fig. 3L-N).

3.4 MHV-A59 infection induces prominent neurochemical and cellular alterations in the brain of female mice.

Given the behavioral and cognitive changes identified post MHV-A59 infection, particularly in female mice, we proceeded to investigate the biochemical and morphological alterations induced by the infection in the brain (Fig. 4A). MHV-A59 RNA viral copies were found in the brains of infected animals at from 2- to 8-dpi, in both sexes. However, the replicative virus was not detected by plaque assay (data not shown). The highest numbers of virus RNA copies were detected on days 5 and 8 dpi, with females having notably more virus at 5 dpi compared to males (Fig. 4B).

A potential mechanism associated with brain damage is neuronal excitotoxicity (Verma et al., 2022). To examine this hypothesis, we assessed intracellular calcium and glutamate levels in isolated nerve terminals, specifically synaptosomes isolated from the hippocampus (Fig. 4C and D, respectively) and cortex (Fig S3A-B, respectively) of both female and male mice at 5- and 30-dpi. Female, but not male mice, exhibited higher levels in intrasynaptosomal calcium concentrations (Fig. 4C) and an increase in hippocampal glutamate levels (Fig. 4D). As for the cortex, no changes were found in glutamate and calcium levels in both sexes (Fig S3A-B). These findings underscore the sex-specific profile in the neurochemical response to MHV-59 infection. Histopathological analysis of the cerebral cortex revealed discrete changes in both sexes, such as the presence of leukocytes surrounding some hyperemic vessels (Fig S3C-D). Immunohistochemical assays showed an increase in the number of IBA-1^{+} (microglia/macrophages) cells in the brain cortex after MHV-A59 infection in both sexes (Fig. 4E). In males, this increase was detected from the 2^{nd} to the 60^{th}-dpi when compared to the mock group, while females showed an increase from the 5^{th}-dpi onwards (Fig 4E). Noteworthy, at 8-dpi, females showed higher numbers of IBA1^{+} cells when compared to males (Fig. 4E). IBA-1 labeling was also performed in the hippocampus and there was a similar profile of IBA-1^{+} cells

in both sexes. Relative to their respective mocks, there was an increase in cells labeled for IBA-1 from 2- to 60-dpi (Fig. 4F). The number of S100B$^+$ astrocytes increased in the brain cortex of female mice after the 2nd-dpi onwards when compared to the mock group. In males, this increase was only observed on the 2nd-dpi (Fig. 4G). Significant difference was observed between females and males at 5 and 16-dpi, with females showing higher numbers than males (Fig. 4G). A similar pattern was detected in the hippocampus (Fig. 4H). Females showed a significant increase in S100B$^+$ cells from 2- to 16-dpi when compared to their control group, while no increase was observed in males. When comparing the sexes, females exhibited higher numbers of hippocampus S100B$^+$ cells at 5-, 8-, and 16-dpi than males (Fig. 4H). The figures demonstrate IBA-1$^+$ and S100B$^+$ cells in the cerebral cortex and hippocampus at the peak of MHV-A59 infection compared to their respective controls.

3.5 MHV-A59 intranasal infection triggers differential accumulation of brain leukocytes and inflammatory mediators.

Next, we evaluated the cellular and molecular profiles involved in MHV-A59-induced CNS inflammation (Fig S4). Both female and male mice infected with MHV-A59 exhibited increased leukocyte accumulation in the brain at 8-dpi when compared to respective controls (Fig. 5A). The number of neutrophils increased in the brains of females at 8-dpi, but not in males (Fig. 5B). Additionally, IBA-1$^+$ cells, indicative of microglia, revealed a pattern of active cells (CD45^{int}CD11b$^+$F4/80$^+$MHCII$^+$) in both sexes also at 8-dpi when compared to the mock groups (Fig. 5C). The expression of iNOS in this population of activated microglia was upregulated in females and was significantly higher when compared to the male group (Fig. 5D).

MHV-A59 infection also prompted a lymphocytic response in brain tissue, which was prominent in infected female mice since they exhibited higher numbers of T CD4$^+$ lymphocytes at 5-dpi than their control group and males at the same time point (Fig. 5E). Additionally, at 5-

dpi, there was an accumulation of a pro-inflammatory subpopulation of T $CD4^+$ lymphocytes in the brain of infected female mice, expressing $CD69^+$, which is a marker of early activation, $Ki67^+$, a marker of cell proliferation, aside from high levels of IFN-γ (Fig. 5F-H). All of these cell markers were significantly increased when compared to males. Regarding the subpopulation of T $CD8^+$ cells, there was an expansion of these cells in the brains of both male and female infected mice at 8-dpi (Fig. 5 I). Similarly, there was an increase in the number of IFN-γ-producing $CD8^+$ T cells and T $CD8^+CD69^+$ cells, although the number of T $CD8^+$ $Ki67^+$ cells only increased in infected females when compared to the control group and male mice (Fig. 5J-L).

In line with the leukocyte infiltration, MHV-A59 induced an increase in CX3CL1 in the prefrontal cortex (PFC) of females at 2- and 5-dpi when compared to the mock group, while in males, such increase occurred only at 2-dpi. Furthermore, this increase was significantly more pronounced in females (Fig. 5M). Females also showed a reduction in BDNF levels at the 8^{th} and 16^{th} -dpi in the PFC, while males showed this reduction only at 2 dpi. At the 30^{th} -dpi, there was a significant difference between the sexes, with males exhibiting lower levels of BDNF than females (Fig. 5N). In contrast, male mice infected with MHV-A59 showed an increase in IL-6 levels in the PFC at 30- and 60-dpi, while infected females showed no alterations (Fig. 5O). MHV-A59 infection also led to an increase at 2-dpi and a reduction at 8-dpi in hippocampus levels of CX3CL1 in female mice. In contrast, CX3CL1 levels in the hippocampus of infected male mice decreased at 5-dpi when compared to mock and were significantly lower than females at 2-, 5-, and 30-dpi (Fig. 5P). Hippocampus BDNF levels decreased at 2-, 5-, 8-, and 16-dpi in infected females and at 2-, 5-, and 8-dpi in infected males, compared to their respective control groups. Nevertheless, no sex-based differences were observed (Fig. 5Q). Quantifying IL-6 levels in the hippocampus indicated a peak in infected female mice at 8-dpi, contrasting with the mock group. Furthermore, a significant increase in IL-6 was observed in infected females compared to

males at this time point (Fig. 5R). Quantification of the cytokine IFN-γ was carried out in the same way as other mediators. However, it was not detected at the protein level.

3.6 MHV-A59-induced CNS dysfunction is dependent on female hormones.

In line with current findings, females appear to be more clinically affected by post-COVID syndrome (Phillips and Williams, 2021). To explore this sex hormone-dependent phenotype, we initially assessed serum levels of estradiol, FSH, and testosterone in female mice infected with MHV-A59. Intranasal infection with MHV-A59 resulted in changes in estradiol levels at 2 dpi and 5 dpi, and it was found to be nearly seven times higher in the long-term (60 dpi) compared to the age-matched control group (Fig. 6A). Plasmatic FSH levels were significantly high at 5 dpi, 16 dpi, 30 dpi and 60 dpi groups in relation to control ($P < 0.05$) (Fig. 6B). Testosterone plasmatic levels, in turn, were reduced about 30% at 5 dpi, 30 dpi and 60 dpi compared to the control group ($P < 0.05$) (Fig 6C). These hormonal changes reflect that the infection can cause temporary or prolonged hormone production dysregulation.

The next step was to study the disease and its sequelae in a female hormones-deficient context. Thus, we ovariectomized (OVX) mice and infected them with MHV-A59 to analyze the role of sex hormones in this infectious process (Fig. 6D). Assessment of viral load in the lungs of SHAM-infected and OVX-infected animals revealed similar amounts of virus at 2 and 5 dpi (Fig. 6E). The histopathological lung damage of infected females subjected to OVX was similar to that of SHAM mice, both at 2- and 5-dpi (Fig. 6F and S6).

Female hormone deficiency in the OVX group protected mice when evaluating the neuropsychiatric sequelae induced by the infection. While MHV-A59 infection triggered a significant reduction in grip strength in all limbs at 5-dpi (Fig. 6G), OVX mice had no alterations in the grip strength of the limbs in the acute phase of infection (Fig. 6G). No significant changes in neuromuscular function were found 16 days after MHV-A59 infection (Figure 6H).

Importantly, ovariectomy also prevented the MHV-A59-associated anhedonia-like behavior and spatial working memory deficit at 34- and 60-dpi, respectively (Fig. 6I-J).

Regarding viral load in the brain at 2 e 5 dpi, SHAM and OVX animals did not show significant differences (Fig. 6K). Accordingly, calcium concentration in the hippocampus of SHAM-infected animals increased relative to their control group at 30 dpi, while OVX-infected mice exhibited no significant alterations at the same time point (Fig. 6L). In contrast, glutamate release increased similarly in the hippocampus of both SHAM and OVX-infected groups (Fig. 6M). Accordingly, OVX prevented the mild histopathological damage induced by MHV-A59 in brain tissue compared with the SHAM-infected group at the corresponding time point of infection (Fig. 6N).

Immunohistochemical assays showed an increase in the number of IBA-1^+ cells in the cerebral cortex of infected OVX mice at 2 and 5 dpi when compared to the control group (Fig. 6O), whereas there were no changes in the number of IBA-1^+ cells in the hippocampus of these animals (Fig. 6P). Furthermore, no significant quantitative change was observed in $S100^+$ cells in the cerebral cortex of OVX and infected mice (Fig 6Q), but an increase in the number of $S100B^+$ cells was observed in the hippocampus of these mice at 5 and 60 dpi (Fig 6R).

4. Discussion

As defined by the World Health Organization (WHO), Post-COVID syndrome (PCS) is a condition that encompasses fatigue, shortness of breath, cognitive dysfunction, and other symptoms due to previous SARS-CoV-2 infection that cannot be explained by another diagnosis. Symptoms usually appear 3 months after the onset of COVID-19 and last for at least 2 months (Soriano et al., 2022). Post-COVID syndrome has been reported to affect between 7.5% and 89% of COVID-19 patients (Chen et al., 2022; Nasserie et al., 2021; Subramanian et al., 2022). It is noteworthy that PCS is not limited to severe cases, as 29.6% of patients with mild illness are

affected by this condition (Cazé et al., 2023). Considering that most COVID-19 patients (about 80%) develop mild disease (Huang et al., 2020), it is of great importance to study this condition in mild models of coronavirus infection. Here, through a robust characterization of MHV-A59 lung infection and central nervous system dysfunctions, we showed, to the best of our knowledge for the first time, that intranasal instillation of murine betacoronavirus MHV-A59 induced: (I) transient infection and mild lung disease in wild-type C57BL/6J mice; (II) more severe inflammatory response in the lung of female mice, characterized by a robust T cell response; (III) behavioral and cognitive changes, mainly in female mice, that persisted for up to 2 months; (IV) more severe inflammatory response in the brain of female mice (comparing with male counterparts) characterized by neutrophil infiltrate, microglial activation, and IFN-γ response; (V) female hormone-dependent disease phenotype on brain and behavioral sequelae.

The emergence of SARS-CoV-2 and the risk of new coronavirus outbreaks, which had been overlooked for decades (Morens et al., 2004), has emphasized the need to develop models to better understand the pathogen-host interaction and to evaluate potential therapeutic treatments and vaccines for coronavirus infections. Intranasal instillation of different MHV strains in mice has been used as an *in vivo* platform to study coronavirus lung disease (Andrade et al., 2021; Pimenta et al., 2023; Queiroz-Junior et al. 2023; De Albuquerque et al., 2006; Yang et al., 2014). In a prior study, Yang et al. characterized MHV-A59 lung infection in C57BL/6 mice as a model for acute respiratory distress syndrome (Yang et al., 2014). MHV-A59 was able to induce acute lung inflammation in C57BL/6 mice with leukocyte infiltration and hemorrhage, as well as increased mRNA expression of pro-inflammatory mediators such as CXCL10, IFN-γ, TNF, and IL-1β (Yang et al., 2014). Here, MHV-A59 infection also induced mild clinical pulmonary signs, with mild and transient histopathologic lung changes. Mice also exhibited acute lung dysfunction, as evidenced by decreased lung volume and compliance. This stiff behavior of the respiratory system is consistent with pulmonary restrictive disease (Mortola 2019), and COVID-

19 patients also show impairment in lung function, including those with mild respiratory symptoms (Mo et al., 2020; Altmann et al., 2023). Fibrosis is an important factor associated with impaired lung function, and COVID-19 patients showed abnormal collagen deposition in lung tissue (Schaller et al., 2020). Despite the increased levels of TGF-β, a key regulator of collagen deposition (Meng et al., 2016), in the lungs of MHV-A59-infected mice at post-acute time points, we did not observe pulmonary fibrosis throughout the course of the disease. Together with the recovery of lung volume and compliance 30 days post-infection, this suggests that the impaired lung function observed in MHV-A59-infected mice is primarily related to the acute phase of lung disease rather than persistent structural changes in lung tissue.

The immune response against MHV-A59 infection had a distinct sex-related phenotype. Indeed, several pieces of evidence suggest that biological sex is an important factor that impacts COVID-19 immune response, outcome, and development of PCS symptoms (Scully et al., 2020; Takahashi et al., 2020). Here, female MHV-A59 infected-mice had a robust lung T cell response, with higher levels of IFN-γ compared to male infected-mice. Conversely, male MHV-A59 infected-mice had prolonged levels of pulmonary chemokines involved in innate immune cell recruitment, such as CCL3, CCL5 and CXCL1. Accordingly, in COVID-19 patients, males have a more robust induction of innate immune response, with higher levels of IL-8, IL-18, and CCL5, and accumulation of non-classical monocytes in lung tissue, while female patients have more abundant activated T cells (Takahashi et al., 2020). This highlights that female and male MHV-A59 infected mice may differ regarding innate and adaptive immune response in the lung tissue, as observed in COVID-19 patients.

Mice infected with MHV-A59 completely cleared the virus in the lung tissue, indicating the host's ability to cope with the infection. In addition, replicating MHV-A59 could not be detected in the plasma or spleen but in the liver, and viral RNA copies in brain, suggesting limited viral spread to extrapulmonary sites. In terms of systemic changes, MHV-A59 infection leads to

a transient increase in NLR in the blood, which is also seen in COVID-19 patients and is an indicator of disease severity and mortality (Henry et al., 2020; Liao et al., 2020; Ponti et al., 2020). Of note, mice fully recovered from the imbalance in NLR mediated by MHV-A59 infection. Therefore, this model was characterized by mild lung disease with mild systemic alterations and viral dissemination, constituting a suitable platform to study sequelae post-coronavirus infection. Importantly, infection with MHV-1, another murine betacoronavirus, was recently shown to recapitulate some aspects of PCS in mice (Masciarella et al., 2023). The long COVID model proposed so far shows that mice infected with MHV-1 present congested blood vessels, perivascular cavitation, pericellular halos, vacuolation of neutrophils, pyknotic nuclei, acute eosinophilic necrosis, necrotic neurons with fragmented nuclei, and vacuolation in the brain cortex after 12 months of infection. Furthermore, these changes were associated with increased reactive astrocytes and microglia, hyperphosphorylated TDP-43 and tau, and a decrease in synaptic protein synaptophysin-1 (Paidas et al., 2022).

In the current model, female mice infected with MHV-A59 showed acute olfactory discrimination dysfunction. Olfactory loss is a core symptom of acute COVID-19 (Harapan and Yoo, 2021) as well as PCS (Winter et al., 2023). MHV-A59 infection also triggered motor impairment in female mice, affecting muscular strength of the forelimbs in both sexes at 16-dpi. This feature has recently been reported in patients with PCS (Ramírez-Vélez et al., 2023). In addition, both female and male mice presented anhedonic-like behavior, corroborating previous studies with PCS patients (Lamontagne et al., 2021; Sayed et al., 2021). Interestingly, only female mice demonstrated impairment in spatial working memory and short-term aversive memory in the Y-maze test and in the step-down inhibitory avoidance test, respectively, at 60-dpi. These cognitive deficits have been more commonly observed in women with long-COVID compared to men (Bai et al., 2022). Hence, the present model provides, for the first time,

supporting evidence for the predominance of behavioral and cognitive impairments observed in PCS, particularly among females.

Previous findings from our research group demonstrated that synaptosomes from MHV-3 infected mice have increased glutamate release and intracellular calcium levels (Pimenta et al., 2023). In the current model, MHV-A59-infected female mice also had significant glutamate release and increased intracellular Ca^{2+} levels in the hippocampus at 30-dpi. This is suggestive of neuronal excitotoxicity, as viral infections, including HIV, ZIKA and H1N1, have already been shown to impair glutamatergic transmission, thus impairing neural signaling (Costa et al., 2017; Düsedau et al., 2021; Gorska and Eugenin, 2020). Importantly, a greater number of microglia/macrophage (IBA-1) and astrocytes (S100B) were found in the cerebral cortex and hippocampus of female mice when compared to male mice. The increased number of these cells is suggestive of enhanced neuroinflammation and possibly neurodegeneration (Kwon and Koh, 2020; Vandenbark et al., 2021). Moreover, microglia of infected female mice but no male mice showed high expression of inducible nitric oxide synthase (iNOS). Nitric oxide (NO) is essential in synaptic transmission and brain plasticity, mainly in the cortex and hippocampus. However, high levels of NO and nitrergic/oxidative stress can lead to synaptic impairment and early neurodegeneration (Balez and Ooi, 2016).

The more robust neuroinflammation in female mice was further confirmed by detection of immune cells in the brain. MHV-A59-infected female mice presented increased number of IFN-γ^{+}-releasing $CD4^{+}$ T lymphocytes in the brain, with $Ki67^{+}$ (cell proliferation marker) and CD69 (cell activation marker) expression, aside higher numbers of $Ki67^{+}$ $CD8^{+}$ T cells in relation to males. T cells are especially important for limiting viral replication, as they can gain access to brain parenchyma through local recognition of viral antigens by T cell receptors (Steinbach et al., 2016). The interaction between microglia and T cells is also crucial within the CNS parenchyma, since the effector functions of these lymphocytes depend on this communication

(Ai and Klein, 2020). However, when this response is not finely regulated, the results can be deleterious. A study demonstrated that T cells might be associated with neurocognitive sequelae in surviving animals during neuropathogenic viral infections, such as ZIKV and West Nile Virus (WNV). This occurs mainly through the signaling of IFN-γ released by specific $CD8^+$ T cells infiltrating the CNS, which induces the activation of microglia (Garber et al., 2019). This microglial activation is correlated with several neurotoxic effects, such as excessive complement-mediated synapse elimination, neurodegeneration and decreased adult neurogenesis (Klein et al., 2019). WT mice infected with MHV V5A13.1 presented CNS inflammation and demyelination significantly less severe than T $CD4^{-/-}$ mice (Lane et al., 2000). Regarding other inflammatory mediators, MHV-A59 infection did not alter IL-6 levels in the PFC of female mice compared to controls. In males, IL-6 levels increased at 30- and 60-dpi. However, in the hippocampus, females exhibited increased IL-6 at 8-dpi compared to the mock group and infected males. SARS-CoV-2-induced IL-6 may influence working memory and cognitive systems (Alnefeesi et al., 2021). Increased expression of systemic IL-6 induced by SARS-CoV-2 infection can cross the blood-brain barrier to activate microglia and interfere with memory (Alnefeesi et al., 2021; Vos et al., 2022). Although IL-6 is mostly characterized by its proinflammatory profile, it has been demonstrated that it also participates in neurogenesis, in the response of mature neurons and glial cells in conditions of brain homeostasis (Erta et al., 2012). It is possible that, in the acute infection, especially in females, IL-6 is exerting its pro-inflammatory role in response to MHV-A59, while its later increase in males appears to be a compensatory/protective response to the system to return to homeostasis.

In addition to the inflammatory burden, MHV-A59 triggered an impairment in neurotrophic factors. MHV-A59 infection decreased BDNF levels in the PFC in females at 8- and 16-dpi and in males at 8-dpi. In the hippocampus, females exhibited reduction from 2- to 16-dpi, while males showed this reduction only from 2- to 8-dpi. Such delayed recovery of BDNF

in infected females may have contributed to the neuropsychiatric symptoms. BDNF is a key factor in survival, synaptic plasticity, and reorganization of the brain microenvironment (Chen et al., 2020). BDNF may play an antidepressant role in the PFC (Li et al., 2018) and hippocampus (Li et al., 2017), besides reducing anxiety-like behavior in rats (Cirulli et al., 2004). The levels of CX3CL1 showed a general pattern of increase followed by decrease in the PFC and hippocampus of female and male mice, suggesting a homeostatic response to control the acute effects of infection. The CX3CL1/CX3CR1 axis is important for neuron-microglia communication and the predominant function of CX3CL1 in the CNS is believed to reduce the pro-inflammatory response (Subbarayan et al., 2022). Furthermore, the impairment of this axis has been associated with the development of neuropsychiatric conditions (Chamera et al., 2020).

Biological sex affects innate and adaptive immune responses to infections and vaccination (Klein and Flanagan, 2016). Accordingly, biological sex has been implicated as an important factor influencing the immune response, outcomes, and sequelae of COVID-19 (Scully et al., 2020; Sylvester et al., 2022; Takahashi et al., 2020). Most epidemiological studies on COVID-19 have shown a sex-related mortality trend, with males being more vulnerable (Solis et al., 2022). Male laboratory animals are also more susceptible to SARS-CoV and SARS-CoV-2 infection than females (Channappanavar et al., 2017; Dhakal et al., 2021; Ruiz-Bedoya et al., 2022). Regarding sequelae, females appear to be more likely to develop post-COVID syndrome (Bai et al., 2022). Given the phenotype of CNS sequelae in female mice following MHV-A59 infection, we investigated the involvement of estradiol, FSH, and testosterone hormones in this context.

Our model identified high estradiol levels at the acute phase (2 and 5 dpi) and a peak at 60 dpi. Additionally, we observed increased FSH levels several time points after infection. Collectively, these data suggest that the infection compromised the estradiol signaling in the hypothalamus-pituitary-gonadal axis. Evidence shows that the SARS-CoV-2 spike protein binds

to and modulates estrogen receptors (Solis et al., 2022). Ding and colleagues (2020) found that estradiol (E2) may protect females during COVID-19 by regulating cytokines linked to infection severity. While female hormones can offer benefits in the acute phase, they may also sustain the hyperinflammatory state even after recovery (Bienvenu et al., 2020; Mohamed et al., 2021). Regarding FSH levels, women have been shown to have increased levels during COVID-19 (Cai et al., 2022), but studies on the relationship of this hormone with long COVID are scarce.

Our model also demonstrated a decrease in testosterone in female mice at 5, 30 and 60 dpi. A recent study showed that low testosterone levels in both sexes are associated with the immunological profile observed in women with long-term COVID-19, which includes a strong T-cell-mediated response (Silva et al., 2024). A previous study by this same research group demonstrated that high levels of antibodies against herpesviruses (EBV, CMV and HSV-2) are predominantly observed in females with PCS (Klein et al., 2023). It was subsequently observed that greater reactivity to these viruses is associated with low testosterone levels (Silva et al., 2024). Low testosterone levels in women may contribute to their higher susceptibility to autoimmune diseases (Bupp and Jorgensen, 2018). Since androgen receptors are expressed in immune cells, testosterone levels are believed to directly influence individual immune profiles (Bupp and Jorgensen, 2018).

Based on these findings, we set out to understand the sequelae in the context of hormonal deficiency triggered by ovariectomy, showing that ovariectomized female mice presented lung lesions similar to those of infected SHAM mice, but excitotoxicity, behavioral and cognitive impairments were significantly prevented. Regarding the profile of IBA-1+ and S100B+ cells, there was no complete reversion of these cell types in infected OVX mice, but we observed that the return to homeostasis is faster. This slight recovery positively impacts the behavioral phenotype.

Estrogen is known to be an important modulator of the immune system, so there is a question whether ovariectomy would impair the ability of mice to fight infection; however, despite small amounts, this hormone can be synthesized in secondary tissues such as brain, kidneys, bones, skin, and adipose tissue (Harding & Heaton 2022). Thus, we suggest that infected ovariectomized female mice did not present greater difficulty dealing with the virus than the infected SHAM group. In line with these results, an experimental study demonstrated that estradiol treatment did not minimize pulmonary complications in male hamsters infected with SARS-CoV-2 (Dhakal et al., 2021). Therefore, hormonal changes, not only estrogen, are associated with sequelae, as there is already evidence that dysfunctions of the hypothalamic-pituitary-gonadal axis are more prevalent in patients with long-term COVID-19 (Angum et al., 2020).

In conclusion, this is the first time that an experimental study recapitulates several aspects of the human post-COVID syndrome, clearly showing the sex differences regarding cognitive and behavioral outcomes. MHV-A59 induced mild acute lung inflammation and triggered chronic neuropsychiatric and musculoskeletal disorders, which were dependent on female hormones. This model offers a distinct platform to study the pathogenesis of PCS within a BSL2 structure. Its significance lies in addressing the challenge of studying behavioral and cognitive impairment in BSL3 laboratories mandated for SARS-CoV-2. Additionally, it facilitates the exploration of the therapeutic efficacy of antiviral, anti-inflammatory, or neuroprotective strategies, enhancing the overall management of COVID-19. Importantly, although transgenic mice expressing human ACE2 (hACE2) have been used to investigate SARS-CoV-2 pathophysiological processes, many of these transgenic models have failed to recapitulate the full spectrum of COVID-19, particularly extrapulmonary manifestations and its persistent symptoms (Knight et al., 2021). In this context, developing new and diverse models is pivotal to advance the field (Fan et al., 2022; Muñoz-Fontela et al., 2022). Although our findings are

remarkably novel, we understand that our study bears limitations. Further mechanistic studies are needed to answer how dysfunctions in the hypothalamic-pituitary-gonadal axis can be modulated to prevent CNS sequelae induced by coronavirus infection. Another limitation relies on the assessment of reinfection and its impact on the cognitive and behavioral aspects, as this is an event of great importance in the current COVID-19 scenario.

Table 1. Antibodies, reagents, cells, viral strain, mice and softwares.

REAGEANT or RESOURCE	SOURCE	IDENTIFIER
Antibodies and reagentes		
Human/Mouse BDNF	R&D system	DY248
CD11b Monoclonal Antibody, Super Bright™ 600	ThermoFisher	63-0112-82
CD11c Monoclonal Antibody, Super Bright™ 645	ThermoFisher	64-0114-82
CD3 Monoclonal Antibody, Super Bright™ 600	ThermoFisher	63-0032-82
CD4 Monoclonal Antibody, PE-Cyanine7	ThermoFisher	25-0041-82
CD45 Monoclonal Antibody, Pacific Orange™	ThermoFisher	MCD4505
CD45.2 Mouse Antibody, PerCP-Cy™5.5	Biolegend	109828
CD69 Monoclonal Antibody, Alexa Fluor™ 700	ThermoFisher	56-0691-82
CD8a Monoclonal Antibody, eFluor™ 450	ThermoFisher	48-0081-82
Estradiol (E2)	Monobind Inc	4925-300
F4/80 Monoclonal Antibody , APC	ThermoFisher	17-4801-82
Goat Anti-Mouse IgG Fc-HRP	Southern Biotech	AB_2737432
Goat Anti-Mouse IgM-HRP	Southern Biotech	AB_2794240
IBA1 Polyclonal Antibody	Invitrogen	PA5-21274
IFN gamma Monoclonal Antibody, APC-eFluor™ 780	ThermoFisher	47-7311-82

iNOS Monoclonal Antibody, PE-eFluor™ 610	ThermoFisher	61-5920-82
Ki-67 Monoclonal Antibody, FITC	ThermoFisher	11-5698-82
L-10 Monoclonal Antibody, Alexa Fluor™ 700	ThermoFisher	56-7101-82
LIVE/DEAD™ Fixable Aqua Dead Cell Stain Kit	ThermoFisher	L34957
Ly-6G/Ly-6C (Gr-1) Biotin anti-mouse Antibody	Biolegend	108403
MHC Class II (I-A/I-E) Monoclonal Antibody, APC-eFluor™ 780	ThermoFisher	47-5321-82
Mouse CCL2/JE/MCP-1	R&D system	DY479
Mouse CCL3/MIP-1 alpha	R&D system	DY450
Mouse CCL5/RANTES	R&D system	DY478
Mouse CX3CL1/Fractalkine	R&D system	DY472
Mouse CXCL1/KC	R&D system	DY453
Mouse IFN-gamma	R&D system	DY485
Mouse IL-1 beta/IL-1F2	R&D system	DY401
Mouse IL-10	R&D system	DY417
Mouse IL-6	R&D system	DY406
Mouse TGF-beta 1	R&D system	DY1679
Mouse TNF	R&D system	DY410
NK1.1 Monoclonal Antibody, PerCP-Cyanine5.5	ThermoFisher	45-5941-82

S100 beta antibody	Abcam	ab41548
Streptavidin, Pacific Orange™ conjugate	ThermoFisher	S32365
Cells		
L929	ATCC	CCL-1 ™
Viral strain		
Murine hepatitis Virus-A59 (MHV-A59)	ATCC	VR-764 ™
Mice		
C57BL/6 (Wild-type)	Central Animal House of the UFMG	C57BL/6Junib
Softwares		
GraphPad Prism v9 software	GraphPad	https://www.graphpad.com/
FlowJo V10.4.11	Becton, Dickinson (BD)	https://www.flowjo.com/
ImageJ 1.54g	National Institutes of Health	https://imagej.net/ij
LabChart v7	AdInstruments	https://www.adinstruments.com/

FIGURES

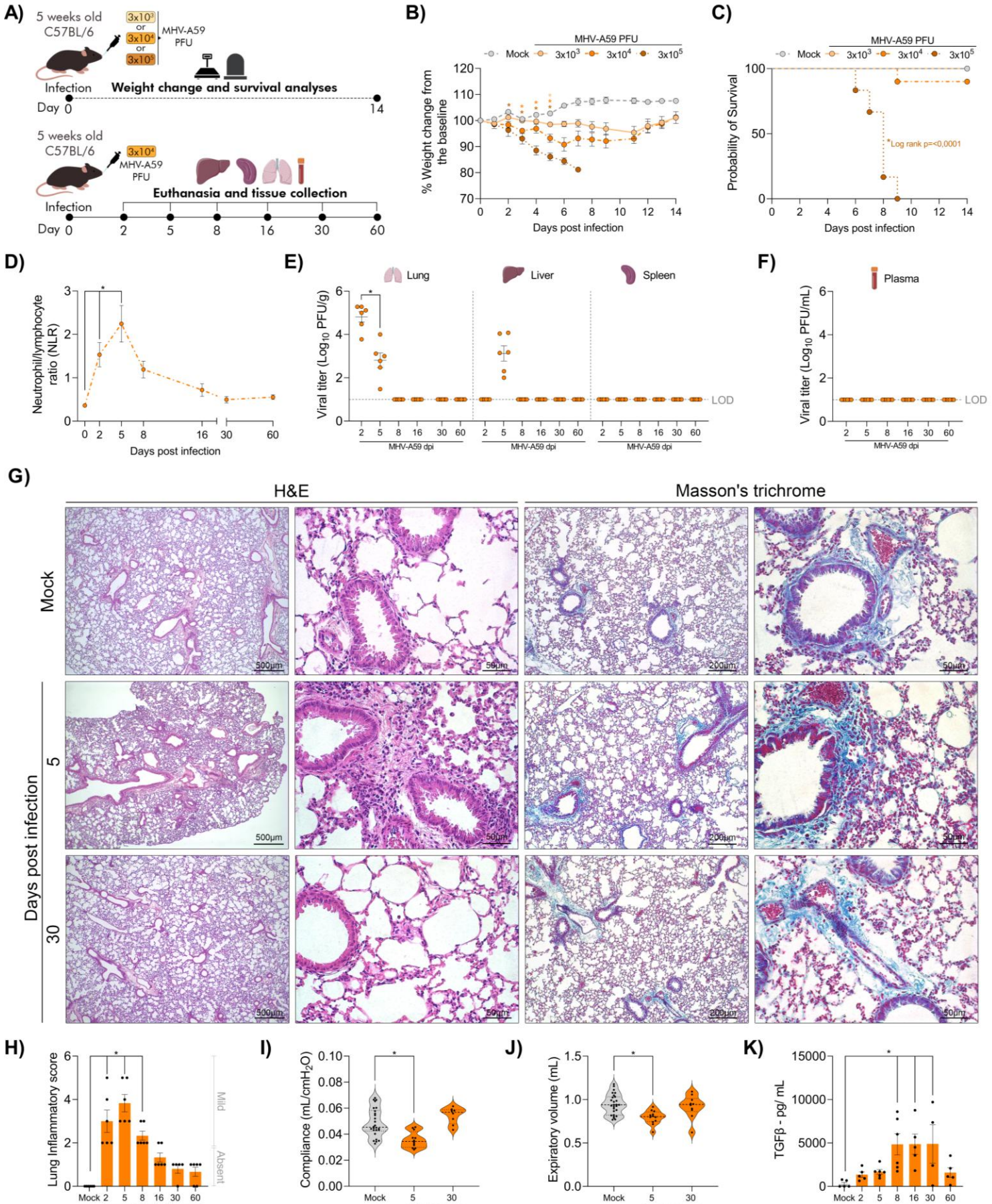
A)
5 weeks old C57BL/6
3x10³ or 3x10⁴ or 3x10⁵
MHV-A59 PFU
Infection
Weight change and survival analyses
Day 0
14
5 weeks old C57BL/6
3x10⁴
MHV-A59 PFU
Euthanasia and tissue collection
Infection
Day 0 2 5 8 16 30 60
B)
MHV-A59 PFU
Mock 3x10³ 3x10⁴ 3x10⁵
% Weight change from the baseline
Days post infection
C)
MHV-A59 PFU
Mock 3x10³ 3x10⁴ 3x10⁵
Probability of Survival
*Log rank p=<0,0001
Days post infection
D)
Neutrophil/lymphocyte ratio (NLR)
Days post infection
E)
Lung
Liver
Spleen
Viral titer (Log10 PFU/g)
LOD
MHV-A59 dpi
F)
Plasma
Viral titer (Log10 PFU/mL)
LOD
MHV-A59 dpi
G)
H&E
Masson's trichrome
Mock
Days post infection
5
30
500µm
50µm
200µm
H)
Lung Inflammatory score
Mild
Absent
Mock 2 5 8 16 30 60
MHV-A59 dpi
I)
Compliance (mL/cmH2O)
Mock 5 30
MHV-A59 dpi
J)
Expiratory volume (mL)
Mock 5 30
MHV-A59 dpi
K)
TGFβ - pg/ mL
Mock 2 5 8 16 30 60
MHV-A59 dpi

Figure 1. Intranasal instillation of MHV-A59 in mice results in transitory lung injury and function impairment. (A) Experimental design. (B) Body weight percentage changes upon infection with $3x10^3$, $3x10^4$ or $3x10^5$ PFU/30 μL of MHV-A59 versus mock controls. Significance was determined by Two-way ANOVA and Dunnet's multiple comparison test *p < 0.05 (n = 8-10). (C) Survival curve of MHV-A59-infected mice versus mock controls. Significance was determined by Simple Kaplan-Meier survival analysis *p < 0.05 (n = 6-10). (D) Blood neutrophil for lymphocyte ratio (NLR). Significance was determined by Two-way ANOVA and Dunnet's multiple comparison test *p < 0.01 (n = 6). Viral load determined in lung, liver, and spleen extracts (E), and plasma (F) of MHV-A59-infected mice by plaque assay. The results are presented as $\log_{10}$ PFU per gram of tissue or milliliter of plasma. Significance was determined by Student's t-test *p < 0.05 (n = 6). (G) Hematoxylin and eosin (H&E) and Masson's trichrome staining of lung sections of mock controls and 5 and 30-dpi MHV-A59-infected mice. (H) Histopathological assessment in relation to overall lung inflammatory score. Significance was determined by Two-way ANOVA and Dunnet's multiple comparison test *p < 0.01 (n = 5-6). (I) Analysis of total lung volume (vital capacity) and (J) pulmonary compliance of mock controls and 5 and 30-dpi MHV-A59 infected mice. Significance was determined by Two-way ANOVA and Dunnet's multiple comparison test *p < 0.05 (n = 9-28). (K) Lung tissue levels of TGF-β. Significance was determined by Two-way ANOVA and Dunnet's multiple comparison test *p < 0.05 (n = 4-6). L.O.D. (limit of detection).

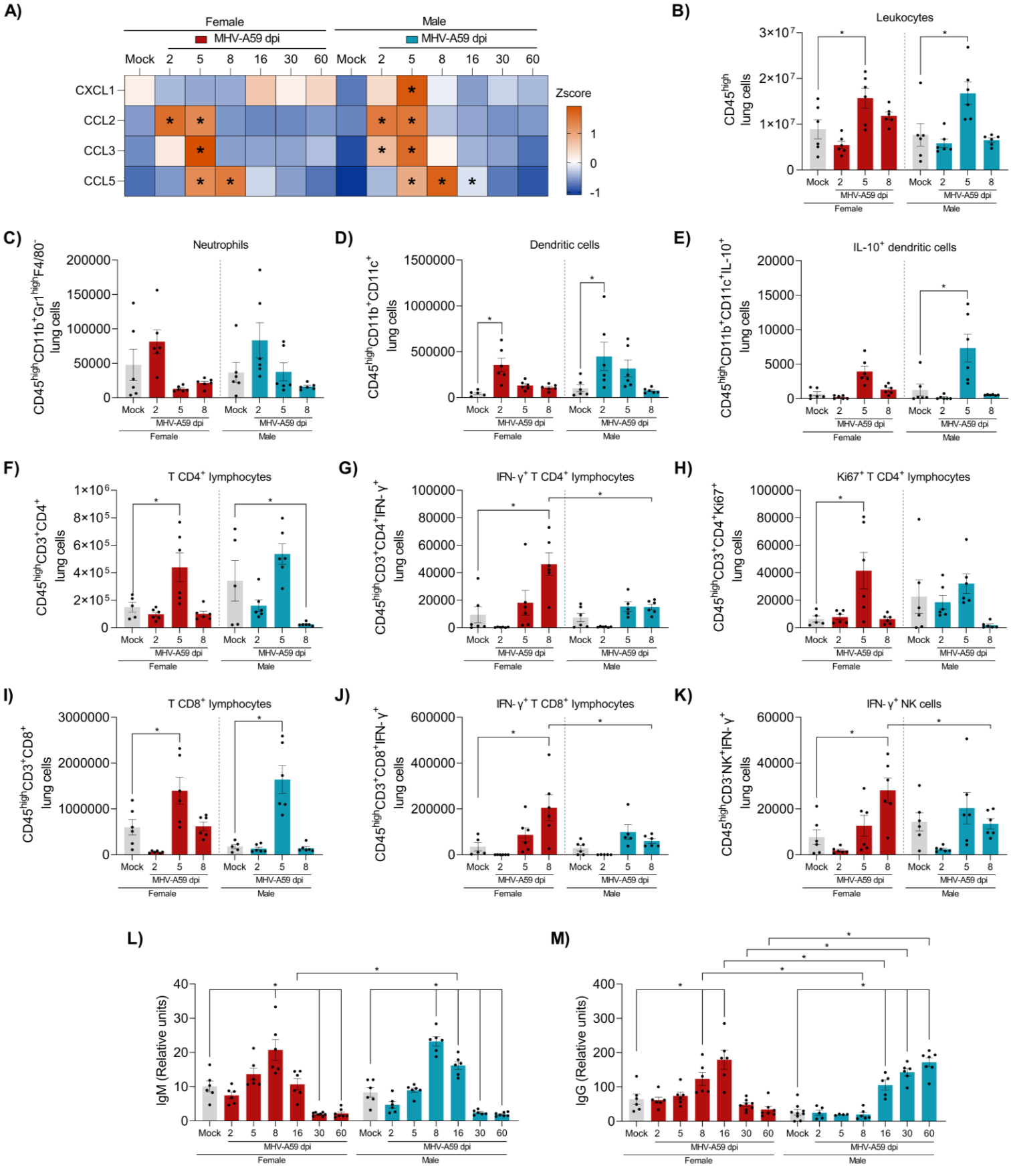
A)
Female
MHV-A59 dpi
Male
MHV-A59 dpi
Mock 2 5 8 16 30 60 Mock 2 5 8 16 30 60
CXCL1
CCL2
CCL3
CCL5
Zscore
1
0
-1
B)
Leukocytes
CD45high lung cells
3×10^7
2×10^7
1×10^7
0
Mock 2 5 8 Mock 2 5 8
MHV-A59 dpi
Female
Male
C)
Neutrophils
CD45highCD11b+Gr1highF4/80- lung cells
200000
150000
100000
50000
0
D)
Dendritic cells
CD45highCD11b+CD11c+ lung cells
1500000
1000000
500000
0
E)
IL-10+ dendritic cells
CD45highCD11b+CD11c+IL-10+ lung cells
20000
15000
10000
5000
0
F)
T CD4+ lymphocytes
CD45highCD3+CD4+ lung cells
1×10^6
8×10^5
6×10^5
4×10^5
2×10^5
0
G)
IFN-γ+ T CD4+ lymphocytes
CD45highCD3+CD4+IFN-γ+ lung cells
100000
80000
60000
40000
20000
0
H)
Ki67+ T CD4+ lymphocytes
CD45highCD3+CD4+Ki67+ lung cells
100000
80000
60000
40000
20000
0
I)
T CD8+ lymphocytes
CD45highCD3+CD8+ lung cells
3000000
2000000
1000000
0
J)
IFN-γ+ T CD8+ lymphocytes
CD45highCD3+CD8+IFN-γ+ lung cells
600000
400000
200000
0
K)
IFN-γ+ NK cells
CD45highCD3-NK+IFN-γ+ lung cells
60000
40000
20000
0
L)
IgM (Relative units)
40
30
20
10
0
Mock 2 5 8 16 30 60 Mock 2 5 8 16 30 60
MHV-A59 dpi
Female
Male
M)
IgG (Relative units)
400
300
200
100
0
Mock 2 5 8 16 30 60 Mock 2 5 8 16 30 60
MHV-A59 dpi
Female
Male

Figure 2. Intranasal infection with MHV-A59 promotes differential accumulation of pulmonary chemokines and leukocytes. (A) Z Score representation of pulmonary levels of CXCL1, CCL2, CCL3, CCL5 measured by ELISA assay. Significance was determined by Two-way ANOVA and Dunnet's multiple comparison test *$p < 0.01$ ($n = 4$-6). Number of pulmonary leukocytes **(B)**, neutrophils **(C)**, dendritic cells **(D)**, IL-10^+ dendritic cells **(E)**, $CD4^+$ T lymphocytes **(F)**, $Ki67^+$ $CD4^+$ T lymphocytes **(G)**, IFN-γ^+ $CD4^+$ T lymphocytes **(H)**, $CD8^+$ T lymphocytes **(I)**, IFN-γ^+ $CD8^+$ T lymphocytes **(J)**, and IFN-γ^+ NK cells **(K)**, assessed by flow cytometry. Significance was determined by Two-way ANOVA and Dunnet's multiple comparison test to analyze the differences between mock controls and infected mice of respective sex at different time points. Significance was determined by Two-way ANOVA and the Šídák multiple comparison test to analyze the differences between the sexes at the respective infection time points. *$p < 0.05$ to data that passed Shapiro-Wilk test and *$p < 0.01$ to data that did not pass Shapiro-Wilk test ($n = 5$-6). Plasma levels of IgM **(L)** and IgG **(M)**. Significance was determined by Two-way ANOVA and Dunnet's multiple comparison test to analyze the differences between mock controls and infected mice of respective sex at different time points. Significance was determined by Two-way ANOVA and the Šídák multiple comparison test to analyze the differences between the sexes at the respective infection time points *$p < 0.05$ ($n =$ 6-8).

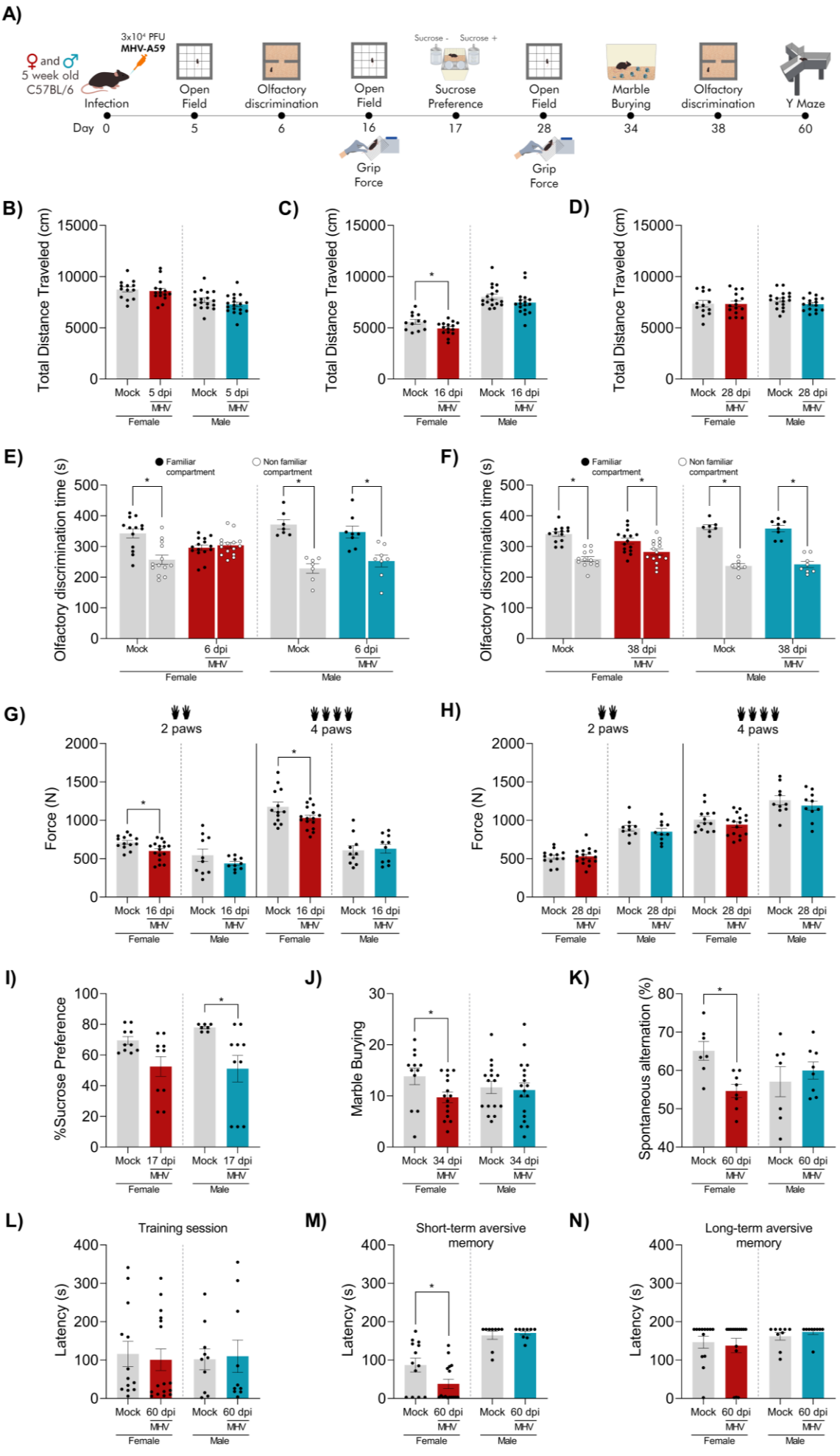
A)
3x10⁴ PFU
MHV-A59
♀ and ♂
5 week old
C57BL/6
Infection
Day 0
Open Field
5
Olfactory discrimination
6
Open Field
16
Grip Force
Sucrose - Sucrose +
Sucrose Preference
17
Open Field
28
Grip Force
Marble Burying
34
Olfactory discrimination
38
Y Maze
60
B)
Total Distance Traveled (cm)
Mock 5 dpi MHV
Female
Male
C)
Mock 16 dpi MHV
D)
Mock 28 dpi MHV
E)
Olfactory discrimination time (s)
Familiar compartment
Non familiar compartment
Mock 6 dpi MHV
F)
Mock 38 dpi MHV
G)
2 paws
4 paws
Force (N)
Mock 16 dpi MHV
H)
Mock 28 dpi MHV
I)
%Sucrose Preference
Mock 17 dpi MHV
J)
Marble Burying
Mock 34 dpi MHV
K)
Spontaneous alternation (%)
Mock 60 dpi MHV
L)
Training session
Latency (s)
M)
Short-term aversive memory
N)
Long-term aversive memory

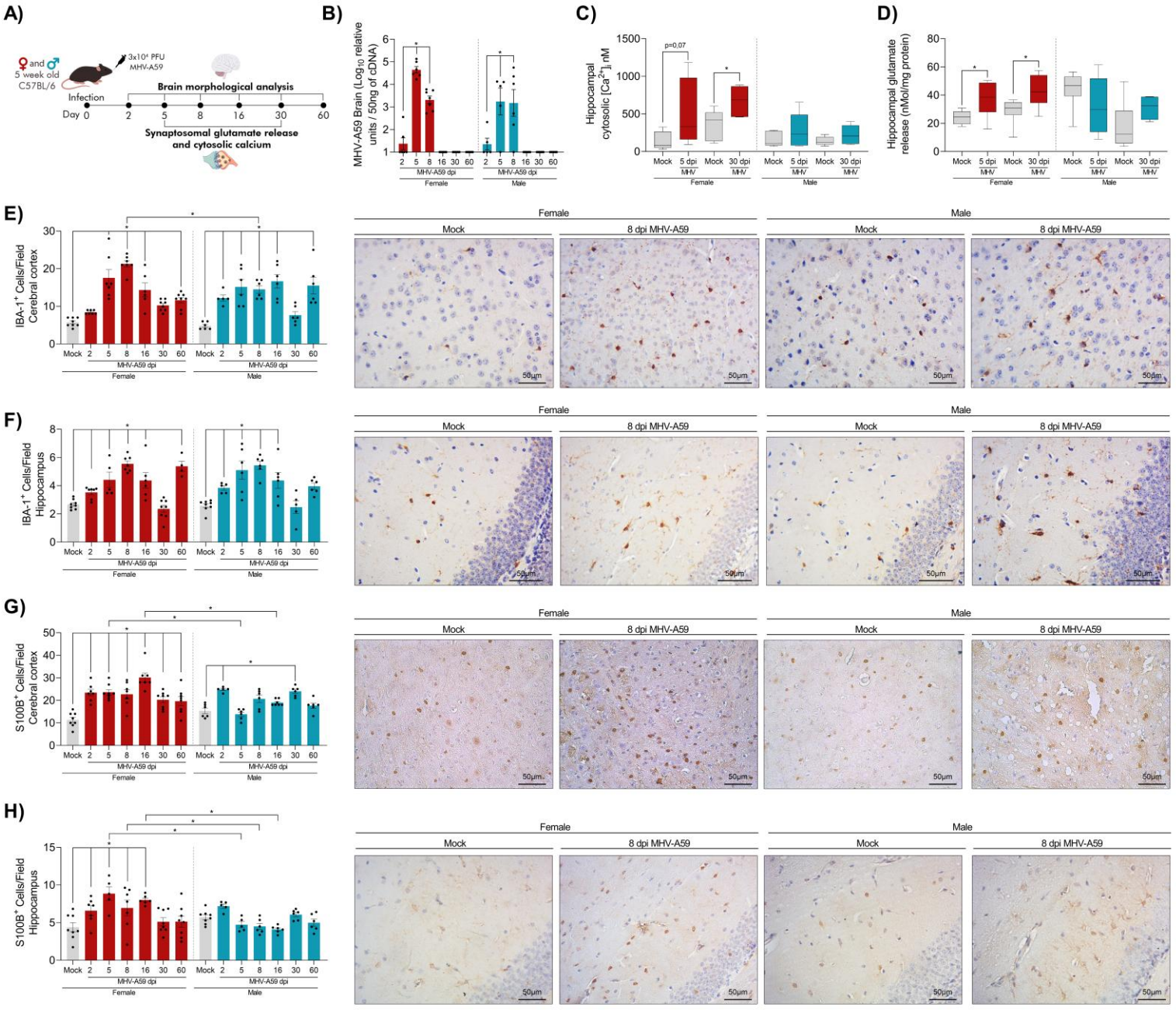

Figure 4. MHV-A59 infection induces more prominent neurochemical and cellular alterations in females. (A) Experimental design. **(B)** MHV-A59 brain viral load measured by PCR. Significance was determined by Two-way ANOVA and Dunnet's multiple comparison test to analyze the differences between infected mice of each sex at different time points or by Two-way ANOVA and the Šídák multiple comparison test to analyze the differences between the sexes at the respective infection time points *p < 0.01 (n = 5-7). **(C)** Hippocampal

intrasynaptosomal calcium concentration (n = 5-7) and **(D)** glutamate release (n = 6-8)**.** Significance was determined by Student's t-test to data that passed Shapiro-Wilk test and Mann-Whitney test to data that did not pass Shapiro-Wilk test *$p < 0.05$. **(E)** IBA-1^+ cells in the cerebral cortex (n = 6-8) and **(F)** hippocampus (n = 4-8). **(G)** $S100B^+$ cells in the cerebral cortex (n =5-8) and **(H)** hippocampus (n = 5-8). Significance was determined by Two-way ANOVA and Dunnet's multiple comparison test to analyze the differences between mock controls and infected mice of respective sex at different time points or by Two-way ANOVA and the Šídák multiple comparison test to analyze the differences between the sexes at the respective infection time points. *$p < 0.05$ to data that passed Shapiro-Wilk test and *$p < 0.01$ to data that did not pass Shapiro-Wilk test.

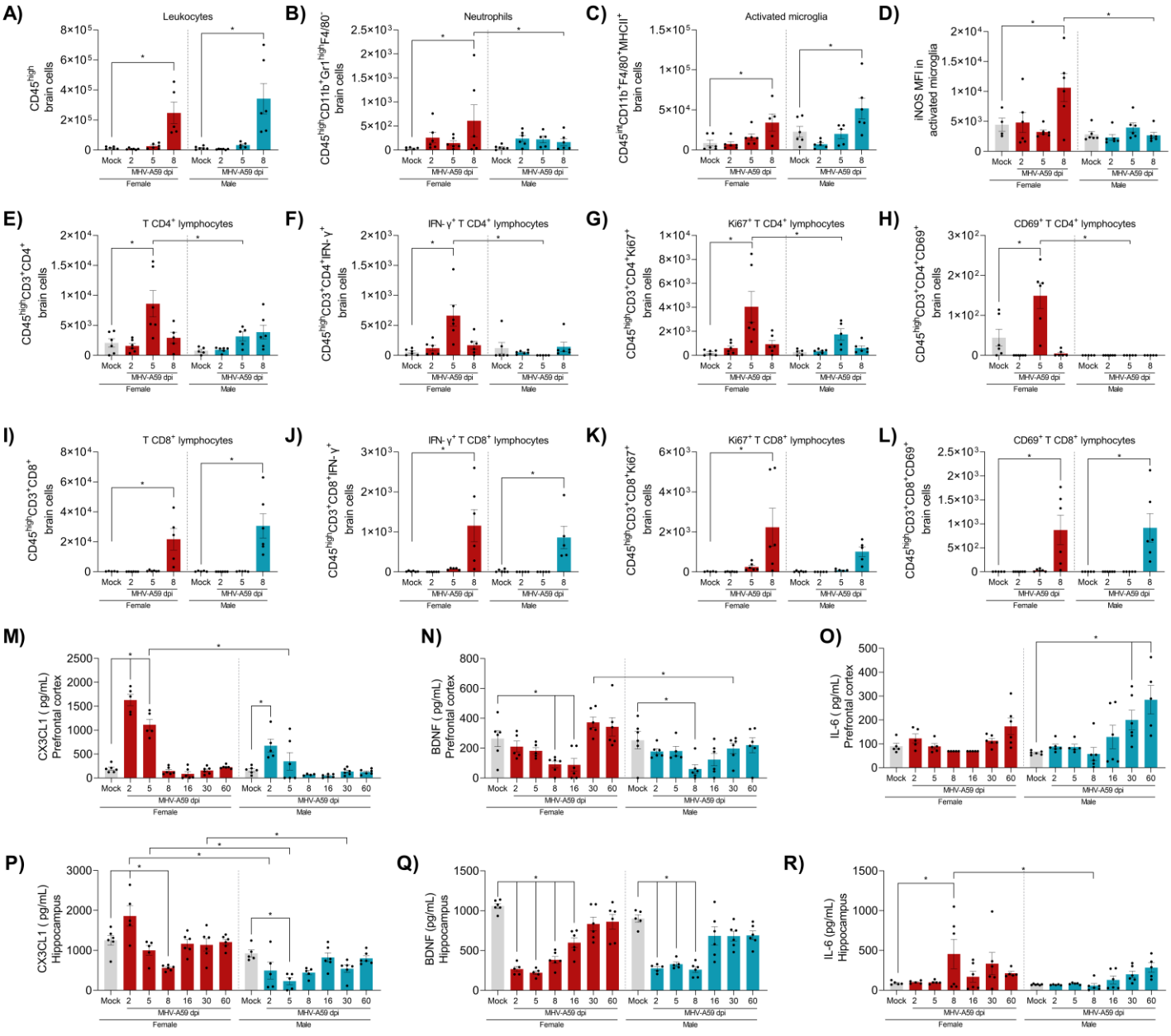

Figure 5. MHV-A59 infection triggers differential accumulation of leukocytes and inflammatory mediators in the brain. (A) Number of brain leukocytes, **(B)** neutrophils, **(C)** activated microglia, **(D)** iNOS MFI in activated microglia, **(E)** $CD4^+$ T lymphocytes, **(F)** $INF\text{-}\gamma^+$ $CD4^+$ T lymphocytes, **(G)** $Ki67^+$ $CD4^+$ T lymphocytes, **(H)** $CD69^+$ $CD4^+$ T lymphocytes, **(I)** $CD8^+$ T lymphocytes, **(J)** $IFNy^+$ $CD8^+$ T lymphocytes, **(K)** $Ki67^+$ $CD8^+$ T lymphocytes, and **(L)** $CD69^+$ $CD8^+$ T lymphocytes, assessed by flow cytometry. Significance was determined by Two-

way ANOVA and Dunnet's multiple comparison test to analyze the differences between mock controls and infected mice of respective sex at different time points and by Two-way ANOVA and the Šídák multiple comparison test to analyze the differences between the sexes at the respective infection time points. *p < 0.05 to data that passed Shapiro-Wilk test and *p < 0.01 to data that did not pass Shapiro-Wilk test (n = 5-6). Prefrontal cortex levels of **(M)** CX3CL1, **(N)** BDNF, and **(O)** IL-6, and hippocampal levels of **(P)** CX3CL1, **(Q)** BDNF, and **(R)** IL-6, measured by ELISA assay. Significance was determined by Two-way ANOVA and Dunnet's multiple comparison test to analyze the differences between mock controls and infected mice of respective sex at different time points and by Two-way ANOVA and the Šídák multiple comparison test to analyze the differences between the sexes at the respective infection time points. *p < 0.05 to data that passed Shapiro-Wilk test and *p < 0.01 to data that did not pass Shapiro-Wilk test (n = 5-6).

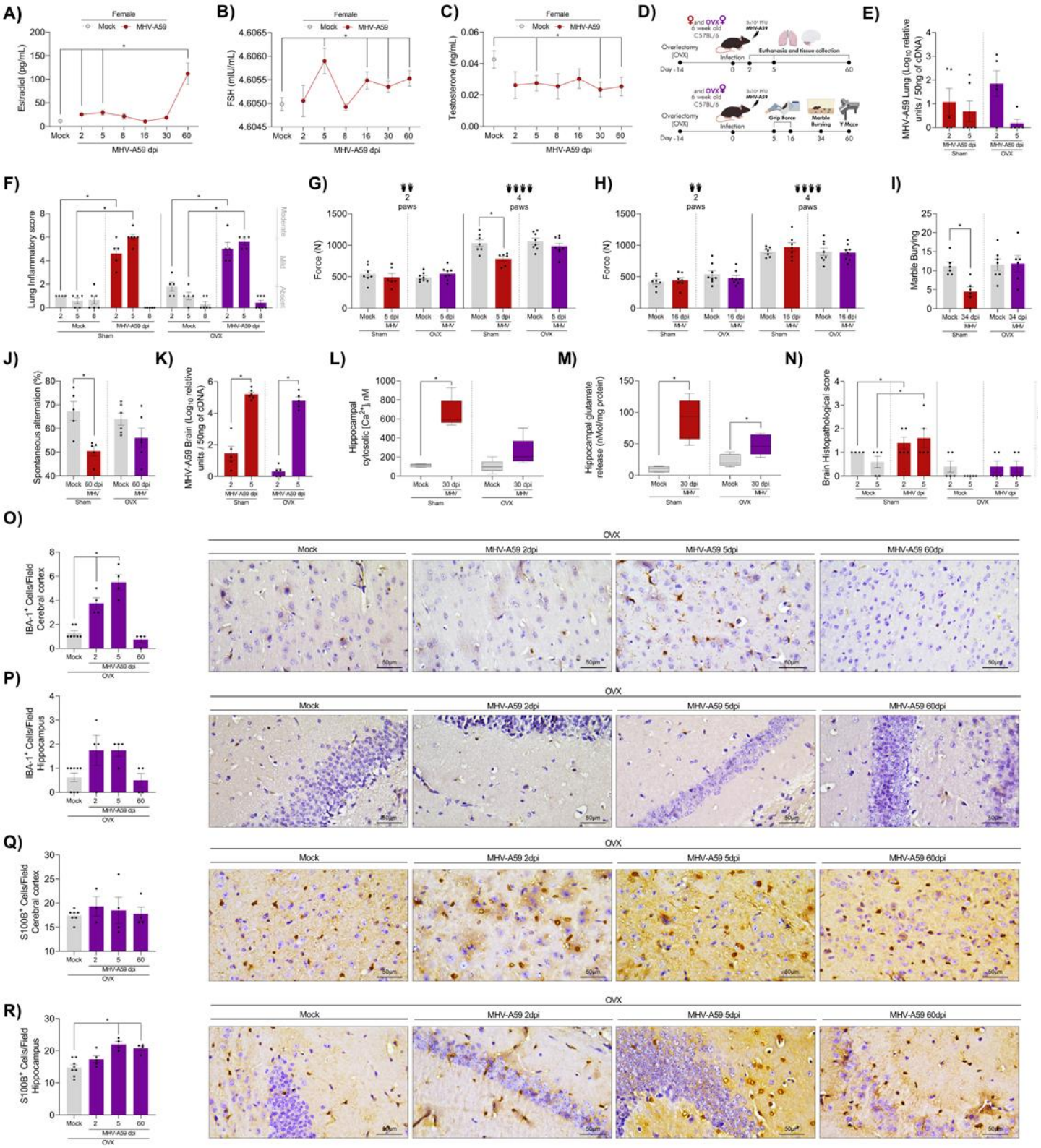
A)
Female
Mock
MHV-A59
Estradiol (pg/mL)
MHV-A59 dpi
B)
FSH (mIU/mL)
C)
Testosterone (ng/mL)
D)
Ovariectomy (OVX)
Infection
Euthanasia and tissue collection
Grip Force
Marble Burying
Y Maze
E)
MHV-A59 Lung (Log10 relative units / 50ng of cDNA)
F)
Lung Inflammatory score
Moderate
Mild
Absent
G)
2 paws
4 paws
Force (N)
H)
I)
Marble Burying
J)
Spontaneous alternation (%)
K)
MHV-A59 Brain (Log10 relative units / 50ng of cDNA)
L)
Hippocampal cytosolic [Ca2+]i nM
M)
Hippocampal glutamate release (nMol/mg protein)
N)
Brain Histopathological score
O)
IBA-1+ Cells/Field Cerebral cortex
OVX
Mock
MHV-A59 2dpi
MHV-A59 5dpi
MHV-A59 60dpi
P)
IBA-1+ Cells/Field Hippocampus
Q)
S100B+ Cells/Field Cerebral cortex
R)
S100B+ Cells/Field Hippocampus

Figure 6. Ovariectomy (OVX) reduces histopathological brain damage, prevents behavioral alterations, and minimizes neurochemical imbalance in the hippocampus induced by MHV-A59 infection. (A) Plasma estradiol levels in mock and MHV-A59-infected female mice. Significance was determined by Student's t-test *p < 0.05. (n = 5-12). **(B)** Plasma FSH levels in mock and MHV-A59-infected female mice. Significance was determined by Student's t-test to data that passed Shapiro-Wilk test and Mann–Whitney test to data that did not pass Shapiro-Wilk test *p < 0.05. (n = 5-7). **(C)** Plasma testosterone levels in mock and MHV-A59-infected female mice. Significance was determined by Student's t-test *p < 0.05. (n = 6-7). **(D)** Experimental design. **(E)** MHV-A59 lung viral load measured by PCR. Significance was determined by Two-way ANOVA and Dunnet's multiple comparison test *p < 0.01 (n = 5-6) **(F)** Overall lung inflammatory score. Significance was determined by Three-way ANOVA and Tukey's multiple comparison test to analyze the differences between sham or OVX, mock or infected mice, at different time points *p < 0.01 (n = 4-7). Force in newtons (N) in 2 or 4 paws grip force test **(G)** 5- and **(H)** 16-days post-infection **(**n = 6-8). **(I)** Marble burying test 34 days post-infection (n = 6-7). **(J)** Spontaneous alternation in Y-maze test 60 days post-infection (n = 5-6). Significance was determined by Student's t-test to data that passed Shapiro-Wilk test and Mann–Whitney test to data that did not pass Shapiro-Wilk test *p < 0.05. **(K)** MHV-A59 brain viral load measured by PCR. Significance was determined by Two-way ANOVA and Dunnet's multiple comparison test *p < 0.01 (n= 5-6) **(L)** Hippocampal intrasynaptosomal calcium concentration (n = 5) and **(M)** glutamate release (n = 5-7)**.** Significance was determined by Student's t-test to data that passed Shapiro-Wilk test and Mann–Whitney test to data that did not pass Shapiro-Wilk test *p < 0.05. **(N)** Overall brain histopathological score (n = 4-5). Significance was determined by Three-way ANOVA and Tukey's multiple comparison test to analyze the differences between sham or OVX, mock or infected mice, at different time points *p < 0.01.

Supplementary Materials

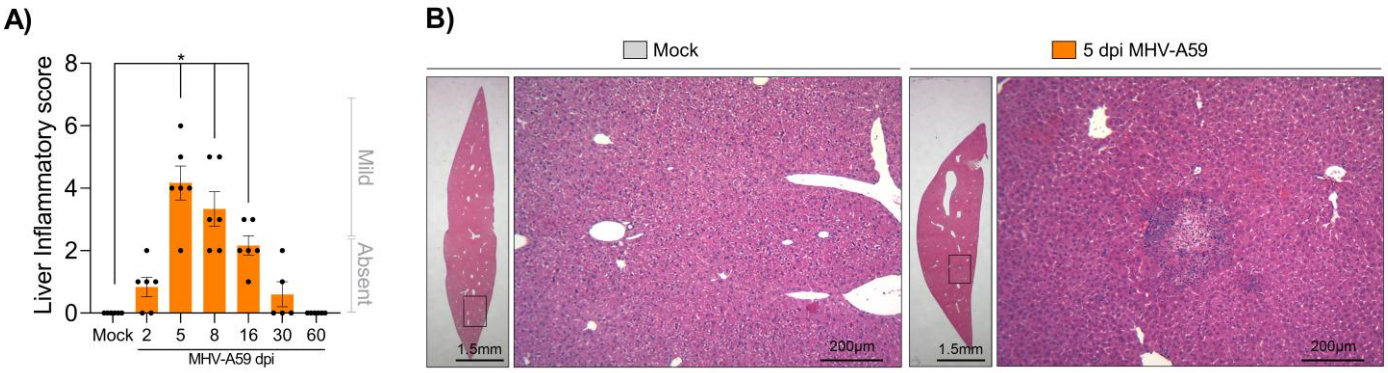

Supplementary figure 1. Intranasal instillation of MHV-A59 in mice results in transitory and mild liver injury. (A) Histopathological assessment in relation to overall liver inflammatory score. Significance was determined by Two-way ANOVA and Dunnet's multiple comparison test *p < 0.01 (n = 5-6). **(B)** Representative images of H&E-stained liver sections of mock controls and 5-dpi MHV-A59-infected mice.

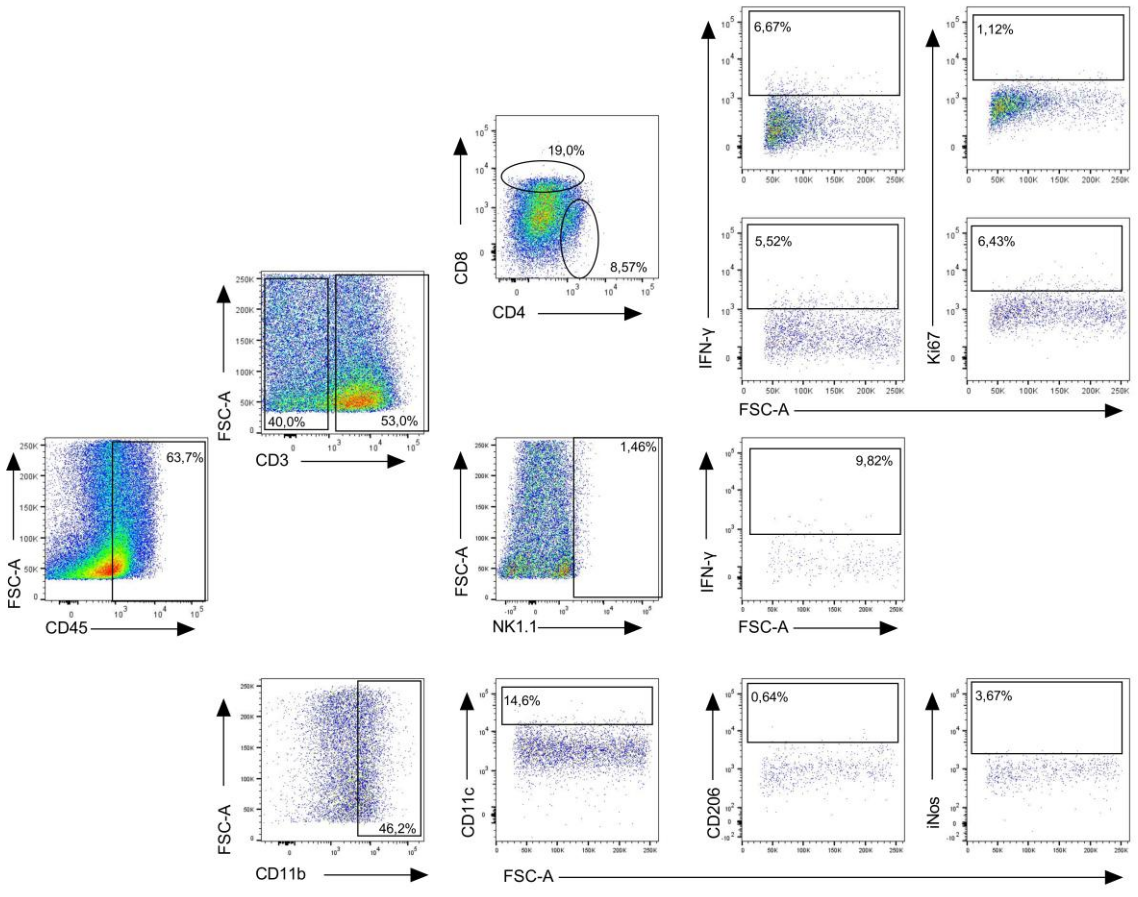

Supplementary Figure 2. Flow cytometry gates for leukocytes (CD45high), dendritic cells ($CD45highCD11b^{+}CD11c^{+}$), T $CD4^{+}$ lymphocytes ($CD45highCD3^{+}CD4^{+}$), T $CD8^{+}$ lymphocytes ($CD45highCD3^{+}CD8^{+}$), NK cells ($CD45highCD3^{-}NK^{+}$), and markers (IFN-γ^{+}, Ki67, IL-10).

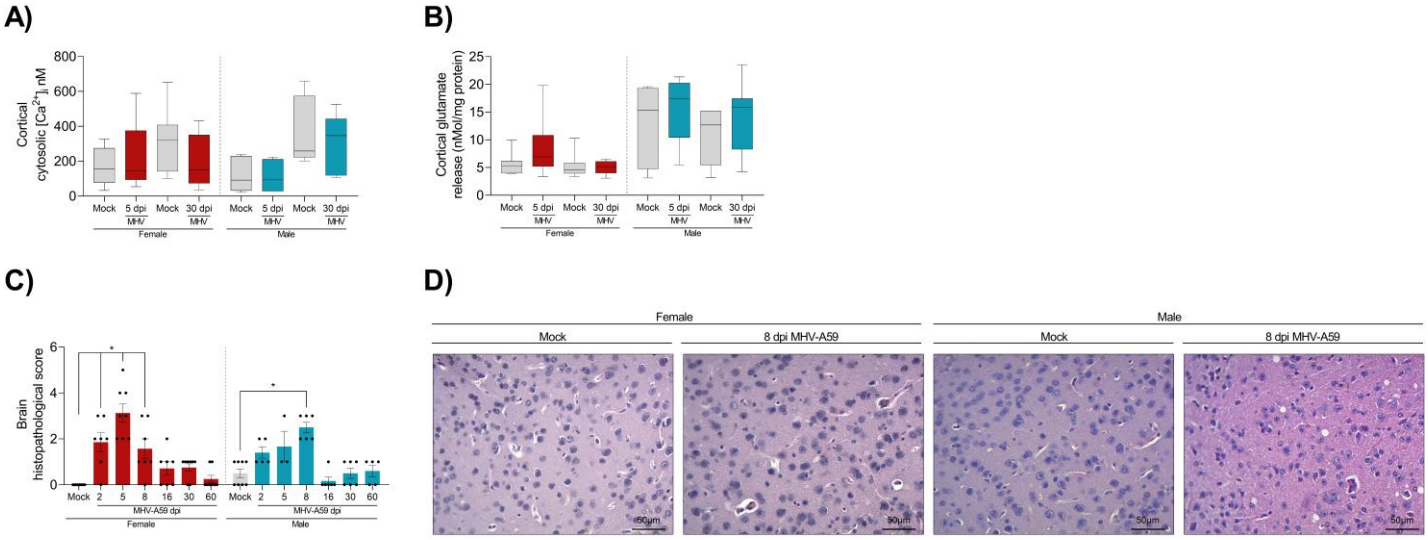

Supplementary Figure 3. (A) Hippocampal intrasynaptosomal calcium concentration (n = 5-7) and **(B)** glutamate release. Significance was determined by Student's t-test to data that passed Shapiro-Wilk test and Mann–Whitney test to data that did not pass Shapiro-Wilk test *$p < 0.05$ (n = 6-8). **(C)** Brain histopathological score. Significance was determined by Two-way ANOVA and Dunnet's multiple comparison test to analyze the differences between mock controls and infected mice of respective sex at different time points. Significance was determined by Two-way ANOVA and the Šídák multiple comparison test to analyze the differences between the sexes at the respective infection time points. *$p < 0.01$ (n = 3-8). **(D)** Representative images of H&E-stained brain sections of mock controls and 8-dpi MHV-A59-infected mice.

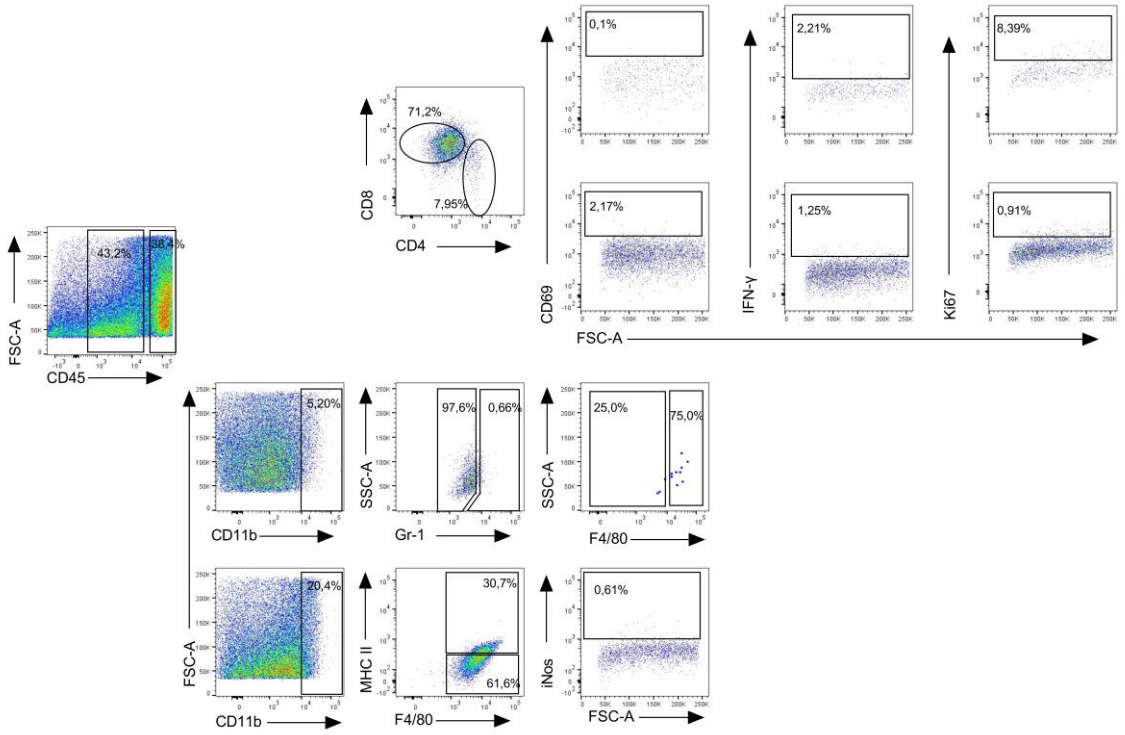

Supplementary Figure 4. Flow cytometry gates for leukocytes (CD45high), activated microglia ($CD45^{int}CD11b^{+}F4/80^{+}MHCII^{+}$), T $CD4^{+}$ lymphocytes ($CD45^{high}CD3^{+}CD4^{+}$), T $CD8^{+}$ lymphocytes ($CD45^{high}CD3^{+}CD8^{+}$), and markers (IFN-$\gamma^{+}$, CD69, Ki67).

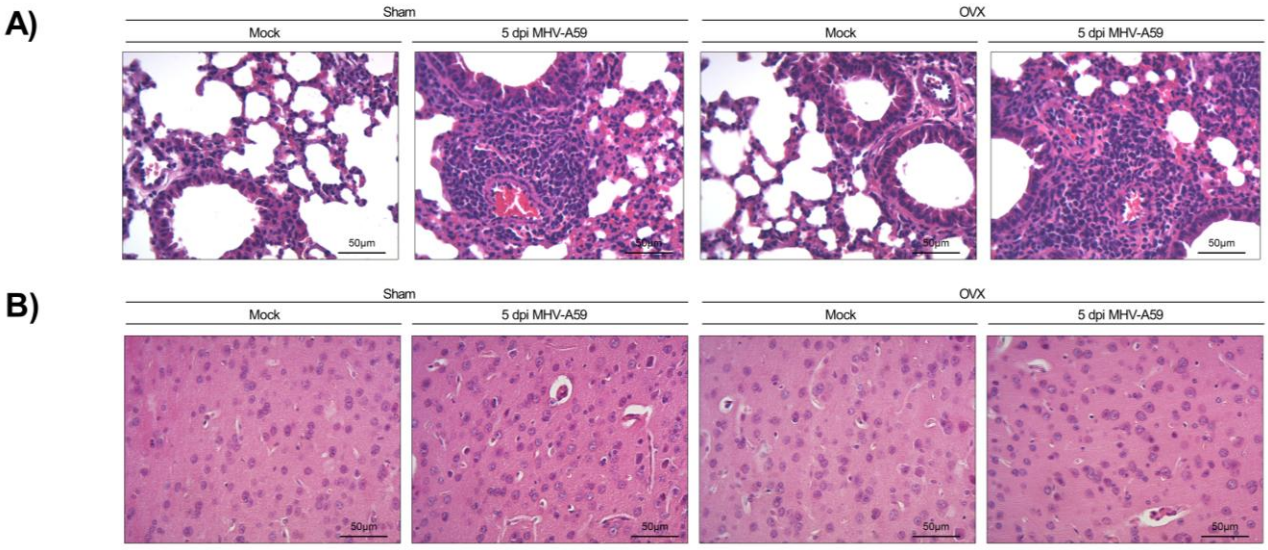

Supplementary Figure 5. (A) Representative images of H&E-stained lung sections of sham and OVX mock controls and 5-dpi MHV-A59-infected mice. **(B)** Representative images of H&E-stained brain sections of sham and OVX mock controls and 5-dpi MHV-A59-infected mice.

Supplementary Table 1. Gender and proportion of animals that developed PCS after MHV-A59 infection.

Test	Day post infection	Gender	Mice % that developed PCS
Open Field Test	16	female	86.6%
2 Paws Grip-force	16	female	81.25%
4 Paws Grip-force Test	16	female	80%
Sucrose Preference Test	17	male	80%
Marble Burying Test	34	female	100%
Y-Labyrinth maze test	60	female	100%
Step-down inhibitory avoidance (short-term aversive memory)	60	female	100%

For the behavioral tests where statistical significance was found between mock and infected animals, the median score of the mock group was used as a threshold to determine whether PCS developed.

Funding

This study was funded by the Fundação de Amparo à Pesquisa do Estado de Minas Gerais grant numbers: RED-00202-22, 29568-1, APQ-02618-23, APQ-04650-23, APQ-02281-18, APQ-00826-21; APQ-01078-21, APQ-02402-23, and APQ-04983-24. Conselho Nacional de Desenvolvimento Científico e Tecnológico by the following grants 442731/2020-5; 408482/2022-2, 305932/2022-5 and 422002/2023-2. This work was also supported by grants from Coordenação de Aperfeiçoamento de Pessoal de Nível Superior –CAPES/Brazil (Projeto: CAPES - Programa: 9951 - Programa Estratégico Emergencial de Prevenção e Combate a Surtos, Endemias, Epidemias e Pandemias AUX 0641/2020 - Processo 88881.507175/2020-01) and CAPES 11/2020 Epidemias, Nº 88887.506690/2020-00. This work also received support from the National Institute of Science and Technology in Dengue and Host-Microorganism Interaction (INCT em Dengue), sponsored by the Conselho Nacional de Desenvolvimento Científico e Tecnológico (CNPq; Brazil) (Processo CNPQ: 465425 /2014-3) and the Fundação de Amparo à Pesquisa do Estado de Minas Gerais (FAPEMIG; Brazil) (Processo FAPEMIG: 25036). And by FINEP - Financiadora de Estudos e Projetos under MCTI/FINEP – MS/SCTIE/DGITIS/CGITS (6205283B-BB28-4F9C-AA65-808FE4450542) grant.

Declaration of Competing Interest: The authors declare that they have no known competing financial interests or personal relationships that could have appeared to influence the work reported in this paper.

Acknowledgements

We are grateful to Ilma Marçal de Souza, Rosemeire Oliveira, Letícia Soldati and Tânia Colina for their technical assistance. We also thank the support of the Technological Center for Advanced and Innovative Therapies - CT - Terapias UFMG and the Experimental Platforms of

UFMG (flow cytometry - Laboratório Institucional de Pesquisa em Biomarcadores (LINBIO) at Pharmacy Faculty/UFMG, Neurological and behavioral analysis - Laboratório de Neurobiologia “Profa Conceição Machado” at ICB/UFMG, *in vivo* platforms of viral infections - GPAV at ICB/UFMG) for providing the facilities and expertise for the conduction of the experiments. VVC and ASM also thanked “Para mulheres na Ciência Prize” provided by L'oréal, UNESCO and ABC.

Data availability

The data that support the findings of this study are included within the article and are available upon request.

References

Ai, S., Klein, R.S., 2020. Update on T cells in the virally infected brain: friends and foes. Curr Opin Neurol 33, 405. https://doi.org/10.1097/WCO.0000000000000825

Al-kuraishy, H.M., Al-Gareeb, A.I., Faidah, H., Al-Maiahy, T.J., Cruz-Martins, N., Batiha, G.E.S., 2021. The Looming Effects of Estrogen in Covid-19: A Rocky Rollout. Front Nutr 8. https://doi.org/10.3389/FNUT.2021.649128

Alnefeesi, Y., Siegel, A., Lui, L.M.W., Teopiz, K.M., Ho, R.C.M., Lee, Y., Nasri, F., Gill, H., Lin, K., Cao, B., Rosenblat, J.D., McIntyre, R.S., 2021. Impact of SARS-CoV-2 Infection on Cognitive Function: A Systematic Review. Front Psychiatry 11. https://doi.org/10.3389/FPSYT.2020.621773

Altmann, C. H., Zvonova, E., Richter, L., & Schüller, P. O. (2023). Pulmonary recovery directly after COVID-19 and in Long-COVID. Respiratory physiology & neurobiology, 315, 104112. https://doi.org/10.1016/j.resp.2023.104112

Andrade, A.C. dos S.P., Campolina-Silva, G.H., Queiroz-Junior, C.M., de Oliveira, L.C., Lacerda, L. de S.B., Gaggino, J.C.P., de Souza, F.R.O., de Meira Chaves, I., Passos, I.B., Teixeira, D.C., Bittencourt-Silva, P.G., Valadão, P.A.C., Rossi-Oliveira, L., Antunes, M.M., Figueiredo, A.F.A., Wnuk, N.T., Temerozo, J.R., Ferreira, A.C., Cramer, A., Oliveira, C.A., Durães-Carvalho, R., Weis Arns, C., Guimarães, P.P.G., Costa, G.M.J., de Menezes, G.B., Guatimosim, C., da Silva, G.S.F., Souza, T.M.L., Barrioni, B.R., Pereira, M. de M., de Sousa, L.P., Teixeira, M.M., Costa, V.V., 2021a. A Biosafety Level 2 Mouse Model for Studying Betacoronavirus-Induced Acute Lung Damage and Systemic Manifestations. J Virol 95, 1276–1297. https://doi.org/10.1128/JVI.01276-21

Angum, F., Khan, T., Kaler, J., Siddiqui, L., & Hussain, A. (2020). The Prevalence of Autoimmune Disorders in Women: A Narrative Review. *Cureus*, *12*(5), e8094. https://doi.org/10.7759/cureus.8094

Badenoch, J.B., Rengasamy, E.R., Watson, C., Jansen, K., Chakraborty, S., Sundaram, R.D., Hafeez, D., Burchill, E., Saini, A., Thomas, L., Cross, B., Hunt, C.K., Conti, I., Ralovska, S., Hussain, Z., Butler, M., Pollak, T.A., Koychev, I., Michael, B.D., Holling, H., Nicholson, T.R., Rogers, J.P., Rooney, A.G., 2022. Persistent neuropsychiatric symptoms after COVID-19: a systematic review and meta-analysis. Brain Commun 4. https://doi.org/10.1093/BRAINCOMMS/FCAB297

Bai, F., Tomasoni, D., Falcinella, C., Barbanotti, D., Castoldi, R., Mulè, G., Augello, M., Mondatore, D., Allegrini, M., Cona, A., Tesoro, D., Tagliaferri, G., Viganò, O., Suardi, E., Tincati, C., Beringheli, T., Varisco, B., Battistini, C.L., Piscopo, K., Vegni, E., Tavelli, A., Terzoni, S., Marchetti, G., Monforte, A. d. A., 2022. Female gender is associated with long COVID syndrome: a prospective cohort study. Clinical Microbiology and Infection 28, 611.e9. https://doi.org/10.1016/J.CMI.2021.11.002

Balez, R., Ooi, L., 2016. Getting to NO Alzheimer's Disease: Neuroprotection versus Neurotoxicity Mediated by Nitric Oxide. Oxid Med Cell Longev 2016. https://doi.org/10.1155/2016/3806157

Ballering, A. V., van Zon, S.K.R., olde Hartman, T.C., Rosmalen, J.G.M., 2022. Persistence of somatic symptoms after COVID-19 in the Netherlands: an observational cohort study. Lancet 400, 452–461. https://doi.org/10.1016/S0140-6736(22)01214-4

Bienvenu, L.A., Noonan, J., Wang, X., Peter, K., 2020. Higher mortality of COVID-19 in males: sex differences in immune response and cardiovascular comorbidities. Cardiovasc Res 116, 2197–2206. https://doi.org/10.1093/CVR/CVAA284

Bupp, M.R.G., Jorgensen, T.N., 2018. Androgen-Induced Immunosuppression. Front Immunol 9. https://doi.org/10.3389/FIMMU.2018.00794

Cai, Z., Zhong, J., Jiang, Y., Zhang, J., 2022. Associations between COVID-19 infection and sex steroid hormones. Front Endocrinol (Lausanne) 13, 940675. https://doi.org/10.3389/FENDO.2022.940675/BIBTEX

Carrillo, J., Izquierdo-Useros, N., Ávila-Nieto, C., Pradenas, E., Clotet, B., Blanco, J., 2021. Humoral immune responses and neutralizing antibodies against SARS-CoV-2; implications in pathogenesis and protective immunity. Biochem Biophys Res Commun 538, 187–191. https://doi.org/10.1016/J.BBRC.2020.10.108

Cazé, A.B., Cerqueira-Silva, T., Bomfim, A.P., de Souza, G.L., Azevedo, A.C.A., Brasil, M.Q.A., Santos, N.R., Khouri, R., Dan, J., Bandeira, A.C., Cavalcanti, L.P.G., Barral-Netto, M., Barral, A., Barbosa, C.G., Boaventura, V.S., 2023. Prevalence and risk factors for long COVID after mild disease: A cohort study with a symptomatic control group. J Glob Health 13. https://doi.org/10.7189/JOGH.13.06015

Chamera, K., Trojan, E., Szuster-Głuszczak, M., Basta-Kaim, A., 2020. The Potential Role of Dysfunctions in Neuron-Microglia Communication in the Pathogenesis of Brain Disorders. Curr Neuropharmacol 18, 408. https://doi.org/10.2174/1570159X17666191113101629

Channappanavar, R., Fett, C., Mack, M., Ten Eyck, P.P., Meyerholz, D.K., Perlman, S., 2017. Sex-Based Differences in Susceptibility to Severe Acute Respiratory Syndrome Coronavirus Infection. J Immunol 198, 4046–4053. https://doi.org/10.4049/JIMMUNOL.1601896

Chen, C., Haupert, S.R., Zimmermann, L., Shi, X., Fritsche, L.G., Mukherjee, B., 2022. Global Prevalence of Post-Coronavirus Disease 2019 (COVID-19) Condition or Long COVID: A Meta-Analysis and Systematic Review. J Infect Dis 226, 1593–1607. https://doi.org/10.1093/INFDIS/JIAC136

Chen, J., Shehadah, A., Pal, A., Zacharek, A., Cui, X., Cui, Y., Roberts, C., Lu, M., Zeitlin, A., Hariri, R., Chopp, M., 2020. Neurotrophic Factor BDNF, Physiological Functions and Therapeutic Potential in Depression, Neurodegeneration and Brain Cancer. International Journal of Molecular Sciences 2020, Vol. 21, Page 7777 21, 7777. https://doi.org/10.3390/IJMS21207777

Chen, T., Song, J., Liu, H., Zheng, H., Chen, C., 2021. Positive Epstein–Barr virus detection in coronavirus disease 2019 (COVID-19) patients. Scientific Reports 2021 11:1 11, 1–7. https://doi.org/10.1038/s41598-021-90351-y

Cirulli, F., Berry, A., Chiarotti, F., Alleva, E., 2004. Intrahippocampal administration of BDNF in adult rats affects short-term behavioral plasticity in the Morris water maze and performance in the elevated plus-maze. Hippocampus 14, 802–807. https://doi.org/10.1002/HIPO.10220

Comelli, A., Viero, G., Bettini, G., Nobili, A., Tettamanti, M., Galbussera, A.A., Muscatello, A., Mantero, M., Canetta, C., Martinelli Boneschi, F., Arighi, A., Brambilla, P., Vecchi, M., Lampertico, P., Bonfanti, P., Contoli, M., Blasi, F., Gori, A., Bandera, A., 2022. Patient-Reported Symptoms and Sequelae 12 Months After COVID-19 in Hospitalized Adults: A Multicenter Long-Term Follow-Up Study. Front Med (Lausanne) 9, 834354. https://doi.org/10.3389/FMED.2022.834354

Costa, V.V., Fagundes, C.T, Valadão, D.F., Ávila, T.V., Cisalpino, D., Rocha, R.F., Ribeiro, L.S., Ascenção, F.R., Kangussu, L.M., Queiroz-Junior, C.M., Astigarraga, R.G., Gouveia, F.L.,

Silva, T.A., Bonaventura, D., Sampaio, D.A., Leite, A.C., Teixeira, M.M., Souza, D.G. Subversion of early innate antiviral responses during antibody-dependent enhancement of Dengue virus infection induces severe disease in immunocompetent mice, 2014. Med Microbiol Immunol. 203(4):231-50. https://doi.org/10.1007/s00430-014-0334-5.

Costa, V.V., Del Sarto, J.L., Rocha, R.F., Silva, F.R., Doria, J.G., Olmo, I.G., Marques, R.E., Queiroz-Junior, C.M., Foureaux, G., Araújo, J.M.S., Cramer, A., Real, A.L.C.V., Ribeiro, L.S., Sardi, S.I., Ferreir, A.J., Machado, F.S., De Oliveira, A.C., Teixeira, A.L., Nakaya, H.I., Souza, D.G., Ribeiro, F.M., Teixeira, M.M., 2017. N-Methyl-d-Aspartate (NMDA) Receptor Blockade Prevents Neuronal Death Induced by Zika Virus Infection. mBio 8. https://doi.org/10.1128/MBIO.00350-17

Crunfli, F., Carregari, V.C., Veras, F.P., Silva, L.S., Nogueira, M.H., Antunes, A.S.L.M., Vendramini, P.H., Valença, A.G.F., Brandão-Teles, C., da Silva Zuccoli, G., Reis-De-Oliveira, G., Silva-Costa, L.C., Saia-Cereda, V.M., Smith, B.J., Codo, A.C., de Souza, G.F., Muraro, S.P., Parise, P.L., Toledo-Teixeira, D.A., de Castro, I.M.S., Melo, B.M., Almeida, G.M., Firmino, E.M.S., Paiva, I.M., Silva, B.M.S., Guimarães, R.M., Mendes, N.D., Ludwig, R.L., Ruiz, G.P., Knittel, T.L., Davanzo, G.G., Gerhardt, J.A., Rodrigues, P.B., Forato, J., Amorim, M.R., Brunetti, N.S., Martini, M.C., Benatti, M.N., Batah, S.S., Siyuan, L., João, R.B., Aventurato, I.K., de Brito, M.R., Mendes, M.J., da Costa, B.A., Alvim, M.K.M., da Silva Junior, J.R., Damião, L.L., de Sousa, I.M.P., da Rocha, E.D., Gonçalves, S.M., Lopes da Silva, L.H., Bettini, V., Campos, B.M., Ludwig, G., Tavares, L.A., Pontelli, M.C., Viana, R.M.M., Martins, R.B., Vieira, A.S., Alves-Filho, J.C., Arruda, E., Podolsky-Gondim, G.G., Santos, M.V., Neder, L., Damasio, A., Rehen, S., Vinolo, M.A.R., Munhoz, C.D., Louzada-Junior, P., Oliveira, R.D., Cunha, F.Q., Nakaya, H.I., Mauad, T., Duarte-Neto, A.N., da Silva, L.F.F., Dolhnikoff, M., Saldiva, P.H.N., Farias, A.S., Cendes, F., Moraes-Vieira, P.M.M., Fabro, A.T., Sebollela, A., Proença-Modena, J.L., Yasuda, C.L., Mori, M.A., Cunha, T.M., Martins-De-Souza, D., 2022.

Morphological, cellular, and molecular basis of brain infection in COVID-19 patients. Proc Natl Acad Sci U S A 119, e2200960119. https://doi.org/10.1073/pnas.2200960119

Davis, H.E., Assaf, G.S., McCorkell, L., Wei, H., Low, R.J., Re'em, Y., Redfield, S., Austin, J.P., Akrami, A., 2021. Characterizing long COVID in an international cohort: 7 months of symptoms and their impact. EClinicalMedicine 38, 101019. https://doi.org/10.1016/j.eclinm.2021.101019

Davis, H.E., McCorkell, L., Vogel, J.M., Topol, E.J., 2023. Long COVID: major findings, mechanisms and recommendations. Nature Reviews Microbiology 2023 21:3 21, 133–146. https://doi.org/10.1038/s41579-022-00846-2

De Albuquerque, N., Baig, E., Ma, X., Zhang, J., He, W., Rowe, A., Habal, M., Liu, M., Shalev, I., Downey, G.P., Gorczynski, R., Butany, J., Leibowitz, J., Weiss, S.R., McGilvray, I.D., Phillips, M.J., Fish, E.N., Levy, G.A., 2006. MurineHepatitis Virus Strain 1 Produces a Clinically Relevant Model of Severe Acute Respiratory Syndrome in A/J Mice. J Virol 80, 10382–10394. https://doi.org/10.1128/JVI.00747-06

De Bundel, D., Gangarossa, G., Biever, A., Bonnefont, X., Valjent, E., 2013. Cognitive dysfunction, elevated anxiety, and reduced cocaine response in circadian clock-deficient cryptochrome knockout mice. Front Behav Neurosci 7. https://doi.org/10.3389/FNBEH.2013.00152

Dhakal, S., Ruiz-Bedoya, C.A., Zhou, R., Creisher, P.S., Villano, J.S., Littlefield, K., Castillo, J.R., Marinho, P., Jedlicka, A.E., Ordonez, A.A., Bahr, M., Majewska, N., Betenbaugh, M.J., Flavahan, K., Mueller, A.R.L., Looney, M.M., Quijada, D., Mota, F., Beck, S.E., Brockhurst, J., Braxton, A.M., Castell, N., Stover, M., D'alessio, F.R., Metcalf Pate, K.A., Karakousis, P.C., Mankowski, J.L., Pekosz, A., Jain, S.K., Klein, S.L., 2021. Sex Differences in Lung Imaging and

SARS-CoV-2 Antibody Responses in a COVID-19 Golden Syrian Hamster Model. mBio 12. https://doi.org/10.1128/MBIO.00974-21

Ding, T., Zhang, J., Wang, T., Cui, P., Chen, Z., Jiang, J., Zhou, S., Dai, J., Wang, B., Yuan, S., Ma, W., Ma, L., Rong, Y., Chang, J., Miao, X., Ma, X., & Wang, S. (2021). Potential Influence of Menstrual Status and Sex Hormones on Female Severe Acute Respiratory Syndrome Coronavirus 2 Infection: A Cross-sectional Multicenter Study in Wuhan, China. *Clinical infectious diseases : an official publication of the Infectious Diseases Society of America*, *72*(9), e240–e248. https://doi.org/10.1093/cid/ciaa1022

Dinnon, K.H., Leist, S.R., Schäfer, A., Edwards, C.E., Martinez, D.R., Montgomery, S.A., West, A., Yount, B.L., Hou, Y.J., Adams, L.E., Gully, K.L., Brown, A.J., Huang, E., Bryant, M.D., Choong, I.C., Glenn, J.S., Gralinski, L.E., Sheahan, T.P., Baric, R.S., 2020. A mouse-adapted model of SARS-CoV-2 to test COVID-19 countermeasures. Nature 2020 586:7830 586, 560–566. https://doi.org/10.1038/s41586-020-2708-8

Dunkley, P.R., Heath, J.W., Harrison, S.M., Jarvie, P.E., Glenfield, P.J., Rostas, J.A.P., 1988. A rapid Percoll gradient procedure for isolation of synaptosomes directly from an S1 fraction: homogeneity and morphology of subcellular fractions. Brain Res 441, 59–71. https://doi.org/10.1016/0006-8993(88)91383-2

Düsedau, H.P., Steffen, J., Figueiredo, C.A., Boehme, J.D., Schultz, K., Erck, C., Korte, M., Faber-Zuschratter, H., Smalla, K.H., Dieterich, D., Kröger, A., Bruder, D., Dunay, I.R., 2021. Influenza A Virus (H1N1) Infection Induces Microglial Activation and Temporal Dysbalance in Glutamatergic Synaptic Transmission. mBio 12. https://doi.org/10.1128/MBIO.01776-21

Erta, M., Quintana, A., Hidalgo, J., 2012. Interleukin-6, a Major Cytokine in the Central Nervous System. Int J Biol Sci 8, 1254. https://doi.org/10.7150/IJBS.4679

Frere, J.J., Serafini, R.A., Pryce, K.D., Zazhytska, M., Oishi, K., Golynker, I., Panis, M., Zimering, J., Horiuchi, S., Hoagland, D.A., Møller, R., Ruiz, A., Kodra, A., Overdevest, J.B., Canoll, P.D., Borczuk, A.C., Chandar, V., Bram, Y., Schwartz, R., Lomvardas, S., Zachariou, V., tenOever, B.R., 2022. SARS-CoV-2 infection in hamsters and humans results in lasting and unique systemic perturbations after recovery. Sci Transl Med 14, 3059.https://doi.org/10.1126/scitranslmed.abq3059

Garber, C., Soung, A., Vollmer, L.L., Kanmogne, M., Last, A., Brown, J., Klein, R.S., 2019. T cells promote microglia-mediated synaptic elimination and cognitive dysfunction during recovery from neuropathogenic flaviviruses. Nature Neuroscience 2019 22:8 22, 1276–1288. https://doi.org/10.1038/s41593-019-0427-y

García-González, L., Martí-Sarrias, A., Puertas, M.C., Bayón-Gil, Á., Resa-Infante, P., Martinez-Picado, J., Navarro, A., Acosta, S., 2023. Understanding the neurological implications of acute and long COVID using brain organoids. Dis Model Mech 16. https://doi.org/10.1242/DMM.050049

Gorska, A.M., Eugenin, E.A., 2020. The Glutamate System as a Crucial Regulator of CNS Toxicity and Survival of HIV Reservoirs. Front Cell Infect Microbiol 10, 523638. https://doi.org/10.3389/fcimb.2020.00261

Grynkiewicz, G., Poenie, M., Tsien, R.Y., 1985. A new generation of Ca2+ indicators with greatly improved fluorescence properties. Journal of Biological Chemistry 260, 3440–3450. https://doi.org/10.1016/S0021-9258(19)83641-4

Gu, H., Chen, Q., Yang, G., He, L., Fan, H., Deng, Y.Q., Wang, Y., Teng, Y., Zhao, Z., Cui, Y., Li, Yuchang, Li, X.F., Li, J., Zhang, N.N., Yang, Xiaolan, Chen, S., Guo, Y., Zhao, G., Wang, X., Luo, D.Y., Wang, H., Yang, Xiao, Li, Yan, Han, G., He, Y., Zhou, X., Geng, S., Sheng, X.,

Jiang, S., Sun, S., Qin, C.F., Zhou, Y., 2020. Adaptation of SARS-CoV-2 in BALB/c mice for testing vaccine efficacy. Science 369. https://doi.org/10.1126/SCIENCE.ABC4730

Hao, X., Ou, M., Zhang, D., Zhao, W., Yang, Y., Liu, J., Yang, H., Zhu, T., Li, Y., & Zhou, C. (2020). The Effects of General Anesthetics on Synaptic Transmission. *Current neuropharmacology*, *18*(10), 936–965. https://doi.org/10.2174/1570159X18666200227125854

Harapan, B.N., Yoo, H.J., 2021. Neurological symptoms, manifestations, and complications associated with severe acute respiratory syndrome coronavirus 2 (SARS-CoV-2) and coronavirus disease 19 (COVID-19). Journal of Neurology 2021 268:9 268, 3059–3071. https://doi.org/10.1007/S00415-021-10406-Y

Harding, A. T., & Heaton, N. S. (2022). The Impact of Estrogens and Their Receptors on Immunity and Inflammation during Infection. *Cancers*, *14*(4), 909. https://doi.org/10.3390/cancers14040909

Hefner, K., Holmes, A., 2007. Ontogeny of fear-, anxiety- and depression-related behavior across adolescence in C57BL/6J mice. Behavioural brain research 176, 210–215. https://doi.org/10.1016/J.BBR.2006.10.001

Henry, B.M., De Oliveira, M.H.S., Benoit, S., Plebani, M., Lippi, G., 2020. Hematologic, biochemical and immune biomarker abnormalities associated with severe illness and mortality in coronavirus disease 2019 (COVID-19): A meta-analysis. Clin Chem Lab Med 58, 1021–1028. https://doi.org/10.1515/cclm-2020-0369

Hikmet, F., Méar, L., Edvinsson, Å., Micke, P., Uhlén, M., Lindskog, C., 2020. The protein expression profile of ACE2 in human tissues. Mol Syst Biol 16, e9610. https://doi.org/10.15252/MSB.20209610

Huang, C., Wang, Y., Li, X., Ren, L., Zhao, J., Hu, Y., Zhang, L., Fan, G., Xu, J., Gu, X., Cheng, Z., Yu, T., Xia, J., Wei, Y., Wu, W., Xie, X., Yin, W., Li, H., Liu, M., Xiao, Y., Gao, H., Guo, L., Xie, J., Wang, G., Jiang, R., Gao, Z., Jin, Q., Wang, J., Cao, B., 2020. Clinical features of patients infected with 2019 novel coronavirus in Wuhan, China. The Lancet 395, 497–506. https://doi.org/10.1016/S0140-6736(20)30183-5

Jiang, Y., Cheng, Y., Xiao, J., Wang, Y., Chen, G., Zhang, Y., 2023. Analysis of the correlation between heart rate variability and palpitation symptoms in female patients with long COVID. Front Cardiovasc Med 10, 1273156. https://doi.org/10.3389/fcvm.2023.1273156

Kalueff, A. V., Gallagher, P.S., Murphy, D.L., 2006. Are serotonin transporter knockout mice "depressed"? hypoactivity but no anhedonia. Neuroreport 17, 1347–1351. https://doi.org/10.1097/01.WNR.0000230514.08962.76

Klein, J., Wood, J., Jaycox, J. R., Dhodapkar, R. M., Lu, P., Gehlhausen, J. R., Tabachnikova, A., Greene, K., Tabacof, L., Malik, A. A., Silva Monteiro, V., Silva, J., Kamath, K., Zhang, M., Dhal, A., Ott, I. M., Valle, G., Peña-Hernández, M., Mao, T., … Iwasaki, A. (2023). Distinguishing features of long COVID identified through immune profiling. *Nature 2023 623:7985*, *623*(7985), 139–148. https://doi.org/10.1038/s41586-023-06651-y

Klein, R.S., Garber, C., Funk, K.E., Salimi, H., Soung, A., Kanmogne, M., Manivasagam, S., Agner, S., Cain, M., 2019. Neuroinflammation During RNA Viral Infections. https://doi.org/10.1146/annurev-immunol-042718-041417

Klein, S.L., Flanagan, K.L., 2016. Sex differences in immune responses. Nature Reviews Immunology 2016 16:10 16, 626–638. https://doi.org/10.1038/nri.2016.90

Kocanova, S., Mazaheri, M., Caze-Subra, S., Bystricky, K., 2010. Ligands specify estrogen receptor alpha nuclear localization and degradation. BMC Cell Biol 11. https://doi.org/10.1186/1471-2121-11-98

Kolisnyk, B., Guzman, M. S., Raulic, S., Fan, J., Magalhães, A. C., Feng, G., Gros, R., Prado, V. F., & Prado, M. A. M. (2013). ChAT-ChR2-EYFP mice have enhanced motor endurance but show deficits in attention and several additional cognitive domains. *The Journal of Neuroscience : The Official Journal of the Society for Neuroscience*, *33*(25), 10427–10438. https://doi.org/10.1523/JNEUROSCI.0395-13.2013

Körner, R.W., Majjouti, M., Alejandre Alcazar, M.A., Mahabir, E., 2020. Of Mice and Men: The Coronavirus MHV and Mouse Models as a Translational Approach to Understand SARS-CoV-2. Viruses 2020, Vol. 12, Page 880 12, 880. https://doi.org/10.3390/V12080880

Kwon, H.S., Koh, S.H., 2020. Neuroinflammation in neurodegenerative disorders: the roles of microglia and astrocytes. Translational Neurodegeneration 2020 9:1 9, 1–12. https://doi.org/10.1186/S40035-020-00221-2

Lamontagne, S.J., Winters, M.F., Pizzagalli, D.A., Olmstead, M.C., 2021. Post-acute sequelae of COVID-19: Evidence of mood & cognitive impairment. Brain Behav Immun Health 17, 100347. https://doi.org/10.1016/J.BBIH.2021.100347

Lane, T.E., Liu, M.T., Chen, B.P., Asensio, V.C., Samawi, R.M., Paoletti, A.D., Campbell, I.L., Kunkel, S.L., Fox, H.S., Buchmeier, M.J., 2000. A Central Role for CD4+ T Cells and RANTES in Virus-Induced Central Nervous System Inflammation and Demyelination. J Virol 74, 1415. https://doi.org/10.1128/JVI.74.3.1415-1424.2000

Li, H., Wang, T., Shi, C., Yang, Y., Li, X., Wu, Y., Xu, Z.Q.D., 2018. Inhibition of GALR1 in PFC Alleviates Depressive-Like Behaviors in Postpartum Depression Rat Model by

Upregulating CREB-BNDF and 5-HT Levels. Front Psychiatry 9. https://doi.org/10.3389/FPSYT.2018.00588

Li, M., Li, C., Yu, H., Cai, X., Shen, X., Sun, X., Wang, J., Zhang, Y., Wang, C., 2017. Lentivirus-mediated interleukin-1β (IL-1β) knock-down in the hippocampus alleviates lipopolysaccharide (LPS)-induced memory deficits and anxiety- and depression-like behaviors in mice. J Neuroinflammation 14. https://doi.org/10.1186/S12974-017-0964-9

Liao, D., Zhou, F., Luo, L., Xu, M., Wang, H., Xia, J., Gao, Y., Cai, L., Wang, Z., Yin, P., Wang, Y., Tang, L., Deng, J., Mei, H., Hu, Y., 2020. Haematological characteristics and risk factors in the classification and prognosis evaluation of COVID-19: a retrospective cohort study. Lancet Haematol 7, e671–e678. https://doi.org/10.1016/S2352-3026(20)30217-9

Limjunyawong, N., Fallica, J., Horton, M.R., Mitzner, W., 2015. Measurement of the Pressure-volume Curve in Mouse Lungs. J Vis Exp 52376. https://doi.org/10.3791/52376

Long, B., Brady, W.J., Koyfman, A., Gottlieb, M., 2020. Cardiovascular complications in COVID-19. Am J Emerg Med 38, 1504–1507. https://doi.org/10.1016/J.AJEM.2020.04.048

Liu M, Yang S, Yang J, Lee Y, Kou J, Wang C. Neuroprotective and Memory-Enhancing Effects of Antioxidant Peptide From Walnut (Juglans regia L.) Protein Hydrolysates. *Natural Product Communications*. 2019;14(7). doi:10.1177/1934578X19865838

Mao, L., Jin, H., Wang, M., Hu, Y., Chen, S., He, Q., Chang, J., Hong, C., Zhou, Y., Wang, D., Miao, X., Li, Y., Hu, B., 2020a. Neurologic Manifestations of Hospitalized Patients with Coronavirus Disease 2019 in Wuhan, China. JAMA Neurol 77, 683–690. https://doi.org/10.1001/JAMANEUROL.2020.1127

Mao, R., Qiu, Y., He, J.S., Tan, J.Y., Li, X.H., Liang, J., Shen, J., Zhu, L.R., Chen, Y., Iacucci, M., Ng, S.C., Ghosh, S., Chen, M.H., 2020b. Manifestations and prognosis of gastrointestinal and liver involvement in patients with COVID-19: a systematic review and meta-analysis. Lancet Gastroenterol Hepatol 5, 667–678. https://doi.org/10.1016/S2468-1253(20)30126-6

Masciarella, A.D., Di Gregorio, D.M., Ramamoorthy, R., Hussain, H., Jayakumar, A.R., Paidas, M.J., 2023. A Mouse Model of MHV-1 Virus Infection for Study of Acute and Long COVID Infection. Curr Protoc 3, e896. https://doi.org/10.1002/cpz1.896

Mendes de Almeida, V., Engel, D.F., Ricci, M.F., Cruz, C.S., Lopes, Í.S., Alves, D.A., d' Auriol, M., Magalhães, J., Machado, E.C., Rocha, V.M., Carvalho, T.G., Lacerda, L.S.B., Pimenta, J.C., Aganetti, M., Zuccoli, G.S., Smith, B.J., Carregari, V.C., da Silva Rosa, E., Galvão, I., Dantas Cassali, G., Garcia, C.C., Teixeira, M.M., André, L.C., Ribeiro, F.M., Martins, F.S., Saia, R.S., Costa, V.V., Martins-de-Souza, D., Hansbro, P.M., Marques, J.T., Aguiar, E.R.G.R., Vieira, A.T., 2023. Gut microbiota from patients with COVID-19 cause alterations in mice that resemble post-COVID symptoms. Gut Microbes 15. https://doi.org/10.1080/19490976.2023.2249146

Meng, X.M., Nikolic-Paterson, D.J., Lan, H.Y., 2016. TGF-β: the master regulator of fibrosis. Nature Reviews Nephrology 2016 12:6 12, 325–338. https://doi.org/10.1038/nrneph.2016.48

Mo, X., Jian, W., Su, Z., Chen, M., Peng, H., Peng, P., Lei, C., Chen, R., Zhong, N., Li, S., 2020. Abnormal pulmonary function in COVID-19 patients at time of hospital discharge. Eur Respir J 55. https://doi.org/10.1183/13993003.01217-2020

Mohamed, M.S., Moulin, T.C., Schiöth, H.B., 2021. Sex differences in COVID-19: the role of androgens in disease severity and progression. Endocrine 71, 3–8. https://doi.org/10.1007/S12020-020-02536-6

Möller, M., Borg, K., Janson, C., Lerm, M., Normark, J., Niward, K., 2023. Cognitive dysfunction in post-COVID-19 condition: Mechanisms, management, and rehabilitation. J Intern Med 294, 563–581. https://doi.org/10.1111/JOIM.13720

Morens, D.M., Folkers, G.K., Fauci, A.S., 2004. The challenge of emerging and re-emerging infectious diseases. Nature 430, 242–249. https://doi.org/10.1038/nature02759

Mortola J. P. (2019). How to breathe? Respiratory mechanics and breathing pattern. Respiratory physiology & neurobiology, 261, 48–54. https://doi.org/10.1016/j.resp.2018.12.005

Nasserie, T., Hittle, M., Goodman, S.N., 2021. Assessment of the Frequency and Variety of Persistent Symptoms Among Patients With COVID-19: A Systematic Review. JAMA Netw Open 4. https://doi.org/10.1001/JAMANETWORKOPEN.2021.11417

Nicholls, D.G., Sihra, T.S., Sanchez-Prieto, J., 1987. Calcium-Dependent and Independent Release of Glutamate from Synaptosomes Monitored by Continuous Fluorometry. J Neurochem 49, 50–57. https://doi.org/10.1111/J.1471-4159.1987.TB03393.X

Paidas, M.J., Cosio, D.S., Ali, S., Kenyon, N.S., Jayakumar, A.R., 2022. Long-Term Sequelae of COVID-19 in Experimental Mice. Mol Neurobiol 59, 5970–5986. https://doi.org/10.1007/S12035-022-02932-1

Pereira, R. das D., Rabelo, R.A.N., Oliveira, N.F. de M., Porto, S.L.T., Andrade, A.C. dos S.P., Queiroz-Junior, C.M., Barbosa, C.L.N., de Souza-Costa, L.P., Santos, F.R. da S., Oliveira, F.B.R., da Silva, B.L.V., Umezu, H.L., Ferreira, R., da Silva, G.S.F., Cruz, J.S., Teixeira, M.M., Costa, V.V., Machado, F.S., 2023. A 5-Lipoxygenase Inhibitor, Zileuton, Modulates Host Immune Responses and Improves Lung Function in a Model of Severe Acute Respiratory Syndrome (SARS) Induced by Betacoronavirus. Viruses 2023, Vol. 15, Page 2049 15, 2049. https://doi.org/10.3390/V15102049

Phillips, S., Williams, M.A., 2021. Confronting Our Next National Health Disaster - Long-Haul Covid. N Engl J Med 385, 577–579. https://doi.org/10.1056/NEJMP2109285

Pimenta, J., Da Silva Oliveira, B., Lima, A.L.D., Machado, C.A., De Souza Barbosa Lacerda, L., Rossi, L., Queiroz-Junior, C.M., De Souza-Costa, L.P., Andrade, A.C.S.P., Gonçalves, M.R., Mota, B., Marim, F.M., Aguiar, R.S., Guimarães, P.P.G., Teixeira, A.L., Vieira, L.B., Guatimosim, C., Teixeira, M.M., De Miranda, A.S., Costa, V.V., 2023. A suitable model to investigate acute neurological consequences of coronavirus infection. Inflammation Research 72, 2073–2088. https://doi.org/10.1007/S00011-023-01798-W

Ponti, G., Maccaferri, M., Ruini, C., Tomasi, A., Ozben, T., 2020. Biomarkers associated with COVID-19 disease progression. https://doi.org/10.1080/10408363.2020.1770685.

Prediger, R.D.S., Aguiar, A.S., Rojas-Mayorquin, A.E., Figueiredo, C.P., Matheus, F.C., Ginestet, L., Chevarin, C., Del Bel, E., Mongeau, R., Hamon, M., Lanfumey, L., Raisman-Vozari, R., 2010. Single intranasal administration of 1-methyl-4-phenyl-1,2,3,6-tetrahydropyridine in C57BL/6 mice models early preclinical phase of Parkinson's disease. Neurotox Res 17, 114–129. https://doi.org/10.1007/S12640-009-9087-0

Proal, A.D., VanElzakker, M.B., Aleman, S., Bach, K., Boribong, B.P., Buggert, M., Cherry, S., Chertow, D.S., Davies, H.E., Dupont, C.L., Deeks, S.G., Eimer, W., Ely, E.W., Fasano, A., Freire, M., Geng, L.N., Griffin, D.E., Henrich, T.J., Iwasaki, A., Izquierdo-Garcia, D., Locci, M., Mehandru, S., Painter, M.M., Peluso, M.J., Pretorius, E., Price, D.A., Putrino, D., Scheuermann, R.H., Tan, G.S., Tanzi, R.E., VanBrocklin, H.F., Yonker, L.M., Wherry, E.J., 2023. SARS-CoV-2 reservoir in post-acute sequelae of COVID-19 (PASC). Nat Immunol 24, 1616–1627. https://doi.org/10.1038/S41590-023-01601-2

Proal, A.D., VanElzakker, M.B., 2021. Long COVID or Post-acute Sequelae of COVID-19 (PASC): An Overview of Biological Factors That May Contribute to Persistent Symptoms. Front Microbiol 12, 698169. https://doi.org/10.3389/FMICB.2021.698169/BIBTEX

Queiroz-Junior, C.M., Santos, A.C.P.M., Gonçalves, M.R., Brito, C.B., Barrioni, B., Almeida, P.J., Gonçalves-Pereira, M.H., Silva, T., Oliveira, S.R., Pereira, M.M., Santiago, H.C., Teixeira, M.M., Costa, V. V., 2023. Acute coronavirus infection triggers a TNF-dependent osteoporotic phenotype in mice. Life Sci 324. https://doi.org/10.1016/J.LFS.2023.121750

Ramírez-Vélez, R., Legarra-Gorgoñon, G., Oscoz-Ochandorena, S., García-Alonso, Y., García-Alonso, N., Oteiza, J., Lorea, A.E., Correa-Rodríguez, M., Izquierdo, M., 2023. Reduced muscle strength in patients with long-COVID-19 syndrome is mediated by limb muscle mass. J Appl Physiol (1985) 134, 50–58. https://doi.org/10.1152/JAPPLPHYSIOL.00599.2022

Rice, James, Laurence Coutellier, Jeffrey L. Weiner, e Chen Gu. 2019. "Region-Specific Interneuron Demyelination and Heightened Anxiety-like Behavior Induced by Adolescent Binge Alcohol Treatment". *Acta Neuropathologica Communications* 7 (1): 173. https://doi.org/10.1186/s40478-019-0829-9.

Robichaud, A., Fereydoonzad, L., Limjunyawong, N., Rabold, R., Allard, B., Benedetti, A., Martin, J.G., Mitzner, W., 2017. Automated full-range pressure-volume curves in mice and rats. J Appl Physiol (1985) 123, 746–756. https://doi.org/10.1152/JAPPLPHYSIOL.00856.2016

Rodrigues, D.H., Vilela, M. de C., Lacerda-Queiroz, N., Miranda, A.S. de, Sousa, L.F. da C., Reis, H.J. dos, Teixeira, A.L., 2011. Behavioral investigation of mice with experimental autoimmune encephalomyelitis. Arq Neuropsiquiatr 69, 938–942. https://doi.org/10.1590/S0004-282X2011000700018

Romero, M., Caicedo, M., Díaz, A., Ortega, D., Llanos, C., Concha, A., Vallejo, A., Valdés, F., González, C., 2023. Post-COVID-19 syndrome: Descriptive analysis based on a survivors' cohort in Colombia. Glob Epidemiol 6, 100126. https://doi.org/10.1016/J.GLOEPI.2023.100126

Rossi, L., Santos, K.B.S., Mota, B.I.S., Pimenta, J., Oliveira, B., Machado, C.A., Fernandes, H.B., Barbosa, L.A., Rodrigues, H.A., Teixeira, G.H.M., Gomes-Martins, G.A., Chaimowicz, G.F., Queiroz-Junior, C.M., Chaves, I., Tapia, J.C., Teixeira, M.M., Costa, V. V., Miranda, A.S., Guatimosim, C., 2023. Neuromuscular defects after infection with a beta coronavirus in mice. Neurochem Int 169. https://doi.org/10.1016/J.NEUINT.2023.105567

Ruiz-Bedoya, C.A., Mota, F., Ordonez, A.A., Foss, C.A., Singh, A.K., Praharaj, M., Mahmud, F.J., Ghayoor, A., Flavahan, K., De Jesus, P., Bahr, M., Dhakal, S., Zhou, R., Solis, C. V., Mulka, K.R., Bishai, W.R., Pekosz, A., Mankowski, J.L., Villano, J., Klein, S.L., Jain, S.K., 2022. 124I-Iodo-DPA-713 Positron Emission Tomography in a Hamster Model of SARS-CoV-2 Infection. Mol Imaging Biol 24, 135–143. https://doi.org/10.1007/S11307-021-01638-5

Sayed, S. El, Shokry, D., Sarah, |, Gomaa, M., Samir, C., Sayed, E., 2021. Post-COVID-19 fatigue and anhedonia: A cross-sectional study and their correlation to post-recovery period. Neuropsychopharmacol Rep 41, 50–55. https://doi.org/10.1002/NPR2.12154

Schaller, T., Hirschbühl, K., Burkhardt, K., Braun, G., Trepel, M., Märkl, B., Claus, R., 2020. Postmortem Examination of Patients With COVID-19. JAMA 323, 2518–2520. https://doi.org/10.1001/JAMA.2020.8907

Scully, E.P., Haverfield, J., Ursin, R.L., Tannenbaum, C., Klein, S.L., 2020. Considering how biological sex impacts immune responses and COVID-19 outcomes. Nature Reviews Immunology 2020 20:7 20, 442–447. https://doi.org/10.1038/s41577-020-0348-8

Silva, J., Takahashi, T., Wood, J., Lu, P., Tabachnikova, A., Gehlhausen, J. R., Greene, K., Bhattacharjee, B., Monteiro, V. S., Lucas, C., Dhodapkar, R. M., Tabacof, L., Peña-Hernandez, M., Kamath, K., Mao, T., Mccarthy, D., Medzhitov, R., van Dijk, D., Krumholz, H. M., Guan, L., Iwasaki, A. (2024). Sex differences in symptomatology and immune profiles of Long COVID. *medRxiv: the preprint server for health sciences*, 2024.02.29.24303568. https://doi.org/10.1101/2024.02.29.24303568

Simani, L., Ramezani, M., Darazam, I.A., Sagharichi, M., Aalipour, M.A., Ghorbani, F., Pakdaman, H., 2021. Prevalence and correlates of chronic fatigue syndrome and post-traumatic stress disorder after the outbreak of the COVID-19. J Neurovirol 27, 154–159. https://doi.org/10.1007/S13365-021-00949-1

Solis, O., Beccari, A.R., Iaconis, D., Talarico, C., Ruiz-Bedoya, C.A., Nwachukwu, J.C., Cimini, A., Castelli, V., Bertini, R., Montopoli, M., Cocetta, V., Borocci, S., Prandi, I.G., Flavahan, K., Bahr, M., Napiorkowski, A., Chillemi, G., Ooka, M., Yang, X., Zhang, S., Xia, M., Zheng, W., Bonaventura, J., Pomper, M.G., Hooper, J.E., Morales, M., Rosenberg, A.Z., Nettles, K.W., Jain, S.K., Allegretti, M., Michaelides, M., 2022a. The SARS-CoV-2 spike protein binds and modulates estrogen receptors. Sci Adv 8, 4150. https://doi.org/10.1126/SCIADV.ADD4150

Soriano, J. B., Murthy, S., Marshall, J. C., Relan, P., Diaz, J. V., & WHO Clinical Case Definition Working Group on Post-COVID-19 Condition (2022). A clinical case definition of post-COVID-19 condition by a Delphi consensus. *The Lancet. Infectious diseases*, *22*(4), e102–e107. https://doi.org/10.1016/S1473-3099(21)00703-9

Spudich, S., Nath, A., 2022. Nervous system consequences of COVID-19. Science (1979) 375, 267–269. https://doi.org/10.1126/SCIENCE.ABM2052

Sylvester, S. V., Rusu, R., Chan, B., Bellows, M., O'Keefe, C., Nicholson, S., 2022. Sex differences in sequelae from COVID-19 infection and in long COVID syndrome: a review. Curr Med Res Opin 38, 1391–1399. https://doi.org/10.1080/03007995.2022.2081454

Stallmach, A., Kesselmeier, M., Bauer, M., Gramlich, J., Finke, K., Fischer, A., Fleischmann-Struzek, C., Heutelbeck, A., Katzer, K., Mutschke, S., Pletz, M.W., Quickert, S., Reinhart, K., Stallmach, Z., Walter, M., Scherag, A., Reuken, P.A., 2022. Comparison of fatigue, cognitive dysfunction and psychological disorders in post-COVID patients and patients after sepsis: is there a specific constellation? Infection 50, 661. https://doi.org/10.1007/S15010-021-01733-3

Stein, S.R., Ramelli, S.C., Grazioli, A., Chung, J.Y., Singh, M., Yinda, C.K., Winkler, C.W., Sun, J., Dickey, J.M., Ylaya, K., Ko, S.H., Platt, A.P., Burbelo, P.D., Quezado, M., Pittaluga, S., Purcell, M., Munster, V.J., Belinky, F., Ramos-Benitez, M.J., Boritz, E.A., Lach, I.A., Herr, D.L., Rabin, J., Saharia, K.K., Madathil, R.J., Tabatabai, A., Soherwardi, S., McCurdy, M.T., Babyak, A.L., Perez Valencia, L.J., Curran, S.J., Richert, M.E., Young, W.J., Young, S.P., Gasmi, B., Sampaio De Melo, M., Desar, S., Tadros, S., Nasir, N., Jin, X., Rajan, S., Dikoglu, E., Ozkaya, N., Smith, G., Emanuel, E.R., Kelsall, B.L., Olivera, J.A., Blawas, M., Star, R.A., Hays, N., Singireddy, S., Wu, J., Raja, K., Curto, R., Chung, J.E., Borth, A.J., Bowers, K.A., Weichold, A.M., Minor, P.A., Moshref, M.A.N., Kelly, E.E., Sajadi, M.M., Scalea, T.M., Tran, D., Dahi, S., Deatrick, K.B., Krause, E.M., Herrold, J.A., Hochberg, E.S., Cornachione, C.R., Levine, A.R., Richards, J.E., Elder, J., Burke, A.P., Mazzeffi, M.A., Christenson, R.H., Chancer, Z.A., Abdulmahdi, M., Sopha, S., Goldberg, T., Sangwan, Y., Sudano, K., Blume, D., Radin, B., Arnouk, M., Eagan, J.W., Palermo, R., Harris, A.D., Pohida, T., Garmendia-Cedillos, M., Dold, G., Saglio, E., Pham, P., Peterson, K.E., Cohen, J.I., de Wit, E., Vannella, K.M., Hewitt, S.M., Kleiner, D.E., Chertow, D.S., 2022. SARS-CoV-2 infection and persistence in the human body and brain at autopsy. Nature 612, 758–763. https://doi.org/10.1038/S41586-022-05542-Y

Steinbach, K., Vincenti, I., Kreutzfeldt, M., Page, N., Muschaweckh, A., Wagner, I., Drexler, I., Pinschewer, D., Korn, T., Merkler, D., 2016. Brain-resident memory T cells represent an autonomous cytotoxic barrier to viral infection. Journal of Experimental Medicine 213, 1571–1587. https://doi.org/10.1084/JEM.20151916

Subbarayan, M.S., Joly-Amado, A., Bickford, P.C., Nash, K.R., 2022. CX3CL1/CX3CR1 signaling targets for the treatment of neurodegenerative diseases. Pharmacol Ther 231, 107989. https://doi.org/10.1016/J.PHARMTHERA.2021.107989

Subramanian, A., Nirantharakumar, K., Hughes, S., Myles, P., Williams, T., Gokhale, K.M., Taverner, T., Chandan, J.S., Brown, K., Simms-Williams, N., Shah, A.D., Singh, M., Kidy, F., Okoth, K., Hotham, R., Bashir, N., Cockburn, N., Lee, S.I., Turner, G.M., Gkoutos, G. V., Aiyegbusi, O.L., McMullan, C., Denniston, A.K., Sapey, E., Lord, J.M., Wraith, D.C., Leggett, E., Iles, C., Marshall, T., Price, M.J., Marwaha, S., Davies, E.H., Jackson, L.J., Matthews, K.L., Camaradou, J., Calvert, M., Haroon, S., 2022. Symptoms and risk factors for long COVID in non-hospitalized adults. Nat Med 28, 1706–1714. https://doi.org/10.1038/S41591-022-01909-W

Synowiec, A., Szczepański, A., Barreto-Duran, E., Lie, L.K., Pyrc, K., 2021. Severe acute respiratory syndrome coronavirus 2 (SARS-CoV-2): A systemic infection. Clin Microbiol Rev 34, 1–32. https://doi.org/10.1128/CMR.00133-20

Takahashi, T., Ellingson, M.K., Wong, P., Israelow, B., Lucas, C., Klein, J., Silva, J., Mao, T., Oh, J.E., Tokuyama, M., Lu, P., Venkataraman, A., Park, A., Liu, F., Meir, A., Sun, J., Wang, E.Y., Casanovas-Massana, A., Wyllie, A.L., Vogels, C.B.F., Earnest, R., Lapidus, S., Ott, I.M., Moore, A.J., Anastasio, K., Askenase, M.H., Batsu, M., Beatty, H., Bermejo, S., Bickerton, S., Brower, K., Bucklin, M.L., Cahill, S., Campbell, M., Cao, Y., Courchaine, E., Datta, R., DeIuliis, G., Geng, B., Glick, L., Handoko, R., Kalinich, C., Khoury-Hanold, W., Kim, D., Knaggs, L., Kuang, M., Kudo, E., Lim, J., Linehan, M., Lu-Culligan, A., Malik, A.A., Martin, A., Matos, I.,

McDonald, D., Minasyan, M., Mohanty, S., Muenker, M.C., Naushad, N., Nelson, A., Nouws, J., Nunez-Smith, M., Obaid, A., Ott, I., Park, H.J., Peng, X., Petrone, M., Prophet, S., Rahming, H., Rice, T., Rose, K.A., Sewanan, L., Sharma, L., Shepard, D., Silva, E., Simonov, M., Smolgovsky, M., Song, E., Sonnert, N., Strong, Y., Todeasa, C., Valdez, J., Velazquez, S., Vijayakumar, P., Wang, H., Watkins, A., White, E.B., Yang, Y., Shaw, A., Fournier, J.B., Odio, C.D., Farhadian, S., Dela Cruz, C., Grubaugh, N.D., Schulz, W.L., Ring, A.M., Ko, A.I., Omer, S.B., Iwasaki, A., 2020. Sex differences in immune responses that underlie COVID-19 disease outcomes. Nature 2020 588:7837 588, 315–320. https://doi.org/10.1038/s41586-020-2700-3

Tsuchida, T., Yoshimura, N., Ishizuka, K., Katayama, K., Inoue, Y., Hirose, M., Nakagama, Y., Kido, Y., Sugimori, H., Matsuda, T., Ohira, Y., 2023. Five cluster classifications of long COVID and their background factors: A cross-sectional study in Japan. Clin Exp Med 23, 3663–3670. https://doi.org/10.1007/s10238-023-01057-6

Vandenbark, A.A., Offner, H., Matejuk, S., Matejuk, A., 2021. Microglia and astrocyte involvement in neurodegeneration and brain cancer. Journal of Neuroinflammation 2021 18:1 18, 1–16. https://doi.org/10.1186/S12974-021-02355-0

Verma, M., Lizama, B.N., Chu, C.T., 2022. Excitotoxicity, calcium and mitochondria: a triad in synaptic neurodegeneration. Transl Neurodegener 11. https://doi.org/10.1186/S40035-021-00278-7

Vos, T., Hanson, S.W., Abbafati, C., Aerts, J.G., Al-Aly, Z., Ashbaugh, C., Ballouz, T., Blyuss, O., Bobkova, P., Bonsel, G., Borzakova, S., Buonsenso, D., Butnaru, D., Carter, A., Chu, H., De Rose, C., Diab, M.M., Ekbom, E., Tantawi, M. El, Fomin, V., Frithiof, R., Gamirova, A., Glybochko, P. V., Haagsma, J.A., Haghjooy Javanmard, S., Hamilton, E.B., Harris, G., Heijenbrok-Kal, M.H., Helbok, R., Hellemons, M.E., Hillus, D., Huijts, S.M., Hultström, M., Jassat, W., Kurth, F., Larsson, I.M., Lipcsey, M., Liu, C., Loflin, C.D., Malinovschi, A., Mao,

W., Mazankova, L., McCulloch, D., Menges, D., Mohammadifard, N., Munblit, D., Nekliudov, N.A., Ogbuoji, O., Osmanov, I.M., Peñalvo, J.L., Petersen, M.S., Puhan, M.A., Rahman, M., Rass, V., Reinig, N., Ribbers, G.M., Ricchiuto, A., Rubertsson, S., Samitova, E., Sarrafzadegan, N., Shikhaleva, A., Simpson, K.E., Sinatti, D., Soriano, J.B., Spiridonova, E., Steinbeis, F., Svistunov, A.A., Valentini, P., Van De Water, B.J., Van Den Berg-Emons, R., Wallin, E., Witzenrath, M., Wu, Y., Xu, H., Zoller, T., Adolph, C., Albright, J., Amlag, J.O., Aravkin, A.Y., Bang-Jensen, B.L., Bisignano, C., Castellano, R., Castro, E., Chakrabarti, S., Collins, J.K., Dai, X., Daoud, F., Dapper, C., Deen, A., Duncan, B.B., Erickson, M., Ewald, S.B., Ferrari, A.J., Flaxman, A.D., Fullman, N., Gamkrelidze, A., Giles, J.R., Guo, G., Hay, S.I., He, J., Helak, M., Hulland, E.N., Kereselidze, M., Krohn, K.J., Lazzar-Atwood, A., Lindstrom, A., Lozano, R., Malta, D.C., Månsson, J., Mantilla Herrera, A.M., Mokdad, A.H., Monasta, L., Nomura, S., Pasovic, M., Pigott, D.M., Reiner, R.C., Reinke, G., Ribeiro, A.L.P., Santomauro, D.F., Sholokhov, A., Spurlock, E.E., Walcott, R., Walker, A., Wiysonge, C.S., Zheng, P., Bettger, J.P., Murray, C.J.L., 2022. Estimated Global Proportions of Individuals with Persistent Fatigue, Cognitive, and Respiratory Symptom Clusters Following Symptomatic COVID-19 in 2020 and 2021. JAMA 328, 1604–1615. https://doi.org/10.1001/JAMA.2022.18931

Wiersinga, W.J., Rhodes, A., Cheng, A.C., Peacock, S.J., Prescott, H.C., 2020. Pathophysiology, Transmission, Diagnosis, and Treatment of Coronavirus Disease 2019 (COVID-19): A Review. JAMA 324, 782–793. https://doi.org/10.1001/JAMA.2020.12839

Winter, A.L., Henecke, S., Lundström, J.N., Thunell, E., 2023. Impairment of quality of life due to COVID-19-induced long-term olfactory dysfunction. Front Psychol 14, 1165911. https://doi.org/10.3389/fpsyg.2023.1165911

Woodruff, M.C., Ramonell, R.P., Haddad, N.S., Anam, F.A., Rudolph, M.E., Walker, T.A., Truong, A.D., Dixit, A.N., Han, J.E., Cabrera-Mora, M., Runnstrom, M.C., Bugrovsky, R., Hom,

J., Connolly, E.C., Albizua, I., Javia, V., Cashman, K.S., Nguyen, D.C., Kyu, S., Singh Saini, A., Piazza, M., Tipton, C.M., Khosroshahi, A., Gibson, G., Martin, G.S., Maier, C.L., Esper, A., Jenks, S.A., Lee, F.E.H., Sanz, I., 2022. Dysregulated naive B cells and de novo autoreactivity in severe COVID-19. Nature 2022 611:7934 611, 139–147. https://doi.org/10.1038/s41586-022-05273-0

World Health Organization (WHO). WHO COVID-19 dashboard. Available: https://data.who.int/dashboards/covid19/deaths?n=o. Access: Dec 18, 2024.

Xu, E., Xie, Y., Al-Aly, Z., 2022. Long-term neurologic outcomes of COVID-19. Nature Medicine 2022 28:11 28, 2406–2415. https://doi.org/10.1038/s41591-022-02001-z

Yang, Z., Du, J., Chen, G., Zhao, J., Yang, X., Su, L., Cheng, G., Tang, H., 2014. Coronavirus MHV-A59 infects the lung and causes severe pneumonia in C57BL/6 mice. Virol Sin 29, 393–402. https://doi.org/10.1007/s12250-014-3530-y

Zeng, N., Zhao, Y.M., Yan, W., Li, C., Lu, Q.D., Liu, L., Ni, S.Y., Mei, H., Yuan, K., Shi, L., Li, P., Fan, T.T., Yuan, J.L., Vitiello, M. V., Kosten, T., Kondratiuk, A.L., Sun, H.Q., Tang, X.D., Liu, M.Y., Lalvani, A., Shi, J., Bao, Y.P., Lu, L., 2023. A systematic review and meta-analysis of long term physical and mental sequelae of COVID-19 pandemic: call for research priority and action. Mol Psychiatry 28, 423. https://doi.org/10.1038/S41380-022-01614-7

Zheng, X., Zhao, Y., Yang, L., 2020. Acute Kidney Injury in COVID-19: The Chinese Experience. Semin Nephrol 40, 430–442. https://doi.org/10.1016/J.SEMNEPHROL.2020.09.001

3.3 Resultados não publicados

A COVID-19 deixou sequelas duradouras em milhões de pessoas em todo o mundo. A COVID longa, caracterizada por uma ampla gama de sintomas, incluindo fadiga crônica, dificuldades cognitivas e problemas respiratórios, tem um impacto significativo na qualidade de vida dos pacientes. Em particular, os sintomas neurológicos, como a "névoa cerebral" e a perda de memória, têm sido relatados por muitos pacientes, destacando a necessidade de mais pesquisas relacionadas ao desenvolvimento de tratamentos eficazes (Al-Aly & Topol, 2024). Em um estudo recente, nosso grupo de pesquisa demonstrou que o tratamento com Angio (1-7), um anti-inflamatório e pró-resolutivo, durante a fase aguda de infecções por betacoronavírus, como MHV-3 e SARS-CoV-2, resultou em uma redução significativa da inflamação, da carga viral e do dano pulmonar, aumentando a taxa de sobrevivência dos animais infectados (Lima et al., 2024). Diante desses resultados, investigamos se esse tratamento na fase aguda poderia evitar ou minimizar as sequelas neuropsiquiátricas induzidas pela infecção por betacoronavírus. Para tanto, foi utilizado o modelo de COVID longa induzido pelo MHV-A59.

3.3.1 Material e Métodos

O peptídeo Angio (1–7) (Bachem Inc.) foi diluído em (solução salina 0,9% + 0,02% DMSO) e administrado por via i.p na dose de 30 µg/camundongo. A dose de Ang (1–7) foi baseada no estudo anterior do nosso grupo (Lima et al., 2024). O regime de tratamento começou 24h após a infecção e continuou 36, 48, 60,72,84,96h depois. O grupo veículo recebeu solução salina 0,9% + 0,02% DMSO. Como controle positivo para o experimento, tratamos um grupo de animais com o antiviral Remdesivir (RDV) Veklury® (25 mg/kg, ip., 2x/dia - GILEAD Sciences, São Paulo, Brasil), iniciando o tratamento 24h antes da inoculação do vírus até 96h depois. Os experimentos foram realizados com camundongos C57BL/6 WT de 5 semanas de idade.

I. Angio (1-7)

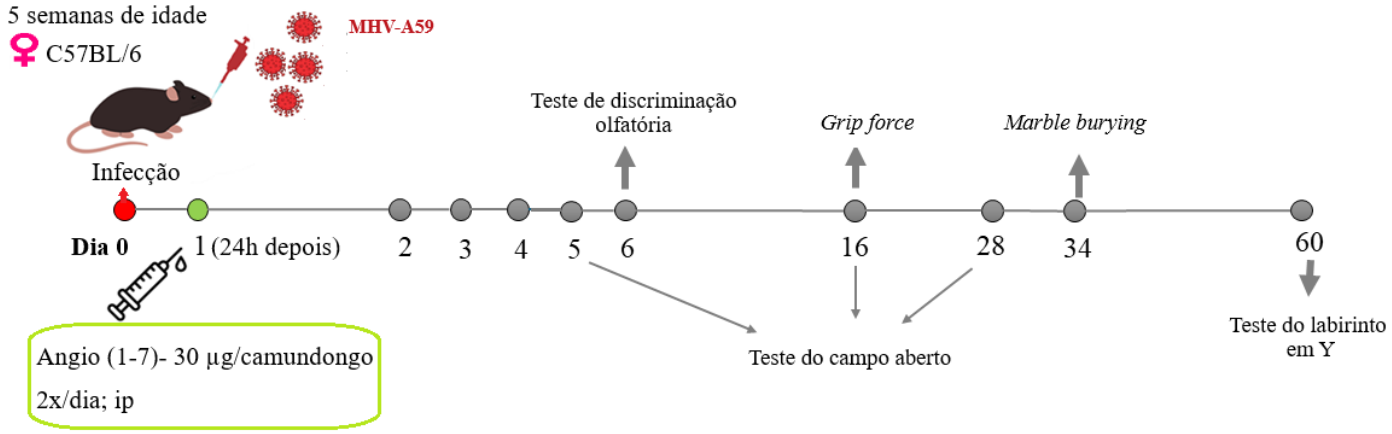

II. Remdesivir (RDV)

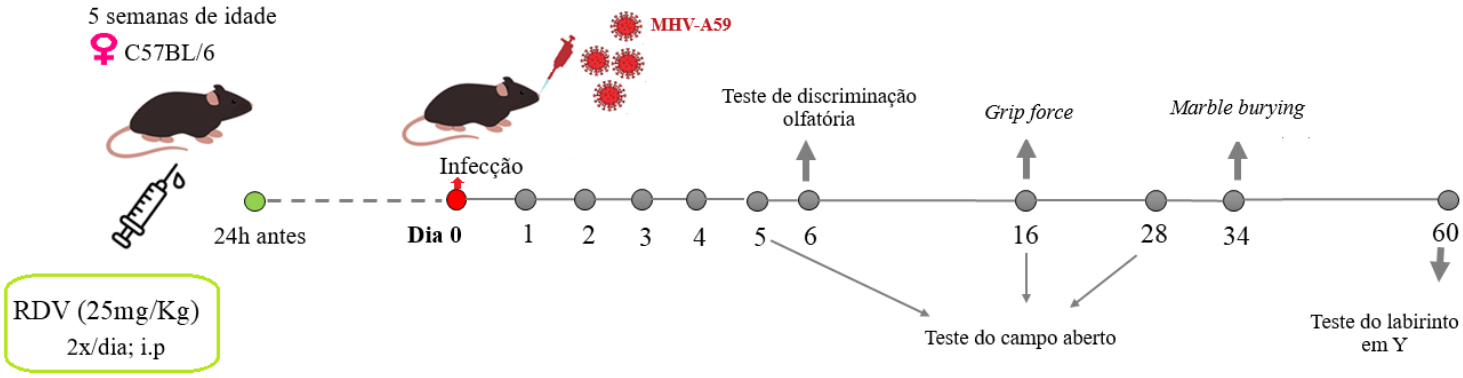

Figura 5: Desenho experimental dos tratamentos administrados na fase aguda da infecção por MHV-A59. Camundongos fêmeas C57BL/6 WT, com 5 semanas de idade, foram infectados por via intranasal com MHV-A59. (I) O tratamento com Angio (1-7) se iniciou 24h após infecção e o com RDV (II) começou 24h antes da infecção, ambos por via i.p e até o 4° dpi. Os testes comportamentais foram realizados no 5°,6°, 16°, 28°, 34° e 60° dpi.

3.3.2 Resultados

O tratamento com Angio (1-7) foi capaz de prevenir sequelas neuropsiquiátricas induzidas pela infecção por MHV-A59

A falta de compreensão completa do mecanismo da COVID longa impede o desenvolvimento de tratamentos específicos. Assim, a prática clínica atual concentra-se em abordagens de suporte, como reabilitação e exercícios, além de terapias sintomáticas, como antidepressivos e anticoagulantes, para aliviar os sintomas dessa condição (G Li et al., 2023). Nesse sentido, tratamos os camundongos infectados com o peptídeo Angio (1-7) ainda na fase aguda da doença e observamos se, posteriormente, as sequelas neuropsiquiátricas seriam evitadas ou minimizadas. Como controle positivo, utilizamos um antiviral, o RDV (Veklury®), por ser um medicamento amplamente utilizado na clínica para o tratamento da COVID-19 (Gottlieb et al., 2022). Além disso, o RDV foi utilizado na fase aguda da infecção por betacoronavírus em experimentos do nosso grupo e se mostrou eficaz em reduzir os títulos virais viáveis e cópias de RNA viral, além de reduzir a lesão pulmonar induzida pelo MHV-A59 (dados não mostrados).
Os camundongos C57BL/6 fêmeas foram primeiramente tratados e depois infectados com MHV-A59, no caso do RDV, que foi administrado 24 h antes da infecção (via i.p, a cada 12 h) até o 4° dpi. Para Angio (1-7), os animais foram infectados e tratados 24 h após a inoculação viral (via i.p, a cada 12 h) até o 4° dpi. Alguns testes comportamentais importantes foram selecionados para validar o efeito dos tratamentos neste contexto de sequelas ao longo dos 60 dias de infecção. Demonstramos através do teste do campo aberto, que os animais tratados com veículo apresentaram comprometimento na locomoção quando comparado ao grupo mock, enquanto os animais tratados com Angio (1-7) e com RDV se locomoveram de maneira semelhante ao grupo mock (Fig. 6A). Esse teste também foi realizado nos dias 16 e 28 pós infecção e nenhum grupo apresentou dificuldade na locomoção (Fig 6B e 6C, respectivamente). O teste de discriminação olfatória revelou que o tratamento com Angio (1-7) e RDV evitou que os animais infectados apresentassem comprometimento no olfato no 6° dpi, enquanto os animais do grupo infectado e tratado com veículo apresentam comprometimento da memória olfatória (Fig. 6D). O teste de força de preensão foi realizado 16 dpi para avaliar a força em duas (patas dianteiras) e nas quatro patas dos animais. Foi demonstrado que os animais infectados tratados com Angio (1-7) assim como aqueles infectados e tratados com RDV apresentaram força similar ao grupo mock, enquanto os animais infectados do grupo veículo tiveram seu nível de força comprometido em todos os membros (Fig 6E). Além disso, foi realizado o teste de *Marble Burying* no 34° dpi para

avaliar o perfil de anedonia ou compulsividade dos animais. Os camundongos infectados e tratados com veículo e com RDV apresentaram comportamento do tipo anedônico, pois enterraram menos bolinhas de gude, enquanto o tratamento com Angio (1-7) evitou a anedonia induzida pela infecção (Fig 6F). Por fim, 60 dpi, o teste do labirinto em Y foi realizado para avaliar a memória espacial dos animais e, consequentemente, o aprendizado. O teste demonstrou que os animais infectados tratados com veículo e RDV apresentaram prejuízo na memória espacial, enquanto o tratamento com Angio (1-7) foi capaz de prevenir o comprometimento cognitivo.

Figura 6: O tratamento com Angio (1-7) foi capaz de prevenir sequelas neuropsiquiátricas induzidas pela infecção por MHV-A59. (A) Distância total percorrida no teste de campo aberto em 5, (B) 16 e (C) 28 dpi (n = 10). (D) Tempo de discriminação olfatória no 6° dpi (n = 10-20). (E) Força em newtons (N) no teste de força de preensão de 2 ou 4 patas, 16 dpi (n = 10). (F) *Teste Marble Burying*, 34 dpi (n = 10). (G) Alternância espontânea no teste do labirinto em Y 60 dpi (n= 9-10). A significância foi determinada pelo teste t de Student para dados que passaram no teste de Shapiro-Wilk e pelo teste de Mann-Whitney para dados que não passaram no teste de Shapiro-Wilk *p < 0,05.

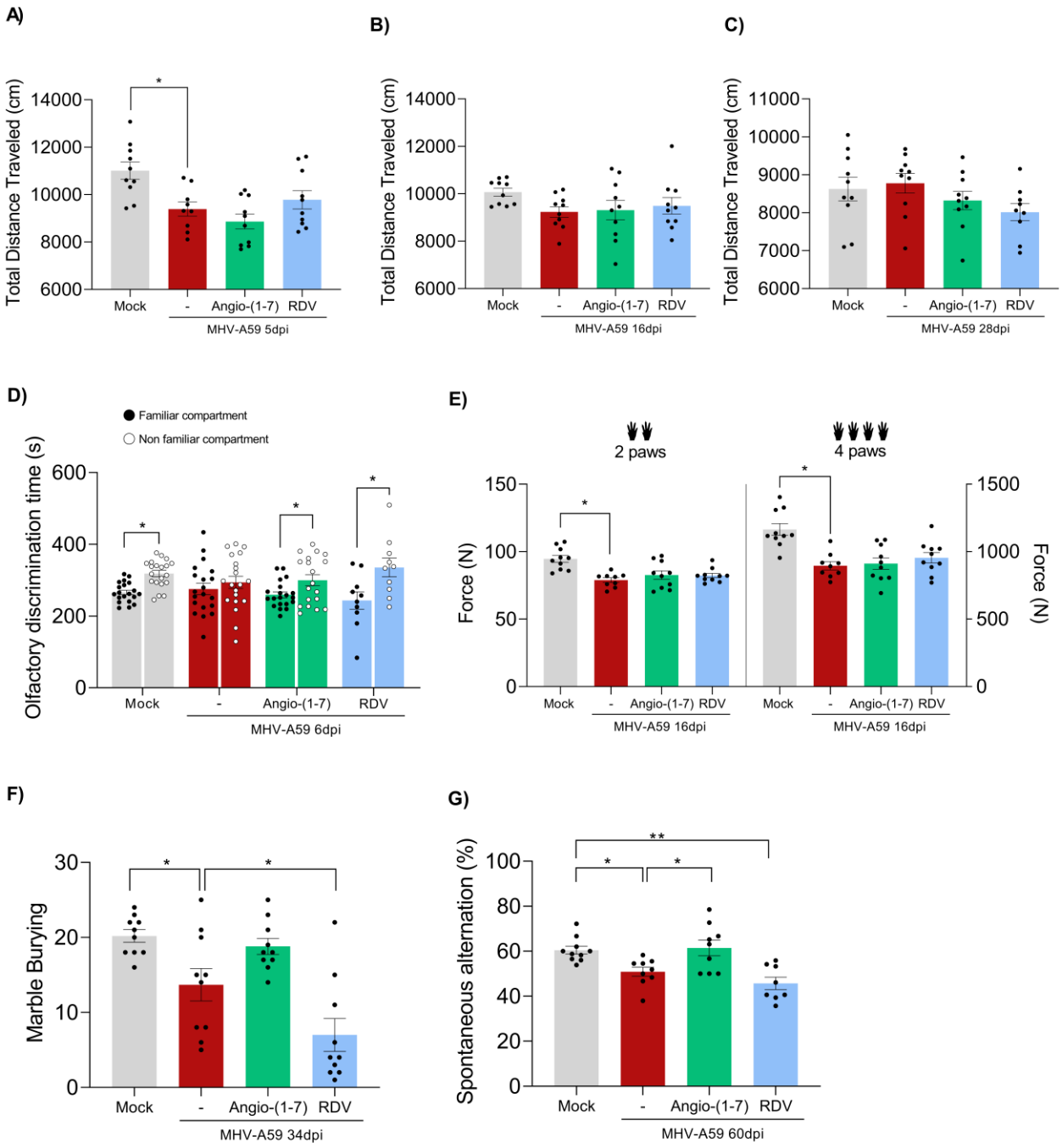

4. DISCUSSÃO

A COVID-19, com sua ampla gama de manifestações clínicas, tem sido também caracterizada por alterações neuropsiquiátricas. O acometimento do SNC já havia sido documentado na epidemia de SARS-CoV (Desforges et al, 2014). A maior parte das condições que acometem o SNC apresentam mecanismos fisiopatológicos complexos e a falta de uma compreensão mais profunda desses processos dificulta a identificação de alvos terapêuticos (Nagappan et al, 2020). Além da doença aguda causada pelo SARS-CoV-2, com o decorrer da pandemia começou a surgir sintomas persistentes após a infecção, conhecida como COVID longa. Estima-se que mais de 65 milhões de pessoas em todo o mundo lidam com as consequências de longo prazo dessa doença, que se manifesta em diversos sistemas do organismo, incluindo o SNC. (Davis et al., 2023). Essa condição, que pode durar meses ou até anos, emergiu como um grave problema de saúde pública mundial (Davis et al., 2023; Silva & Iwasaki, 2024), impulsionada pela escassez de conhecimento sobre seus mecanismos e pela ausência de tratamentos eficazes. Modelos que avaliam alterações celulares, morfológicas e comportamentais no contexto de infecção por betacoronavírus no SNC são limitados. Nesse sentido, o objetivo desse trabalho foi compreender melhor as alterações agudas e crônicas no SNC induzidas pela infecção por coronavírus.

De maneira geral, as alterações no modelo de infecção aguda, incluem: (i) o betacoronavírus MHV-3, inoculado por via intranasal, é capaz de infectar e se replicar no SNC, provocando alterações histopatológicas leves em camundongos C57BL/6 selvagens; (ii) a infecção pelo MHV-3 leva ao aumento da liberação de glutamato, elevação dos níveis de cálcio intracelular e maior produção de mediadores pró-inflamatórios no córtex; (iii) a infecção pelo MHV-3 reduz a síntese de mediadores neuroprotetores, como BDNF e CX3CL1, no córtex; (iv) os camundongos infectados pelo MHV-3 exibiram comportamentos do tipo ansioso, anedonia e comprometimento motor, com maior impacto observado em fêmeas. Já no modelo de COVID longa, demonstramos que (i) o betacoronavírus MHV-A59 provoca uma doença pulmonar leve e transitória em camundongos C57BL/6 selvagens; (ii) camundongos fêmeas exibem uma resposta inflamatória intensa nos pulmões, marcada por uma resposta robusta de células T; (iii) alterações comportamentais, aem fêmeas, persistentes por até dois meses após a infecção; (iv) fêmeas apresentam uma resposta inflamatória mais acentuada no cérebro, em comparação aos machos, caracterizada por infiltrado de neutrófilos, ativação de micróglia e resposta de IFN-γ; (v) o fenótipo da doença e as sequelas estão associados à influência dos hormônios sexuais; (vi) o tratamento agudo com RDV e Angio (1-7) evitou comprometimento motor (5 dpi), olfatório (6

dpi) e de força (16 dpi); (vii) o tratamento agudo com Angio (1-7) evitou anedonia (34 dpi) e comprometimento de memória espacial (60 dpi), induzidos pela infecção por MHV-A59.

O modelo de infecção intranasal utilizando um betacoronavírus murino (MHV-3) demonstrou que, apesar de seu hepatotropismo, pode ser útil como plataforma para recapitular os aspectos neurológicos e psiquiátricos observados em pacientes com COVID-19 grave. Todas as análises foram realizadas até o 5° dpi e isso pode ser justificado pelo fato de que no 3° dpi identificamos o pico pulmonar e no 6° dpi os animais já começam a sucumbir (Andrade et al., 2021). Inicialmente, demonstramos que o MHV-3 apresenta tropismo pelo tecido cerebral e capacidade de replicação no SNC a partir do 5° dpi. Além disso, a análise histopatológica do cérebro revelou lesão leve com presença de vasos sanguíneos dilatados nas meninges, assim como discreto infiltrado inflamatório e poucos vasos hiperêmicos no córtex cerebral. Esses achados estão alinhados com a literatura, que aponta a detecção de SARS-CoV-2 no cérebro *pos-mortem* em 53% dos pacientes com COVID-19, utilizando qRT-PCR *(Quantitative Reverse Transcription Polymerase Chain Reaction*) ou imunocoloração, sendo as lesões neuropatológicas geralmente leves (Matschke et al, 2020). Em outros estudos, o material genético de SAR-CoV-2 não foi encontrado ou foi identificado em níveis baixos no tecido cerebral (Solomon et al, 2020; Wichmann et al., 2020). Um outro trabalho demonstrou que a quantidade de RNA viral no córtex frontal de pacientes *pos-mortem* é mínima e só pôde ser detectada por meio de um método muito sensível, a PCR digital, mostrando que 88% das amostras analisadas apresentava o material genético de SARS-CoV-2, ao passo que a qRT- PCR foi capaz de detectar somente em 11% das amostras (Gagliardi et al, 2021).

Além disso, realizamos a análise quantitativa de neurônios (NeuN), micróglias/macrófagos (IBA-1), astrócitos (S100B) e avaliamos apoptose (caspase-3 clivada). Nenhum desses marcadores se mostrou alterado no córtex cerebral dos animais infectados no 5° dpi quando comparados ao grupo controle. No entanto, isso não significa que as células, como micróglia e astrócito não estejam alteradas, pois são necessários experimentos mais específicos para analisar o perfil de ativação dessas células, como citometria de fluxo com marcadores específicos. De fato, já foi comprovado que em tecidos cerebrais coletados de indivíduos que morreram de COVID-19, a micróglia expressou abundantemente o marcador lisossomal CD68, que indica aumento na sua atividade fagocítica, especialmente em áreas do bulbo olfatório e cerebelo (Matschke et al, 2020). Da mesma forma, não podemos afirmar que não há morte celular neuronal nesse processo infeccioso, visto que as células podem morrer por outras vias que não a apoptose, ou ainda por ser tratar de uma infecção grave, os camundongos podem sucumbir antes da ocorrência de eventos como neurodegeneração e morte celular. Boroujeni e colaboradores

(2021) mostraram que a resposta inflamatória na COVID-19 provocou morte neuronal no córtex cerebral (*pos-mortem)* de pacientes graves. Nossa quantificação de NeuN mostrou um número semelhante de neurônios positivos para o marcador quando comparamos os grupos infectados e controle. Porém, a análise da ultraestrutura do córtex cerebral de animais infectados pelo MHV-3 revelou a presença de neurônios escurecidos, conhecidos como *Dark Neurons* (DNs), que indicam degeneração em curso. Nessas amostras também foi observado a presença de complexos de Golgi e retículos endoplasmáticos dilatados e mitocôndrias com cristas rompidas. A quantificação de NeuN não mostrou alterações e isso pode ser justificado pelo fato de que cerca de 90-99% dos DNs se recuperam após um tempo, enquanto uma pequena quantidade de neurônios, de fato, morre (Csordás, et al., 2003). Estudos de microscopia eletrônica demonstraram que esses DNs tem uma baixa atividade funcional, apesar de apresentarem intensa síntese proteica devido a maior expressão de alguns genes. No entanto, a origem e o mecanismo do surgimento desses neurônios escuros permanecem indefinidos (Csordás, et al., 2003; Zimatkin & Bon', 2018). Ademais, não se sabe se os neurônios voltam a exercer suas funções de maneira adequada.

Além de alterações estruturais, investigamos a liberação de glutamato e o influxo de cálcio nesse contexto de infecção. O sistema glutamatérgico, é o principal sistema de neurotransmissão excitatória do SNC nos mamíferos, sendo importante para o desenvolvimento do cérebro, para a plasticidade sináptica e em processos fisiológicos de aprendizado e memória (Stevens, 2008). Entretanto, a alta liberação de glutamato na fenda sinápticas, com o consequente aumento do influxo de cálcio, podem levar à morte neuronal e neurodegeneração via excitotoxicidade (Wang & Qin, 2010). O excesso de glutamato e cálcio contribui para o desenvolvimento e progressão de várias condições do SNC, como trauma, isquemia e doenças neurodegenerativas (Lau & Tymianski, 2010). Nossos dados mostram que no 5º dpi os camundongos infectados com MHV-3 exibiram maior liberação de glutamato e influxo de cálcio no córtex quando comparados com o grupo não infectado. Em modelo de infecção pelo ZIKV, já foi demonstrado que há morte neuronal e que ao tratarem os animais infectados com um inibidor não competitivo do receptor de glutamato N-metil-D-aspartato (NMDA), memantina, a morte neuronal e a microgliose induzidas pela infecção foram inibidas tanto *in vitro* como *in vivo* (Costa et al., 2017). Resultados semelhantes foram descritos em um modelo de neuroinfecção pelo parasita *Plasmodium falciparum*, causador da malária, em que o aumento da liberação de glutamato no córtex de animais com malária cerebral estava associado a alterações neurológicas e comportamentais (Miranda et al, 2010), prevenidas com o inibidor do receptor NMDA, MK801 (Miranda et al., 2017).

Partindo do pressuposto que um dos maiores agravantes da COVID-19 é a tempestade de citocinas (Coperchini et al., 2020), mensuramos mediadores inflamatórios no córtex pré-frontal, hipocampo e estriado. Encontramos que a infecção pelo MHV-3 induziu aumento da citocina IL-6 no córtex pré-frontal, hipocampo e estriado, ao passo que IFN-γ teve uma maior concentração somente no córtex dos animais infectados ao compará-los com os controles. De maneira importante, estudos epidemiológicos e genéticos reforçam o papel dos mediadores inflamatórios nos sintomas neuropsiquiátricos observados em pacientes com COVID-19 aguda ou no pós-COVID-19, pois mostram que muitos marcadores de inflamação em concentrações séricas elevadas, como a IL-6, estão diretamente associados à depressão nesses indivíduos (Milaneschi et al, 2021).

Um modelo de neuroinfecção utilizando o vírus HSV-1 mostrou um aumento de IL-6 no hipocampo associado a apoptose neuronal e dano hipocampal (Toscano et al., 2020). O aumento da inflamação no estriado está relacionado com redução da conectividade funcional dessa região com o córtex pré-frontal, o que resulta em sintomas como anedonia e lentidão psicomotora (Felger et al., 2016). Esses resultados corroboram com o perfil de IL-6 do hipocampo e do estriado dos animais infectados com coronavírus observados no atual trabalho. Em relação ao IFN-γ, outro marcador inflamatório importante, quando utilizado no tratamento de pacientes com hepatite C, foi capaz de induzir episódio depressivo em ¼ desses pacientes (Udina, et al., 2012). Nossos resultados sugeriram comprometimento locomotor nos animais após a infecção pelo MHV-3. Dados semelhantes foram encontrados em animais infectados por via intracranial pelo vírus do Dengue-3 (DENV-3), em que o curso da doença foi caracterizado por alteração motora associada ao aumento de mediadores inflamatórios no SNC (Amaral et al., 2011).

A neuroinflamação pode levar a alterações na estrutura e/ou na função dos circuitos do SNC relacionados à ansiedade, tornando o cérebro vulnerável a esse transtorno (Won & Kim, 2020). Pacientes pós-COVD-19 têm apresentado vários distúrbios como depressão, ansiedade, sintomas obsessivos-compulsivos, que podem ser consequência da neuroinflamação decorrente da doença (Mazza et al, 2020). Ao realizar o teste de labirinto em cruz elevado, os animais infectados com MHV-3 apresentaram comportamento do tipo ansioso. Validando nossos achados, um estudo anterior de encefalite causada por DENV-3 demonstrou que os camundongos infectados apresentaram comportamento do tipo ansioso, bem como um aumento da expressão de RNAm de citocinas pró-inflamatórias no hipocampo associado à perda neuronal (de Miranda et al.,2012). Em modelo de malária cerebral, os camundongos infectados com *Plasmodium berghei* também apresentaram comportamento do tipo ansioso associado ao aumento dos níveis de citocinas pró-inflamatórias e alterações histopatológicas, como meningite focal, com presença

principalmente de linfócitos e macrófagos, sequestro de leucócitos na microvasculatura (tampão vascular) no córtex, tronco cerebral e hipocampo (de Miranda et al., 2011).

Além de mediadores envolvidos na inflamação do SNC, existem os mediadores que atuam em respostas neuromoduladoras/neuroprotetoras. CX3CL1 é uma quimiocina que no SNC é produzida por neurônios e através do receptor CX3CR1, presente na micróglia, ocorre a sinalização neuroglial. A sinalização CX3CL1/CX3CR1 parece ser imprescindível para a homeostase cerebral (Subbarayan et al., 2022). Acredita-se que no cérebro adulto, a CX3CL1 ou também conhecida como fractalquina (FQN), mantenha a micróglia em estado homeostático (Sheridan & Murphy, 2013). O BDNF, uma neurotrofina, é um regulador da neuroplasticidade e funções cerebrais como memória e cognição (Dechant & Neumann, 2002), sendo o córtex cerebral uma das principais fontes de secreção central do BDNF(Anders et al., 2020). A propósito, o BDNF é um protetor crítico da hipóxia e danos neurais induzidos pela inflamação (Lima Giacobbo et al., 2019). Pouco se sabe sobre CX3CL1 e BDNF no contexto da COVID-19 e os resultados ainda são controversos. Os estudos existentes de BDNF no curso da infecção pelo SARS-CoV-2 dosaram concentrações séricas desta neurotrofina. Enquanto alguns observaram níveis mais baixos de BDNF em pacientes hospitalizados com COVID-19 (Asgarzadeh et al., 2022; Azoulay et al. 2020), outros encontraram níveis maiores de BDNF em pacientes com COVID-19 em comparação com controles saudáveis (Ong et al., 2021 ; Chan et al., 2021).

Nossos resultados mostraram redução na concentração de CX3CL1 e BDNF no córtex cerebral de animais infectados com MHV-3 quando comparados aos animais controle, o que sugere uma perda da homeostase nesse ambiente. Níveis baixos de BDNF, principalmente corticais e hipocampais, têm sido associados à depressão (Kojima et al, 2019), o que vai ao encontro dos nossos dados comportamentais de anedonia. O BDNF é essencial em processos anti-inflamatórios e anti-apoptóticos em modelos experimentais de meningite por *S. pneumoniae* (Braun et al., 2017), ao passo que sua redução foi correlacionada à apoptose neuronal em modelos pré-clínicos de HIV (Michael et al., 2020). Em síntese, nossos resultados indicam que o modelo baseado no MHV-3 é eficiente em reproduzir as graves consequências agudas no SNC observadas em pacientes com COVID-19. Contudo, a alta letalidade induzida por esse betacoronavírus limita a possibilidade de investigar potenciais sequelas comportamentais e cognitivas associadas à infecção

Nesse sentido, iniciamos a caracterização de um modelo para estudo de sequelas pulmonares e neuropsiquiátricas decorrentes da infecção por coronavírus. Foi escolhida uma cepa menos virulenta e com maior tropismo pulmonar, o MHV-A59 que permitisse a sobrevivência dos animais e estudo da COVID longa. O inóculo foi determinado por meio de

uma curva de sobrevivência e pela variação do peso corporal dos animais em resposta à infecção. De acordo com a definição da OMS, PASC são caracterizadas por sintomas como fadiga, dificuldade respiratória, comprometimento cognitivo e outras manifestações que persistem após a infecção pelo SARS-CoV-2, sem explicação atribuída a outros diagnósticos. É importante destacar que a PASC não se restringe a casos graves da doença, uma vez que 29,6% dos pacientes que apresentaram quadros leves também são afetados por essa condição (Cazé et al., 2023). Dado que cerca de 80% dos casos de COVID-19 são classificados como leves (Huang et al., 2020), torna-se essencial investigar essa síndrome em modelos experimentais que reflitam infecções de baixa gravidade.

Neste trabalho, por meio de uma análise detalhada da infecção pulmonar pelo betacoronavírus murino MHV-A59 e suas consequências no SNC, apresentamos pela primeira vez os seguintes achados: infecção transitória e doença pulmonar leve em camundongos C57BL/6J de tipo selvagem; (II) resposta inflamatória mais grave no pulmão de camundongos fêmeas, caracterizada por uma resposta robusta de células T; (III) alterações comportamentais e cognitivas, principalmente em camundongos fêmeas, que persistiram por até 2 meses; (IV) resposta inflamatória mais grave no cérebro de camundongos fêmeas (em comparação com os machos), caracterizada por infiltrado de neutrófilos, ativação microglial e resposta de IFN-γ; (V) fenótipo da doença dependente de hormônios sexuais.

O surgimento do SARS-CoV-2 e o risco de novos surtos de coronavírus, anteriormente subestimados (Morens et al., 2004), destacaram a necessidade de desenvolver modelos para investigar a interação patógeno-hospedeiro e avaliar tratamentos e vacinas para infecções por coronavírus. A instilação intranasal de cepas de MHV em camundongos tem sido amplamente utilizada como modelo *in vivo* para estudar doenças pulmonares associadas aos coronavírus (Andrade et al., 2021; Pimenta et al., 2023; Queiroz-Junior et al., 2023). Estudo anterior demonstrou que a infecção por MHV-A59 em camundongos C57BL/6 provoca inflamação pulmonar aguda com infiltração leucocitária, hemorragia e aumento de mediadores pró-inflamatórios, como CXCL10, IFN-γ, TNF e IL-1β (Yang et al., 2014).

Neste trabalho, observamos que o MHV-A59 induz sinais clínicos pulmonares leves e alterações histopatológicas transitórias, acompanhadas de disfunção pulmonar aguda, como redução do volume pulmonar e da complacência, características de doenças restritivas (Mortola, 2019). Em pacientes com COVID-19, disfunções pulmonares similares também são relatadas mesmo em casos leves (Mo et al., 2020; Altmann et al., 2023). Embora os níveis de TGF-β, um regulador-chave da deposição de colágeno (Meng et al., 2016), tenham aumentado nos camundongos infectados, não foi detectada fibrose pulmonar ao longo da doença. A recuperação

do volume pulmonar e da complacência em 30 dias sugere que a disfunção observada está restrita à fase aguda, sem alterações estruturais permanentes no tecido pulmonar.

A resposta imunológica à infecção por MHV-A59 apresentou diferenças marcantes relacionadas ao sexo. Evidências sugerem que o sexo biológico desempenha um papel significativo na modulação da resposta imune, no desfecho clínico e no desenvolvimento de sintomas da PASC (Scully et al., 2020; Takahashi et al., 2020). Em nosso estudo, camundongos fêmeas infectados com MHV-A59 exibiram uma forte resposta de células T no pulmão, acompanhada de níveis elevados de IFN-γ em comparação aos camundongos machos infectados. Em contrapartida, camundongos machos apresentaram níveis altos de quimiocinas nos pulmões, como CCL3, CCL5 e CXCL1, associadas ao recrutamento de células imunes inatas. De forma semelhante, em pacientes com COVID-19, homens geralmente apresentam uma resposta imune inata mais intensa, caracterizada por níveis elevados de IL-8, IL-18 e CCL5, além do acúmulo de monócitos no pulmão, ao passo que as mulheres apresentam uma ativação mais proeminente de células T (Takahashi et al., 2020). Esses achados sugerem que camundongos machos e fêmeas infectados com MHV-A59 refletem diferenças nas respostas imunológicas inata e adaptativa no tecido pulmonar, espelhando padrões observados em pacientes com COVID-19.

Camundongos infectados com MHV-A59 demonstraram capacidade de eliminar o vírus do tecido pulmonar, indicando uma resposta eficaz no controle da infecção. A replicação viral não foi detectada no plasma e no baço, mas foi observada no fígado e cópias de RNA viral foram identificadas no cérebro, sugerindo uma disseminação viral limitada. No contexto sistêmico, a infecção por MHV-A59 provocou um aumento transitório na razão neutrófilo/linfócito (NLR) no sangue, padrão também observado em pacientes com COVID-19, onde é considerado um marcador de gravidade e mortalidade da doença (Henry et al., 2020; Liao et al., 2020; Ponti et al., 2020). Notavelmente, os camundongos infectados se recuperaram completamente do desequilíbrio na NLR causado pela infecção.

Esse modelo experimental foi caracterizado por doença pulmonar leve, acompanhada de alterações sistêmicas discretas e disseminação viral limitada, tornando-se uma ferramenta valiosa para investigar as sequelas pós-infecção por coronavírus. Em apoio a isso, estudos recentes demonstraram que o MHV-1, outro betacoronavírus murino, reproduz alguns aspectos da PASC em camundongos (Masciarella et al., 2023). Modelos baseados no MHV-1 mostraram alterações como congestão vascular, cavitação perivascular, halos pericelulares, vacuolização de neutrófilos, necrose aguda com presença de eosinófilos, neurônios necróticos com fragmentação nuclear e vacuolização no córtex cerebral após 12 meses de infecção (Paidas et al., 2022).

Como prova de conceito das alterações induzidas pelo MHV-A59 no SNC, realizamos testes comportamentais. Observamos que camundongos fêmeas infectados com o MHV-A59 apresentaram disfunção na capacidade de discriminar odores no início da infecção, indicando comprometimento do olfato. Esse sintoma é amplamente encontrado tanto na COVID-19 aguda (Harapan e Yoo, 2021) quanto em pacientes com sintomas pós-COVID (Winter et al., 2023). Além disso, a infecção por MHV-A59 levou a prejuízos motores, incluindo redução da força muscular das patas dianteiras em camundongos de ambos os sexos aos 16 dpi. De forma semelhante, comprometimentos motores têm sido relatados em pacientes com COVID longa (Ramírez-Vélez et al., 2023). Outro achado relevante foi a presença de comportamento do tipo anedônico em camundongos de ambos os sexos, o que está de acordo com observações em estudos de pacientes com PASC (Lamontagne et al., 2021; Sayed et al., 2021). No entanto, apenas as fêmeas apresentaram déficits de memória, como prejuízo na memória de trabalho espacial avaliado pelo teste do labirinto em Y, e na memória aversiva de curto prazo, observado no teste de esquiva inibitória, aos 60 dpi. Esses déficits cognitivos foram mais frequentemente relatados em mulheres com COVID longa em comparação aos homens (Bai et al., 2022), assim como observado no nosso modelo.

Pesquisas anteriores conduzidas por nosso grupo demonstraram que sinaptossomas de camundongos infectados com MHV-3 apresentaram aumento na liberação de glutamato e nos níveis intracelulares de cálcio (Pimenta et al., 2023). No modelo de MHV-A59, camundongos fêmeas infectados também exibiram liberação significativa de glutamato e elevação dos níveis intracelulares de Ca^{2+} no hipocampo aos 30 dias após a infecção. Esses resultados indicam a ocorrência de um desequilíbrio neuroquímico, uma vez que infecções virais, como as causadas por HIV, ZIKA e H1N1, já foram associadas a prejuízos na transmissão glutamatérgica, comprometendo a sinalização neural (Costa et al., 2017; Düsedau et al., 2021; Gorska e Eugenin, 2020). Adicionalmente, foi observado um aumento significativo no número de micróglia/macrófagos (marcados por IBA-1) e de astrócitos (marcados por S100B) no córtex cerebral e no hipocampo de camundongos fêmeas em vários tempos de infecção em comparação aos machos. Esse aumento celular sugere um estado ampliado de neuroinflamação, associado potencialmente à neurodegeneração (Kwon e Koh, 2020; Vandenbark et al., 2021). Outro dado relevante é que, nas fêmeas infectadas, mas não nos machos, a micróglia apresentou alta expressão da enzima óxido nítrico sintase induzível (iNOS). O óxido nítrico (NO) desempenha um papel fundamental na transmissão sináptica e na plasticidade cerebral, especialmente no córtex e no hipocampo. Entretanto, níveis elevados de NO e o consequente estresse oxidativo

podem acarretar prejuízos sinápticos e contribuir para a neurodegeneração precoce (Balez e Ooi, 2016).

A presença de uma neuroinflamação mais intensa em camundongos fêmeas foi reforçada pela identificação de células imunes no cérebro. As fêmeas infectadas com MHV-A59 apresentaram um aumento significativo no número de linfócitos T CD4 produtores de IFN-γ, com expressão dos marcadores Ki67 (indicativo de proliferação celular) e CD69 (associado à ativação celular). Além disso, essas fêmeas exibiram um número maior de células T $CD8^+$ $Ki67^+$ em comparação aos machos. As células T desempenham um papel essencial no controle da replicação viral, acessando o parênquima cerebral ao reconhecer antígenos virais locais por meio de seus receptores específicos (Steinbach et al., 2016).

A interação entre micróglia e células T no parênquima SNC é particularmente relevante, pois as funções efetoras das células T dependem dessa comunicação (Ai e Klein, 2020). Contudo, uma resposta imune desregulada pode ter consequências prejudiciais. Estudos indicam que células T podem contribuir para sequelas neurocognitivas após infecções virais, como as causadas pelo ZIKV e pelo vírus do Nilo Ocidental. Esse efeito ocorre devido à sinalização do IFN-γ, liberado por células T $CD8^+$ específicas que se infiltram no SNC, promovendo a ativação da micróglia (Garber et al., 2019). Tal ativação está associada a efeitos neurotóxicos, incluindo a eliminação excessiva de sinapses mediada por complemento e neurodegeneração (Klein et al., 2019).

Em relação a outros mediadores inflamatórios, a infecção por MHV-A59 teve diferentes impactos nos níveis de IL-6 conforme o sexo e a região cerebral. No córtex pré-frontal (PFC), os níveis de IL-6 em camundongos fêmeas infectadas permaneceram semelhantes aos controles, enquanto nos machos houve um aumento em 30 e 60 dpi. No entanto, no hipocampo, as fêmeas mostraram elevações significativas de IL-6 em 8 dpi em comparação ao grupo controle e aos machos infectados. Essa citocina, conhecida por sua ação pró-inflamatória, também está associada ao comprometimento da memória de trabalho e de funções cognitivas em infecções como a causada pelo SARS-CoV-2 (Alnefeesi et al., 2021). O aumento sistêmico da IL-6 induzido por infecções pode atravessar a BHE, ativar micróglia e interferir em processos cognitivos (Alnefeesi et al., 2021; Vos et al., 2022). Apesar de ser predominantemente pró-inflamatória, a IL-6 também desempenha funções neuroprotetoras em condições de homeostase cerebral, incluindo a neurogênese e a resposta de neurônios maduros e células gliais (Erta et al., 2012). É possível que na fase aguda da infecção por MHV-A59, especialmente em fêmeas, a IL-6 exerça um papel predominantemente pró-inflamatório, enquanto o aumento tardio dessa

citocina em camundongos machos infectados sugira uma resposta compensatória e protetora para restaurar a homeostase cerebral.

Além dos impactos inflamatórios, a infecção por MHV-A59 também interferiu no nível de mediadores neuromoduladores. Em camundongos fêmeas infectadas, os níveis de BDNF foram reduzidos no PFC aos 8 e 16 dias dpi, enquanto nos machos, essa redução foi observada apenas aos 8 dpi. No hipocampo, as fêmeas apresentaram uma queda nos níveis de BDNF entre 2 e 16 dpi, enquanto nos machos essa redução ocorreu apenas de 2 a 8 dpi. A recuperação mais lenta dos níveis de BDNF nas fêmeas pode estar relacionada ao surgimento de sintomas neuropsiquiátricos. O BDNF desempenha um papel essencial na sobrevivência celular, plasticidade sináptica e reorganização do microambiente cerebral (Chen et al., 2020). Sua ação no PFC tem sido associada a efeitos antidepressivos (Li et al., 2018), enquanto no hipocampo está relacionada tanto à redução de sintomas depressivos (Li et al., 2017) quanto à modulação de comportamentos ansiosos em modelos de ratos (Cirulli et al., 2004). Já os níveis de CX3CL1 nos camundongos infectados seguiram um padrão geral de aumento inicial seguido por redução, tanto no PFC quanto no hipocampo, em fêmeas e machos. Esse comportamento sugere uma tentativa homeostática de controlar os efeitos agudos da infecção. O eixo CX3CL1/CX3CR1 é fundamental para a comunicação entre neurônios e micróglia e tem como função principal atenuar respostas pró-inflamatórias no SNC (Subbarayan et al., 2022). Alterações nesse eixo têm sido associadas ao desenvolvimento de transtornos neuropsiquiátricos (Chamera et al., 2020).

O sexo fisiológico exerce influência nas respostas imunes frente a infecções e à vacinação (Klein e Flanagan, 2016). Estudos epidemiológicos sobre a COVID-19 indicam uma tendência de mortalidade associada ao sexo, com os homens apresentando maior vulnerabilidade (Solis et al., 2022). Da mesma forma, animais de laboratório do sexo masculino demonstram maior suscetibilidade à infecção por SARS-CoV e SARS-CoV-2 em comparação com os do sexo feminino (Channappanavar et al., 2017; Dhakal et al., 2021; Ruiz-Bedoya et al., 2022). No que diz respeito às sequelas, as mulheres parecem apresentar maior predisposição ao desenvolvimento da PASC (Bai et al., 2022). Considerando o fenótipo das sequelas no SNC em camundongos fêmeas após a infecção por MHV-A59, foi analisado o papel dos hormônios estradiol, FSH e testosterona nesse contexto.

Nosso modelo revelou níveis elevados de estradiol durante a fase aguda da infecção (2 e 5 dpi), com um pico observado em 60 dpi. Paralelamente, detectamos um aumento nos níveis de FSH em vários momentos ao longo do curso da infecção. Esses achados sugerem que a infecção alterou a sinalização do estradiol no eixo hipotálamo-hipófise-gonadal. Evidências apontam que a proteína spike do SARS-CoV-2 interage e modula os receptores de estrogênio (Solis et al.,

2022). O estudo de Ding e colaboradores (2020) mostrou que o estradiol (E2) pode proteger as mulheres durante a COVID-19, regulando citocinas associadas à gravidade da doença. No entanto, enquanto os hormônios femininos parecem oferecer benefícios na fase aguda, eles também podem perpetuar um estado hiper inflamatório mesmo após a recuperação (Bienvenu et al., 2020; Mohamed et al., 2021). Quanto ao FSH, pesquisas mostram níveis aumentados desse hormônio em mulheres durante a COVID-19 (Cai et al., 2022), embora a relação entre o FSH, COVID-19 e a COVID longa ainda careçam de estudos mais aprofundados. Em outros contextos, sabe-se que o FSH influencia neurônios e aumenta a expressão de proteínas associadas a processos degenerativos (Xiong et al., 2022). Um estudo demonstrou que a utilização de um anticorpo FSHβ para tratar a doença de Alzheimer em camundongos induziu uma redução nos níveis de Aβ, sugerindo um potencial efeito neuroprotetor da inibição do FSH (Xiong et al., 2023).

Em relação à testosterona, foi observada uma redução em camundongos fêmeas nos dias 5, 30 e 60 dpi. Um estudo recente, identificou respostas imunológicas específicas em mulheres com COVID longa, incluindo maior ativação de linfócitos, evidenciada pela produção de citocinas como IFN-γ, IL-2, IL-4 e IL-6, além de um aumento na exaustão de células T e uma redução nas células T $CD4^+$ e $CD8^+$ *naive* em repouso (Silva et al., 2024; Yin et al., 2024). Essas características parecem estar associadas a alterações hormonais específicas, como a redução de testosterona em indivíduos com COVID longa, em comparação aos sem a condição Silva et al., 2024)., como demonstrado em nosso modelo murino (Em mulheres, a redução da testosterona também pode contribuir para uma maior predisposição a doenças autoimunes (Bupp e Jorgensen, 2018).

Com base nesses achados, buscamos compreender as sequelas no contexto da deficiência hormonal induzida pela ovariectomia. Observamos que camundongos fêmeas ovariectomizadas (OVX) apresentaram lesões pulmonares semelhantes às observadas em camundongos SHAM infectadas. No entanto, a excitotoxicidade, bem como os comprometimentos comportamentais e cognitivos, foram significativamente prevenidos. Em relação ao perfil das células IBA-1^+ e $S100B^+$, não houve reversão completa desses tipos celulares nas fêmeas OVX infectadas. Contudo, notamos que o retorno à homeostase em fêmeas OVX ocorreu de forma mais acelerada, resultando em uma leve recuperação que impactou positivamente o fenótipo comportamental.

O estrogênio exerce um papel fundamental como modulador do sistema imunológico, suscitando a hipótese de que a ovariectomia possa comprometer a capacidade dos camundongos de enfrentar infecções. No entanto, mesmo em pequenas quantidades, esse hormônio pode ser produzido por outros tecidos, como o cérebro, rins, ossos, pele e tecido adiposo (Harding e Heaton, 2022). Com

base nisso, sugerimos que as fêmeas ovariectomizadas infectadas não demonstraram maior dificuldade em combater o vírus em comparação com o grupo SHAM infectado. Esses achados estão alinhados com evidências experimentais, como o estudo de Dhakal et al. (2021), que mostrou que o tratamento com estradiol não reduziu complicações pulmonares em hamsters machos infectados com SARS-CoV-2. Isso sugere que outros hormônios, além do estrogênio, podem estar associados às sequelas. Ademais, já há indícios de que disfunções no eixo hipotálamo-hipófise-gonadal são mais frequentes em pacientes com COVID longa (Angum et al.,2020).

A terapia da COVID-19 apresentou avanços significativos, com a aprovação de diversas moléculas antivirais (nirmatrelvir-ritonavir, remdesivir e molnupiravir) juntamente com uma gama de anticorpos monoclonais (G. Li et al., 2023). Ademais, indivíduos hospitalizados com quadros graves podem ainda ser tratados com agentes imunomoduladores, principalmente, o glicocorticoide dexametasona (Li et al., 2023).

Outros vírus também possuem o potencial de gerar sequelas a longo prazo, especialmente no âmbito neuropsiquiátrico, como o vírus Zika (ZIKV), o vírus da encefalite japonesa e o vírus do Nilo Ocidental. (Llorente et al., 2024). Nesse contexto, destaca-se o sofosbuvir, um antiviral utilizado clinicamente no tratamento do vírus da hepatite C, que é uma substância aprovada pela FDA com eficácia comprovada contra o ZIKV, conforme demonstrado em um estudo realizado com camundongos infectados, no qual o tratamento com esse medicamento preveniu déficits de memória nesses animais (Ferreira et al., 2017).

Em 2023 foi publicado um artigo mostrando que o uso do molnupiravir foi relacionado a uma diminuição no risco de desenvolver PASC em indivíduos não vacinados, naqueles que receberam uma ou duas doses da vacina, ou uma dose de reforço, bem como em casos de infecção primária por SARS-CoV-2 e reinfecção. Além disso, essa redução de risco foi observada em diversos subgrupos, considerando fatores como idade, raça, gênero, tabagismo, presença de câncer, doenças cardiovasculares, renais, pulmonares crônicas, diabetes e disfunção imunológica. Quando comparado à ausência de tratamento, o uso de molnupiravir também esteve associado à redução do risco em oito de 13 sequelas pré-estabelecidas, incluindo disritmia, embolia pulmonar, trombose venosa profunda, fadiga e mal-estar, doença hepática, lesão renal aguda, dor muscular e comprometimento neurocognitivo (Xie et al., 2023). No entanto, a maioria dos estudos sobre tratamentos para a COVID longa ainda são limitados e estão em fases iniciais, por isso o manejo dessas condições tem se concentrado, sobretudo, em terapias voltadas para a redução dos sintomas (G Li et al., 2023).

Recentemente, foi demonstrado que o peptídeo Ang (1–7) modula a resposta inflamatória durante a infecção pelos betacoronavírus MHV-3 e SARS-CoV-2, restaurando a linfopenia, reduzindo a carga viral e os danos pulmonares, com consequente aumento nas taxas de sobrevida dos animais (Lima et al., 2024). Também foi reportado recentemente que a administração lipossomal intranasal de Angio (1-7) reduz a inflamação e a carga viral nos pulmões de camundongos transgênicos K18-hACE2 durante a infecção por SARS-CoV-2 (Mendes et al., 2024). Com base nesses estudos, utilizamos o modelo de COVID longa para investigar se os efeitos do tratamento com Angio (1-7) e com o antiviral RDV (controle positivo) poderiam prevenir ou minimizar as sequelas neuropsiquiátricas.

O RDV, aprovado pela Agência Europeia de Medicamentos (EMA), é atualmente o antiviral recomendado para pacientes hospitalizados com COVID-19. Estudos têm demonstrado que o tratamento precoce com RDV reduz significativamente o risco de hospitalização ou óbito quando comparado ao placebo (Brown et al., 2023). No entanto, investigações focadas nos sintomas associados à PASC sugerem que o uso de RDV durante a hospitalização não oferece benefícios clinicamente relevantes na prevenção dessas sequelas (Nevalainen et al., 2022; Patrick-Brown et al., 2024). Esses achados estão em consonância com os resultados obtidos no presente estudo.

Durante a fase aguda da infecção, ambos os tratamentos demonstraram eficácia em evitar déficits motores (5 dpi) e olfatórios (6 dpi), destacando seu impacto na preservação das funções neurológicas em comparação ao grupo que recebeu o veículo. Aos 16 dpi, os resultados continuaram favoráveis, com os animais tratados mantendo a força muscular, diferentemente do grupo veículo que apresentou comprometimentos. No entanto, em estágios mais avançados da infecção somente a Angio (1-7) foi capaz de prevenir comportamentos associados à anedonia aos 34 dpi e preservar a memória espacial aos 60 dpi. De fato, já foi demonstrado que a Angio (1-7) possui efeito anti-inflamatório direto na micróglia (Liu et al., 2015), o que pode contribuir para uma menor neuroinflamação e reversão das sequelas. Dessa forma, enquanto o RDV e a Angio (1-7) demonstram eficácia na fase aguda da infecção, nossos dados destacam que o Angio (1-7) apresenta um efeito protetor prolongado. Este tratamento emerge como uma abordagem terapêutica promissora para mitigar as sequelas neuropsiquiátricas associadas ao coronavírus.

Estudos recentes têm avançado na compreensão da COVID longa, e este trabalho experimental representa um marco ao recapitular diversos aspectos dessa condição em um modelo animal. A infecção por MHV-A59, ao induzir uma leve inflamação pulmonar aguda, desencadeou alterações neuropsiquiátricas e musculoesqueléticas crônicas associadas à influência de hormônios sexuais. Esses achados reforçam a importância de modelos que, dentro

de uma estrutura NB-2, sejam capazes de estudar a patogênese da PASC de maneira abrangente, especialmente diante das restrições associadas aos laboratórios NB-3, exigidos para pesquisas com SARS-CoV-2.

A relevância desse modelo não reside apenas na sua aplicabilidade ao estudo de comprometimentos comportamentais e cognitivos, mas também na possibilidade de testar estratégias terapêuticas antivirais, anti-inflamatórias e neuroprotetoras. Cabe ressaltar que modelos transgênicos de camundongos expressando hECA-2, amplamente utilizados para investigar os efeitos fisiopatológicos induzidos pelo SARS-CoV-2, apresentam limitações significativas, particularmente no que diz respeito às manifestações extrapulmonares e sintomas persistentes da doença. Assim, a necessidade de desenvolver modelos mais diversos e representativos torna-se imperativa para ampliar a compreensão dos mecanismos subjacentes à PASC. Ainda que este estudo traga contribuições inovadoras, é importante reconhecer suas limitações. Investigações adicionais são necessárias para compreender como as disfunções no eixo hipotálamo-hipófise-gonadal podem ser moduladas com vistas à prevenção de sequelas neurológicas induzidas por coronavírus. Além disso, a avaliação dos efeitos da reinfecção nos desfechos cognitivos e comportamentais se apresenta como uma lacuna a ser preenchida, dada sua relevância no contexto atual. Esses desafios sublinham a importância de esforços contínuos para aprofundar o entendimento e o manejo das consequências da COVID-19.

5. CONCLUSÃO

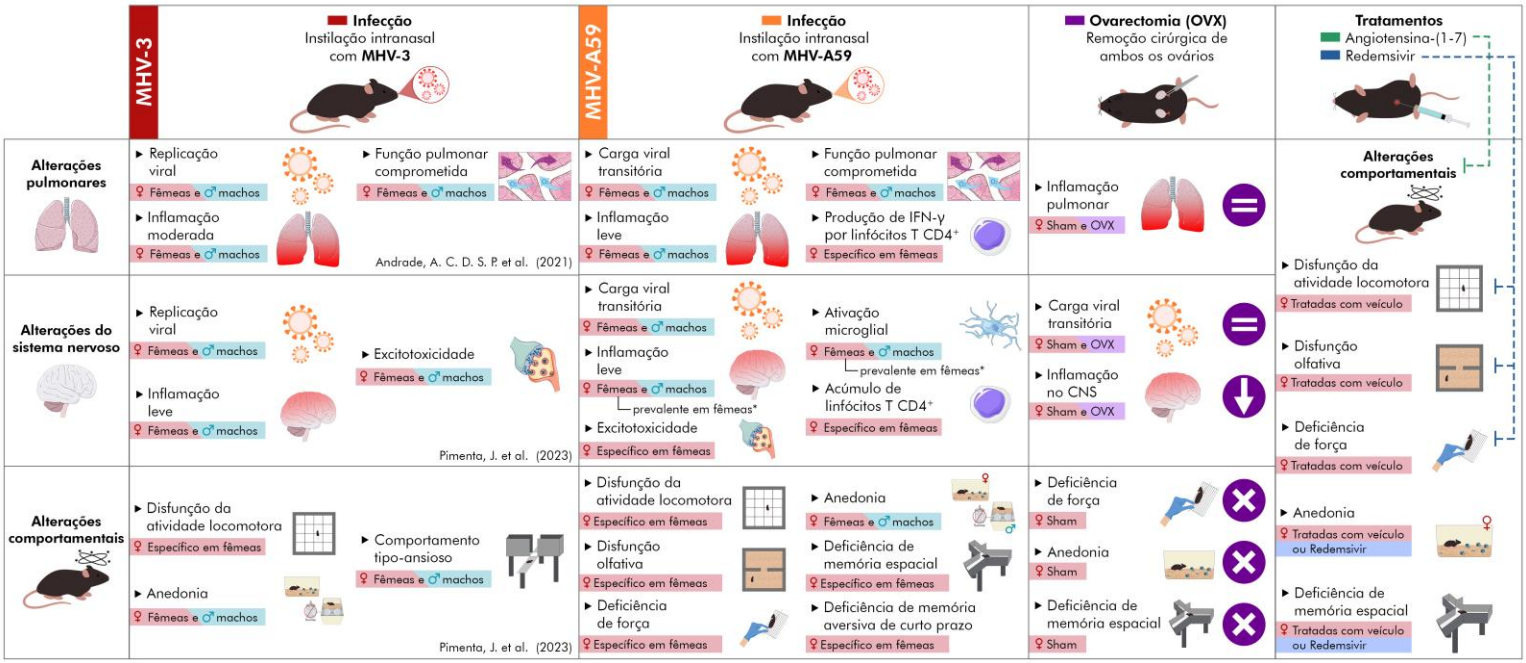

Figura 7: Alterações pulmonares agudas e neuropsiquiátricas agudas e crônicas associadas à infecção por coronavírus. O modelo de MHV-3 evidenciou neuroinflamação com comprometimento locomotor, olfatório e de força, além de comportamento do tipo ansioso e anedonia. O modelo de MHV-A59 revelou lesão pulmonar transitória e auto resolutiva, acompanhada de sequelas neuropsiquiátricas crônicas, predominantes em fêmeas. A ovariectomia reverteu essas sequelas neuropsiquiátricas sem alterar o fenótipo pulmonar. O tratamento com Angio (1-7), um anti-inflamatório e pró-resolutivo, na fase aguda da infecção preveniu as alterações comportamentais.

REFERÊNCIAS BIBLIOGRÁFICAS

1. Aly, Z., & Topol, E. (2024). Solving the puzzle of Long Covid. *Science*, *383*(6685), 830–832. https://doi.org/10.1126/SCIENCE.ADL0867/ASSET/40C5582A-51A6-4C0A-9FF9-634A2AEE04A3/ASSETS/SCIENCE.ADL0867-F1.SVG

2. Almutairi, M. M., Sivandzade, F., Albekairi, T. H., Alqahtani, F., & Cucullo, L. (2021). Neuroinflammation and Its Impact on the Pathogenesis of COVID-19. Frontiers in medicine, 8, 745789. https://doi.org/10.3389/fmed.2021.745789

3. Amaral, D. C., Rachid, M. A., Vilela, M. C., Campos, R. D., Ferreira, G. P., Rodrigues, D. H., Lacerda-Queiroz, N., Miranda, A. S., Costa, V. V., Campos, M. A., Kroon, E. G., Teixeira, M. M., & Teixeira, A. L. (2011). Intracerebral infection with dengue-3 virus induces meningoencephalitis and behavioral changes that precede lethality in mice. Journal of neuroinflammation, 8, 23. https://doi.org/10.1186/1742-2094-8-23

4. Amruta, N., Chastain, W. H., Paz, M., Solch, R. J., Murray-Brown, I. C., Befeler, J. B., Gressett, T. E., Longo, M. T., Engler-Chiurazzi, E. B., & Bix, G. (2021). SARS-CoV-2 mediated neuroinflammation and the impact of COVID-19 in neurological disorders. *Cytokine & Growth Factor Reviews*, *58*, 1–15. https://doi.org/10.1016/J.CYTOGFR.2021.02.002

5. Anders, Q. S., Ferreira, L., Rodrigues, L., & Nakamura-Palacios, E. M. (2020). BDNF mRNA Expression in Leukocytes and Frontal Cortex Function in Drug Use Disorder. Frontiers in psychiatry, 11, 469. https://doi.org/10.3389/fpsyt.2020.00469

6. Andrade ACDSP, Campolina-Silva GH, Queiroz-Junior CM, et al. A Biosafety Level 2 Mouse Model for Studying Betacoronavirus-Induced Acute Lung Damage and Systemic Manifestations. J Virol. 2021;95(22):e0127621. doi: 10.1128/JVI.01276-21

7. Andrews, M. G., Mukhtar, T., Eze, U. C., Simoneau, C. R., Ross, J., Parikshak, N., Wang, S., Zhou, L., Koontz, M., Velmeshev, D., Siebert, C. V., Gemenes, K. M., Tabata, T., Perez, Y., Wang, L., Mostajo-Radji, M. A., de Majo, M., Donohue, K. C., Shin, D., Salma, J., … Kriegstein, A. R. (2022). Tropism of SARS-CoV-2 for human cortical astrocytes. Proceedings of the National Academy of Sciences of the United States of America, 119(30), e2122236119. https://doi.org/10.1073/pnas.2122236119

8. Arnold, D. T., Milne, A., Samms, E., Stadon, L., Maskell, N. A., & Hamilton, F. W. (2021). Symptoms After COVID-19 Vaccination in Patients With Persistent Symptoms After Acute Infection: A Case Series. *Annals of Internal Medicine*, *174*(9), 1334–1336. https://doi.org/10.7326/M21-1976

9. Aschman T, Mothes R, Heppner FL, Radbruch H. What SARS-CoV-2 does to our brains. Immunity. 2022 Jul 12;55(7):1159-1172. doi: 10.1016/j.immuni.2022.06.013. Epub 2022 Jun 20. PMID: 35777361; PMCID: PMC9212726.

10. Asgarzadeh, A., Fouladi, N., Asghariazar, V., Sarabi, S. F., Khiavi, H. A., Mahmoudi, M., & Safarzadeh, E. (2022). Serum Brain-Derived Neurotrophic Factor (BDNF) in COVID-19 Patients and its Association with the COVID-19 Manifestations. Journal of molecular neuroscience: MN, 1–11. Advance online publication. https://doi.org/10.1007/s12031-022-02039-1

11. Ashour, H. M., Elkhatib, W. F., Rahman, M. M., & Elshabrawy, H. A. (2020). Insights into the Recent 2019 Novel Coronavirus (SARS-CoV-2) in Light of Past Human Coronavirus Outbreaks. *Pathogens (Basel, Switzerland)*, *9*(3), 186. https://doi.org/10.3390/pathogens9030186

12. Azoulay, D., Shehadeh, M., Chepa, S., Shaoul, E., Baroum, M., Horowitz, N. A., & Kaykov, E. (2020). Recovery from SARS-CoV-2 infection is associated with serum BDNF restoration. The Journal of infection, 81(3), e79–e81. https://doi.org/10.1016/j.jinf.2020.06.038

13. Bai, F., Tomasoni, D., Falcinella, C., Barbanotti, D., Castoldi, R., Mulè, G., Augello, M., Mondatore, D., Allegrini, M., Cona, A., Tesoro, D., Tagliaferri, G., Viganò, O., Suardi, E., Tincati, C., Beringheli, T., Varisco, B., Battistini, C. L., Piscopo, K., … Monforte, A. d. A. (2021). Female gender is associated with long COVID syndrome: a prospective cohort study. *Clinical Microbiology and Infection*, *28*(4), 611.e9. https://doi.org/10.1016/J.CMI.2021.11.002

14. Baig, A. M., Khaleeq, A., Ali, U., & Syeda, H. (2020). Evidence of the COVID-19 Virus Targeting the CNS: Tissue Distribution, Host-Virus Interaction, and Proposed Neurotropic Mechanisms. ACS chemical neuroscience, 11(7), 995–998. https://doi.org/10.1021/acschemneuro.0c00122

15. Bao, L., Deng, W., Huang, B., Gao, H., Liu, J., Ren, L., Wei, Q., Yu, P., Xu, Y., Qi, F., Qu, Y., Li, F., Lv, Q., Wang, W., Xue, J., Gong, S., Liu, M., Wang, G., Wang, S., … Qin, C. (2020). The pathogenicity of SARS-CoV-2 in hACE2 transgenic mice. *Nature*, *583*(7818), 830–833. https://doi.org/10.1038/S41586-020-2312-Y

16. Barthold, S. W., Beck, D. S., & Smith, A. L. (1993). Enterotropic coronavirus (mouse hepatitis virus) in mice: influence of host age and strain on infection and disease. Laboratory animal science, 43(4), 276–284.

17. Bayat, A. H., Azimi, H., Hassani Moghaddam, M., Ebrahimi, V., Fathi, M., Vakili, K., Mahmoudiasl, G. R., Forouzesh, M., Boroujeni, M. E., Nariman, Z., Abbaszadeh, H. A., Aryan, A., Aliaghaei, A., & Abdollahifar, M. A. (2022). COVID-19 causes neuronal degeneration and reduces neurogenesis in human hippocampus. Apoptosis: an international journal on programmed cell death, 1–17. Advance online publication. https://doi.org/10.1007/s10495-022-01754-9

18. Bergmann, C. C., Lane, T. E., & Stohlman, S. A. (2006). Coronavirus infection of the central nervous system: host-virus stand-off. Nature reviews. Microbiology, 4(2), 121–132. https://doi.org/10.1038/nrmicro1343

19. Boldrini M., Canoll P.D., Klein R.S. How COVID-19 Affects the Brain. JAMA psychiatry. 2021;78(6):682. doi:10.1001/jamapsychiatry.2021.0500

20. Boroujeni, M. E., Simani, L., Bluyssen, H., Samadikhah, H. R., Zamanlui Benisi, S., Hassani, S., Akbari Dilmaghani, N., Fathi, M., Vakili, K., Mahmoudiasl, G. R., Abbaszadeh, H. A., Hassani Moghaddam, M., Abdollahifar, M. A., & Aliaghaei, A. (2021). Inflammatory Response Leads to Neuronal Death in Human Post-Mortem Cerebral Cortex in Patients with COVID-19. ACS chemical neuroscience, 12(12), 2143–2150. https://doi.org/10.1021/acschemneuro.1c00111

21. Bougakov D, Podell K, Goldberg E. Multiple Neuroinvasive Pathways in COVID-19. Mol Neurobiol. 2021;58(2):564-575. doi:10.1007/s12035-020-02152-5

22. Braun, D. J., Kalinin, S., & Feinstein, D. L. (2017). Conditional Depletion of Hippocampal Brain-Derived Neurotrophic Factor Exacerbates Neuropathology in a Mouse Model of Alzheimer's Disease. ASN neuro, 9(2), 1759091417696161. https://doi.org/10.1177/1759091417696161

23. Braz-de-Melo, H. A., Faria, S. S., Pasquarelli-do-Nascimento, G., Santos, I. de O., Kobinger, G. P., & Magalhães, K. G. (2021). The Use of the Anticoagulant Heparin and Corticosteroid Dexamethasone as Prominent Treatments for COVID-19. *Frontiers in Medicine*, *8*. https://doi.org/10.3389/FMED.2021.615333

24. Brison, E., Jacomy, H., Desforges, M., & Talbot, P. J. (2011). Glutamate excitotoxicity is involved in the induction of paralysis in mice after infection by a human coronavirus with a single point mutation in its spike protein. Journal of virology, 85(23), 12464–12473. https://doi.org/10.1128/JVI.05576-11

25. Brown, S. M., Katz, M. J., Ginde, A. A., Juneja, K., Ramchandani, M., Schiffer, J. T., Vaca, C., Gottlieb, R. L., Tian, Y., Elboudwarej, E., Hill, J. A., Gilson, R., Rodriguez, L., Hedskog, C., Chen, S., Montezuma-Rusca, J. M., Osinusi, A., & Paredes, R. (2023). Consistent Effects of Early Remdesivir on Symptoms and Disease Progression Across At-Risk Outpatient Subgroups: Treatment Effect Heterogeneity in PINETREE Study. *Infectious Diseases and Therapy*, *12*(4), 1189–1203. https://doi.org/10.1007/S40121-023-00789-Y/FIGURES/4

26. Bupp, M. R. G., & Jorgensen, T. N. (2018). Androgen-Induced Immunosuppression. *Frontiers in Immunology*, *9*(APR). https://doi.org/10.3389/FIMMU.2018.00794

27. Burks SM, Rosas-Hernandez H, Alejandro Ramirez-Lee M, Cuevas E, Talpos JC. Can SARS-CoV-2 infect the central nervous system via the olfactory bulb or the blood-brain barrier? Brain Behav Immun. 2021; 95:7-14. doi: 10.1016/j.bbi.2020.12.031

28. Cai, Z., Zhong, J., Jiang, Y., & Zhang, J. (2022). Associations between COVID-19 infection and sex steroid hormones. *Frontiers in Endocrinology*, *13*. https://doi.org/10.3389/FENDO.2022.940675

29. Camargos, Q. M., Silva, B. C., Silva, D. G., Toscano, E. C. B., Oliveira, B. D. S., Bellozi, P. M. Q., Jardim, B. L. O., Vieira, É. L. M., de Oliveira, A. C. P., Sousa, L. P., Teixeira, A. L., de Miranda, A. S., & Rachid, M. A. (2020). Minocycline treatment prevents depression

and anxiety-like behaviors and promotes neuroprotection after experimental ischemic stroke. *Brain research bulletin*, *155*, 1–10. https://doi.org/10.1016/j.brainresbull.2019.11.009

30. Camargos, V. N., Foureaux, G., Medeiros, D. C., da Silveira, V. T., Queiroz-Junior, C. M., Matosinhos, A., Figueiredo, A., Sousa, C., Moreira, T. P., Queiroz, V. F., Dias, A., Santana, K., Passos, I., Real, A., Silva, L. C., Mourão, F., Wnuk, N. T., Oliveira, M., Macari, S., Silva, T., Souza, D. G. (2019). In-depth characterization of congenital Zika syndrome in immunocompetent mice: Antibody-dependent enhancement and antiviral peptide therapy. EBioMedicine, 44, 516–529. https://doi.org/10.1016/j.ebiom.2019.05.014

31. Cañas, C. A. (2020). The triggering of post-COVID-19 autoimmunity phenomena could be associated with both transient immunosuppression and an inappropriate form of immune reconstitution in susceptible individuals. *Medical Hypotheses*, *145*, 110345. https://doi.org/10.1016/J.MEHY.2020.110345

32. Carson, G., & Long Covid Forum Group (2021). Research priorities for Long Covid: refined through an international multi-stakeholder forum. BMC medicine, 19(1), 84. https://doi.org/10.1186/s12916-021-01947-0

33. Chan, Y. H., Young, B. E., Fong, S. W., Ding, Y., Goh, Y. S., Chee, R. S., Tan, S. Y., Kalimuddin, S., Tambyah, P. A., Leo, Y. S., Ng, L., Lye, D. C., & Renia, L. (2021). Differential Cytokine Responses in Hospitalized COVID-19 Patients Limit Efficacy of Remdesivir. Frontiers in immunology, 12, 680188. https://doi.org/10.3389/fimmu.2021.680188

34. Chang, R., Yen-Ting Chen, T., Wang, S. I., Hung, Y. M., Chen, H. Y., & Wei, C. C. J. (2023). Risk of autoimmune diseases in patients with COVID-19: a retrospective cohort study. *EClinicalMedicine*, *56*, 101783. https://doi.org/10.1016/J.ECLINM.2022.101783

35. Channappanavar, R., Fett, C., Mack, M., Ten Eyck, P. P., Meyerholz, D. K., & Perlman, S. (2017). Sex-Based Differences in Susceptibility to Severe Acute Respiratory Syndrome Coronavirus Infection. *Journal of Immunology (Baltimore, Md. : 1950)*, *198*(10), 4046–4053. https://doi.org/10.4049/JIMMUNOL.1601896

36. Cheng Q, Yang Y, Gao J. Infectivity of human coronavirus in the brain. EBioMedicine (2020) 56. doi: 10.1016/j.ebiom.2020.102799

37. Choutka, J., Jansari, V., Hornig, M., & Iwasaki, A. (2022). Unexplained post-acute infection syndromes. *Nature Medicine 2022 28:5*, *28*(5), 911–923. https://doi.org/10.1038/s41591-022-01810-6

38. Coperchini, F., Chiovato, L., Croce, L., Magri, F., & Rotondi, M. (2020). The cytokine storm in COVID-19: An overview of the involvement of the chemokine/chemokine-receptor system. Cytokine & growth factor reviews, 53, 25–32. https://doi.org/10.1016/j.cytogfr.2020.05.003

39. Costa VV, Del Sarto JL, Rocha RF, Silva FR, Doria JG, Olmo IG, Marques RE, Queiroz-Junior CM, Foureaux G, Araújo JMS, Cramer A, Real ALCV, Ribeiro LS, Sardi SI, Ferreir

AJ, Machado FS, De Oliveira AC, Teixeira AL, Nakaya HI, Souza DG, Ribeiro FM, Teixeira MM. 2017. N-Methyl-D-aspartate (NMDA) receptor blockade prevents neuronal death induced by Zika virus infection. mBio 8: e00350-17. https://doi.org/10.1128/mBio.00350-17

40. Cowley TJ, Weiss SR. 2010. Murine coronavirus neuropathogenesis: determinants of virulence. J Neurovirol 16:427–434. doi:10.1007/BF03210848

41. Crunfli, F., Carregari, V. C., Veras, F. P., Silva, L. S., Nogueira, M. H., Antunes, A. S. L. M., Vendramini, P. H., Valença, A. G. F., Brandão-Teles, C., da Silva Zuccoli, G., Reis-De-Oliveira, G., Silva-Costa, L. C., Saia-Cereda, V. M., Smith, B. J., Codo, A. C., de Souza, G. F., Muraro, S. P., Parise, P. L., Toledo-Teixeira, D. A., … Martins-De-Souza, D. (2022). Morphological, cellular, and molecular basis of brain infection in COVID-19 patients. *Proceedings of the National Academy of Sciences of the United States of America*, *119*(35), e2200960119. https://doi.org/10.1073/PNAS.2200960119/SUPPL_FILE/PNAS.2200960119.SAPP.PDF

42. Csordás, A., Mázló, M., & Gallyas, F. (2003). Recovery versus death of "dark" (compacted) neurons in non-impaired parenchymal environment: light and electron microscopic observations. Acta neuropathologica, 106(1), 37–49. https://doi.org/10.1007/s00401-003-0694-1.

43. Cui, J., Li, F., & Shi, Z. L. (2019). Origin and evolution of pathogenic coronaviruses. *Nature reviews. Microbiology*, *17*(3), 181–192. https://doi.org/10.1038/s41579-018-0118-9

44. Czura, C. J., & Tracey, K. J. (2005). Autonomic neural regulation of immunity. Journal of internal medicine, 257(2), 156–166. https://doi.org/10.1111/j.1365-2796.2004.01442.x.

45. Das Sarma J. (2010). A mechanism of virus-induced demyelination. Interdisciplinary perspectives on infectious diseases, 2010, 109239. https://doi.org/10.1155/2010/109239

46. Das Sarma, J., Fu, L., Tsai, J. C., Weiss, S. R., & Lavi, E. (2000). Demyelination determinants map to the spike glycoprotein gene of coronavirus mouse hepatitis virus. Journal of virology, 74(19), 9206–9213. https://doi.org/10.1128/jvi.74.19.9206-9213.2000

47. Datta, S. D., Talwar, A., & Lee, J. T. (2020). A Proposed Framework and Timeline of the Spectrum of Disease Due to SARS-CoV-2 Infection: Illness Beyond Acute Infection and Public Health Implications. JAMA, 324(22), 2251–2252. https://doi.org/10.1001/jama.2020.22717

48. Davis, H. E., Assaf, G. S., McCorkell, L., Wei, H., Low, R. J., Re'em, Y., Redfield, S., Austin, J. P., & Akrami, A. (2021). Characterizing long COVID in an international cohort: 7 months of symptoms and their impact. *EClinicalMedicine*, *38*, 101019. https://doi.org/10.1016/j.eclinm.2021.101019

49. de Miranda, A. S., Brant, F., Vieira, L. B., Rocha, N. P., Vieira, É. L. M., Rezende, G. H. S., de Oliveira Pimentel, P. M., Moraes, M. F. D., Ribeiro, F. M., Ransohoff, R. M., Teixeira, M. M., Machado, F. S., Rachid, M. A., & Teixeira, A. L. (2017). A Neuroprotective Effect

of the Glutamate Receptor Antagonist MK801 on Long-Term Cognitive and Behavioral Outcomes Secondary to Experimental Cerebral Malaria. *Molecular neurobiology*, *54*(9), 7063–7082. https://doi.org/10.1007/s12035-016-0226-3

50. de Miranda, A. S., Lacerda-Queiroz, N., de Carvalho Vilela, M., Rodrigues, D. H., Rachid, M. A., Quevedo, J., & Teixeira, A. L. (2011). Anxiety-like behavior and proinflammatory cytokine levels in the brain of C57BL/6 mice infected with *Plasmodium berghei* (strain ANKA). Neuroscience letters, 491(3), 202–206. https://doi.org/10.1016/j.neulet.2011.01.038

51. de Miranda, A. S., Rodrigues, D. H., Amaral, D. C., de Lima Campos, R. D., Cisalpino, D., Vilela, M. C., Lacerda-Queiroz, N., de Souza, K. P., Vago, J. P., Campos, M. A., Kroon, E. G., da Glória de Souza, D., Teixeira, M. M., Teixeira, A. L., & Rachid, M. A. (2012). Dengue-3 encephalitis promotes anxiety-like behavior in mice. Behavioural brain research, 230(1), 237–242. https://doi.org/10.1016/j.bbr.2012.02.020

52. Dechant, G., & Neumann, H. (2002). Neurotrophins. Advances in experimental medicine and biology, 513, 303–334. https://doi.org/10.1007/978-1-4615-0123-7_11

53. Desforges, M., Le Coupanec, A., Stodola, J. K., Meessen-Pinard, M., & Talbot, P. J. (2014). Human coronaviruses: viral and cellular factors involved in neuroinvasiveness and neuropathogenesis. Virus research, 194, 145–158. https://doi.org/10.1016/j.virusres.2014.09.011

54. Diaz-Castro, B., Bernstein, A. M., Coppola, G., Sofroniew, M. V., & Khakh, B. S. (2021). Molecular and functional properties of cortical astrocytes during peripherally induced neuroinflammation. *Cell reports*, *36*(6), 109508. https://doi.org/10.1016/j.celrep.2021.109508

55. Diener, K. R., Al-Dasooqi, N., Lousberg, E. L., & Hayball, J. D. (2013). The multifunctional alarmin HMGB1 with roles in the pathophysiology of sepsis and cancer. Immunology and cell biology, 91(7), 443–450. https://doi.org/10.1038/icb.2013.25

56. Ding, T., Wang, T., Zhang, J., Cui, P., Chen, Z., Zhou, S., Yuan, S., Ma, W., Zhang, M., Rong, Y., Chang, J., Miao, X., Ma, X., & Wang, S. (2021). Analysis of Ovarian Injury Associated With COVID-19 Disease in Reproductive-Aged Women in Wuhan, China: An Observational Study. *Frontiers in Medicine*, *8*, 635255. https://doi.org/10.3389/FMED.2021.635255/FULL

57. Dokubo, E. K., Wendland, A., Mate, S. E., Ladner, J. T., Hamblion, E. L., Raftery, P., Blackley, D. J., Laney, A. S., Mahmoud, N., Wayne-Davies, G., Hensley, L., Stavale, E., Fakoli, L., Gregory, C., Chen, T. H., Koryon, A., Roth Allen, D., Mann, J., Hickey, A., … Fallah, M. P. (2018). Persistence of Ebola virus after the end of widespread transmission in Liberia: an outbreak report. *The Lancet. Infectious Diseases*, *18*(9), 1015–1024. https://doi.org/10.1016/S1473-3099(18)30417-1

58. Dragin, N., Nancy, P., Villegas, J., Roussin, R., Le Panse, R., & Berrih-Aknin, S. (2017). Balance between Estrogens and Proinflammatory Cytokines Regulates Chemokine

Production Involved in Thymic Germinal Center Formation. *Scientific Reports*, *7*(1). https://doi.org/10.1038/S41598-017-08631-5

59. Dunkley, P. R., Heath, J. W., Harrison, S. M., Jarvie, P. E., Glenfield, P. J., & Rostas, J. A. (1988). A rapid Percoll gradient procedure for isolation of synaptosomes directly from an S1 fraction: homogeneity and morphology of subcellular fractions. *Brain research*, *441*(1-2), 59–71. https://doi.org/10.1016/0006-8993(88)91383-2

60. Eimer, W. A., Vijaya Kumar, D. K., Navalpur Shanmugam, N. K., Rodriguez, A. S., Mitchell, T., Washicosky, K. J., György, B., Breakefield, X. O., Tanzi, R. E., & Moir, R. D. (2018). Alzheimer's Disease-Associated β-Amyloid Is Rapidly Seeded by Herpesviridae to Protect against Brain Infection. *Neuron*, *99*(1), 56-63.e3. https://doi.org/10.1016/J.NEURON.2018.06.030/ATTACHMENT/88E7209B-D58C-412A-BE49-8C2884A78734/MMC2.PDF

61. Elliot J Lefkowitz, Donald M Dempsey, Robert Curtis Hendrickson, Richard J Orton, Stuart G Siddell, Donald B Smith, Virus taxonomy: the database of the International Committee on Taxonomy of Viruses (ICTV), *Nucleic Acids Research*, Volume 46, Issue D1, 4 January 2018, Pages D708–D717, https://doi.org/10.1093/nar/gkx932

62. Eltokhi, A., Kurpiers, B., & Pitzer, C. (2021). Baseline Depression-Like Behaviors in Wild-Type Adolescent Mice Are Strain and Age but Not Sex Dependent. *Frontiers in behavioral neuroscience*, *15*, 759574. https://doi.org/10.3389/fnbeh.2021.759574

63. Fan, C., Wu, Y., Rui, X., Yang, Y., Ling, C., Liu, S., Liu, S., & Wang, Y. (2022). Animal models for COVID-19: advances, gaps and perspectives. *Signal Transduction and Targeted Therapy 2022 7:1*, *7*(1), 1–24. https://doi.org/10.1038/s41392-022-01087-8

64. Felger, J. C., Li, Z., Haroon, E., Woolwine, B. J., Jung, M. Y., Hu, X., & Miller, A. H. (2016). Inflammation is associated with decreased functional connectivity within corticostriatal reward circuitry in depression. Molecular psychiatry, 21(10), 1358–1365. https://doi.org/10.1038/mp.2015.168

65. Fernández-Castañeda, A., Lu, P., Geraghty, A. C., Song, E., Lee, M. H., Wood, J., O'Dea, M. R., Dutton, S., Shamardani, K., Nwangwu, K., Mancusi, R., Yalçın, B., Taylor, K. R., Acosta-Alvarez, L., Malacon, K., Keough, M. B., Ni, L., Woo, P. J., Contreras-Esquivel, D., Monje, M. (2022). Mild respiratory COVID can cause multi-lineage neural cell and myelin dysregulation. *Cell*, *185*(14), 2452. https://doi.org/10.1016/J.CELL.2022.06.008

66. Ferreira, A. C., Zaverucha-Do-Valle, C., Reis, P. A., Barbosa-Lima, G., Vieira, Y. R., Mattos, M., Silva, P. D. P., Sacramento, C., De Castro Faria Neto, H. C., Campanati, L., Tanuri, A., Brüning, K., Bozza, F. A., Bozza, P. T., & Souza, T. M. L. (2017). Sofosbuvir protects Zika virus-infected mice from mortality, preventing short- and long-term sequelae. *Scientific Reports 2017 7:1*, *7*(1), 1–9. https://doi.org/10.1038/s41598-017-09797-8

67. Finnigan, L. E. M., Cassar, M. P., Koziel, M. J., Pradines, J., Lamlum, H., Azer, K., Kirby, D., Montgomery, H., Neubauer, S., Valkovič, L., & Raman, B. (2023). Efficacy and tolerability of an endogenous metabolic modulator (AXA1125) in fatigue-predominant long

COVID: a single-centre, double-blind, randomised controlled phase 2a pilot study. *EClinicalMedicine*, *59*, 101946. https://doi.org/10.1016/J.ECLINM.2023.101946

68. Fujinami, R. S., von Herrath, M. G., Christen, U., & Whitton, J. L. (2006). Molecular mimicry, bystander activation, or viral persistence: infections and autoimmune disease. *Clinical microbiology reviews*, *19*(1), 80–94. https://doi.org/10.1128/CMR.19.1.80-94.2006

69. Gagliardi, S., Poloni, E. T., Pandini, C., Garofalo, M., Dragoni, F., Medici, V., Davin, A., Visonà, S. D., Moretti, M., Sproviero, D., Pansarasa, O., Guaita, A., Ceroni, M., Tronconi, L., & Cereda, C. (2021). Detection of SARS-CoV-2 genome and whole transcriptome sequencing in frontal cortex of COVID-19 patients. Brain, behavior, and immunity, 97, 13–21. https://doi.org/10.1016/j.bbi.2021.05.012.

70. Gao, Q., Li, X., Huang, T., Gao, L., Wang, S., Deng, Y., Wang, F., Xue, X., & Duan, R. (2024). Angiotensin-(1-7) relieves behavioral defects and α-synuclein expression through NEAT1/miR-153-3p axis in Parkinson's disease. *Aging*, *16*(21), 13304–13322. https://doi.org/10.18632/aging.206028

71. Ge, H., Wang, X., Yuan, X., Xiao, G., Wang, C., Deng, T., Yuan, Q., & Xiao, X. (2020). The epidemiology and clinical information about COVID-19. *European journal of clinical microbiology & infectious diseases : official publication of the European Society of Clinical Microbiology*, *39*(6), 1011–1019. https://doi.org/10.1007/s10096-020-03874-z

72. Geng, L. N., Bonilla, H., Hedlin, H., Jacobson, K. B., Tian, L., Jagannathan, P., Yang, P. C., Subramanian, A. K., Liang, J. W., Shen, S., Deng, Y., Shaw, B. J., Botzheim, B., Desai, M., Pathak, D., Jazayeri, Y., Thai, D., O'Donnell, A., Mohaptra, S., Singh, U. (2024). Nirmatrelvir-Ritonavir and Symptoms in Adults With Postacute Sequelae of SARS-CoV-2 Infection: The STOP-PASC Randomized Clinical Trial. *JAMA Internal Medicine*, *184*(9), 1024–1034. https://doi.org/10.1001/JAMAINTERNMED.2024.2007

73. Getts, D. R., Chastain, E. M. L., Terry, R. L., & Miller, S. D. (2013). Virus infection, antiviral immunity, and autoimmunity. *Immunological Reviews*, *255*(1), 197–209. https://doi.org/10.1111/IMR.12091

74. Gilhus, N.E., Deuschl, G. Neuroinflammation- a common thread in neurological disorders. Nat Rev Neurol 15, 429–430 (2019). https://doi.org/10.1038/s41582-019-0227-8

75. Giovannoni, F., & Quintana, F. J. (2020). The Role of Astrocytes in CNS Inflammation. *Trends in immunology*, *41*(9), 805–819. https://doi.org/10.1016/j.it.2020.07.007

76. Giron, L. B., Peluso, M. J., Ding, J., Kenny, G., Zilberstein, N. F., Koshy, J., Hong, K. Y., Rasmussen, H., Miller, G. E., Bishehsari, F., Balk, R. A., Moy, J. N., Hoh, R., Lu, S., Goldman, A. R., Tang, H. Y., Yee, B. C., Chenna, A., Winslow, J. W., Abdel-Mohsen, M. (2022). Markers of fungal translocation are elevated during post-acute sequelae of SARS-CoV-2 and induce NF-κB signaling. *JCI Insight*, *7*(15), e160989. https://doi.org/10.1172/JCI.INSIGHT.160989

77. Gottlieb, R. L., Vaca, C. E., Paredes, R., Mera, J., Webb, B. J., Perez, G., Oguchi, G., Ryan, P., Nielsen, B. U., Brown, M., Hidalgo, A., Sachdeva, Y., Mittal, S., Osiyemi, O., Skarbinski, J., Juneja, K., Hyland, R. H., Osinusi, A., Chen, S., … Hill, J. A. (2022). Early Remdesivir to Prevent Progression to Severe Covid-19 in Outpatients. *The New England Journal of Medicine*, *386*(4), 305–315. https://doi.org/10.1056/NEJMOA2116846

78. Grynkiewicz, G., Poenie, M., & Tsien, R. Y. (1985). A new generation of Ca2+ indicators with greatly improved fluorescence properties. *The Journal of biological chemistry*, *260*(6), 3440–3450.

79. Hansen, K. S., Mogensen, T. H., Agergaard, J., Schiøttz-Christensen, B., Østergaard, L., Vibholm, L. K., & Leth, S. (2022). High-dose coenzyme Q10 therapy versus placebo in patients with post COVID-19 condition: a randomized, phase 2, crossover trial. *The Lancet Regional Health - Europe*, *24*, 100539. https://doi.org/10.1016/J.LANEPE.2022.100539

80. Harapan, B. N., & Yoo, H. J. (2021). Neurological symptoms, manifestations, and complications associated with severe acute respiratory syndrome coronavirus 2 (SARS-CoV-2) and coronavirus disease 19 (COVID-19). *Journal of neurology*, *268*(9), 3059–3071. https://doi.org/10.1007/s00415-021-10406-y

81. Harding, A. T., & Heaton, N. S. (2022). The Impact of Estrogens and Their Receptors on Immunity and Inflammation during Infection. *Cancers*, *14*(4). https://doi.org/10.3390/CANCERS14040909

82. Haroon, E., Miller, A. H., & Sanacora, G. (2017). Inflammation, Glutamate, and Glia: A Trio of Trouble in Mood Disorders. Neuropsychopharmacology: official publication of the American College of Neuropsychopharmacology, 42(1), 193–215. https://doi.org/10.1038/npp.2016.199

83. Hoffmann, M., Kleine-Weber, H., Schroeder, S., Krüger, N., Herrler, T., Erichsen, S., Schiergens, T. S., Herrler, G., Wu, N. H., Nitsche, A., Müller, M. A., Drosten, C., & Pöhlmann, S. (2020). SARS-CoV-2 Cell Entry Depends on ACE2 and TMPRSS2 and Is Blocked by a Clinically Proven Protease Inhibitor. Cell, 181(2), 271–280.e8. https://doi.org/10.1016/j.cell.2020.02.052

84. Homberger, F. R., Zhang, L., & Barthold, S. W. (1998). Prevalence of enterotropic and polytropic mouse hepatitis virus in enzootically infected mouse colonies. *Laboratory animal science*, *48*(1), 50–54.

85. Hopkins, C., Surda, P., Whitehead, E., & Kumar, B. N. (2020). Early recovery following new onset anosmia during the COVID-19 pandemic - an observational cohort study. *Journal of otolaryngology - head & neck surgery = Le Journal d'oto-rhino-laryngologie et de chirurgie cervico-faciale*, *49*(1), 26. https://doi.org/10.1186/s40463-020-00423-8

86. Huang, C., Huang, L., Wang, Y., Li, X., Ren, L., Gu, X., Kang, L., Guo, L., Liu, M., Zhou, X., Luo, J., Huang, Z., Tu, S., Zhao, Y., Chen, L., Xu, D., Li, Y., Li, C., Peng, L., Li, Y., … Cao, B. (2021). 6-month consequences of COVID-19 in patients discharged from hospital: a cohort study. *Lancet (London, England)*, *397*(10270), 220–232. https://doi.org/10.1016/S0140-6736(20)32656-8

87. Hulswit, R. J., de Haan, C. A., & Bosch, B. J. (2016). Coronavirus Spike Protein and Tropism Changes. *Advances in virus research*, *96*, 29–57. https://doi.org/10.1016/bs.aivir.2016.08.004

88. Hurst, K. R., Koetzner, C. A., & Masters, P. S. (2009). Identification of in vivo-interacting domains of the murine coronavirus nucleocapsid protein. *Journal of virology*, *83*(14), 7221–7234. https://doi.org/10.1128/JVI.00440-09

89. International Committee on Taxonomy of Viruses Virus Taxonomy: 2019 Release, EC 51. Acesso em 05 de janeiro 2025)]; https://talk.ictvonline.org/taxonomy

90. Issa, H., Eid, A. H., Berry, B., Takhviji, V., Khosravi, A., Mantash, S., Nehme, R., Hallal, R., Karaki, H., Dhayni, K., Faour, W. H., Kobeissy, F., Nehme, A., & Zibara, K. (2021). Combination of Angiotensin (1-7) Agonists and Convalescent Plasma as a New Strategy to Overcome Angiotensin Converting Enzyme 2 (ACE2) Inhibition for the Treatment of COVID-19. *Frontiers in Medicine*, *8*, 620990. https://doi.org/10.3389/FMED.2021.620990

91. Janig, W., & Green, P. G. (2014). Acute inflammation in the joint: its control by the sympathetic nervous system and by neuroendocrine systems. Autonomic neuroscience: basic & clinical, 182, 42–54. https://doi.org/10.1016/j.autneu.2014.01.001

92. Kee, J., Thudium, S., Renner, D. M., Glastad, K., Palozola, K., Zhang, Z., Li, Y., Lan, Y., Cesare, J., Poleshko, A., Kiseleva, A. A., Truitt, R., Cardenas-Diaz, F. L., Zhang, X., Xie, X., Kotton, D. N., Alysandratos, K. D., Epstein, J. A., Shi, P. Y., … Korb, E. (2022). SARS-CoV-2 disrupts host epigenetic regulation via histone mimicry. *Nature*, *610*(7931), 381. https://doi.org/10.1038/S41586-022-05282-Z

93. Keita, A. K., Koundouno, F. R., Faye, M., Düx, A., Hinzmann, J., Diallo, H., Ayouba, A., Le Marcis, F., Soropogui, B., Ifono, K., Diagne, M. M., Sow, M. S., Bore, J. A., Calvignac-Spencer, S., Vidal, N., Camara, J., Keita, M. B., Renevey, A., Diallo, A., Magassouba, N. F. (2021). Resurgence of Ebola virus in 2021 in Guinea suggests a new paradigm for outbreaks. *Nature*, *597*(7877), 539–543. https://doi.org/10.1038/S41586-021-03901-9

94. Keita, A. K., Vidal, N., Toure, A., Diallo, M. S. K., Magassouba, N., Baize, S., Mateo, M., Raoul, H., Mely, S., Subtil, F., Kpamou, C., Koivogui, L., Traore, F., Sow, M. S., Ayouba, A., Etard, J. F., Delaporte, E., Peeters, M., & PostEbogui Study Group (2019). A 40-Month Follow-Up of Ebola Virus Disease Survivors in Guinea (PostEbogui) Reveals Long-Term Detection of Ebola Viral Ribonucleic Acid in Semen and Breast Milk. *Open forum infectious diseases*, *6*(12), ofz482. https://doi.org/10.1093/ofid/ofz482

95. Kim, B., Kaistha, S. D., & Rouse, B. T. (2006). Viruses and autoimmunity. *Autoimmunity*, *39*(1), 71–77. https://doi.org/10.1080/08916930500484708

96. Kim, W.-K., Corey, S., Alvarez, X., & Williams, K. (2003). Monocyte/macrophage traffic in HIV and SIV encephalitis. *Journal of Leukocyte Biology*, *74*(5), 650–656. https://doi.org/10.1189/JLB.0503207

97. Klausegger, A., Strobl, B., Regl, G., Kaser, A., Luytjes, W., & Vlasak, R. (1999). Identification of a coronavirus hemagglutinin-esterase with a substrate specificity different from those of influenza C virus and bovine coronavirus. *Journal of virology*, *73*(5), 3737–3743. https://doi.org/10.1128/JVI.73.5.3737-3743.1999

98. Klein, S. L., & Flanagan, K. L. (2016). Sex differences in immune responses. *Nature Reviews. Immunology*, *16*(10), 626–638. https://doi.org/10.1038/NRI.2016.90

99. Klírová, M., Adamová, A., Biačková, N., Laskov, O., Renková, V., Stuchlíková, Z., Odnohová, K., & Novák, T. (2024). Transcranial direct current stimulation (tDCS) in the treatment of neuropsychiatric symptoms of long COVID. *Scientific Reports*, *14*(1). https://doi.org/10.1038/S41598-024-52763-4

100. Knight, A. C., Montgomery, S. A., Fletcher, C. A., & Baxter, V. K. (2021). Mouse Models for the Study of SARS-CoV-2 Infection. *Comparative Medicine*, *71*(5), 383–397. https://doi.org/10.30802/AALAS-CM-21-000031

101. Kojima, M., Matsui, K. & Mizui, T. BDNF pro-peptide: physiological mechanisms and implications for depression. Cell Tissue Res 377, 73–79 (2019). https://doi.org/10.1007/s00441-019-03034-6

102. Körner, R. W., Majjouti, M., Alejandre Alcazar, M. A., & Mahabir, E. (2020). Of Mice and Men: The Coronavirus MHV and Mouse Models as a Translational Approach to Understand SARS-CoV-2. *Viruses*, *12*(8), 880. https://doi.org/10.3390/V12080880

103. Krasemann, S., Haferkamp, U., Pfefferle, S., Woo, M. S., Heinrich, F., Schweizer, M., Appelt-Menzel, A., Cubukova, A., Barenberg, J., Leu, J., Hartmann, K., Thies, E., Littau, J. L., Sepulveda-Falla, D., Zhang, L., Ton, K., Liang, Y., Matschke, J., Ricklefs, F., Sauvigny, T., Pless, O. (2022). The blood-brain barrier is dysregulated in COVID-19 and serves as a CNS entry route for SARS-CoV-2. *Stem cell reports*, *17*(2), 307–320. https://doi.org/10.1016/j.stemcr.2021.12.011

104. Kuba, K., Yamaguchi, T., & Penninger, J. M. (2021). Angiotensin-Converting Enzyme 2 (ACE2) in the Pathogenesis of ARDS in COVID-19. Frontiers in immunology, 12, 732690. https://doi.org/10.3389/fimmu.2021.732690

105. Lau, A., & Tymianski, M. (2010). Glutamate receptors, neurotoxicity and neurodegeneration. Pflugers Archiv: European journal of physiology, 460(2), 525–542. https://doi.org/10.1007/s00424-010-0809-1

106. Lau, R. I., Su, Q., Lau, I. S. F., Ching, J. Y. L., Wong, M. C. S., Lau, L. H. S., Tun, H. M., Mok, C. K. P., Chau, S. W. H., Tse, Y. K., Cheung, C. P., Li, M. K. T., Yeung, G. T. Y., Cheong, P. K., Chan, F. K. L., & Ng, S. C. (2024). A synbiotic preparation (SIM01) for post-acute COVID-19 syndrome in Hong Kong (RECOVERY): a randomised, double-blind, placebo-controlled trial. *The Lancet Infectious Diseases*, *24*(3), 256–265. https://doi.org/10.1016/S1473-3099(23)00685-0

107. Li, J., Zhou, Y., Ma, J., Zhang, Q., Shao, J., Liang, S., Yu, Y., Li, W., & Wang, C. (2023). The long-term health outcomes, pathophysiological mechanisms and multidisciplinary

management of long COVID. *Signal Transduction and Targeted Therapy 2023 8:1*, *8*(1), 1–19. https://doi.org/10.1038/s41392-023-01640-z

108. Li, T., Chen, X., Zhang, C., Zhang, Y., & Yao, W. (2019). An update on reactive astrocytes in chronic pain. *Journal of neuroinflammation*, *16*(1), 140. https://doi.org/10.1186/s12974-019-1524-2

109. Li, Z., Liu, T., Yang, N., Han, D., Mi, X., Li, Y., Liu, K., Vuylsteke, A., Xiang, H., & Guo, X. (2020). Neurological manifestations of patients with COVID-19: potential routes of SARS-CoV-2 neuroinvasion from the periphery to the brain. *Frontiers of Medicine*, *14*(5), 533–541. https://doi.org/10.1007/S11684-020-0786-5/METRICS

110. Lima Giacobbo, B., Doorduin, J., Klein, H. C., Dierckx, R., Bromberg, E., & de Vries, E. (2019). Brain-Derived Neurotrophic Factor in Brain Disorders: Focus on Neuroinflammation. Molecular neurobiology, 56(5), 3295–3312. https://doi.org/10.1007/s12035-018-1283-6

111. Lima, E. B. de S., Carvalho, A. F. S., Zaidan, I., Monteiro, A. H. A., Cardoso, C., Lara, E. S., Carneiro, F. S., Oliveira, L. C., Resende, F., Santos, F. R. da S., Souza-Costa, L. P., Chaves, I. de M., Queiroz-Junior, C. M., Russo, R. C., Santos, R. A. S., Tavares, L. P., Teixeira, M. M., Costa, V. V., & Sousa, L. P. (2024). Angiotensin-(1-7) decreases inflammation and lung damage caused by betacoronavirus infection in mice. *Inflammation Research: Official Journal of the European Histamine Research Society [et Al.]*, *73*(11), 2009–2022. https://doi.org/10.1007/S00011-024-01948-8

112. Linnerbauer, M., Wheeler, M. A., & Quintana, F. J. (2020). Astrocyte Crosstalk in CNS Inflammation. *Neuron*, *108*(4), 608–622. https://doi.org/10.1016/j.neuron.2020.08.012

113. Liu, M., Shi, P., & Sumners, C. (2015). Direct anti-inflammatory effects of angiotensin-(1–7) on microglia. *Journal of Neurochemistry*, *136*(1), 163. https://doi.org/10.1111/JNC.13386

114. Llorente, F., Cody, S. G., Adam, A., Siniavin, A., Kang, S. S., & Wang, T. (2024). Flaviviruses—Induced Neurological Sequelae. *Pathogens 2025, Vol. 14, Page 22*, *14*(1), 22. https://doi.org/10.3390/PATHOGENS14010022

115. Lobo, S. M., Plantefève, G., Nair, G., Joaquim Cavalcante, A., Franzin de Moraes, N., Nunes, E., Barnum, O., Berdun Stadnik, C. M., Lima, M. P., Lins, M., Hajjar, L. A., Lipinski, C., Islam, S., Ramos, F., Simon, T., Martinot, J. B., Guimard, T., Desclaux, A., Lioger, B., Morelot-Panzini, C. (2024). Efficacy of oral 20-hydroxyecdysone (BIO101), a MAS receptor activator, in adults with severe COVID-19 (COVA): a randomized, placebo-controlled, phase 2/3 trial. *EClinicalMedicine*, *68*, 102383. https://doi.org/10.1016/J.ECLINM.2023.102383

116. Louveau, A., Smirnov, I., Keyes, T. J., Eccles, J. D., Rouhani, S. J., Peske, J. D., Derecki, N. C., Castle, D., Mandell, J. W., Lee, K. S., Harris, T. H., & Kipnis, J. (2015). Structural and functional features of central nervous system lymphatic vessels. Nature, 523(7560), 337–341. https://doi.org/10.1038/nature14432

117. Martins-Gonçalves, R., Hottz, E. D., & Bozza, P. T. (2023). Acute to post-acute COVID-19 thromboinflammation persistence: Mechanisms and potential consequences. *Current research in immunology*, *4*, 100058. https://doi.org/10.1016/j.crimmu.2023.100058

118. Mathys, H., Davila-Velderrain, J., Peng, Z., Gao, F., Mohammadi, S., Young, J. Z., Menon, M., He, L., Abdurrob, F., Jiang, X., Martorell, A. J., Ransohoff, R. M., Hafler, B. P., Bennett, D. A., Kellis, M., & Tsai, L. H. (2019). Single-cell transcriptomic analysis of Alzheimer's disease. *Nature*, *570*(7761), 332–337. https://doi.org/10.1038/s41586-019-1195-2

119. Matschke, J., Lütgehetmann, M., Hagel, C., Sperhake, J. P., Schröder, A. S., Edler, C., Mushumba, H., Fitzek, A., Allweiss, L., Dandri, M., Dottermusch, M., Heinemann, A., Pfefferle, S., Schwabenland, M., Sumner Magruder, D., Bonn, S., Prinz, M., Gerloff, C., Püschel, K., Krasemann, S., Glatzel, M. (2020). Neuropathology of patients with COVID-19 in Germany: a post-mortem case series. The Lancet. Neurology, 19(11), 919–929. https://doi.org/10.1016/S1474-4422(20)30308-2

120. Mattson, M. P., & Magnus, T. (2006). Ageing and neuronal vulnerability. *Nature reviews. Neuroscience*, *7*(4), 278–294. https://doi.org/10.1038/nrn1886

121. Mazza, M. G., Palladini, M., De Lorenzo, R., Magnaghi, C., Poletti, S., Furlan, R., Ciceri, F., COVID-19 BioB Outpatient Clinic Study group, Rovere-Querini, P., & Benedetti, F. (2021). Persistent psychopathology and neurocognitive impairment in COVID-19 survivors: Effect of inflammatory biomarkers at three-month follow-up. Brain, behavior, and immunity, 94, 138–147. https://doi.org/10.1016/j.bbi.2021.02.021

122. Mazza, M. G., Palladini, M., Poletti, S., & Benedetti, F. (2022). Post-COVID-19 Depressive Symptoms: Epidemiology, Pathophysiology, and Pharmacological Treatment. CNS drugs, 36(7), 681–702. https://doi.org/10.1007/s40263-022-00931-3

123. McCray, P. B., Jr, Pewe, L., Wohlford-Lenane, C., Hickey, M., Manzel, L., Shi, L., Netland, J., Jia, H. P., Halabi, C., Sigmund, C. D., Meyerholz, D. K., Kirby, P., Look, D. C., & Perlman, S. (2007). Lethal infection of K18-hACE2 mice infected with severe acute respiratory syndrome coronavirus. Journal of virology, 81(2), 813–821. https://doi.org/10.1128/JVI.02012-06

124. Meinhardt, J., Radke, J., Dittmayer, C., Franz, J., Thomas, C., Mothes, R., Laue, M., Schneider, J., Brünink, S., Greuel, S., Lehmann, M., Hassan, O., Aschman, T., Schumann, E., Chua, R. L., Conrad, C., Eils, R., Stenzel, W., Windgassen, M., … Heppner, F. L. (2021). Olfactory transmucosal SARS-CoV-2 invasion as a port of central nervous system entry in individuals with COVID-19. *Nature Neuroscience*, *24*(2), 168–175. https://doi.org/10.1038/s41593-020-00758-5

125. Mendes, S., Guimarães, L. C., Costa, P. A. C., Fernandez, C. C., Figueiredo, M. M., Teixeira, M. M., Dos Santos, R. A. S., Guimarães, P. P. G., & Frézard, F. (2024). Intranasal liposomal angiotensin-(1-7) administration reduces inflammation and viral load in the lungs during SARS-CoV-2 infection in K18-hACE2 transgenic mice. *Antimicrobial Agents and Chemotherapy*, *68*(12), e0083524. https://doi.org/10.1128/AAC.00835-24

126. Merad, M., Blish, C. A., Sallusto, F., & Iwasaki, A. (2022). The immunology and immunopathology of COVID-19. *Science (New York, N.Y.)*, *375*(6585), 1122–1127. https://doi.org/10.1126/science.abm8108

127. Michael, H., Mpofana, T., Ramlall, S., & Oosthuizen, F. (2020). The Role of Brain Derived Neurotrophic Factor in HIV-Associated Neurocognitive Disorder: From the Bench-Top to the Bedside. Neuropsychiatric disease and treatment, 16, 355–367. https://doi.org/10.2147/NDT.S232836

128. Miesbach, W. (2020). Pathological Role of Angiotensin II in Severe COVID-19. *TH Open: Companion Journal to Thrombosis and Haemostasis*, *4*(2), e138. https://doi.org/10.1055/S-0040-1713678

129. Milaneschi, Y., Kappelmann, N., Ye, Z., Lamers, F., Moser, S., Jones, P. B., Burgess, S., Penninx, B., & Khandaker, G. M. (2021). Association of inflammation with depression and anxiety: evidence for symptom-specificity and potential causality from UK Biobank and NESDA cohorts. Molecular psychiatry, 26(12), 7393–7402. https://doi.org/10.1038/s41380-021-01188-w

130. Miner, J. J., & Diamond, M. S. (2016). Mechanisms of restriction of viral neuroinvasion at the blood-brain barrier. *Current Opinion in Immunology*, *38*, 18–23. https://doi.org/10.1016/J.COI.2015.10.008

131. Miranda, A. S., Vieira, L. B., Lacerda-Queiroz, N., Souza, A. H., Rodrigues, D. H., Vilela, M. C., Gomez, M. V., Machado, F. S., Rachid, M. A., & Teixeira, A. L. (2010). Increased levels of glutamate in the central nervous system are associated with behavioral symptoms in experimental malaria. *Brazilian journal of medical and biological research = Revista brasileira de pesquisas medicas e biologicas*, *43*(12), 1173–1177. https://doi.org/10.1590/s0100-879x2010007500130

132. Mody, I., & MacDonald, J. F. (1995). NMDA receptor-dependent excitotoxicity: the role of intracellular Ca^{2+} release. Trends in pharmacological sciences, 16(10), 356–359. https://doi.org/10.1016/s0165-6147(00)89070-7

133. Muñoz-Fontela, C., Widerspick, L., Albrecht, R. A., Beer, M., Carroll, M. W., de Wit, E., Diamond, M. S., Dowling, W. E., Funnell, S. G. P., García-Sastre, A., Gerhards, N. M., de Jong, R., Munster, V. J., Neyts, J., Perlman, S., Reed, D. S., Richt, J. A., Riveros-Balta, X., Roy, C. J., Barouch, D. H. (2022). Advances and gaps in SARS-CoV-2 infection models. *PLoS Pathogens*, *18*(1), e1010161. https://doi.org/10.1371/JOURNAL.PPAT.1010161

134. Mushebenge, A. G. A., Ugbaja, S. C., Mbatha, N. A., B. Khan, R., & Kumalo, H. M. (2023). Assessing the Potential Contribution of In Silico Studies in Discovering Drug Candidates That Interact with Various SARS-CoV-2 Receptors. *International Journal of Molecular Sciences 2023, Vol. 24, Page 15518*, *24*(21), 15518. https://doi.org/10.3390/IJMS242115518

135. Nagappan, P. G., Chen, H., & Wang, D. Y. (2020). Neuroregeneration and plasticity: a review of the physiological mechanisms for achieving functional recovery

postinjury. Military Medical Research, 7(1), 30. https://doi.org/10.1186/s40779-020-00259-3

136. Nakagawara, K., Morita, A., Namkoong, H., Terai, H., Chubachi, S., Asakura, T., Tanaka, H., Ito, F., Matsuyama, E., Kaji, M., Saito, A., Takaoka, H., Okada, M., Sunata, K., Watase, M., Yagi, K., Ohgino, K., Miyata, J., Kamata, H., Fukunaga, K. (2023). Longitudinal long COVID symptoms in Japanese patients after COVID-19 vaccinations. *Vaccine: X*, *15*, 100381. https://doi.org/10.1016/J.JVACX.2023.100381

137. Netland, J., Meyerholz, D. K., Moore, S., Cassell, M., & Perlman, S. (2008). Severe acute respiratory syndrome coronavirus infection causes neuronal death in the absence of encephalitis in mice transgenic for human ACE2. Journal of virology, 82(15), 7264–7275. https://doi.org/10.1128/JVI.00737-08

138. Nevalainen, O. P. O., Horstia, S., Laakkonen, S., Rutanen, J., Mustonen, J. M. J., Kalliala, I. E. J., Ansakorpi, H., Kreivi, H. R., Kuutti, P., Paajanen, J., Parkkila, S., Paukkeri, E. L., Perola, M., Pourjamal, N., Renner, A., Rosberg, T., Rutanen, T., Savolainen, J., Solidarity Finland Investigators, Haukka, J. K., Tikkinen, K. A. O. (2022). Effect of remdesivir post hospitalization for COVID-19 infection from the randomized SOLIDARITY Finland trial. *Nature communications*, *13*(1), 6152. https://doi.org/10.1038/s41467-022-33825-5

139. Ngai, J. C., Ko, F. W., Ng, S. S., To, K. W., Tong, M., & Hui, D. S. (2010). The long-term impact of severe acute respiratory syndrome on pulmonary function, exercise capacity and health status. Respirology (Carlton, Vic.), 15(3), 543–550. https://doi.org/10.1111/j.1440-1843.2010.01720.x

140. Nicholls, D. G., Sihra, T. S., & Sanchez-Prieto, J. (1987). Calcium-Dependent and-Independent Release of Glutamate from Synaptosomes Monitored by Continuous Fluorometry. *Journal of Neurochemistry*, *49*(1), 50–57. https://doi.org/10.1111/j.1471-4159.1987.tb03393.x

141. Oliveira, T. P. D., Gonçalves, B. D. C., Oliveira, B. S., de Oliveira, A. C. P., Reis, H. J., Ferreira, C. N., Aguiar, D. C., de Miranda, A. S., Ribeiro, F. M., Vieira, E. M. L., Palotás, A., & Vieira, L. B. (2021). Negative Modulation of the Metabotropic Glutamate Receptor Type 5 as a Potential Therapeutic Strategy in Obesity and Binge-Like Eating Behavior. *Frontiers in neuroscience*, *15*, 631311. https://doi.org/10.3389/fnins.2021.631311

142. Ong, S., Fong, S. W., Young, B. E., Chan, Y. H., Lee, B., Amrun, S. N., Chee, R. S., Yeo, N. K., Tambyah, P., Pada, S., Tan, S. Y., Ding, Y., Renia, L., Leo, Y. S., Ng, L., & Lye, D. C. (2021). Persistent Symptoms and Association With Inflammatory Cytokine Signatures in Recovered Coronavirus Disease 2019 Patients. Open forum infectious diseases, 8(6), ofab156. https://doi.org/10.1093/ofid/ofab156

143. O'Sullivan O. (2021). Long-term sequelae following previous coronavirus epidemics. Clinical medicine (London, England), 21(1), e68–e70. https://doi.org/10.7861/clinmed.2020-0204

144. Patrick-Brown, T. D. J. H., Barratt-Due, A., Trøseid, M., Dyrhol-Riise, A. M., Nezvalova-Henriksen, K., Kåsine, T., Aukrust, P., Olsen, I. C., & NOR Solidarity consortium (2024). The effects of remdesivir on long-term symptoms in patients hospitalised for COVID-19: a pre-specified exploratory analysis. *Communications medicine*, *4*(1), 231. https://doi.org/10.1038/s43856-024-00650-4

145. Paz-Bailey, G., Rosenberg, E. S., Doyle, K., Munoz-Jordan, J., Santiago, G. A., Klein, L., Perez-Padilla, J., Medina, F. A., Waterman, S. H., Adams, L. E., Lozier, M. J., Bertrán-Pasarell, J., Garcia Gubern, C., Alvarado, L. I., & Sharp, T. M. (2017). Persistence of Zika Virus in Body Fluids - Final Report. *The New England Journal of Medicine*, *379*(13), 1234–1243. https://doi.org/10.1056/NEJMOA1613108

146. Peluso, M. J., Deitchman, A. N., Torres, L., Iyer, N. S., Munter, S. E., Nixon, C. C., Donatelli, J., Thanh, C., Takahashi, S., Hakim, J., Turcios, K., Janson, O., Hoh, R., Tai, V., Hernandez, Y., Fehrman, E. A., Spinelli, M. A., Gandhi, M., Trinh, L., Henrich, T. J. (2021). Long-term SARS-CoV-2-specific immune and inflammatory responses in individuals recovering from COVID-19 with and without post-acute symptoms. *Cell Reports*, *36*(6), 109518. https://doi.org/10.1016/J.CELREP.2021.109518

147. Peluso, M. J., Deveau, T. M., Munter, S. E., Ryder, D., Buck, A., Beck-Engeser, G., Chan, F., Lu, S., Goldberg, S. A., Hoh, R., Tai, V., Torres, L., Iyer, N. S., Deswal, M., Ngo, L. H., Buitrago, M., Rodriguez, A., Chen, J. Y., Yee, B. C., Henrich, T. J. (2023). Chronic viral coinfections differentially affect the likelihood of developing long COVID. *The Journal of Clinical Investigation*, *133*(3), e163669. https://doi.org/10.1172/JCI163669

148. Pennisi, M., Lanza, G., Falzone, L., Fisicaro, F., Ferri, R., & Bella, R. (2020). SARS-CoV-2 and the Nervous System: From Clinical Features to Molecular Mechanisms. *International Journal of Molecular Sciences*, *21*(15), 5475. https://doi.org/10.3390/IJMS21155475

149. Podhorna, J., & Brown, R. E. (2002). Strain differences in activity and emotionality do not account for differences in learning and memory performance between C57BL/6 and DBA/2 mice. *Genes, brain, and behavior*, *1*(2), 96–110. https://doi.org/10.1034/j.1601-183x.2002.10205.x

150. Prediger, R. D., Aguiar, A. S., Jr, Rojas-Mayorquin, A. E., Figueiredo, C. P., Matheus, F. C., Ginestet, L., Chevarin, C., Bel, E. D., Mongeau, R., Hamon, M., Lanfumey, L., & Raisman-Vozari, R. (2010). Single intranasal administration of 1-methyl-4-phenyl-1,2,3,6-tetrahydropyridine in C57BL/6 mice models early preclinical phase of Parkinson's disease. *Neurotoxicity research*, *17*(2), 114–129. https://doi.org/10.1007/s12640-009-9087-0

151. Proal, A. D., VanElzakker, M. B., Aleman, S., Bach, K., Boribong, B. P., Buggert, M., Cherry, S., Chertow, D. S., Davies, H. E., Dupont, C. L., Deeks, S. G., Eimer, W., Ely, E. W., Fasano, A., Freire, M., Geng, L. N., Griffin, D. E., Henrich, T. J., Iwasaki, A., … Wherry, E. J. (2023a). SARS-CoV-2 reservoir in post-acute sequelae of COVID-19 (PASC). *Nature Immunology 2023 24:10*, *24*(10), 1616–1627. https://doi.org/10.1038/s41590-023-01601-2

152. RECOVERY Collaborative Group, Horby, P., Lim, W. S., Emberson, J. R., Mafham, M., Bell, J. L., Linsell, L., Staplin, N., Brightling, C., Ustianowski, A., Elmahi, E., Prudon, B., Green, C., Felton, T., Chadwick, D., Rege, K., Fegan, C., Chappell, L. C., Faust, S. N., Jaki, T., Landray, M. J. (2021). Dexamethasone in Hospitalized Patients with Covid-19. *The New England journal of medicine*, *384*(8), 693–704. https://doi.org/10.1056/NEJMoa2021436

153. Reza-Zaldívar, E. E., Hernández-Sapiéns, M. A., Minjarez, B., Gómez-Pinedo, U., Márquez-Aguirre, A. L., Mateos-Díaz, J. C., Matias-Guiu, J., & Canales-Aguirre, A. A. (2021). Infection Mechanism of SARS-COV-2 and Its Implication on the Nervous System. *Frontiers in immunology*, *11*, 621735. https://doi.org/10.3389/fimmu.2020.621735

154. Rhodes, C. H., Priemer, D. S., Karlovich, E., Perl, D. P., & Goldman, J. (2022). B-Amyloid Deposits in Young COVID Patients. *SSRN Electronic Journal*. https://doi.org/10.2139/SSRN.4003213

155. Rodrigues, H. A., Fonseca, M.deC., Camargo, W. L., Lima, P. M., Martinelli, P. M., Naves, L. A., Prado, V. F., Prado, M. A., & Guatimosim, C. (2013). Reduced expression of the vesicular acetylcholine transporter and neurotransmitter content affects synaptic vesicle distribution and shape in mouse neuromuscular junction. *PloS one*, *8*(11), e78342. https://doi.org/10.1371/journal.pone.0078342

156. Russell, K., Hills, S. L., Oster, A. M., Porse, C. C., Danyluk, G., Cone, M., Brooks, R., Scotland, S., Schiffman, E., Fredette, C., White, J. L., Ellingson, K., Hubbard, A., Cohn, A., Fischer, M., Mead, P., Powers, A. M., & Brooks, J. T. (2017). Male-to-Female Sexual Transmission of Zika Virus-United States, January-April 2016. *Clinical Infectious Diseases: An Official Publication of the Infectious Diseases Society of America*, *64*(2), 211–213. https://doi.org/10.1093/CID/CIW692

157. Ryu, J. K., Yan, Z., Montano, M., Sozmen, E. G., Dixit, K., Suryawanshi, R. K., Matsui, Y., Helmy, E., Kaushal, P., Makanani, S. K., Deerinck, T. J., Meyer-Franke, A., Rios Coronado, P. E., Trevino, T. N., Shin, M. G., Tognatta, R., Liu, Y., Schuck, R., Le, L., Akassoglou, K. (2024). Fibrin drives thromboinflammation and neuropathology in COVID-19. *Nature 2024 633:8031*, *633*(8031), 905–913. https://doi.org/10.1038/s41586-024-07873-4

158. Ryu, S., Shchukina, I., Youm, Y. H., Qing, H., Hilliard, B., Dlugos, T., Zhang, X., Yasumoto, Y., Booth, C. J., Fernández-Hernando, C., Suárez, Y., Khanna, K., Horvath, T. L., Dietrich, M. O., Artyomov, M., Wang, A., & Dixit, V. D. (2021). Ketogenic diet restrains aging-induced exacerbation of coronavirus infection in mice. *ELife*, *10*, e66522. https://doi.org/10.7554/ELIFE.66522

159. Sarubbo, F., El Haji, K., Vidal-Balle, A., & Bargay Lleonart, J. (2022). Neurological consequences of COVID-19 and brain related pathogenic mechanisms: A new challenge for neuroscience. *Brain, Behavior, & Immunity - Health*, *19*, 100399. https://doi.org/10.1016/J.BBIH.2021.100399

160. Schultheiß, C., Willscher, E., Paschold, L., Gottschick, C., Klee, B., Henkes, S. S., Bosurgi, L., Dutzmann, J., Sedding, D., Frese, T., Girndt, M., Höll, J. I., Gekle, M., Mikolajczyk, R., & Binder, M. (2022). The IL-1β, IL-6, and TNF cytokine triad is associated

with post-acute sequelae of COVID-19. *Cell Reports Medicine*, *3*(6), 100663. https://doi.org/10.1016/J.XCRM.2022.100663

161. Schulze, H., & Bayer, W. (2022). Changes in Symptoms Experienced by SARS-CoV-2-Infected Individuals – From the First Wave to the Omicron Variant. *Frontiers in Virology*, *2*, 880707. https://doi.org/10.3389/FVIRO.2022.880707/BIBTEX

162. Scully, E. P., Haverfield, J., Ursin, R. L., Tannenbaum, C., & Klein, S. L. (2020). Considering how biological sex impacts immune responses and COVID-19 outcomes. *Nature Reviews. Immunology*, *20*(7), 442–447. https://doi.org/10.1038/S41577-020-0348-8

163. Seo, S. M., Son, J. H., Lee, J. H., Kim, N. W., Yoo, E. S., Kang, A. R., Jang, J. Y., On, D. I., Noh, H. A., Yun, J. W., Park, J. W., Choi, K. S., Lee, H. Y., Shin, J. S., Seo, J. Y., Nam, K. T., Lee, H., Seong, J. K., & Choi, Y. K. (2022). Development of transgenic models susceptible and resistant to SARS-CoV-2 infection in FVB background mice. *PloS One*, *17*(7). https://doi.org/10.1371/JOURNAL.PONE.0272019

164. Sheridan, G. K., & Murphy, K. J. (2013). Neuron-glia crosstalk in health and disease: fractalkine and CX3CR1 take centre stage. Open biology, 3(12), 130181. https://doi.org/10.1098/rsob.130181

165. Silva, J., & Iwasaki, A. (2024). Sex differences in postacute infection syndromes. *Science translational medicine*, *16*(773), eado2102. https://doi.org/10.1126/scitranslmed.ado2102

166. Siu, Y. L., Teoh, K. T., Lo, J., Chan, C. M., Kien, F., Escriou, N., Tsao, S. W., Nicholls, J. M., Altmeyer, R., Peiris, J. S., Bruzzone, R., & Nal, B. (2008). The M, E, and N structural proteins of the severe acute respiratory syndrome coronavirus are required for efficient assembly, trafficking, and release of virus-like particles. *Journal of virology*, *82*(22), 11318–11330. https://doi.org/10.1128/JVI.01052-08

167. Slabakova, Y., Gerasoudis, S., Miteva, D., Peshevska-Sekulovska, M., Batselova, H., Snegarova, V., Vasilev, G. V., Vasilev, G. H., Sekulovski, M., Lazova, S., Gulinac, M., Tomov, L., & Velikova, T. (2023). SARS-CoV-2 Variant-Specific Gastrointestinal Symptoms of COVID-19: 2023 Update. *Gastroenterology Insights*, *14*(4), 431-445. https://doi.org/10.3390/gastroent14040032

168. Solomon, I. H., Normandin, E., Bhattacharyya, S., Mukerji, S. S., Keller, K., Ali, A. S., Adams, G., Hornick, J. L., Padera, R. F., Jr, & Sabeti, P. (2020). Neuropathological Features of Covid-19. The New England journal of medicine, 383(10), 989–992. https://doi.org/10.1056/NEJMc2019373

169. Son, K., Jamil, R., Chowdhury, A., Mukherjee, M., Venegas, C., Miyasaki, K., Zhang, K., Patel, Z., Salter, B., Yan Yuen, A. C., Soon-Keen Lau, K., Cowbrough, B., Radford, K., Huang, C., Kjarsgaard, M., Dvorkin-Gheva, A., Smith, J., Li, Q. Z., Waserman, S., Mukherjee, M. (2023). Circulating anti-nuclear autoantibodies in COVID-19 survivors predict long COVID symptoms. *The European Respiratory Journal*, *61*(1). https://doi.org/10.1183/13993003.00970-2022

170. Sousa, L. P., Pinho, V., & Teixeira, M. M. (2020). Harnessing inflammation resolving-based therapeutic agents to treat pulmonary viral infections: What can the future offer to COVID-19? *British Journal of Pharmacology*, *177*(17), 3898–3904. https://doi.org/10.1111/BPH.15164

171. Stein, S. R., Ramelli, S. C., Grazioli, A., Chung, J. Y., Singh, M., Yinda, C. K., Winkler, C. W., Sun, J., Dickey, J. M., Ylaya, K., Ko, S. H., Platt, A. P., Burbelo, P. D., Quezado, M., Pittaluga, S., Purcell, M., Munster, V. J., Belinky, F., Ramos-Benitez, M. J., Chertow, D. S. (2022). SARS-CoV-2 infection and persistence in the human body and brain at autopsy. *Nature*, *612*(7941), 758–763. https://doi.org/10.1038/S41586-022-05542-Y

172. Stevens B. (2008). Neuron-astrocyte signaling in the development and plasticity of neural circuits. *Neuro-Signals*, *16*(4), 278–288. https://doi.org/10.1159/000123038

173. Su, S., Wong, G., Shi, W., Liu, J., Lai, A. C. K., Zhou, J., Liu, W., Bi, Y., & Gao, G. F. (2016). Epidemiology, Genetic Recombination, and Pathogenesis of Coronaviruses. *Trends in microbiology*, *24*(6), 490–502. https://doi.org/10.1016/j.tim.2016.03.003

174. Subbarayan, M. S., Joly-Amado, A., Bickford, P. C., & Nash, K. R. (2022). CX3CL1/CX3CR1 signaling targets for the treatment of neurodegenerative diseases. Pharmacology & therapeutics, 231, 107989. https://doi.org/10.1016/j.pharmthera.2021.107989

175. Tang, N., Li, D., Wang, X., & Sun, Z. (2020). Abnormal coagulation parameters are associated with poor prognosis in patients with novel coronavirus pneumonia. *Journal of Thrombosis and Haemostasis*, *18*(4), 844–847. https://doi.org/10.1111/JTH.14768

176. Thompson, E. J., Williams, D. M., Walker, A. J., Mitchell, R. E., Niedzwiedz, C. L., Yang, T. C., Huggins, C. F., Kwong, A., Silverwood, R. J., Di Gessa, G., Bowyer, R., Northstone, K., Hou, B., Green, M. J., Dodgeon, B., Doores, K. J., Duncan, E. L., Williams, F., OpenSAFELY Collaborative, Steptoe, A., Steves, C. J. (2022). Long COVID burden and risk factors in 10 UK longitudinal studies and electronic health records. Nature communications, 13(1), 3528. https://doi.org/10.1038/s41467-022-30836-0

177. Toscano, E., Sousa, L., Lima, G. K., Mesquita, L. A., Vilela, M. C., Rodrigues, D. H., Ferreira, R. N., Soriani, F. M., Campos, M. A., Kroon, E. G., Teixeira, M. M., de Miranda, A. S., Rachid, M. A., & Teixeira, A. L. (2020). Neuroinflammation is associated with reduced SOCS2 and SOCS3 expression during intracranial HSV-1 infection. Neuroscience letters, 736, 135295. https://doi.org/10.1016/j.neulet.2020.135295

178. Tsukahara, T., Brann, D. H., & Datta, S. R. (2023). Mechanisms of SARS-CoV-2-associated anosmia. *Physiological Reviews*, *103*(4), 2759. https://doi.org/10.1152/PHYSREV.00012.2023

179. Uddin, M., Mustafa, F., Rizvi, T. A., Loney, T., Suwaidi, H. A., Al-Marzouqi, A. H. H., Eldin, A. K., Alsabeeha, N., Adrian, T. E., Stefanini, C., Nowotny, N., Alsheikh-Ali, A., & Senok, A. C. (2020). SARS-CoV-2/COVID-19: Viral Genomics, Epidemiology, Vaccines, and Therapeutic Interventions. *Viruses*, *12*(5), 526. https://doi.org/10.3390/v12050526

180. Udina, M., Castellví, P., Moreno-España, J., Navinés, R., Valdés, M., Forns, X., Langohr, K., Solà, R., Vieta, E., & Martín-Santos, R. (2012). Interferon-induced depression in chronic hepatitis C: a systematic review and meta-analysis. The Journal of clinical psychiatry, 73(8), 1128–1138. https://doi.org/10.4088/JCP.12r07694

181. Valdetaro, L., Thomasi, B., Ricciardi, M. C., de Melo Santos, K., de Mattos Coelho-Aguiar, J., & Tavares-Gomes, A. L. (2023). Enteric nervous system as a target and source of SARS-CoV-2 and other viral infections. In *American Journal of Physiology - Gastrointestinal and Liver Physiology* (Vol. 325, Issue 2, pp. G93–G108). American Physiological Society. https://doi.org/10.1152/ajpgi.00229.2022

182. Valles, S. L., Singh, S. K., Campos-Campos, J., Colmena, C., Campo-Palacio, I., Alvarez-Gamez, K., Caballero, O., & Jorda, A. (2023). Functions of Astrocytes under Normal Conditions and after a Brain Disease. *International journal of molecular sciences*, *24*(9), 8434. https://doi.org/10.3390/ijms24098434

183. Varkey, J. B., Shantha, J. G., Crozier, I., Kraft, C. S., Lyon, G. M., Mehta, A. K., Kumar, G., Smith, J. R., Kainulainen, M. H., Whitmer, S., Ströher, U., Uyeki, T. M., Ribner, B. S., & Yeh, S. (2015). Persistence of Ebola Virus in Ocular Fluid during Convalescence. *The New England Journal of Medicine*, *372*(25), 2423–2427. https://doi.org/10.1056/NEJMOA1500306

184. Verma, D., Church, T. M., & Swaminathan, S. (2021). Epstein-Barr Virus Lytic Replication Induces ACE2 Expression and Enhances SARS-CoV-2 Pseudotyped Virus Entry in Epithelial Cells. *Journal of virology*, *95*(13), e0019221. https://doi.org/10.1128/JVI.00192-21

185. Vieira-Alves, I., Alves, A. R. P., Souza, N. M. V., Melo, T. L., Coimbra Campos, L. M. C., Lacerda, L. S. B., Queiroz-Junior, C. M., Andrade, A. C. D. S. P., Barcelos, L. S., Teixeira, M. M., Costa, V. V., Cortes, S. F., & Lemos, V. S. (2023). TNF/iNOS/NO pathway mediates host susceptibility to endothelial-dependent circulatory failure and death induced by betacoronavirus infection. *Clinical science (London, England: 1979)*, *137*(7), 543–559. https://doi.org/10.1042/CS20220663 Vignuzzi, M., Stone, J. K., Arnold, J. J., Cameron, C. E., & Andino, R. (2006). Quasispecies diversity determines pathogenesis through cooperative interactions in a viral population. *Nature*, *439*(7074), 344–348. https://doi.org/10.1038/nature04388

186. Visvabharathy, L., Hanson, B. A., Orban, Z. S., Lim, P. H., Palacio, N. M., Jimenez, M., Clark, J. R., Graham, E. L., Liotta, E. M., Tachas, G., Penaloza-MacMaster, P., & Koralnik, I. J. (2023). Neuro-PASC is characterized by enhanced CD4+ and diminished CD8+ T cell responses to SARS-CoV-2 Nucleocapsid protein. *Frontiers in Immunology*, *14*, 1155770. https://doi.org/10.3389/FIMMU.2023.1155770/FULL

187. Wallukat, G., Hohberger, B., Wenzel, K., Fürst, J., Schulze-Rothe, S., Wallukat, A., Hönicke, A. S., & Müller, J. (2021). Functional autoantibodies against G-protein coupled receptors in patients with persistent Long-COVID-19 symptoms. *Journal of Translational Autoimmunity*, *4*, 100100. https://doi.org/10.1016/J.JTAUTO.2021.100100

188. Wang, Y., & Qin, Z. H. (2010). Molecular and cellular mechanisms of excitotoxic neuronal death. Apoptosis: an international journal on programmed cell death, 15(11), 1382–1402. https://doi.org/10.1007/s10495-010-0481-0

189. Weiskopf, D., Schmitz, K. S., Raadsen, M. P., Grifoni, A., Okba, N. M. A., Endeman, H., van den Akker, J. P. C., Molenkamp, R., Koopmans, M. P. G., van Gorp, E. C. M., Haagmans, B. L., de Swart, R. L., Sette, A., & de Vries, R. D. (2020). Phenotype and kinetics of SARS-CoV-2-specific T cells in COVID-19 patients with acute respiratory distress syndrome. *Science Immunology*, *5*(48), eabd2071. https://doi.org/10.1126/SCIIMMUNOL.ABD2071

190. Weiss, S. R., & Leibowitz, J. L. (2011). Coronavirus pathogenesis. *Advances in virus research*, *81*, 85–164. https://doi.org/10.1016/B978-0-12-385885-6.00009-2

191. Wichmann, D., Sperhake, J. P., Lütgehetmann, M., Steurer, S., Edler, C., Heinemann, A., Heinrich, F., Mushumba, H., Kniep, I., Schröder, A. S., Burdelski, C., de Heer, G., Nierhaus, A., Frings, D., Pfefferle, S., Becker, H., Bredereke-Wiedling, H., de Weerth, A., Paschen, H. R., Sheikhzadeh-Eggers, S., Kluge, S. (2020). Autopsy Findings and Venous Thromboembolism in Patients With COVID-19: A Prospective Cohort Study. Annals of internal medicine, 173(4), 268–277. https://doi.org/10.7326/M20-2003

192. Williams, R. K., Jiang, G. S., & Holmes, K. V. (1991). Receptor for mouse hepatitis virus is a member of the carcinoembryonic antigen family of glycoproteins. Proceedings of the National Academy of Sciences of the United States of America, 88(13), 5533–5536. https://doi.org/10.1073/pnas.88.13.5533

193. Won, E., & Kim, Y. K. (2020). Neuroinflammation-Associated Alterations of the Brain as Potential Neural Biomarkers in Anxiety Disorders. International journal of molecular sciences, 21(18), 6546. https://doi.org/10.3390/ijms21186546

194. Woo, P. C. Y., Huang, Y., Lau, S. K. P., & Yuen, K. Y. (2010). Coronavirus genomics and bioinformatics analysis. *Viruses*, *2*(8), 1804–1820. https://doi.org/10.3390/v2081803

195. World Health Organization. (2021). A clinical case definition of post COVID-19 condition by a Delphi consensus, 6 October 2021. World Health Organization. https://iris.who.int/handle/10665/345824. License: CC BY-NC-SA 3.0 IGO

196. Wright-Jin, E. C., & Gutmann, D. H. (2019). Microglia as Dynamic Cellular Mediators of Brain Function. *Trends in molecular medicine*, *25*(11), 967–979. https://doi.org/10.1016/j.molmed.2019.08.013

197. Wu, C., Chen, X., Cai, Y., Xia, J., Zhou, X., Xu, S., Huang, H., Zhang, L., Zhou, X., Du, C., Zhang, Y., Song, J., Wang, S., Chao, Y., Yang, Z., Xu, J., Zhou, X., Chen, D., Xiong, W., Xu, L., … Song, Y. (2020). Risk Factors Associated With Acute Respiratory Distress Syndrome and Death in Patients With Coronavirus Disease 2019 Pneumonia in Wuhan, China. *JAMA internal medicine*, *180*(7), 934–943. https://doi.org/10.1001/jamainternmed.2020.0994

198. Xie, Y., Choi, T., & Al-Aly, Z. (2023). Molnupiravir and risk of post-acute sequelae of covid-19: cohort study. *BMJ*, *381*. https://doi.org/10.1136/BMJ-2022-074572

199. Xie, Y., Xu, E., Bowe, B., & Al-Aly, Z. (2022). Long-term cardiovascular outcomes of COVID-19. *Nature medicine*, *28*(3), 583–590. https://doi.org/10.1038/s41591-022-01689-3

200. Xiong, J., Kang, S. S., Wang, M., Wang, Z., Xia, Y., Liao, J., Liu, X., Yu, S. P., Zhang, Z., Ryu, V., Yuen, T., Zaidi, M., & Ye, K. (2023). FSH and ApoE4 contribute to Alzheimer's disease-like pathogenesis via C/EBPβ/δ-secretase in female mice. *Nature Communications*, *14*(1). https://doi.org/10.1038/S41467-023-42282-7

201. Xiong, J., Kang, S. S., Wang, Z., Liu, X., Kuo, T. C., Korkmaz, F., Padilla, A., Miyashita, S., Chan, P., Zhang, Z., Katsel, P., Burgess, J., Gumerova, A., Ievleva, K., Sant, D., Yu, S. P., Muradova, V., Frolinger, T., Lizneva, D., Ye, K. (2022). FSH blockade improves cognition in mice with Alzheimer's disease. *Nature*, *603*(7901), 470–476. https://doi.org/10.1038/S41586-022-04463-0

202. Xu, H., Zhong, L., Deng, J. *et al*. High expression of ACE2 receptor of 2019-nCoV on the epithelial cells of oral mucosa. *Int J Oral Sci* 12, 8 (2020). https://doi.org/10.1038/s41368-020-0074-x

203. Yang, A. C., Kern, F., Losada, P. M., Agam, M. R., Maat, C. A., Schmartz, G. P., Fehlmann, T., Stein, J. A., Schaum, N., Lee, D. P., Calcuttawala, K., Vest, R. T., Berdnik, D., Lu, N., Hahn, O., Gate, D., McNerney, M. W., Channappa, D., Cobos, I., Ludwig, N., Wyss-Coray, T. (2021). Dysregulation of brain and choroid plexus cell types in severe COVID-19. *Nature*, *595*(7868), 565–571. https://doi.org/10.1038/s41586-021-03710-0

204. Yang, Z., Du, J., Chen, G., Zhao, J., Yang, X., Su, L., Cheng, G., & Tang, H. (2014). Coronavirus MHV-A59 infects the lung and causes severe pneumonia in C57BL/6 mice. *Virologica Sinica*, *29*(6), 393–402. https://doi.org/10.1007/s12250-014-3530-y

205. Yin, K., Peluso, M. J., Luo, X., Thomas, R., Shin, M. G., Neidleman, J., Andrew, A., Young, K. C., Ma, T., Hoh, R., Anglin, K., Huang, B., Argueta, U., Lopez, M., Valdivieso, D., Asare, K., Deveau, T. M., Munter, S. E., Ibrahim, R., Roan, N. R. (2024). Long COVID manifests with T cell dysregulation, inflammation and an uncoordinated adaptive immune response to SARS-CoV-2. *Nature Immunology*, *25*(2), 218–225. https://doi.org/10.1038/S41590-023-01724-6

206. Zazhytska, M., Kodra, A., Hoagland, D. A., Frere, J., Fullard, J. F., Shayya, H., McArthur, N. G., Moeller, R., Uhl, S., Omer, A. D., Gottesman, M. E., Firestein, S., Gong, Q., Canoll, P. D., Goldman, J. E., Roussos, P., tenoever, B. R., Jonathan, B. O., & Lomvardas, S. (2022). Non-cell-autonomous disruption of nuclear architecture as a potential cause of COVID-19-induced anosmia. *Cell*, *185*(6), 1052-1064.e12. https://doi.org/10.1016/j.cell.2022.01.024

207. Zhang, L., Zhou, L., Bao, L., Liu, J., Zhu, H., Lv, Q., Liu, R., Chen, W., Tong, W., Wei, Q., Xu, Y., Deng, W., Gao, H., Xue, J., Song, Z., Yu, P., Han, Y., Zhang, Y., Sun, X., Yu, X., … Qin, C. (2021). SARS-CoV-2 crosses the blood-brain barrier accompanied with basement membrane disruption without tight juntions alteration. Signal transduction and targeted therapy, 6(1), 337. https://doi.org/10.1038/s41392-021-00719-9.

208. Zhao, Z. S., Granucci, F., Yeh, L., Schaffer, P. A., & Cantor, H. (1998). Molecular mimicry by herpes simplex virus-type 1: autoimmune disease after viral infection. *Science (New York, N.Y.)*, *279*(5355), 1344–1347. https://doi.org/10.1126/science.279.5355.1344

209. Zimatkin, S. M., & Bon', E. I. (2018). Dark Neurons of the Brain. *Neuroscience and Behavioral Physiology*, *48*(8), 908–912. https://doi.org/10.1007/S11055-018-0648-7/METRICS

210. Zollner, A., Koch, R., Jukic, A., Pfister, A., Meyer, M., Rössler, A., Kimpel, J., Adolph, T. E., & Tilg, H. (2022). Postacute COVID-19 is Characterized by Gut Viral Antigen Persistence in Inflammatory Bowel Diseases. *Gastroenterology*, *163*(2), 495-506.e8. https://doi.org/10.1053/J.GASTRO.2022.04.037

211. Zubair, A. S., McAlpine, L. S., Gardin, T., Farhadian, S., Kuruvilla, D. E., & Spudich, S. (2020). Neuropathogenesis and Neurologic Manifestations of the Coronaviruses in the Age of Coronavirus Disease 2019 A Review. JAMA Neurology, 77(8), 1018. https://doi.org/10.1001/JAMANEUROL.2020.2065

PRODUÇÃO CIENTÍFICA

Artigos publicados - colaboração

AMERICAN SOCIETY FOR MICROBIOLOGY | Journal of Virology®

PATHOGENESIS AND IMMUNITY
November 2021 Volume 95 Issue 22 10.1128/jvi.01276-21
https://doi.org/10.1128/jvi.01276-21

A Biosafety Level 2 Mouse Model for Studying Betacoronavirus-Induced Acute Lung Damage and Systemic Manifestations

Ana Cláudia dos Santos Pereira Andrade[a], Gabriel Henrique Campolina-Silva[b], Celso Martins Queiroz-Junior[a], Leonardo Camilo de Oliveira[a], Larisse de Souza Barbosa Lacerda[a], Jordane C Pimenta[a], Filipe Resende Oliveira de Souza[a], Ian de Meira Chaves[a], Ingredy Beatriz Passos[c], Danielle Cunha Teixeira[a], Paloma Graziele Bittencourt-Silva[d], Priscila Aparecida Costa Valadão[a], Leonardo Rossi-Oliveira[a], Maisa Mota Antunes[a], André Felipe Almeida Figueiredo[a], Natália Teixeira Wnuk[a], Jairo R. Temerozo [e,f], André Costa Ferreira[g,h,i], Allysson Cramer[b], Cleida Aparecida Oliveira[a], Ricardo Durães-Carvalho [j], Clarice Weis Arns[j], Pedro Pires Goulart Guimarães[d], Guilherme Mattos Jardim Costa[a], Gustavo Batista de Menezes[a], Cristina Guatimosim[a], Glauber Santos Ferreira da Silva[d], Thiago Moreno L. Souza[g,h], Breno Rocha Barrioni[k], Marivalda de Magalhães Pereira[k], Lirlândia Pires de Sousa[l], Mauro Martins Teixeira[b], Vivian Vasconcelos Costa [a,b]

[a]Department of Morphology, Institute of Biological Sciences, Universidade Federal de Minas Gerais, Belo Horizonte, MG, Brazil
[b]Department of Biochemistry and Immunology, Institute of Biological Sciences, Universidade Federal de Minas Gerais, Belo Horizonte, MG, Brazil
[c]Department of Microbiology, Institute of Biological Sciences, Universidade Federal de Minas Gerais, Belo Horizonte, MG, Brazil
[d]Department of Physiology and Biophysics, Institute of Biological Sciences, Universidade Federal de Minas Gerais, Belo Horizonte, MG, Brazil
[e]Laboratory on Thymus Research, Oswaldo Cruz Institute, Fiocruz, Rio de Janeiro, RJ, Brazil
[f]National Institute for Science and Technology on Neuroimmunomodulation, Oswaldo Cruz Foundation (Fiocruz), Rio de Janeiro, RJ, Brazil
[g]National Institute for Science and Technology on Innovation on Diseases of Neglected Populations (INCT/IDNP), Center for Technological Development in Health (CDTS), Oswaldo Cruz Foundation (Fiocruz), Rio de Janeiro, RJ, Brazil
[h]Immunopharmacology Laboratory, Oswaldo Cruz Foundation (Fiocruz), Rio de Janeiro, RJ, Brazil
[i]Laboratório de Pesquisas Pré-clínicas, Universidade Iguaçu (UNIG), Rio de Janeiro, RJ, Brazil
[j]Laboratory of Virology, Universidade Estadual de Campinas (UNICAMP), Campinas, SP, Brazil
[k]Department of Metallurgical Engineering and Materials, Federal University of Minas Gerais, School of Engineering, Belo Horizonte, Brazil
[l]Department of Clinical and Toxicological Analysis, Faculty of Pharmacy, Universidade Federal de Minas Gerais, Belo Horizonte, MG, Brazil

ABSTRACT The emergence of life-threatening zoonotic diseases caused by betacoronaviruses, including the ongoing coronavirus disease 19 (COVID-19) pandemic, has highlighted the need for developing preclinical models mirroring respiratory and systemic pathophysiological manifestations seen in infected humans. Here, we showed that C57BL/6J wild-type mice intranasally inoculated with the murine betacoronavirus murine hepatitis coronavirus 3 (MHV-3) develop a robust inflammatory

GUT MICROBES
2023, VOL. 15, NO. 2, 2249146
https://doi.org/10.1080/19490976.2023.2249146

Taylor & Francis
Taylor & Francis Group

RESEARCH PAPER

OPEN ACCESS Check for updates

Gut microbiota from patients with COVID-19 cause alterations in mice that resemble post-COVID symptoms

Viviani Mendes de Almeida[a*], Daiane F. Engel[b*], Mayra F. Ricci[a*], Clênio Silva Cruz[a], Ícaro Santos Lopes[c], Daniele Almeida Alves[d], Mirna d' Auriol[e], João Magalhães[a], Elayne C. Machado[a], Victor M. Rocha[a], Toniana G. Carvalho[f], Larisse S. B. Lacerda[g], Jordane C. Pimenta[g], Mariana Aganetti[a], Giuliana S. Zuccoli[h], Bradley J. Smith[h], Victor C. Carregari[h], Erika da Silva Rosa[a], Izabela Galvão[a], Geovanni Dantas Cassali[i], Cristiana C. Garcia[j], Mauro Martins Teixeira[g], Leiliane C. André[e], Fabiola Mara Ribeiro[f], Flaviano S. Martins[k], Rafael Simone Saia[l], Vivian Vasconcelos Costa[g], Daniel Martins-de-Souza[h,m,n,o], Philip M. Hansbro[p], João Trindade Marques[d,q], Eric R. G. R. Aguiar[c], and Angélica T. Vieira[a]

[a]Laboratory of Microbiota and Immunomodulation - Department of Biochemistry and Immunology, Institute of Biological Sciences, Universidade Federal de Minas Gerais - UFMG, Belo Horizonte, Brazil; [b]Department of Clinical Analysis, School of Pharmacy, Universidade Federal de Ouro Preto - UFOP, Ouro Preto, Brazil; [c]Laboratory of Virus Bioinformatics - Department of Biological Science, Center of Biotechnology and Genetics, Universidade Estadual de Santa Cruz - UESC, Ilhéus, Brazil; [d]Laboratory of RNA Interference and Antiviral Immunity - Department of Biochemistry and Immunology, Institute of Biological Sciences, Universidade Federal de Minas Gerais - UFMG, Belo Horizonte, Brazil; [e]Laboratory of Toxicology - Department of Clinical and Toxicological Analysis, Faculty of Pharmacy, Universidade Federal de Minas Gerais - UFMG, Belo Horizonte, Brazil; [f]Laboratory of Neurobiochemistry - Department of Biochemistry and Immunology, Institute of Biological Sciences, Universidade Federal de Minas Gerais - UFMG, Belo Horizonte, Brazil; [g]Center for Research and Development of Drugs - Department of Morphology, Institute of Biological Sciences, Universidade Federal de Minas Gerais - UFMG, Belo Horizonte, Brazil; [h]Laboratory of Neuroproteomics - Department of Biochemistry and Tissue Biology, Institute of Biology, Universidade do Estado de Campinas - UNICAMP, Campinas, Brazil; [i]Laboratory of Comparative Pathology - Department of Pathology, Universidade Federal de Minas Gerais - UFMG, Belo Horizonte, Brazil; [j]Laboratory of Respiratory Viruses and Measles, Instituto Oswaldo Cruz - Fiocruz, Rio de Janeiro, Brazil; [k]Laboratory of Biotherapeutic Agents - Department of Microbiology, Institute of Biological Sciences, Universidade Federal de Minas Gerais - UFMG, Belo Horizonte, Brazil; [l]Laboratory of Intestinal Physiology - Department of Physiology, Ribeirão Preto Medical School, Universidade de São Paulo, Ribeirão Preto, Brazil; [m]D'Or Institute for Research and Education, São Paulo, Brazil; [n]Experimental Medicine Research Cluster, Universidade do Estado de Campinas - UNICAMP, Campinas, Brazil; [o]National Institute of Biomarkers in Neuropsychiatry, National Council for Scientific and Technological Development, São Paulo, Brazil; [p]Centre for Inflammation, Centenary Institute and University of Technology Sydney, Sydney, Australia; [q]CNRS UPR9022, University of Strasbourg, Strasbourg, France

ABSTRACT

Long-term sequelae of coronavirus disease (COVID)-19 are frequent and of major concern. Severe acute respiratory syndrome coronavirus 2 (SARS-CoV-2) infection affects the host gut microbiota, which is linked to disease severity in patients with COVID-19. Here, we report that the gut microbiota of post-COVID subjects had a remarkable predominance of *Enterobacteriaceae* strains with an antibiotic-resistant phenotype compared to healthy controls. Additionally, short-chain fatty acid (SCFA) levels were reduced in feces. Fecal transplantation from post-COVID subjects to germ-free mice led to lung inflammation and worse outcomes during pulmonary infection by multidrug-resistant *Klebsiella pneumoniae*. transplanted mice also exhibited poor cognitive performance. Overall, we show prolonged impacts of SARS-CoV-2 infection on the gut microbiota that persist after subjects have cleared the virus. Together, these data demonstrate that the gut microbiota can directly contribute to post-COVID sequelae, suggesting that it may be a potential therapeutic target.

ARTICLE HISTORY
Received 24 April 2023
Revised 19 July 2023
Accepted 14 August 2023

KEYWORDS
COVID-19; SARS-CoV-2; post-COVID; microbiota; inflammation; antimicrobial-resistance

Neurochemistry International 169 (2023) 105567

Contents lists available at ScienceDirect

Neurochemistry International

journal homepage: www.elsevier.com/locate/neuint

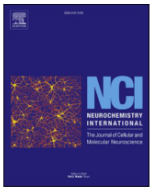

Neuromuscular defects after infection with a beta coronavirus in mice

Leonardo Rossi [a], Kivia B.S. Santos [a], Barbara I.S. Mota [a], Jordane Pimenta [a], Bruna Oliveira [a], Caroline A. Machado [a], Heliana B. Fernandes [a], Leticia A. Barbosa [a], Hermann A. Rodrigues [d], Gabriel H.M. Teixeira [a], Gabriel A. Gomes-Martins [a], Gabriel F. Chaimowicz [a], Celso Martins Queiroz-Junior [a], Ian Chaves [a], Juan C. Tapia [c], Mauro M. Teixeira [b], Vivian V. Costa [a], Aline S. Miranda [a], Cristina Guatimosim [a,*]

[a] Department of Morphology, Institute of Biological Sciences, Universidade Federal de Minas Gerais, Belo Horizonte, MG, Brazil
[b] Department of Biochemistry, Institute of Biological Sciences, Universidade Federal de Minas Gerais, Belo Horizonte, MG, Brazil
[c] School of Medicine, University of Talca, Talca, Chile
[d] Departamento de Ciências Básicas da Vida, Universidade Federal de Juiz de Fora, Campus Governador Valadares, MG, Brazil

A B S T R A C T

COVID-19 affects primarily the lung. However, several other systemic alterations, including muscle weakness, fatigue and myalgia have been reported and may contribute to the disease outcome. We hypothesize that changes in the neuromuscular system may contribute to the latter symptoms observed in COVID-19 patients. Here, we showed that C57BL/6J mice inoculated intranasally with the murine betacoronavirus hepatitis coronavirus 3 (MHV-3), a model for studying COVID-19 in BSL-2 conditions that emulates severe COVID-19, developed robust motor alterations in muscle strength and locomotor activity. The latter changes were accompanied by degeneration and loss of motoneurons that were associated with the presence of virus-like particles inside the motoneuron. At the neuromuscular junction level, there were signs of atrophy and fragmentation in synaptic elements of MHV-3-infected mice. Furthermore, there was muscle atrophy and fiber type switch with alteration in myokines levels in muscles of MHV-3-infected mice. Collectively, our results show that acute infection with a betacoronavirus leads to robust motor impairment accompanied by neuromuscular system alteration.

1. Introduction

In December 2019, a novel coronavirus named severe acute respiratory syndrome coronavirus 2 (SARS-CoV-2) was identified in Wuhan, China. By the middle of 2020, coronavirus disease 2019 (COVID-19, named by WHO on Feb 11, 2020), became a global pandemic, affecting individuals all around the world. The virus is a member of the coronavirus family that caused the 2002–2004 SARS and 2012 MERS outbreaks, and primarily spreads through respiratory droplets produced by the infected people. Noteworthy, it can be transmitted even if the infected person has no symptoms. The clinical manifestations of COVID-19 can range from no symptoms to severe ailment. Fever, cough, headache, myalgia, and difficulty of breathing are among the typical symptoms. Severe symptoms, on the other hand, lead to acute respiratory distress syndrome (ARDS), with systemic inflammatory response, and lung-organ failure, which frequently culminates in the patient's death. Additionally, it is important to note that the severity of COVID-19 disease, although varies widely from person to person, seems to be higher in older adults, people with underlying health conditions, or individuals with compromised immune systems (Del Valle et al., 2020; Lu et al., 2020).

Because of all symptoms described above in humans, animal models for COVID-19 are key to study the disease, providing valuable insights into mechanisms of viral-induced disease (Andrade et al., 2021; Sia et al., 2020; Winkler et al., 2020; Gurumurthy et al., 2020; Rockx et al., 2020). The SARS-CoV-2 virus adsorbs cells via the spike (S) glycoprotein, which has a high affinity (>10 fold more than previous SARS-CoV-1) for ACE2 (angiotensin-converting enzyme 2), localized at the surface of host cells (Bourgonje et al., 2020). Since ACE2 is expressed in several tissues i.e., nasal tissue, lungs, kidneys, liver, blood vessels, gut, brain, immune system, and skeletal muscles; COVID-19 infects not only lung cells but many other cell types and organs throughout the body (Bourgonje et al., 2020; Motta-Santos et al., 2016). Thus, a detailed understanding of the pathophysiological consequences of COVID-19 on various cells and organs remains elusive.

The use of the murine coronavirus has been suggested as a strategy to mimic the key aspects of human coronavirus infection in a biosafety level 2 environment (Albuquerque et al., 2006; Yang et al., 2014;

* Corresponding author.
E-mail address: cguati@icb.ufmg.br (C. Guatimosim).

https://doi.org/10.1016/j.neuint.2023.105567
Received 13 April 2023; Received in revised form 14 June 2023; Accepted 19 June 2023
Available online 20 June 2023

pathogens

MDPI

Article

E3 Ubiquitin Ligase Smurf1 Regulates the Inflammatory Response in Macrophages and Attenuates Hepatic Damage during Betacoronavirus Infection

Luiz P. Souza-Costa [1], Felipe R. S. Santos [1], Jordane C. Pimenta [2], Celso M. Queiroz-Junior [2], Fernanda L. Tana [1], Danielle C. Teixeira [2], Manoela G. G. Couto [2], Natalia F. M. Oliveira [1], Rafaela D. Pereira [1], Vinicius A. Beltrami [2], Pedro A. C. Costa [3], Larisse S. B. Lacerda [2], Josiane T. Andrade-Chaves [1], Pedro P. G. Guimarães [3], Renato S. Aguiar [4], Mauro M. Teixeira [1], Vivian V. Costa [2] and Luis H. Franco [1,*]

[1] Departamento de Bioquímica e Imunologia, Instituto de Ciências Biológicas, Universidade Federal de Minas Gerais, Av. Pres. Antônio Carlos, 6627, Belo Horizonte 31270-901, MG, Brazil; souzaluizpedro@gmail.com (L.P.S.-C.)
[2] Departamento de Morfologia, Instituto de Ciências Biológicas, Universidade Federal de Minas Gerais, Av. Pres. Antônio Carlos, 6627, Belo Horizonte 31270-901, MG, Brazil
[3] Departamento de Fisiologia e Biofísica, Instituto de Ciências Biológicas, Universidade Federal de Minas Gerais, Av. Pres. Antônio Carlos, 6627, Belo Horizonte 31270-901, MG, Brazil
[4] Departamento de Genética e Evolução, Instituto de Ciências Biológicas, Universidade Federal de Minas Gerais, Av. Pres. Antônio Carlos, 6627, Belo Horizonte 31270-901, MG, Brazil
* Correspondence: luisfranco@icb.ufmg.br; Tel.: +55-31-3409-2666

Abstract: The E3 ubiquitin ligase Smurf1 catalyzes the ubiquitination and proteasomal degradation of several protein substrates related to inflammatory responses and antiviral signaling. This study investigated the role of Smurf1 in modulating inflammation induced by Betacoronavirus infection. Bone marrow-derived macrophages (BMDMs) from C57BL/6 (wild-type) or Smurf1-deficient (*Smurf1*$^{-/-}$) mice were infected with MHV-A59 to evaluate the inflammatory response in vitro. Smurf1 was found to be required to downregulate the macrophage production of pro-inflammatory mediators, including TNF, and CXCL1; to control viral release from infected cells; and to increase cell viability. To assess the impact of Smurf 1 in vivo, we evaluated the infection of mice with MHV-A59 through the intranasal route. *Smurf1*$^{-/-}$ mice infected with a lethal inoculum of MHV-A59 succumbed earlier to infection. Intranasal inoculation with a 10-fold lower dose of MHV-A59 resulted in hematological parameter alterations in *Smurf1*$^{-/-}$ mice suggestive of exacerbated systemic inflammation. In the lung parenchyma, Smurf1 expression was essential to promote viral clearance, downregulating IFN-β mRNA and controlling the inflammatory profile of macrophages and neutrophils. Conversely, Smurf1 did not affect IFN-β mRNA regulation in the liver, but it was required to increase TNF and iNOS expression in neutrophils and decrease TNF expression in macrophages. In addition, *Smurf1*$^{-/-}$ mice exhibited augmented liver injuries, accompanied by high serum levels of alanine aminotransferase (ALT). These findings suggest that Smurf1 plays a critical role in regulating the inflammatory response in macrophages and attenuating systemic inflammation during Betacoronavirus infection.

Keywords: Smurf1; Betacoronavirus; MHV-A59; inflammation; macrophages

Citation: Souza-Costa, L.P.; Santos, F.R.S.; Pimenta, J.C.; Queiroz-Junior, C.M.; Tana, F.L.; Teixeira, D.C.; Couto, M.G.G.; Oliveira, N.F.M.; Pereira, R.D.; Beltrami, V.A.; et al. E3 Ubiquitin Ligase Smurf1 Regulates the Inflammatory Response in Macrophages and Attenuates Hepatic Damage during Betacoronavirus Infection. *Pathogens* **2024**, *13*, 871. https://doi.org/10.3390/pathogens13100871

Academic Editor: Luis Martinez-Sobrido

Received: 16 August 2024
Revised: 27 September 2024
Accepted: 1 October 2024
Published: 3 October 2024

1. Introduction

Betacoronavirus is a genus that belongs to the *Coronaviridae* family of viruses, and it includes enveloped viruses with single-stranded, positive-sense RNA. This genus comprises a vast number of members that cause zoonotic and human illnesses, ranging from the common cold to the highly severe acute respiratory coronavirus disease 2019 (COVID-19), responsible for the recent pandemic that led to nearly 7 million deaths [1]. Given the wide geographic distribution of Betacoronaviruses, the recurrence of zoonotic outbreaks, and the potential for

Artigos submetidos- colaboração

This is an automated message.

Journal: Brain Behavior and Immunity
Title: PI3Kγ pathway contributes to neuroinflammation and neuronal death induced by Zika virus infection
Corresponding Author: Dr. Vivian Costa
Co-Authors: Danielle Cunha Teixeira; Gabriel Campolina-Silva; Fernanda Martins Marim; Felipe Rocha Santos; Celso Martins Queiroz-Junior; Pedro Augusto Carvalho Costa; Fernanda Lima Tana; Luiz Pedro Souza-Costa; Jordane Clarisse Pimenta; Júlia Gomes Carvalho; Vinícius Beltrami; Felipe Emanuel Oliveira Rocha; Drielle Viana Vieira; Evandro Gonçalves Dornelas; Giovana Cougo Ferreira; Felipe Ferraz Dias; Pedro Pires Goulart Guimarães; Vinícius Toledo Ribas; Antonio Lucio Teixeira; Aline Silva de Miranda; Mauro Martins Teixeira; Danielle Glória Souza

Manuscript #	JVI02283-24
Current Revision #	0
Submission Date	2024-12-20 14:59:05
Current Stage	Initial QC
Title	Broad-Spectrum Antiviral Efficacy of 7-Deaza-7-Fluoro-2'-C-Methyladenosine Against Multiple Coronaviruses In Vitro and In Vivo
Manuscript Type	Full-Length Text
Special Section	N/A
Journal Section	Vaccines and Antiviral Agents
Manuscript Comment	Letter for waiver Dear Editorial board - Journal of Virology We have submitted a manuscript entitled "Broad-Spectrum Antiviral Efficacy of 7-Deaza-7-Fluoro-2'-C-Methyladenosine Against Multiple Coronaviruses In Vitro and In Vivo". Unfortunately, I am unable to cover the publication fee for this manuscript. Therefore, I would like to request a FULL waiver or, at the very least, a substantial discount, given the ongoing challenges faced by Brazilian research. In recent years, Brazil has continued to endure a political, social, and economic crisis, which has deeply impacted public funding for science and higher education. My research group also does not have grants that allow the payment of fee publications as well as, the dollar is highly valued against BRL (The exchange rate is 6.05 Brazilian reais per US dollar.). Taking into account the arguments presented above, I would like to ask for a FULL waiver of publication fees. I sincerely hope you can accommodate my request for a FULL waiver or a significant reduction in the publication fee. Such support would not only help make this work accessible to the scientific community but also alleviate the challenges posed by the current financial climate in Brazil. Thank you for your attention and understanding. Thanks in advance.
Corresponding Author	Dr. Vivian Vasconcelos Costa (Universidade Federal de Minas Gerais)
Contributing Authors	Ian de Meira Chaves , Filipe Resende Oliveira de Souza , Dr. Celso Martins Queiroz-Junior , Leonardo Camilo Oliveira , Miss Ana Claudia dos Santos Andrade , Victor Rodrigues de Melo Costa , Danielle Cunha Teixeira , Felipe Rocha da Silva Santos , Talita Cristina Martins Fonseca , Larisse de Souza Barbosa Lacerda , Rafaela das Dores Pereira , Jordade Clarisse Pimenta , Dr. Franck Amblard , Dr. Raymond F. Schinazi , Prof. Mauro M Teixeira , Dr. Vivian Vasconcelos Costa (corr-auth)

ANEXOS

ANEXO A

UNIVERSIDADE FEDERAL DE MINAS GERAIS

CEUA
COMISSÃO DE ÉTICA NO USO DE ANIMAIS

CERTIFICADO
Certificamos que o projeto intitulado "Implementação de um modelo de Síndrome Respiratória Aguda Grave (SARS) induzido por coronavírus para testes de potenciais terapias.", protocolo do CEUA: 190/2020 sob a responsabilidade de Vivian Vasconcelos Costa que envolve a produção, manutenção e/ou utilização de animais pertencentes ao filo Chordata, subfilo Vertebrata (exceto o homem) para fins de pesquisa científica (ou ensino) - encontra-se de acordo com os preceitos da Lei nº 11.794, de 8 de outubro de 2008, do Decreto nº 6.899 de 15 de julho de 2009, e com as normas editadas pelo Conselho Nacional de Controle da Experimentação Animal (CONCEA), e foi aprovado pela COMISSÃO DE ÉTICA NO USO DE ANIMAIS (CEUA) DA UNIVERSIDADE FEDERAL DE MINAS GERAIS, em reunião de 05/10/2020.

Vigência da Autorização	05/10/2020 a 04/10/2025
Finalidade	Pesquisa
***Espécie/linhagem**	Camundongo isogênico / C57BL/6
Nº de animais	11
Peso/Idade	16g / 6(semanas)
Sexo	indiferente
Origem	Bioterio Central da UFMG
***Espécie/linhagem**	Camundongo isogênico / C57BL/6
Nº de animais	11
Peso/Idade	16g / 6(semanas)
Sexo	indiferente
Origem	Bioterio Central da UFMG
***Espécie/linhagem**	Camundongo isogênico / C57BL/6
Nº de animais	11
Peso/Idade	16g / 6(semanas)
Sexo	indiferente
Origem	ioterio Central da UFMG
***Espécie/linhagem**	Camundongo isogênico / Balb/c
Nº de animais	11
Peso/Idade	16g / 6(semanas)
Sexo	indiferente
Origem	Bioterio Central
***Espécie/linhagem**	Camundongo isogênico / Balb/c
Nº de animais	11
Peso/Idade	16g / 6(semanas)
Sexo	indiferente
Origem	ioterio Central da UFMG
***Espécie/linhagem**	Camundongo isogênico / Balb/c
Nº de animais	11

ANEXO B

UNIVERSIDADE FEDERAL DE MINAS GERAIS

CEUA
COMISSÃO DE ÉTICA NO USO DE ANIMAIS

CERTIFICADO

Certificamos que o projeto intitulado "Caracterização das sequelas induzidas pela infecção pulmonar com coronavírus murino em um modelo de COVID longa", protocolo do CEUA: 140/2023 sob a responsabilidade de Vivian Vasconcelos Costa que envolve a produção, manutenção e/ou utilização de animais pertencentes ao filo Chordata, subfilo Vertebrata (exceto o homem) para fins de pesquisa científica (ou ensino) - encontra-se de acordo com os preceitos da Lei nº 11.794, de 8 de outubro de 2008, do Decreto nº 6.899 de 15 de julho de 2009, e com as normas editadas pelo Conselho Nacional de Controle da Experimentação Animal (CONCEA), e foi aprovado pela COMISSÃO DE ÉTICA NO USO DE ANIMAIS (CEUA) DA UNIVERSIDADE FEDERAL DE MINAS GERAIS, em reunião de 14/08/2023.

Vigência da Autorização	14/08/2023 a 13/08/2028
Finalidade	Pesquisa
***Espécie/linhagem**	Camundongo isogênico / C57Bl6
Nº de animais	64
Peso/Idade	20g / 6(semanas)
Sexo	masculino
Origem	Biotério Central UFMG
***Espécie/linhagem**	Camundongo isogênico / C57Bl6
Nº de animais	64
Peso/Idade	20g / 6(semanas)
Sexo	feminino
Origem	Biotério Central UFMG
***Espécie/linhagem**	Camundongo isogênico / C57Bl6
Nº de animais	64
Peso/Idade	20g / 6(semanas)
Sexo	masculino
Origem	Biotério Central UFMG
***Espécie/linhagem**	Camundongo isogênico / C57Bl6
Nº de animais	64
Peso/Idade	20g / 6(semanas)
Sexo	feminino
Origem	Biotério Central UFMG
***Espécie/linhagem**	Camundongo isogênico / C57Bl6
Nº de animais	80
Peso/Idade	20g / 6(semanas)
Sexo	masculino
Origem	Biotério Central UFMG
***Espécie/linhagem**	Camundongo isogênico / C57Bl6
Nº de animais	80

ANEXO C

UNIVERSIDADE FEDERAL DE MINAS GERAIS

CEUA
COMISSÃO DE ÉTICA NO USO DE ANIMAIS

CERTIFICADO

Certificamos que o projeto intitulado "Avaliação de potenciais alvos terapêuticos em um modelo experimental de COVID longa induzida por MHV-A59 em camundongos.", protocolo do CEUA: 131/2024 sob a responsabilidade de Vivian Vasconcelos Costa que envolve a produção, manutenção e/ou utilização de animais pertencentes ao filo Chordata, subfilo Vertebrata (exceto o homem) para fins de pesquisa científica (ou ensino) - encontra-se de acordo com os preceitos da Lei nº 11.794, de 8 de outubro de 2008, do Decreto nº 6.899 de 15 de julho de 2009, e com as normas editadas pelo Conselho Nacional de Controle da Experimentação Animal (CONCEA), e foi aprovado pela COMISSÃO DE ÉTICA NO USO DE ANIMAIS (CEUA) DA UNIVERSIDADE FEDERAL DE MINAS GERAIS, em reunião de 01/07/2024.

Vigência da Autorização	01/07/2024 a 30/06/2029
Finalidade	Pesquisa
***Espécie/linhagem**	Camundongo isogênico / C57BL/6
Nº de animais	9
Peso/Idade	15g / 5(semanas)
Sexo	feminino
Origem	Biotério Central da UFMG
***Espécie/linhagem**	Camundongo isogênico / C57BL/6
Nº de animais	9
Peso/Idade	15g / 5(semanas)
Sexo	feminino
Origem	Biotério Central da UFMG
***Espécie/linhagem**	Camundongo isogênico / C57BL/6
Nº de animais	9
Peso/Idade	15g / 5(semanas)
Sexo	feminino
Origem	Biotério Central da UFMG
***Espécie/linhagem**	Camundongo isogênico / C57BL/6
Nº de animais	9
Peso/Idade	15g / 5(semanas)
Sexo	feminino
Origem	Biotério Central da UFMG
***Espécie/linhagem**	Camundongo isogênico / C57BL/6
Nº de animais	9
Peso/Idade	15g / 5(semanas)
Sexo	feminino
Origem	Biotério Central da UFMG
***Espécie/linhagem**	Camundongo isogênico / C57BL/6
Nº de animais	9